

THESE DE DOCTORAT DE L'UNIVERSITÉ DE STRASBOURG

Présentée en vue de l'obtention du titre de docteur de l'Université de Strasbourg
Discipline: Aspects Moléculaires et Cellulaires de la Biologie
Mention: Neurosciences



Cholecystinin and drug abuse: mRNA regulation in drug dependence and alteration of emotional responses after AAV2-shRNA-mediated knock-down in the mouse basolateral amygdala

par

Carolina DEL BOCA

Thèse dirigée par le Pr. Brigitte KIEFFER

soutenue publiquement le 10 juin 2011

à Institut de Génétique et de Biologie Moléculaire et Cellulaire

Membres du jury:

Pr. Ian KITCHEN
Dr. Florence NOBLE
Dr. Michel BARROT
Pr. Brigitte KIEFFER

Rapporteur externe, Surrey (UK)
Rapporteur externe, Paris
Examineur, Strasbourg
Directeur de thèse, Strasbourg

Zona de promesas

Mama sabe bien
Perdí una batalla
Quiero regresar
Solo a besarla

No está mal
Ser mi dueño otra vez
Ni temer que el río sangre y calme
Al contarle mis plegarias

Tarda en llegar
Y al final, al final
Hay recompensa

Mama sabe bien
Pequeña princesa
Cuando regrese
Todo quemaba

No esta mal
Sumergirme otra vez
Ni temer que el río sangre y calme
Se bucear en silencio

Tarda en llegar
Y al final, al final
Hay recompensa
En la zona de promesas

Soda Stereo

ACKNOWLEDGEMENTS

First of all I would like to thank all the members of my jury, Pr. Ian Kitchen, Dr. Florence Noble and Dr. Michel Barrot for having accepted to read and judge my work.

I would particularly like to thank Pr. Brigitte Kieffer for the opportunity to perform my PhD thesis in her lab and her insistence in moments of crisis.

I would like to thank as well all the members of the lab that have shared with me this hard road...

Particularly to Julie for her guidance and advice; to Pascale, not only for the virus preparation but for her constant support, sensitivity and encouragement; to Claire and Katia for having corrected and helped with my manuscript; to Dom for having introduced me in the molecular biology; to Audrey for taking care of so many things in the lab and for her friendship; to Amynah who has always transmitted me peace and optimism and to her beautiful family whom I miss a lot; to Domi for her honest and always very accurate scientific and personal advices; to Jérôme, Pierre-Eric, Chihiro, Eric, David, Abdel...

And very special thanks to the group of wonderful people I've the great opportunity to meet and I hope we keep always in contact: to Manu, Paul, Olivier, Pauline, Raph, Lauren, Megan. Without your support and unconditional help I'm sure I wouldn't be able to do this, thank you for having been the necessary smile (and laugh) to keep fighting!!

And of course! To the second floor for their constant support and joy: Michel, Anne, Aline, Yvan, Xavier and Sercan... And yes, for you I'd need a full page of acknowledgments and still wouldn't be enough, so I'll simply THANK YOU, in capitals, for your unconditional support, help and friendship... l'essentiel est invisible pour les yeux, on ne voit bien qu'avec le coeur.

I would also like to THANK in capitals to Gilles and Djemo for being two incredible people whom have take care not only of my mice but also of me during all this time, merci merci! Vous me manquez déjà!

Next, I would like to thank to Gronnemeyer's team members and so many people in the institute that I'm afraid of forgetting names, so I apologize but I'll do it general... thank you for the great years I've spent in this huge house, because even with all the difficulties, the amazing people I've met here have made of this place a real home for me... Well... I have to thank specially to Mannu, can't avoid your name my brother! ☺ Be strong, you are almost there and you can do it greatly!

And a huge special thank to Maïté for being a great person and essential for the completion of this work.

Then I would like to move outside the IGBMC to thank all my friends here in France, my support, my refuge, my family (and I'm sorry, but I'll switch languages here): Fran, Tina, Fer,

Stefanie, Lucio, Frida (mi tocaya que llegó para robarse un pedacito de mi alma), Murielle, Carlos (... animalito, cuántas cosas vividas, cuántas cosas aprendidas, cuánto camino aun nos queda por delante!! Verdad? ☺), Elena!!! (Qué sería de mi vida sin ti amiga del alma!!! Simplemente no tengo palabras)... Pablo y Naty!! (compañeros de ruta! cada vez tengo menos palabras... Increíble amigos este lazo inquebrantable que siento entre nosotros)... Las gracias en este caso no son a ustedes, son a la vida por cruzarlos en mi camino... Como diría Mercedes Sosa: GRACIAS A LA VIDA, QUE ME HA DADO TANTO TANTO! ☺ (Porque Fer, es bonita la vida, verdad? Gracias por los arcoíris!!!).

And even more far far away, on the other side of the huge puddle, I would also like to thank my friends (and again I switch, I'm sorry)... Tengo que agradecer en especial al Tonga!!! Por ser el verdadero soporte final de mi tesis. Increíble! Segunda vez que me ayudas con esto chanchito!! GRACIAS! A la Juli, negra! Porque llorar, reír y putear de a dos es más fácil, gracias por estar siempre ahí comprendiendo y compartiendo al 100% esta aventura (o desventura?) del doctorado en el extranjero! Y al Gaby, narigón!! Ahora estas de nuevo allá, así que entrás en este apartado, pero sin vos acá tan cerca esto hubiera costado el doble, gracias por tanto aguante!

Y gracias por supuesto a los incondicionales trocitos de mi alma: Juli, Jaz, Flaca, Chete, Choli, Vale, Pili, Andre, Vane, Noe, Romi, Eve, Pato, Flor, Iva, Mauri, Jorge, Gordo, Waldo, Gus, Valen... Porqué sin su apoyo y empuje constante, sin esa fuerza que me da su amor, al que no le importan distancias ni tiempos, no sólo que no habría logrado esto, sino que no sería nada de lo que soy.

Reaching the end, I would like to give VERY special thanks to my family, por el gran esfuerzo que fue para ellos también tenerme lejos de casa, por el apoyo y la confianza constante... A mis hermanos, por ser hermanos y ser amigos, por ser la parte más importante de mi; a mi papá, por ser puro corazón; a mi mamá por ser coraje, por ser la mujer más hermosa del mundo; a mi abuela, por ser la persona más maravillosa del mundo, sin duda alguna; y a mis abuelos que ya no están, por seguir guiándome en mis sueños... A mi familia "política", o más bien del corazón, por ser amor y ser valor, por hacerse querer tanto y quererme tanto.

And finally, I would especially like to thank Dani... If I believed in the concept of "the other half", he would be mine for sure... Gracias mi amor, por vivir conmigo esta aventura, por creer en mí, por TODO lo que me das, por ser una persona increíble, y por este verdadero trabajo de equipo! WE DID IT! ☺

To Dani

SUMMARY

I. General Introduction	1
A. Drug dependence	
1. Definition and theories.....	2
2. Relation of addiction with emotional disorders.....	4
B. Neuronal circuits underlying drug dependence and emotional disorders	
1. Addiction and brain circuits.....	5
a) <i>The mesocorticolimbic dopamine system</i>	6
b) <i>The extended amygdala</i>	7
2. The emotional brain circuits.....	8
a) <i>Frontal-subcortical circuits</i>	8
b) <i>Amygdalar circuit</i>	9
➤ <i>The basolateral nucleus of the amygdala</i>	10
C. Neurotransmitter and neoromodulator systems involved in addiction and emotional disorders	11
An overview of the endogenous opioid system.....	13
D. CHOLECYSTOKININ	16
1. Biosynthesis.....	16
2. Receptors and signal transduction.....	17
3. Intestinal distribution and major effects as a gastrointestinal hormone.....	19
4. Brain distribution and central systems.....	20
5. Major effects as a neuromodulatory peptide.....	21
6. CCK and opioid system interactions.....	24
7. Characterization of the CCK-peptide deficient mice.....	25
E. Aims of the thesis	26

II. Part I.....	29
“CCK mRNA regulation during morphine dependence in the mouse brain”	
A. Introduction.....	30
1. The involvement of BLA and Cg Ctx regions in drug dependence.....	31
2. The autoradiographic film quantification technique.....	32
B. Materials and methods.....	34
C. Results.....	38
1. Mapping of CCK mRNA expression in the mouse brain by <i>in situ</i> hybridization (ISH)	38
2. CCK mRNA expression pattern regulation upon morphine treatment.....	38
D. Discussion.....	40
1. Methodological issues.....	40
2. CCK mRNA distribution in the mouse brain.....	41
3. CCK mRNA regulation upon morphine treatment.....	42
E. Conclusions and perspectives.....	43
III. Part II.....	44
“Emotional behavioral responses after AAV₂-shCCK-mediated knock-down in the mouse brain”	
Summary.....	45
1. Introduction.....	45
a) <i>The shRNA technology</i>	46
b) <i>The viral delivery approach</i>	47
2. Detailed methodology.....	50
a) <i>General procedure</i>	
• <i>Technical optimization of the AAV-shCCK knock-down strategy in Cg Ctx and BLA</i>	50
• <i>Evaluation of the effects of AAV₂-shCCK-mediated knock-down in the BLA on emotional behavioral responses (Manuscript 1)</i>	51

b) Materials and methods	51
• <i>AAV-shCCK vector-based strategy</i>	51
• <i>AAV-shCCK silencing activity evaluation by in situ hybridization (ISH)</i>	53
• <i>Behavioral testing</i>	55
c) Statistical analysis	56
3. Technical optimization of the AAV-shCCK knock-down strategy and preliminary results targeting Cg Ctx and BLA regions	
- <i>Double CMV-U6 promoter-based vector strategy</i>	57
- <i>Setting up of the stereotaxic surgery procedure</i>	58
- <i>Selection of the shCCK sequence producing the best silencing activity</i>	59
- <i>Selection of the best viral serotype to target each region of interest</i>	61
- <i>Pilot experiment on AAV₂-shCCK knock-down quantification</i>	61
4. Manuscript 1:	63
“Genetic silencing of cholecystokinin mRNA in the basolateral amygdala has anxiolytic and antidepressant effects in mice”	
Del Boca C, Le Merrer J, Lutz PE, Koebel P, Kieffer BL. In preparation.	
5. Conclusions and perspectives	95
IV. General discussion and perspectives	97
V. ANNEX	103
“Contribution to other projects in the laboratory. The lithium-CPA paradigm”	
A. Introduction	104
<i>Experimental contribution</i>	104

B. Manuscript 2:	106
“RSK2 signaling in brain habenula mediates place learning”	
Darcq E, Koevel P, Del Boca C, Pannetier S, Kirstetter AS, Garnier JM, Hanauer A, Befort K and Kieffer BL. Submitted.	
C. Manuscript 3:	125
“Deletion of the delta-opioid receptor gene impairs place conditioning but preserves morphine reinforcement”	
Le Merrer J, Plaza-Zabala A, Del Boca C, Matifas A, Maldonado R and Kieffer BL. Biol Psychiatry. 2011	
VI. References	130
VII. Résumé en Français	145

ABBREVIATIONS

5-HT Serotonin	EPM elevated plus-maze test
AAV Adeno-Associated Virus	GABA γ -aminobutyric acid
Am Amygdala	GP Globus Pallidus
BLA Basolateral Amygdala	GPCR G-protein coupled receptor
BNST Bed nucleus of the stria terminalis	Hipp Hippocampus
CCK Cholecystokinin	Hyp Hypothalamus
CCK₁ Cholecystokinin receptor type 1	ISH <i>In situ</i> hybridization
CCK₂ Cholecystokinin receptor type 2	KO knock-out mice
CCK-4 Cholecystokinin tetrapeptide	MOR (μ -) mu-opioid receptor
CCK-8s Cholecystokinin sulfated octapeptide	NAcc Nucleus Accumbens
CCK-IR Cholecystokinin immunoreactivity	OFC Orbitofrontal Cortex
CeA Central Amygdala	PC prohormone convertase
Cg Ctx Cingulate Cortex	PFC Prefrontal Cortex
CNS Central Nervous System	QAR Autoradiographic film quantification
CPA conditional place aversion test	Rph Raphe nuclei
CPP conditional place preference test	shRNA short-hairpin RNA
CPu Caudate-Putamen	SN Substantia Nigra
CRF Corticotropine-releasing factor	Th Thalamus
DA Dopamine	VP Ventral Pallidum
DG Dental Gyrus	VTA Ventral Tegmental Area
DOR (δ -) delta-opioid receptor	WT wild-type mice
	K- kappa-opioid receptor

I. GENERAL INTRODUCTION

A. Drug dependence

1. Definition and theories

Drug addiction is a process that manifests itself in compulsive drug-seeking and drug-taking behaviors with loss of control in limiting intake, and persistence even despite of negative health and social consequences. According to the DSM IV (*Diagnostic and Statistical Manual of Mental Disorder of the American Psychiatric Association* – 5th edition, 2000), addiction is a chronic relapsing brain disorder, defined by the manifestation of at least three of the following seven significant impairments or distresses, occurring during a period of 12 months:

1. Excessive drug-taking and difficulties to control substance abuse;
2. Compulsive and persistent desire to consume the substance;
3. Tolerance to the hedonic effect of the substance characterized by the diminished effect of the same amount of drug and the need of increased amount to achieve the desired effect;
4. Appearance of withdrawal symptoms and a negative emotional states (e.g., dysphoria, anxiety, irritability) when the access to the drug is prevented;
5. Great deal of time spent to obtain the substance;
6. Give up of other recreational and/or social activities;
7. Continued substance use despite knowledge and sufferance of negative consequences.

These key features distinguish drug use from drug abuse and the transition from the occasional and controlled drug-taking to an addictive behavior. Such drug use disorder may begin with initial drug use in vulnerable individuals or individuals at particularly vulnerable developmental periods (e.g., adolescence) and is often accompanied by deficits in the capacity to efficiently process and control reward-related information. Therefore, an emerging deficit in behavioral flexibility and impulse control may represent a crucial component in the development of an addiction (Winstanley et al 2010). Impulsivity is behaviorally defined as a predisposition toward rapid and unplanned reactions to internal and external stimuli without regarding the negative consequences of such reactions (Moeller et al 2001). Compulsivity, on the other hand, is related with the perseveration in responding or persistent reinitiation of habitual acts, in the face of adverse consequences,

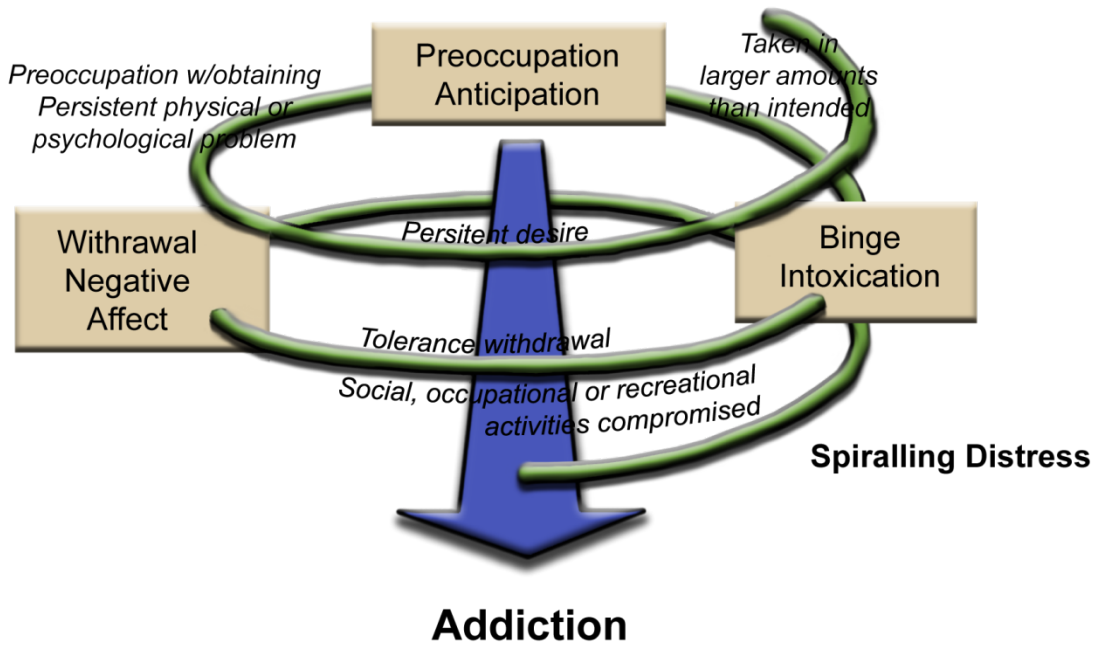


Figure 1: Spiraling addiction cycle. Schematic representation of the major psychological components of the addictive disorder. In this view the addiction is conceptualized as a cycle comprised by 3 stages that interact with each other, increasing their intensity and repetition during chronic drug consumption, and ultimately leading to addiction. Such stages are: preoccupation/anticipation, binge/intoxication, withdrawal/negative affect. (Adapted from Koob and Le Moal, 1997).

Stage of addiction cycle	Animal models	Reference
Binge/Intoxication	Drug-alcohol self-administration	Collins <i>et al</i> , 1984
	Conditioned place preference	Sachis-Segura and Spanagel, 2006
	Brain stimulation reward thresholds	Kometsky and Bain, 1990
Withdrawal Negative affect		Samyai <i>et al</i> , 1995
	Anxiety like responses	Schulteis <i>et al</i> , 1998 Baldwin <i>et al</i> , 1991
	Conditioned place aversion	Tzschentkc, 1998
	Elevated reward thresholds	Markou <i>et al</i> , 1998
		Amhed and Koob, 1998
		Ahmed <i>et al</i> , 2000 Roberts <i>et al</i> , 2000 Kitamura <i>et al</i> , 2006 O' Dell and Koob, 2007; Tomatzky and Miczek, 2000; Amhed and Koob, 1998; Deroche-Gamoner <i>et al</i> , 2004; Vandershur and Everitt, 2004
Preoccupation/Anticipation	Drug-induced reinstated	Sachis-Segura and Spanahel, 2006
	Cue-induced reinstatement	Sachis-Segura and Spanahel, 2006
	Stress-induced reinstatement	Sachis-Segura and Spanahel, 2006

Table 1: Summary of animal laboratory models used for the study of the different stages of the addiction cycle. (From Koob and Volkow, 2010).

or incorrect responses in choice situations (Everitt & Robbins 2005). Accordingly, impulsive disorders could facilitate initial drug consumption guided by the positive reinforcement effects of the substance; and compulsive disorders may be involved in maintaining the consumption when addiction is established. In this step, drug-taking behavior is motivated by an emerging negative reinforcement occurring when stopping drug use (Koob & Volkow 2010). Thus, the transition from drug use to drug abuse may involve a shift from impulsivity to compulsivity and the occurrence of these disorders in collapsed cycles would lead to the development of a spiraling behavior as proposed by Koob and Le Moal (1997). The spiraling addiction cycle is composed of three stages: *i*) binge/intoxication, *ii*) withdrawal/negative affect, and *iii*) preoccupation/anticipation as depicted in [Figure 1](#). Each of these stages has been evaluated by different paradigms developed in animal models as summarized in [Table 1](#). Such models constitute important tools to understand the neuropharmacological action of drugs of abuse and, therefore, the neurobiology of drug dependence.

Several neurobiological theories have been proposed to explain the shift from casual to compulsive drug use. Although early theories were focus only on pleasurable effects of drugs of abuse, it is currently known that this simplify view does not cover the complexity of this disorder (Felteinstein & See 2008). More recent theories have been proposed including positive and negative aspects of drug abuse (Robinson & Berridge 2008; Le Moal & Koob 2007). Following, a brief description of three of these theories is developed since they present the fundamentals of our understanding of addiction processing:

- *Opponent process theory*

Solomon and Corbit (1974) postulated that chronic exposure to a drug of abuse results in a pathological shift of the drug user's hedonic set point to a lower level. The concept is based on a mechanism of opponent processes where the drug is first consumed because of its rewarding properties and then consumption is maintained to avoid withdrawal symptoms. Briefly, there is an initial positive affective or hedonic response to drug intake involving an activation of the brain reward system (process a). This process induces an opposite negative effect that takes place in order to reestablish hedonic homeostasis and may occur by a "switch off" of the rewarding system and the recruitment of stress systems (process b). Chronic drug consumption leads, therefore, to the modification of the hedonic state equilibrium and the establishment of a new allostatic state (Koob et al 2004).

- *Aberrant learning theory*

Everitt and Robbins (2005) proposed that the transition to compulsive consumption would be the result of the ability of drugs of abuse to produce an aberrant learning. According with this theory, initially, the individuals consume drugs because of their reinforcing and hedonic properties; therefore, they have declarative conscious expectations about its reward, and they can perform a cost-benefit analysis. Next, with the chronic drug use, this cognitively and explicitly controlled behavior will switch to an automatic and implicit behavior by the formation of stimulus-response associations. Thus, drug consumption will progressively become habitual and ultimately compulsive.

- *Incentive sensitization theory*

Robinson and Berridge (2008) suggested a dissociation between the hedonic effect of the drug, termed “liking”, and the motivation to seek and take the drug, termed “wanting”. In this theory, the development of addiction is accompanied by a hypersensitivity to this second motivational value of the drug. Chronic drug use results, therefore, in vulnerable individuals to become hypersensitive to the drug and drug-associated cues while the rewarding effects of the substance become lower compared to the first administration.

Altogether, the presented theories, involving both positive and negative reinforcements processing of drug addiction, summarize diverse but complementary aspects of this disorder, given the multilayered complexity of addictive states and their prevalence.

2. Relation of addiction with emotional disorders

The addictive process is closely linked to other mental disorders and patients suffering of psychiatric illness (e.g., bipolar disorder, schizophrenia) are often more vulnerable to drug addiction according to the reports of the National Institute of Mental Health (<http://www.nimh.nih.gov/index.shtml>). Such records also suggest that depression plays a major role in substance abuse since many people try to escape from this negative state by using psychoactive substances. Moreover, evidence from epidemiological and clinical studies has consistently shown a strong association between affective and substance use disorders (SUDs). Individuals with affective psychopathology, including mood and anxiety disorders, demonstrate high rates of comorbidity with SUDs (Cheetham

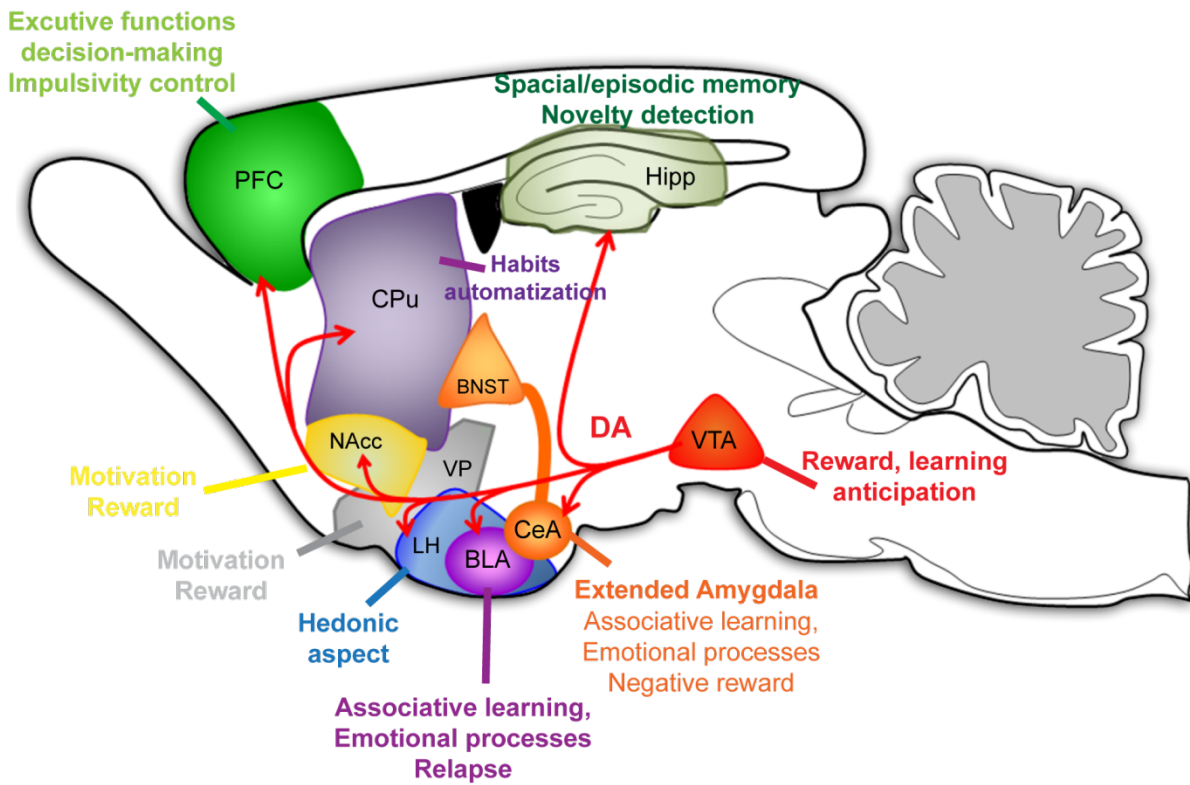


Figure 2: Major mesocorticolimbic dopaminergic pathway. Schematic representation of a rodent sagittal brain section depicting the mesocorticolimbic system consisting in dopamine neurons located in the ventral tegmental area (VTA) and projecting to: prefrontal cortex (PFC), hippocampus (Hipp), caudate-putamen (CPu), nucleus accumbens (NAcc), ventral pallidum (VP), lateral hypothalamus (LH), basolateral nucleus of the amygdala (BLA), and extended amygdala (BNST, bed nucleus of the stria terminalis; CeA, central nucleus of the amygdala). The system is activated by natural rewards and drugs of abuse, main roles of the different brain structures on the addictive disorder are noted in the picture.

et al 2010). In the same direction, there is a large and growing body of clinical and preclinical evidence suggesting an important and complex relationship between stress, anxiety and alcohol use disorders (Silberman et al 2009).

Furthermore, emotional disorders have not only a causal relationship with addictions. Drug abuse, in turn, affects cognitive and emotional processes leading to overvaluation of drug reinforcers, and deficits in inhibitory controls for drug consumption (Goldstein & Volkow 2002). Indeed, clinical studies have documented that exposure to life stressors is correlated with compulsive drug abuse and relapse to drug taking after even long periods of abstinence, influencing treatment prognosis in addicts (Lu et al 2003).

These complex relationships between drug dependence and emotional disorders might be due to common underlying neurobiological processes, involving overlapped neuronal substrates and molecular mechanisms. The following describes some of the key central circuits and molecular components implicated.

B. Neuronal circuits underlying drug dependence and emotional disorders

1. Addiction and brain circuits

Addictive substances were reported to display a wide variety of behavioral and pharmacological effects. Nevertheless, they all share the common ability to produce both feelings of pleasure and relieve of negative emotional states. The same effects are produced by naturally satisfying behaviors. Therefore, researchers have postulated that drugs of abuse may affect a specific brain circuit normally involved in the regulation of fundamental processes to initiate and maintain behaviors important for survival (e.g., eating, sexual activity). This circuit has been called the “natural reward system”, and it is widely accepted that chronic drug use produces dysregulation of specific neurochemical mechanisms leading to neuroadaptations in the brain substrates involved in this circuit. These modifications, therefore, may provide the motivational state that drives addiction. Here I will briefly introduce two main systems contributing to this circuit and to different aspects of the development and maintenance of drug dependence: The mesocorticolimbic dopamine system and the extended amygdala circuit.

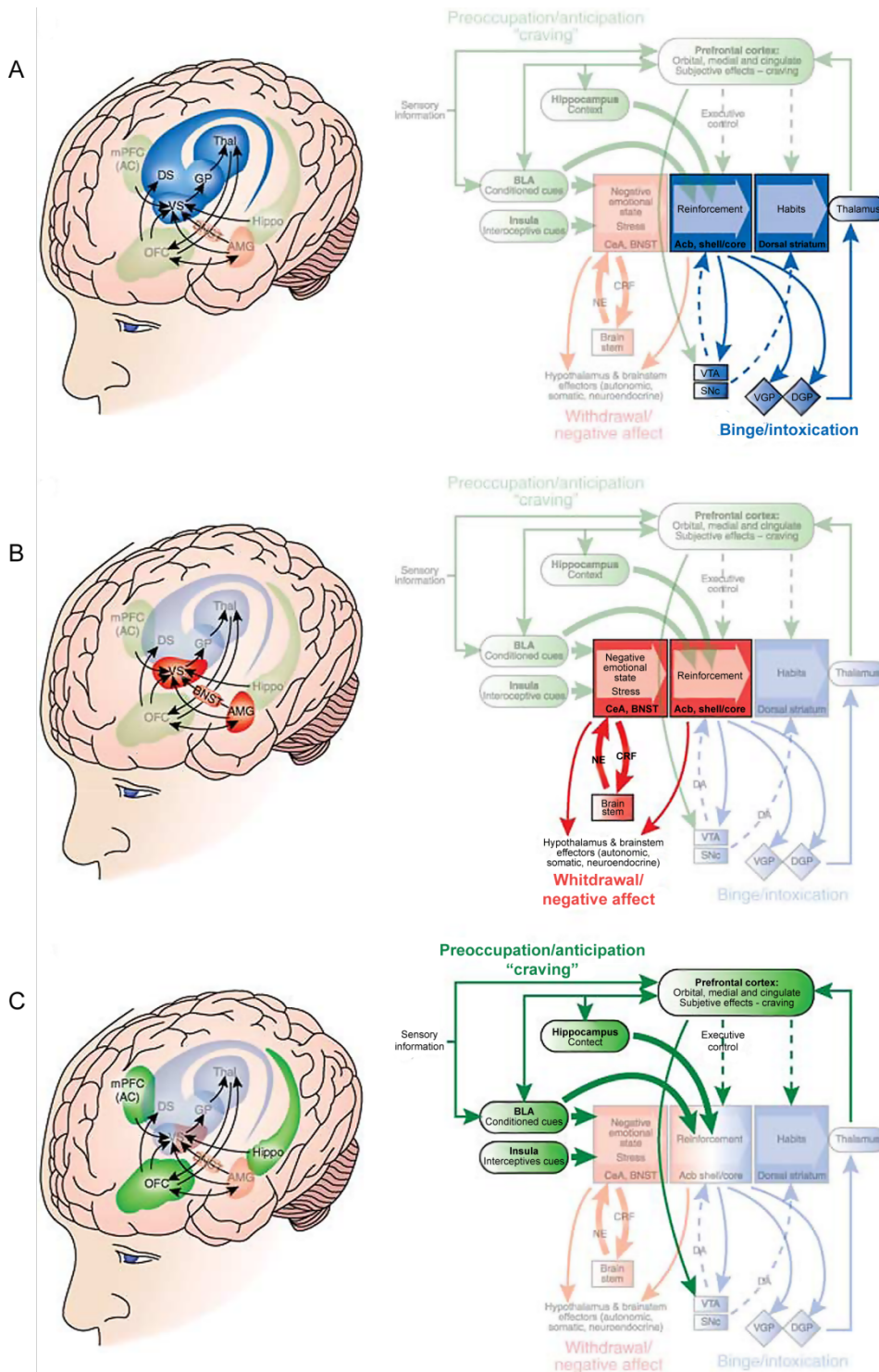


Figure 3: Neural circuitry associated with the three stages of the addiction cycle. (A) *Binge/intoxication* stage in blue, reinforcing effects of drugs engage associative mechanisms in the nucleus accumbens and stimulus-response habits in the dorsal striatum. (B) *Withdrawal/negative affect* stage in red, the negative emotional state of withdrawal engages principally the extended amygdala, involving not only dopaminergic transmission but also corticotropin-releasing factor, norepinephrine, and dynorphin. (C) *Preoccupation/anticipation (craving)* stage in green, this stage involves the processing of conditioned reinforcement in the BLA and the processing of contextual information by the hippocampus, while the executive control depends on the prefrontal cortex. **References:** green/blue arrows, glutamatergic projections; red arrows, dopaminergic projections; pink arrows, GABAergic projections; **Abbreviations:** Ach, nucleus accumbens; BLA, basolateral amygdala; VTA, ventral tegmental area; SNc, substantia nigra pars compacta; VGP, ventral globus pallidus; DGP, dorsal globus pallidus; BNST, bed nucleus of the stria terminalis; CeA, central nucleus of the amygdala; NE, norepinephrine; CRF, corticotropin-releasing factor; PIT, Pavlovian instrumental transfer. (From Koob and Volkow, 2010).

a) *The mesocorticolimbic dopamine system*

This circuit, depicted in [Figure 2](#), consists of dopamine (DA) projections from cell bodies in the ventral tegmental area (VTA) to limbic structures [that is, mesolimbic pathway, including the amygdala (AM), ventral pallidum (VP), hippocampus, and nucleus accumbens (NAcc)] and cortical areas [that is, mesocortical pathway, including the prefrontal cortex (PFC), the orbitofrontal cortex (OFC) and the anterior cingulate (antCg Ctx)] (Feltenstein & See 2008). A large number of studies using intracranial self-administration and intracranial place conditioning (See [Table 1](#)) have implicated this system in the rewarding properties of drugs of abuse (Koob & Volkow 2010). Especially, projections from the VTA to the NAcc were postulated as the main pathway of convergence for addictive behaviors (Nestler 2005); and is of general agreement that the initial reinforcing effects of most drugs of abuse rely on the induction of large and rapid increases in DA levels within the accumbens.

The behavioral functions of mesolimbic DA have been largely investigated and this neurotransmitter has been postulated to play important roles in cognition and motivation. For instance, in the NAcc, DA participates in many functions that are important for instrumental behavior. Thus, in cooperation with learning mechanisms having place in other structures (e.g., hippocampus, amygdala), the reward system underlies behavioral contingencies that act to strengthen the addictive behavior. More specifically, a positive reinforcement procedure links the pleasant sensations with the drug of abuse, leading the individual to search for this associated stimulus (Salamone et al 2007).

As mentioned before, the establishment of an addiction occurs when recreational drug consumption evolves toward uncontrolled drug use, and such transition involves neuroplasticity of the structures forming this mesocorticolimbic dopamine system. Koob and Volkow (2010) explain these neuroadaptations by relating the different brain structures involved in this circuitry with the different stages of the spiraling addiction cycle, as summarized in [Figure 3](#). Briefly, in the *binge/intoxication stage* (A), the NAcc receives massive inputs from several structures such as the AM, PFC and HIP, and modulates the motivational properties of drug-taking; recruiting the dorsal striatum during the development of habit learning; then, for the *withdrawal/negative affect stage* (B) the main neuroanatomical substrate is the Extended Amygdala with the recruitment of stress systems (see below); and finally, the *preoccupation/anticipation stage* (C), also known as “craving”, is composed by the PFC, the basolateral nucleus of the amygdala (BLA) and the

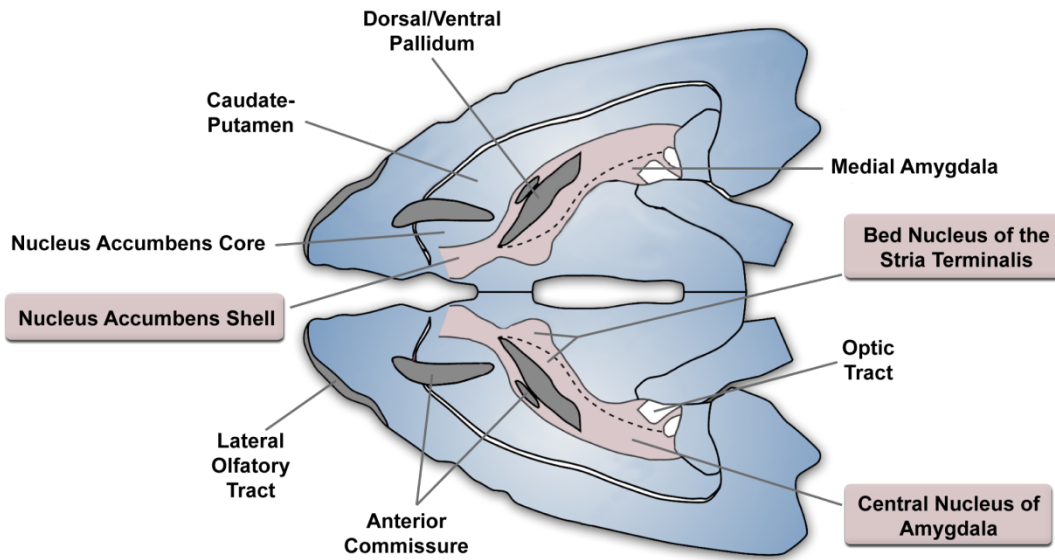


Figure 4: The extended amygdala. Schematic representation of a rodent brain horizontal section depicting the principal structures of the extended amygdala, an anatomical entity that acts as an interface between reward and stress systems involved in the negative emotional states induced by drugs of abuse. (Adapted from Koob, 2008).

Hipp, and constitutes a fundamental element of drug addiction leading drug abusers to relapse.

b) The extended amygdala

During the study of the opponent processes associated with drug dependence, functional observations provided support for the hypothesis of a new neuroanatomical circuitry that forms a separate entity within the basal forebrain. Such circuit was named the “extended amygdala” and is composed of several basal forebrain structures including the bed nucleus of the stria terminalis (BNST), the central medial amygdala, and a transition zone in the posterior part of the medial nucleus accumbens (i.e., posterior shell) (Figure 4) (Koob 2008).

This complex neuronal circuit is divided into medial and central components. On one side, the medial subdivision was associated with neuroendocrine regulation, integrating hormonal and chemosensory signals that regulate social behaviors in a wide variety of mammals (Newman 1999). On the other side, the central subdivision was related with reward processes in the context of drug addiction (Waraczynski 2006).

The concept of “central extended amygdala” stems from developmental studies showing a common origin of BNST and CeA in the fetal brain. This unique structure is later divided into rostral (BNST) and caudal components that will, therefore, share a cellular and histochemical organization. In addition to these structural similarities, both regions also share similar inputs, including afferents from limbic cortices, hippocampus, BLA, and lateral hypothalamus; and efferent connections from the ventral pallidum, VTA and lateral hypothalamus (Fudge & Emiliano 2003). Moreover, a wide range of neurochemical systems are present in the central EA, including those associated with reinforcing effects of drugs of abuse (dopamine and opioid peptides) as well as components of the hypothalamic-pituitary-adrenal (HPA) axis and brain stress systems (GABA, corticotropin-releasing factor (CRF), noradrenaline, galanin and neuropeptide Y) (Edwards & Koob 2010; Koob & Le Moal 2005). Therefore, the central EA may represent a common neuroanatomical substrate integrating stress and hedonic processing systems to produce the emotional state that support negative reinforcement properties of drugs of abuse (Koob & Volkow 2010).

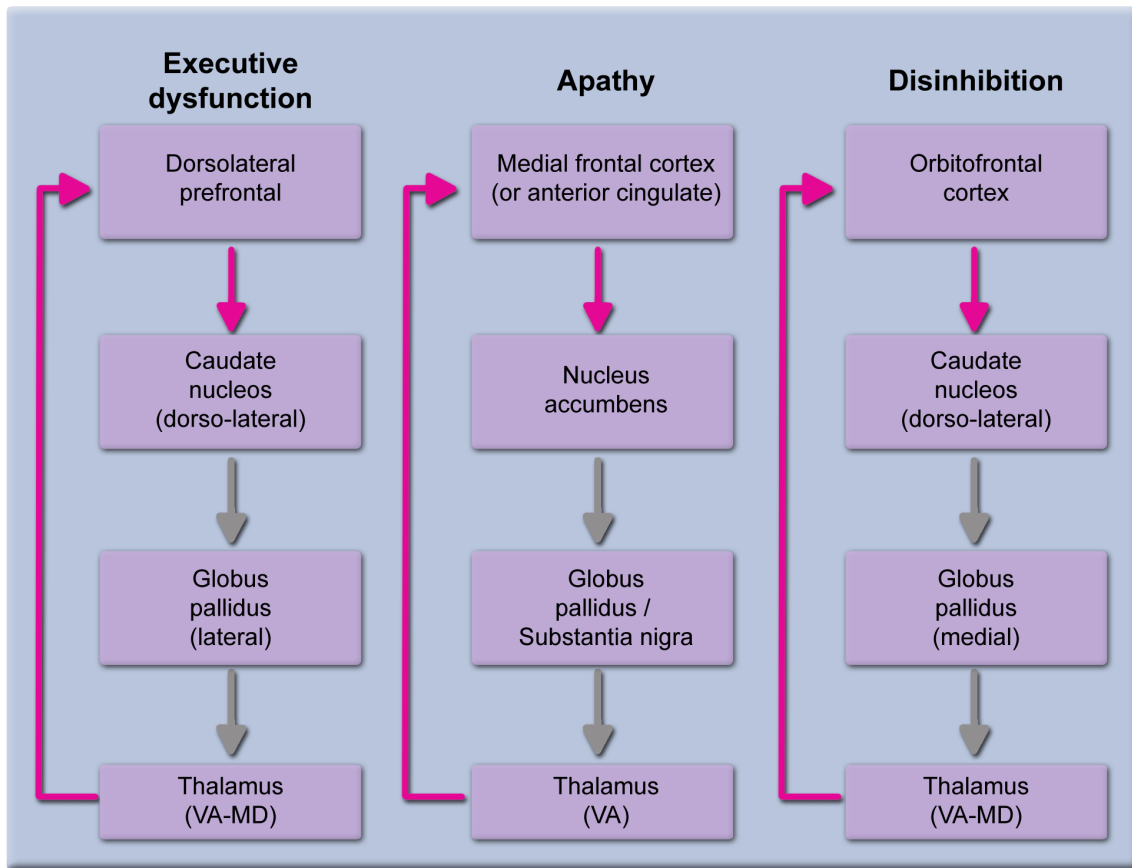


Figure 5: Major fronto-subcortical circuits involved in motivational behavior. Diagram of the three behaviorally relevant pathways connecting the prefrontal cortex with limbic structures and mediating executive functions (dorsolateral prefrontal circuit), motivational behavior (medial frontal cortex circuit), and integration of emotional information into behavioral responses (orbitofrontal circuit). Pink arrows represent glutamatergic projections and grey arrows represent GABAergic projections. Pathophysiology of loops dysfunction are indicated on the top. (Adapted from Bonelli and Cummings, 2007). **Abbreviations:** VA: Ventral Anterior. MD: Media Dorsal

2. The emotional brain circuits

Regarding the relationship between addictive disorders and other mental illnesses, Goodman (2008) has postulated that the addictive process involves not only aberrations in the natural rewarding circuitry but also in other two functional systems: A system involved in affect regulation, which comprises the neurobiological process responsible for maintaining emotional states within normal ranges of intensity and stability, preventing distress, and a system involved in behavioral inhibition and decision-making, whose impairment leads to impulsive and compulsive disorders. Therefore, among the complex neural circuits involved in emotional processing, I will present two main components contributing to such systems: The frontal-subcortical circuit and the amygdalar circuit, with special attention in the latter one, which is essential in emotional regulation and whose imbalance has been shown to be responsible of producing anxiety and depressive disorders.

a) *Frontal-subcortical circuits*

This fronto-limbic system forms the principal mediating network of motor activity and behavior, allowing the organism to interact with the environment. It was described by Alexander et al (1990) who proposed that the basal ganglia and thalamus participate in five parallel segregated circuits with selected cortical areas in the frontal lobe. The basal ganglia is a collection of nuclei located at both sides of the thalamus, and comprised by the corpus striatum (including caudate-putamen nucleus and globus pallidus), and the nucleus accumbens (Boeree, 2006). Among the five major circuits involved in this system, two of them are originated in motor areas (the *motor circuit* and the *oculomotor circuit*) and the other three consist in the most behaviorally relevant pathways of the system which originates in the prefrontal cortex: the *dorsolateral prefrontal circuit*, which mediates executive functions (i.e., organization of information to facilitate a response); the medial frontal cortex or *anterior cingulate circuit*, which is involved in motivational behavior; and the *orbitofrontal circuit* that mediate the integration of emotional information into behavioral responses (Bonelli & Cummings 2007).

As represented in [figure 5](#), the three circuits share the same central anatomical structures. They originate in prefrontal cortex (PFC), project to the striatum (caudate-putamen or ventral striatum), connect to the globus pallidus and substantia nigra and from there to the thalamus. In addition, there are feedback projections to the frontal cortex

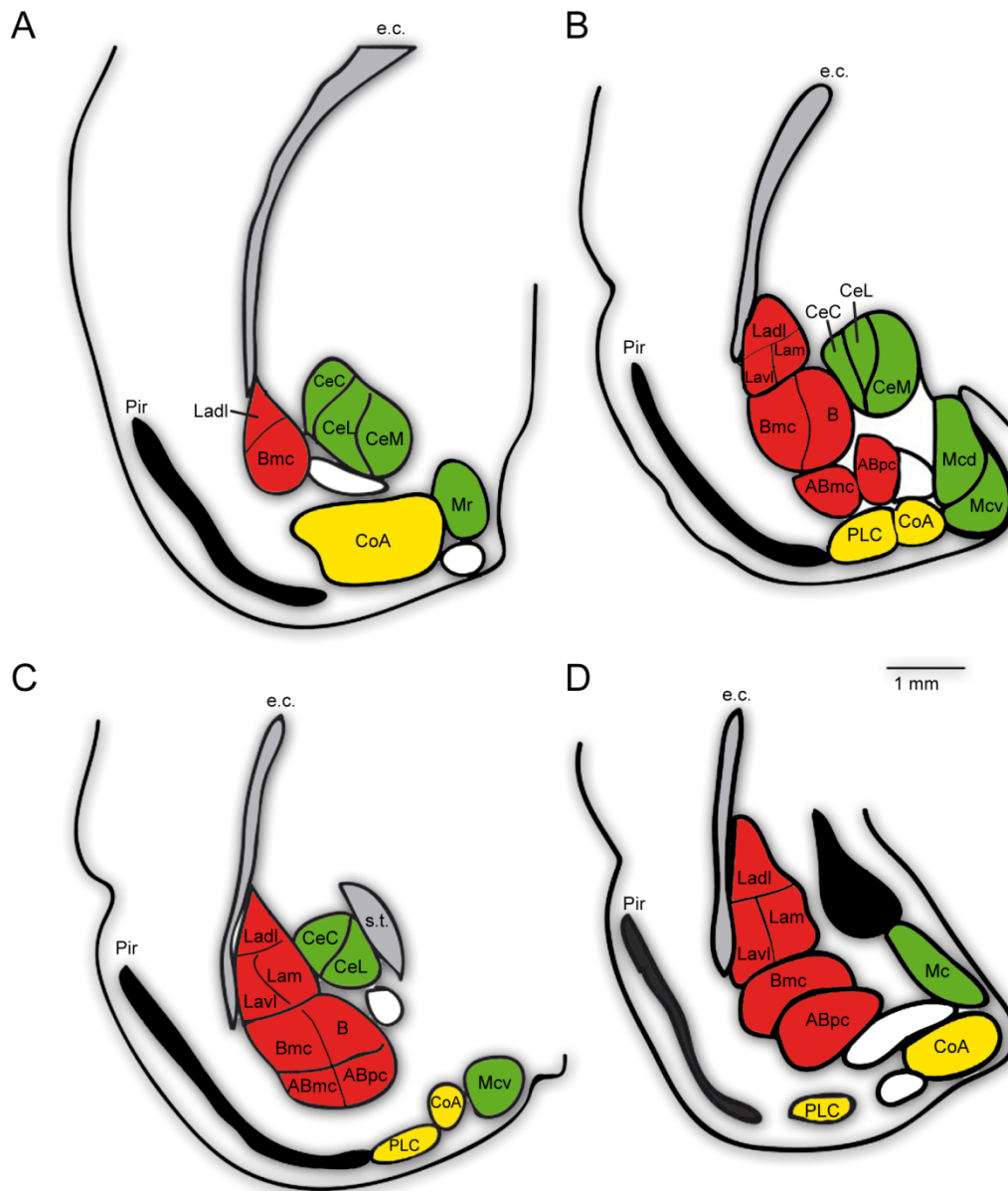


Figure 6: The amygdaloid complex. Schematic representation of a rat brain coronal sections depicting, from rostral (A) to caudal (D) the amygdaloid nuclei divided into three main groups: the basolateral group in red, the centromedial group in green, and the cortical group in yellow. **Abbreviations:** Pir, piriform cortex; e.c., external capsule; s.t., stria terminalis; Ladl, lateral amygdala medial subdivision; Lavl, lateral amygdala ventrolateral subdivision; Lam, lateral amygdala medial subdivision; Bmc, basal magnocellular subdivision; B, basal subdivision; ABmc, accessory basal magnocellular subdivision; ABpc, accessory basal parvicellular subdivision; CeC, central capsular subdivision; CeM, central medial subdivision; CeL, central lateral subdivision; Mcd, medial dorsal subdivision; Mr, medial rostral subdivision; Mcv, medial ventral subdivision; CoA, cortical anterior subdivision; PLC, posterolateral cortical subdivision. (Adapted from Sah et al, 2003).

forming a loop, as well as connections between other cortical and subcortical structures comprising “open loop” associations. From a neurochemical point of view, the substrates of these pathways are mainly glutamatergic (from PFC to the striatum and from thalamus to the PFC) and GABAergic (from the striatum to the globus pallidus and SN, and from there to the thalamus); while dopaminergic and serotonergic systems may provide the main modulatory systems over these pathways (Tekin & Cummings 2002).

A large amount of evidence from both experimental and clinical studies has involved these circuits with a several mental disorders:

- The dorsolateral prefrontal system is related with executive function, including roles in anticipation, goal selection, planning, monitoring, and use of feedback in task performance. Thus, its impairment leads to attentional deficits, difficulties in hypotheses generation, reduced verbal and design fluency, and impairment of memory search and of organizational and constructional strategies on learning. Symptoms that were found manifested also in psychiatric syndromes including schizophrenia, depression, and obsessive-compulsive disorder (Biederman & Faraone 2005).
- The anterior cingulate circuit impairment is closely related with a state of profound apathy, with indifference to pain, thirst, or hunger, and absence of motor or psychic initiative. A syndrome commonly observed in Alzheimer’s disease, where is associated with anterior cingulate hypoperfusion (Ishii et al 2009).
- The orbitofrontal cortex circuit is involved in the determination of the appropriate time, place, and strategy for environmentally elicited behavioral responses. Lesions in this area results in behavioral disinhibition and a prominent emotional lability as well as in the occurrence of impulsive disorders (Chow 2000).

b) Amygdalar circuitry

The amygdala or “amygdaloid complex” is a highly differentiated region near the temporal pole of the mammalian cerebral hemisphere, which has been proposed as a key component of the neural circuitry underlying emotions (LeDoux 2000). This complex is a structurally and functionally heterogeneous region consisting in approximately 13 nuclei distinguished by their cytoarchitecture and histochemistry. Each of these nuclei is further divided into several subregions and they are classified into three main groups depicted in [Figure 6](#) (Sah et al 2003): *i*) the deep basolateral subsystem, including lateral, basal, and

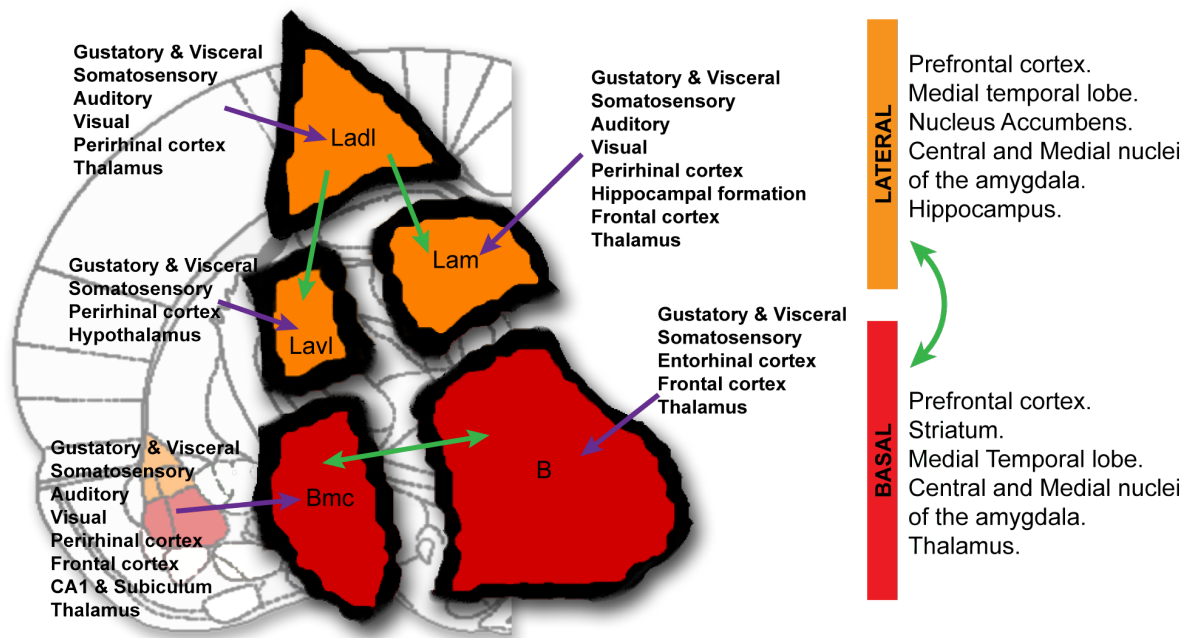


Figure 7: Summary of the major connections of the BLA circuit. Diagram of the different subnucleus that forms the basolateral amygdaloid complex. Depicted main inputs (violet arrows), outputs (in the right, LATERAL and BASAL), and internal connections (green arrows). **Abbreviations:** Ladl, lateral amygdala medial subdivision; Lavi, lateral amygdala ventrolateral subdivision; Lam, lateral medial subdivision; BMC, basal magnocellular subdivision; B, basal subdivision.

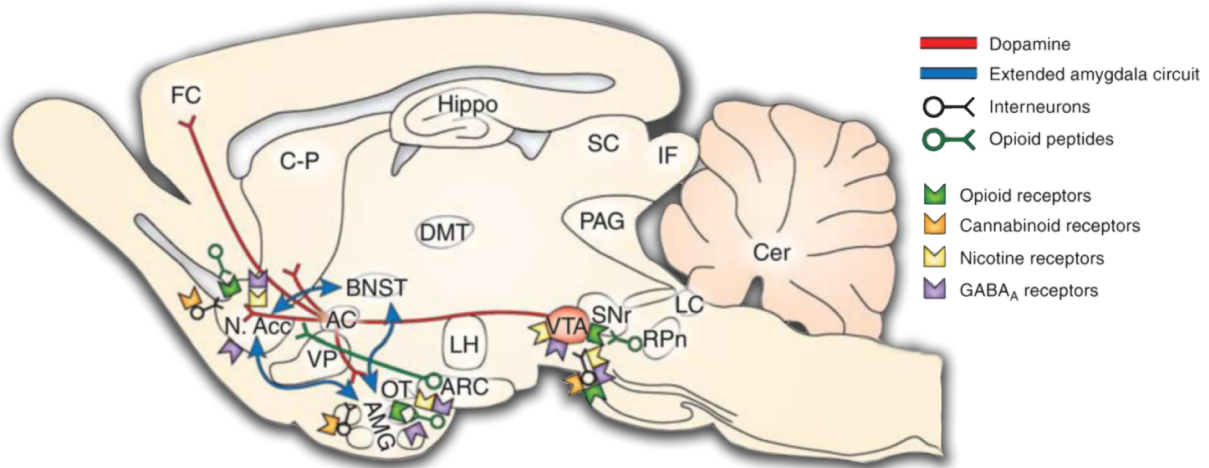


Figure 8: Principal pathways and receptor systems involved in the mediation of drug of abuse effects. Schematic representation of a rodent brain sagittal section depicting the main dopaminergic projections from the VTA to limbic and cortical structures and the receptor systems implicated in the acute reinforcing actions of drugs of abuse. **Abbreviations:** AC, anterior commissure; AMG, amygdala; ARC, arcuate nucleus; BNST, bed nucleus of the stria terminalis; Cer, cerebellum; C-P, caudate-putamen; DMT, dorsomedial thalamus; FC, frontal cortex; Hippo, hippocampus; IF, inferior colliculus; LC, locus coeruleus; LH, lateral hypothalamus; N. Acc., nucleus accumbens; OT, olfactory tract; PAG, periaqueductal gray; RPN, reticular pontine nucleus; SC, superior colliculus; SNr, substantia nigra pars reticulata; VP, ventral pallidum; VTA, ventral tegmental area. (From Koob and Volkow, 2010).

basomedial or accessory basal nuclei; *ii*) the superficial cortical-like subsystem, including cortical nuclei and nucleus of the lateral olfactory tract; and *iii*) the centromedial subsystem composed of the medial and central nuclei. Within these groups, I will focus on the BLA circuitry, a system that has been mostly studied in relation to its role in the acquisition, storage, and expression of fear memory as well as in the processing of pavlovian conditioned learning (LeDoux 2000).

➤ The basolateral nucleus of the amygdala (BLA)

The BLA corresponds to the region originally called “amygdala” by Burdach, who discovered this almond-shape mass of grey matter in the early 19th century. Fifty years later, Meynert proposed the BLA as a ventral temporal lobe extension of the clastrum (the deepest part of the insular cortex); hypothesis that was further confirmed based on embryological considerations and topographic relations (Swanson & Petrovich 1998). Therefore, neurons in the BLA share many features in common with cortical neurons. In this sense, two main types of neurons were described based on Golgi techniques and electrophysiological studies: spiny, pyramidal-like or projection neurons comprise ~70% of the BLA cell population; and local circuit interneurons, which resemble nonspiny stellate cells, complete the content. In terms of synaptic properties, pyramidal-like neurons form the glutamatergic output cells of the BLA while interneurons are GABAergic and can be further divided in different classes according with the presence of different calcium binding proteins (Sah et al 2003). In addition, other types of cells such as extended neurons, cone cells, chandelier cells, and neurogliaform cells have also been described with less important distribution over the structure (McDonald 1985).

Regarding amygdalar connections, the literature is vast and complex. From a practical point of view, inputs to the amygdala can be separated into those which supply information from sensory areas and memory systems, arising in cortical and thalamic structures, and those involved in behavior and autonomic systems, which arise in the hypothalamus or brain stem regions. Moreover, tract tracing studies have revealed that the amygdaloid complex presents extensive intra- and inter-nuclear connectivity. These studies indicate that sensory information enters the amygdala through the BLA, is processed locally and then follows a progression to the centromedial nuclei. Consequently, the CeA acts as an output station with substantial projections to the hypothalamus, the bed nucleus of the stria terminalis and several nuclei in the midbrain, pons and medulla. The role of the BLA

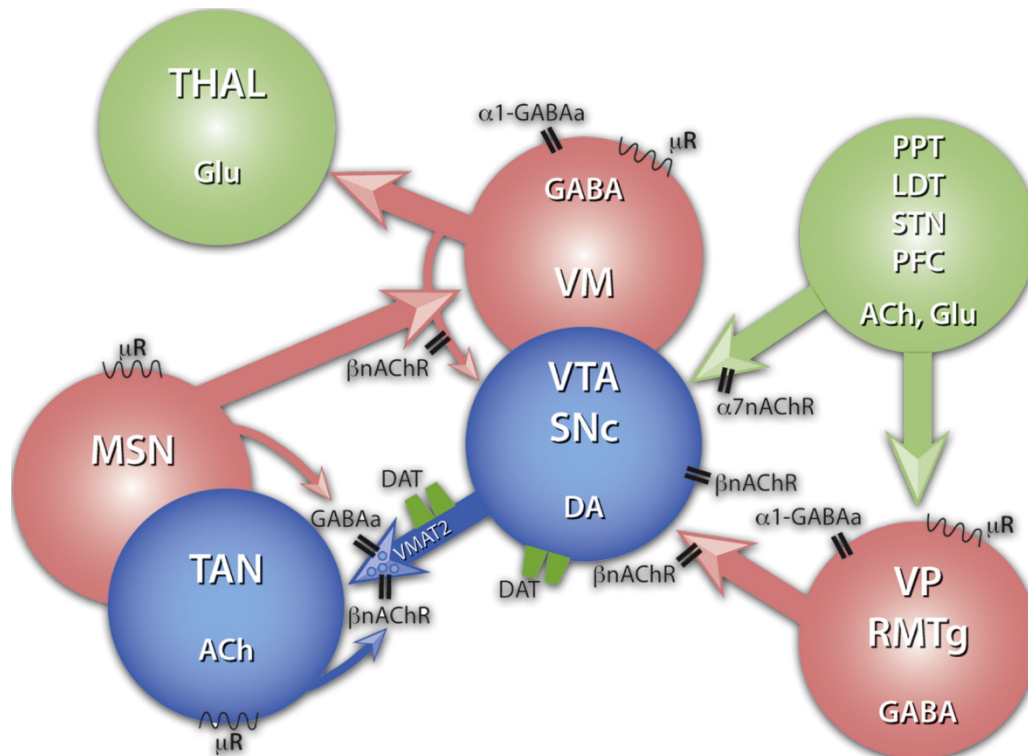


Figure 9: Network model of major molecular pathways regulating the dopaminergic system.

Neurons diagram depicting the main molecular targets that regulate extracellular dopamine (DA) release. Neurons that release conventional excitatory transmitters are in green, inhibitory transmitters in red and modulatory transmitters in blue. According with this model addictive drugs can: *i*) alter DA neuronal firing via excitation or disinhibition: For instance, nicotine excites DA neurons, directly through α -nicotinic acetylcholine receptors (α -nAChR) on glutamatergic presynaptic terminals of axons that innervate DA neurons, and disinhibit DA neurons by inhibiting GABAergic projection neurons that possess axon collaterals modulating DA neuron excitability (through β -nAChR); *ii*) selectively enhance DA transmission also by presynaptic effects: for instance, tonically active neurons that release ACh function to enhance the probability of DA release and nicotine levels reached during smoking are thought to desensitize the DA terminal presynaptic nAChR, resulting in decreased probability of transmitter release. A variety of other presynaptic receptors on DA terminals, including GABA_A receptors, probably produce analogous effects; *iii*) increases extracellular DA by inhibiting reuptake by the dopamine uptake transporter (DAT): Cocaine effect; *iv*) combine multiple cellular effects including effects on synaptic vesicles that possess the vesicular monoamine transporter (VMAT) that together enhance cytosolic DA levels and ultimately release the cytosolic DA via reverse transport across the DAT: Amphetamines effect. **Abbreviations:** THAL, thalamus; MSN, medium spiny neurons; TAN tonicallly active neurons; VM, ventral midbrain; VTA, ventral tegmental area; SNc, substantia nigra compacta; PPT; peduncular pontine tegmentum; LDT; laterodorsal tegmentum; STN, subthalamic nucleus; PFC, prefrontal cortex; VP, ventral pallidum; RMTg, rostralmedial tegmentum. (From Sulzer, 2011).

within this general circuit is depicted in [Figure 7](#). On the one hand, the BLA receives inputs from all sensory modalities (olfactory, somatosensory, gustatory and visceral, auditory, and visual) as well as polymodal information from the prefrontal cortex. On the other hand, major projections are directed to the medial temporal lobe (with afferents in to the hippocampus and perirhinal cortex), the prefrontal cortex, nucleus accumbens and thalamus as well as other substantial projections to hippocampus and striatum (Sah et al 2003).

Altogether, the BLA subsystem is anatomically well positioned for associative learning and emotional coding. Thus, BLA forms a site of convergence of sensory and memory information and an important locus of modulatory influence through efferent projections to other brain regions. In this sense, converging lines of evidence support the role of this region in memory consolidation and storage processes. BLA lesions have shown to disrupt both acquisition and expression of freezing associative responses in conditional fear paradigms (Gale et al 2004; Maren 1999). Moreover, BLA has been postulated to mediate the positive effects of acute stress on learning and memory, throughout a mechanism that enhance memory consolidation by inhibiting GABAergic transmission in this region (Roosendaal et al 2009). Further, the same mechanism of stress-induced impairment of GABA release also underlies the hyperexcitability of the amygdala that leads to stress-related affective disorders (Aroniadou-Anderjaska et al 2007). A recent study on this field, exploring the neural circuits underlying anxiety-disorders by using optogenetic technology, has implicated specific BLA-CeA projections in the control of anxiety-related behaviors (Tye et al 2011).

C. Neurotransmitter and Neuromodulator systems involved in addiction and emotional disorders

Drugs of abuse are able to exert influence over the brain reward pathway either by directly influencing the action of dopamine within the mesocorticolimbic dopamine system, or through a modulatory influence over this pathway by altering the activity of other neurotransmitters and neuromodulatory systems as summarized by Koob and Volkow (2010) ([Figure 8](#)). In this sense, GABAergic (γ -aminobutyric acid), opioidergic, serotonergic, cholinergic and noradrenergic pathways have been shown to interact at various points along this dopamine system and to modulate its activity. Sulzer (2011)

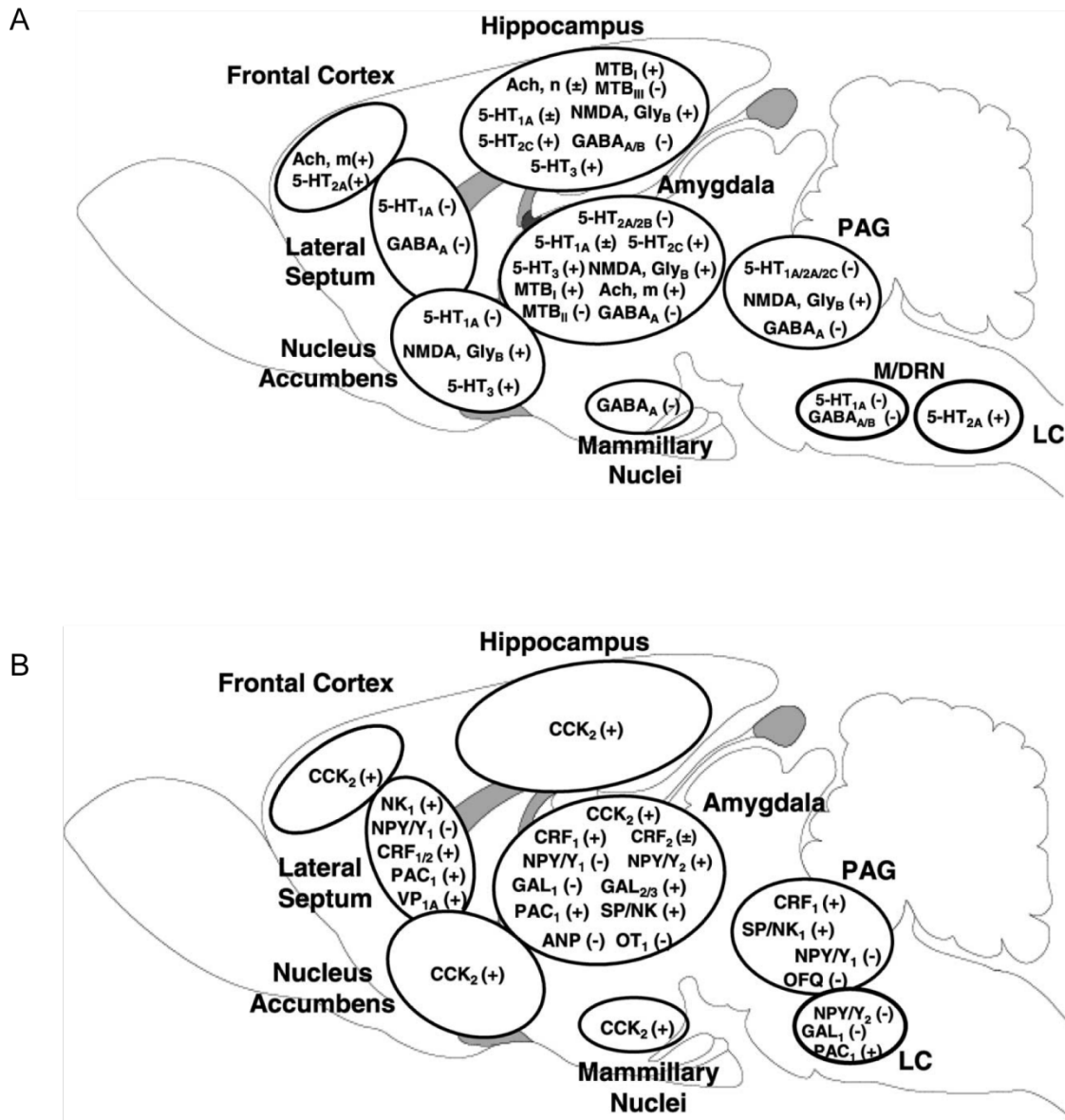


Figure 10: Major molecular components involved in emotional disorders. Schematic representation of a rodent brain sagittal section depicting: the sites of actions of (A) various neurotransmitters and their receptors and (B) various neuropeptides and their receptors in the modulation of anxious states. Anxiolytic actions are indicated by a “+” sign and anxiogenic actions are indicated by a “-” sign: “±” indicates that a broad and balanced mixture of anxiolytic and anxiogenic actions has been reported. **Abbreviations:** GABA, γ -amino-butyric acid; NMDA, *N*-methyl-d-aspartate; GLY_B, glycine_B; MTB, metabotropic glutamatergic; 5-HT, serotonin; Ach/n, acetylcholine/nicotinic; Ach/m, acetylcholine/muscarinic; CCK, cholecystokinin; SP/NK₁, substance P/neurokinin₁; CRF, corticotropin releasing factor; VP, vasopressin; OT, oxytocin; NPY, neuropeptide Y; PAC₁, receptor for pituitary adenyl cyclase activating peptide; GAL, galanin; OFQ, orphaninFQ; GLP1, glucagon-like peptide-1 and ANP, atrial natriuretic peptide. (From Millan, 2003).

summarized such control of dopaminergic system in the frame of drug dependence by a network model of major pathways as depicted in Figure 9. In this model, addictive drugs might in principle act by: *i)* enhancing neuronal firing in response to environmental cues (as do nicotine, opiates, and sedatives); *ii)* inhibiting DA reuptake (as does cocaine); *iii)* altering release probability from the presynaptic terminal (as do nicotine and opiates); and *iv)* releasing DA via reversal of dopamine uptake transporters (as do amphetamines).

Emotional disorders like anxiety, depression and attention deficit hyperactivity disorder (ADHD) have also been linked to chemical imbalance of a variety of specific neurotransmitters, including serotonin, norepinephrine, dopamine and GABA (Figure 10A). This chemical imbalance can be caused by either an excess of neurotransmitter activity, or more commonly, may results from the deficiency of neurotransmitter availability (Millan 2003). Moreover, the actions of numerous modulators have been implicated in the response to stress and in the control of emotional states (Figure 10B).

Altogether, a variety of multiple and convergent biologically neuroactive substances, including neurotransmitters and neuromodulators, are responsible of the development and expression of drug dependence as well as other mental disorders. While neurotransmitters can be subdivided into two major groups based on their chemical nature: biogenic amines and small amino-acids; neuromodulators cover a broad spectrum, ranging from amines to steroids (Figure 11); and among them, the largest subclass is composed by neuropeptides, which are generated from large precursor molecules as showed in Table 2.

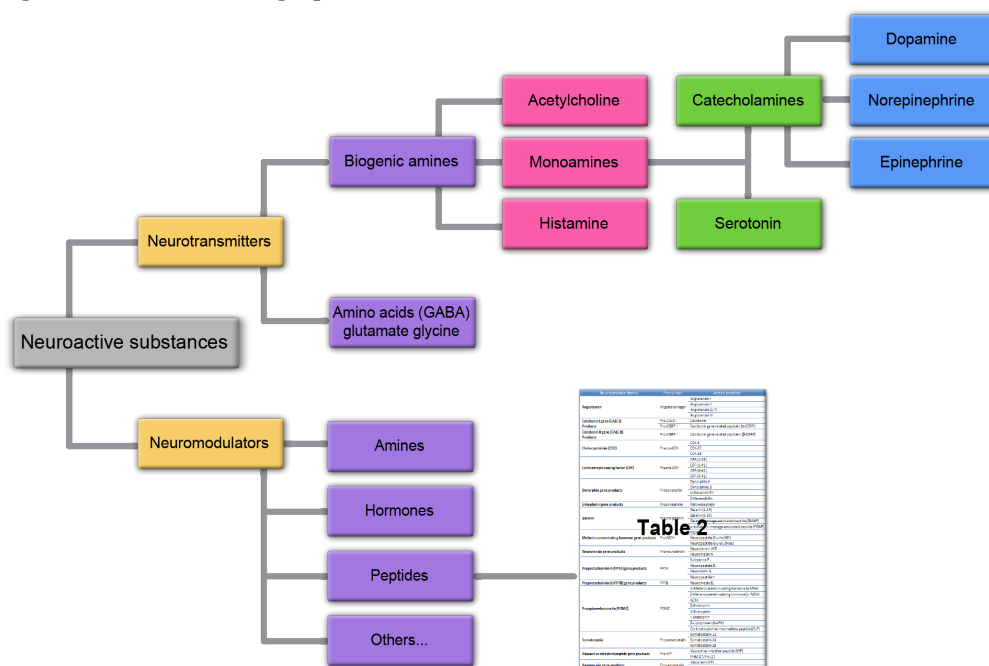


Figure 11: Neuroactive substances. Differentiation of neurotransmitters and neuromodulators based on their chemical structures. (Adapted from von Bohlen und Halbach and Dermietzel, 2006)

Neuropeptide family	Precursor	Active peptide
Angiotensin	Angiotensinogen	Angiotensin I
		Angiotensin II
		Angiotensin (1-7)
		Angiotensin IV
Calcitonin I gene (CALC I) Products	Pro-CALC I	Calcitonin
	Pro-CGRP I	Calcitonin gene related peptide I (α -CGRP)
Calcitonin II gene (CALC II) Products	Pro-CGRP I	Calcitonin gene related peptide II (β -CGRP)
Cholecystokinin (CCK)	Prepro-CCK	CCK-8
		CCK-33
		CCK-58
Corticotropin releasing factor (CRF)	Prepro-CRF	CRF-(1-39)
		CRF-(1-41)
		CRF-(4-41)
		CRF-(9-41)
Dynorphin gene products	Prodynorphin	Dynorphin A
		Dynorphine B
		α -Neoendorfin
		β -Neoendorfin
Enkephalin gene products	Proenkephalin	Met-enkephalin
Galanin	Prepro-galanin	Galanin(1-19)
		Galanin(5-29)
		Galanin message-associated peptide (GMAP)
		pre-Galanin message-associated peptide (PGMP)
Melanin-concentrating hormone gene products	Pro-MCH	MCH
		Neuropeptide Glu-Ile (NEI)
		Neuropeptide Gly-Glu (NGE)
Neurotensin gene products	Proneurotensin	Neurotensin (NT)
		Neuromedin N
Preprotachykinin A (PPTA) gene products	PPTA	Substance P
		Neuropeptide K
		Neurokinin A
		Neuropeptide γ
Preprotachykinin B (PPTB) gene products	PPTB	Neuromedin K
Proopiomelanocortin (POMC)	POMC	α -Melanocyte-stimulating hormone (α -MSH)
		β -Melanocyte-stimulating hormone (β -MSH)
		ACTH
		β -Endorphin
		α -Endorphin
		γ -Endorphin
		β -Lipoprotein (b-LPH)
Corticotropin-like intermediate peptide (CLIP)		
Somatostatin	Prosomatostatin	Somatostatin-12
		Somatostatin-14
		Somatostatin-28
Vasoactive intestinal peptide gene products	Pro-VIP	Vasoactive intestinal peptide (VIP)
		PHM-27/PHI-27
Vasopressin gene products	Provasopressin	Vasopressin(VP)
		Neurophysin II(NP II)

Table 2: Neuropeptides. Summary of neuropeptides present in the central nervous system (non-exhaustive). Highlighted in yellow, members of the CCKergic and opioidergic systems. (Adapted from von Bohlen und Halbach and Dermietzel, 2006)

Although they often reveal neurotransmitter-like characteristics, neuromodulator peptides can be distinguished from the classic neurotransmitters by several criteria (von Bohlen und Halbach & Dermietzel 2006):

- The amount of expression is generally lower than that of neurotransmitters.
- In contrast to neurotransmitters, neuropeptides are effective at low concentrations.
- Normally, they exert slow and long-lasting actions, mainly by affecting G protein-coupled receptors and subsequent second messenger systems.
- Neuropeptides rarely present specific rapid inactivation mechanisms (e.g., re-uptake mechanisms).
- Compared with neurotransmitters, the synthesis of neuropeptides requires complex metabolic pathways and usually occurs in the cell soma.

Among the several neuromodulators presented here, including substance P/neurokinin1, corticotropin releasing factor, vasopressin, oxytocin, neuropeptide Y, and galanin, between others; I will introduce below a short overview of the components, distribution and functions of the endogenous opioid system; a main neuromodulatory system of emotional behaviors largely distributed in both reward and stress systems. Afterward, the focus will be placed on the Cholecystokinin system, which presents a wide distribution in the CNS and a large range of physiological effects, including motivational and emotional processes.

An overview of the endogenous opioid system

The discovery of the opioid system stems from the use of opium in ancient history, when natural alkaloid opiates were extracted from Opium poppy seeds (*Papaver somniferum*) and used as powerful analgesics and for their euphoric properties.

The existence of opioid binding sites in the rat brain was established in 1973, and these receptors were later named as mu (μ) and kappa (κ), in function of their preferred ligand (morphine and ketocyclazocine, respectively), and delta (δ), for being identified in the mouse vas deferens (Lord et al 1977; Martin et al 1976). These three types of opioid receptors are G protein-coupled receptors (GPCRs) with a seven α -helice transmembrane topology, and they have been classified within the GPCR family 1 (or Class A), acting on intracellular adenylate cyclase modulation (Fredriksson et al 2003; Surratt & Adams 2005).

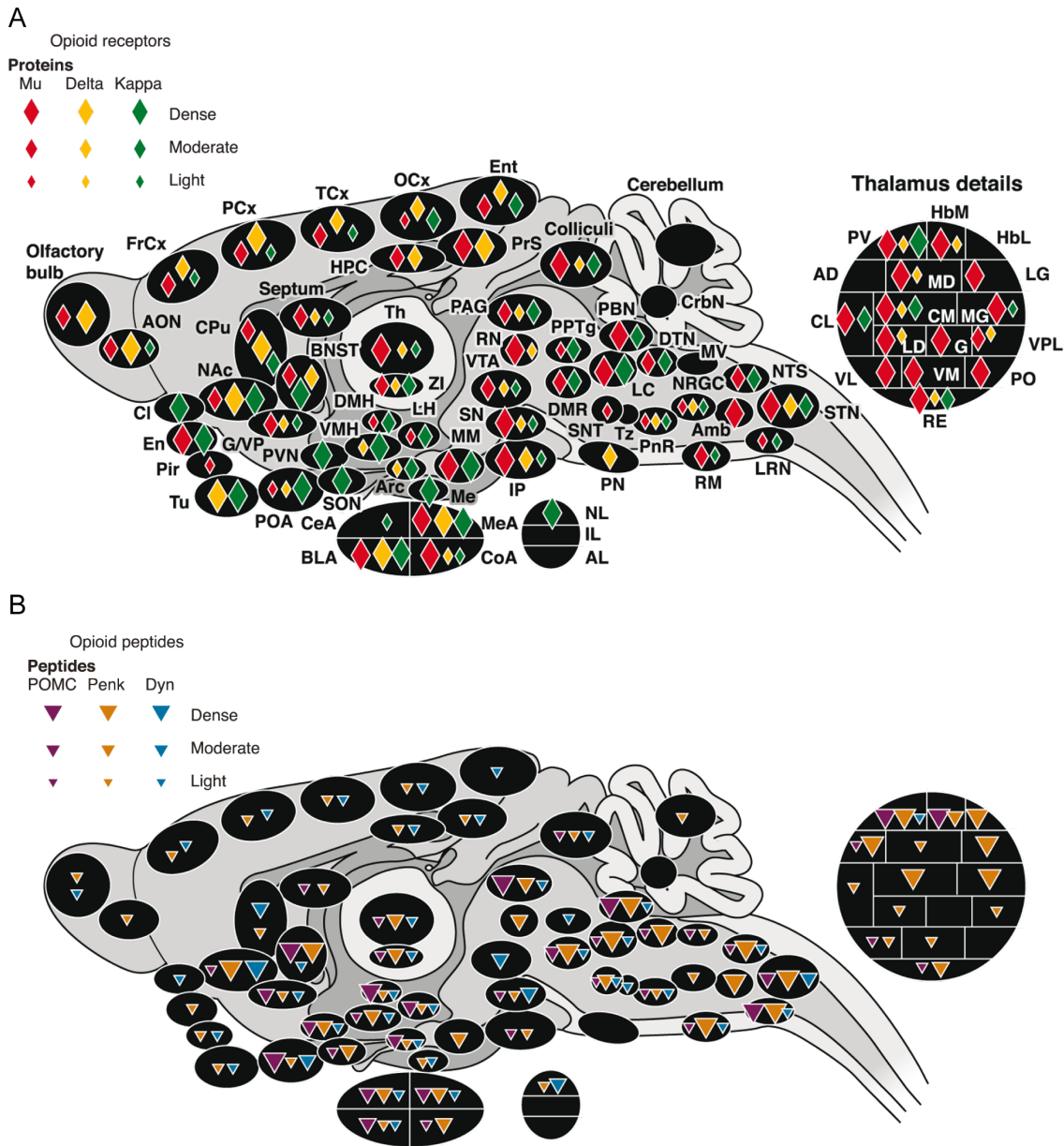


Figure 12: Anatomical distribution of main opioid neural components. Schematic representation of a rodent brain sagittal section depicting the distribution of (A) opioid receptors proteins, and (B) peptides. Densities are represented by symbols of different sizes, from low to high. **Abbreviations:** Amb, nucleus ambiguus; AD, anterodorsal thalamus; AL, anterior lobe, pituitary; AON, anterior olfactory nucleus; Arc, arcuate nucleus, hypothalamus; BLA, basolateral nucleus, amygdala; BNST, bed nucleus of the stria terminalis; CeA, central nucleus, amygdala; Cl, claustrum; CL, centrolateral thalamus; CM, centromedial thalamus; CoA, cortical nucleus, amygdala; CPu, caudate putamen; CrbN, cerebellar nuclei; DMH, dorsomedial hypothalamus; DMR, dorsal and medial raphé; DTN, dorsal tegmental nucleus; En, endopiriform cortex; Ent, entorhinal cortex; FrCx, frontal cortex; G, nucleus gelatinosus, thalamus; G/VP, globus pallidus/ventral pallidum; HbL, lateral habenula; HbM, medial habenula; HPC, hippocampus; IL, intermediate lobe, pituitary; IP, interpeduncular nucleus; LC, locus coeruleus; LD, laterodorsal thalamus; LG, lateral geniculate, thalamus; LH, lateral hypothalamus; LRN, lateral reticular nucleus; MD, mediodorsal thalamus; Me, median eminence; MEA, median nucleus, amygdala; MG, medial geniculate; MM, medial mammillary nucleus; MV, medial vestibular nucleus; NAc, nucleus accumbens; NL, neuronal lobe, pituitary; NRG, nucleus reticularis gigantocellularis; NTS, nucleus tractus solitarius; OCx, occipital cortex; PAG, periaqueductal gray; PCx, parietal cortex; Pir, piriform cortex; PN, pontine nucleus; PnR, pontine reticular; PO, posterior thalamus; POA, preoptic area; PPTg, pedunculopontine nucleus; PrS, presubiculum; PV, paraventricular thalamus; PVN, paraventricular hypothalamus; RE, reuniens thalamus; RN, red nucleus; RM, raphé magnus; SON, supraoptic nucleus; SN, substantia nigra; SNT, sensory trigeminal nucleus; STN, spinal trigeminal nucleus; TCx, temporal cortex; Th, thalamus; Tu, olfactory tubercle; Tz, trapezoid nucleus; VL, ventrolateral thalamus; VM, ventromedial thalamus; VMH, ventromedial hypothalamus; VPL, ventroposterolateral thalamus; VTA, ventral tegmental area; ZI, zona incerta. (From Le Merrer et al, 2009).

The cDNAs coding for the human and rodent μ -, κ -, and δ -receptors have been cloned by sequence homology (for a review see Kieffer 1995).

In 1975, (Hughes et al) characterized the first endogenous ligands for these receptors, the pentapeptides methionine-enkephalin (Met-enk) and leucine-enkephalin (Leu-enk). Since then, many endogenous opioid peptides have been identified, all sharing a common tetrapeptide amino-terminal sequence called “opioid motif”, which interacts with the opioid receptors. These neuropeptides were classified in three families depending on their encoding gene: enkephalins, dynorphins, and endorphins; produced by proteolytic cleavage of large protein precursors known as preproenkephalin (Penk), preprodynorphin (Pdyn), and proopiomelanocortin (POMC), respectively (Akil et al 1998).

Opioid receptors and peptides are both broadly expressed throughout the brain. As depicted in [Figure 12](#) for rodent brain, there is a large overlapping localization and main expression in the cortex, limbic system, and brain stem. Consistent with this widespread anatomical distribution of the components, the opioid system has been involved in a wide range of physiological effects and motivational processes. Indeed, this system has been reported to play a central role in nociception and analgesia as well as in modulating mood, well-being, and addictive behaviors. Moreover, it also regulates numerous physiological functions, including responses to pain, stress, respiratory and cardiovascular functioning, gastrointestinal transit, endocrine and immunological functions as well as learning and memory processing, eating and drinking behaviors, and general activity and locomotion (Bodnar 2010).

Mice lacking the different opioid receptors represent unique tools for functional studies of the opioid system. A summary of the responses to drugs of abuse and spontaneous behavior of κ -, δ - and μ -receptors knockout (KO) is presented in [Figure 13](#). From a general point of view, Kappa-receptors have been primarily involved in motivational circuits mediating the aversive counterpart of hedonic homeostasis and the global negative state developed during drug withdrawal (Gaveriaux-Ruff & Kieffer 2002; Jackson et al 2010). Besides, Delta-receptors were mainly related to nociception, and even if they have shown a minor implication in acute pain, the system was found strongly activated during persistent pain. Accordingly, neuropathic (Nadal et al 2006) and inflammatory (Gaveriaux-Ruff et al 2008) pain were enhanced in delta-receptor KO mice. Moreover, initial studies with this mutant mice also involved delta receptors in emotional responses (Filliol et al 2000); and recent evidence further suggests a role in regulating

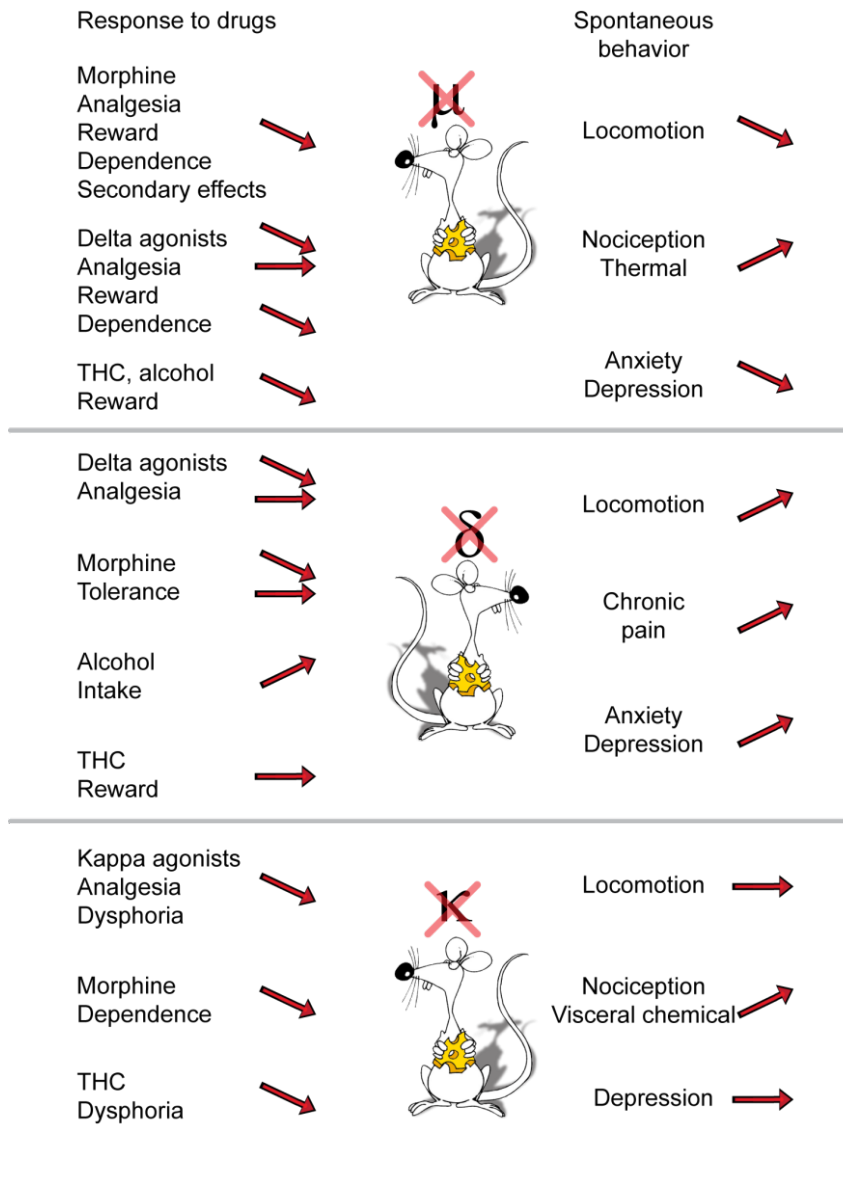


Figure 13: Phenotypes of opioid receptors knockout mice. Summary of the responses to drugs of abuse and spontaneous behavior in opioid receptor KO mice.

References: strongly reduced or abolished; increased; unchanged; unchanged or decreased depending on the experimental conditions. (Adapted from Gavériaux-Ruff and Kieffer, 2002).

mood and emotional states, especially in relation to depressive disorders. Thus, the association between the delta opioid receptor (DOR) system and depression pathology as well as the antidepressant-like effects of delta opioid ligands are being evaluated in preclinical assays, suggesting that these compounds may have therapeutic potential for treating human depression (Jutkiewicz 2006).

Finally, as represented in [Figure 13](#), Mu-receptors knockout mice (MOR-KO) exhibit reduced locomotor activity, and decreased anxiety and depressive-like behaviors as evaluated in the elevated plus-maze and the forced swim test respectively (Filliol et al 2000), a phenotype that was recently confirmed by Ide et al (2010). Moreover, MOR mutant mice also showed phenotypic modifications in models of acute nociception, modulating heat, mechanical and chemical nociception (Martin et al 2003). In this sense, current preclinical and clinical studies still focus the development of potent analgesics through the use of mu-opioid receptors (Pasternak & Pan 2011). Furthermore, a deficit of maternal attachment has been reported in MOR-KO pups (Moles et al 2004) and recently found as well in rhesus macaques (*Macaca mulatta*), in which a single nucleotide polymorphism of mu-opioid receptor (OPRM1) predicts individual differences in infant affiliation for mothers (Higham et al 2011). In addition, food intake studies reported a decreased motivation to eat in MOR-KO mutant mice as compared to control WT (Papaleo et al 2007). These results suggest a role of mu-receptors in the mediation of natural reinforcers both in the context of social interactions and in motivational properties of food intake.

In the field of addictions, Mu-receptors were mainly shown to be mainly involved in the reinforcing processes. Mu receptor signaling was found activated by several drugs of abuse (opioid and non-opioid) both on pharmacological studies and genetics approaches, as review in Contet et al (2004). In this frame, conditioned place preference (CPP) and self-administration paradigms have been used to analyze reinforcing properties of morphine, alcohol, Δ^9 -tetrahydrocannabinol (THC) and nicotine, and results demonstrated the requirement of μ -receptors for the rewarding activities of all the evaluated compounds. Similar results were also obtained for cocaine CCP and self-administration paradigms (Becker et al 2002; Mathon et al 2005). These aspects of μ -receptors opioid activity in relation to opioid and non-opioid drugs of abuse have been also recently reviewed consistently with the previous studies (e.g., Berrendero et al 2010; Gianoulakis 2009). Mu

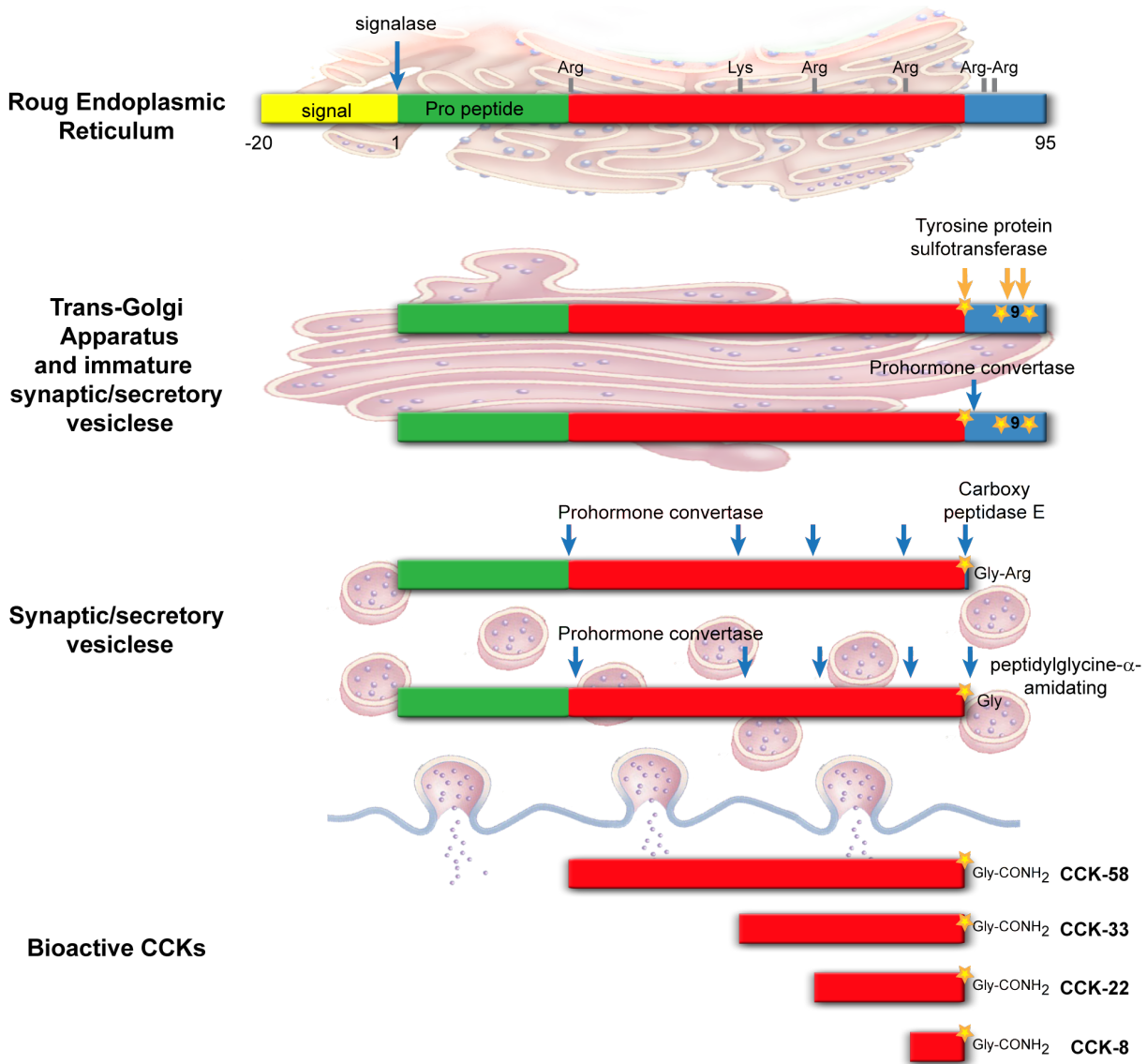


Figure 14: Biosynthesis of CCK biological active peptide fragments. Model of preprocholecystokinin processing adapted from Beinfeld et al, 2003a and Rehfeld, 2004. See text for detailed explanation.

receptors, therefore, were postulated as a convergent molecular gate in the initiation of addictive behaviors and a potential therapeutics target for the treatment of drug addiction.

D. CHOLECYSTOKININ

CCK was first identified in the small intestine and characterized as a gastrointestinal hormone (Mutt & Jorpes 1968) and later reported in the brain (Vanderhaeghen et al 1975), where it was described as the most abundant neuromodulatory peptide in mammals (Beinfeld et al 1981b).

1. Biosynthesis

The biosynthesis of CCK resembles all other secretory peptides and the model of processing is schematically represented in [Figure 14](#). Briefly, CCK is synthesized as a 115 amino acid prepro-polypeptide that is directed to the endoplasmic reticulum where the sequence signal is removed. Next, different modifications take place in the trans-golgi network: 3 tyrosines residues are sulfated by a tyrosine sulfotransferase and a primary endoproteolytic cleavage remove the S9S peptide fragment on the carboxyl-terminal of the molecule. Then, sulfated pro-CCK is sorted into regulated secretory granules together with the enzymes responsible of its processing. Post-translational cleavage generates CCK-58, the largest circulating form of the peptide that further undergoes throughout endoproteolytic cleavage and generates the shorter bioactives forms of CCK. Different pro-hormone convertases run these cleavages occurring sequentially from the amino terminus at the carboxyl-terminal arginine residues. After each cleavage, the arginine residues are removed by a carboxypaptidase E, and the glycine residues are amidated by a peptidylglycine- α -amidating monooxygenase (Beinfeld 2003a; Rehfeld 2004).

CCK post-translational processing displays important tissue- and species-specific differences. The main tissue-specific distinction is found between the brain and the intestine; while the brain present mainly CCK-8 and CCK-4 fragments, the intestine contains larger forms like CCK 12, 22, 33 and 58 peptide. These differences may be due to different processing by the pro-hormone convertases (PC). Indeed, in the brain, PC1, PC2 and PC5 have been postulated to form a redundant system to ensure production of CCK-8S

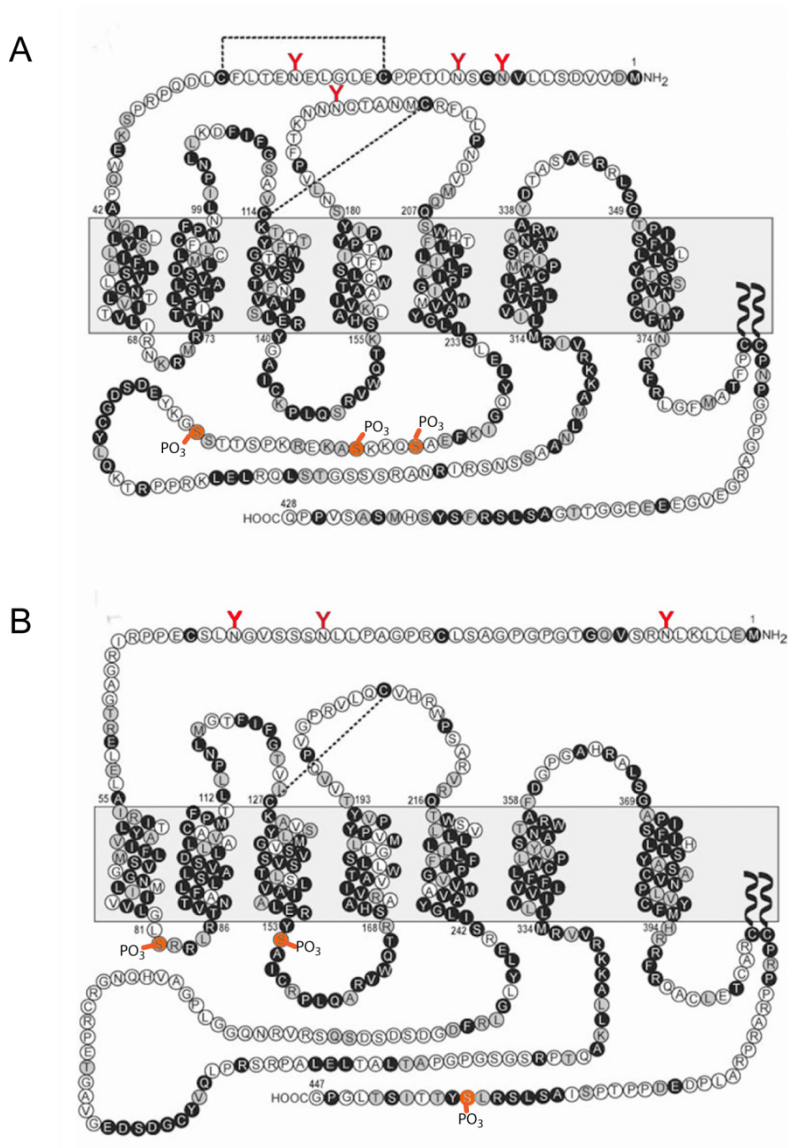


Figure 15: Snake diagrams of the amino-acid sequences of CCK receptors. Proposed topology of the (A) CCK₁ and (B) CCK₂ receptors. The filled black circles represent conserved identical residues, while white and grey circles represent homologous residues. Dotted lines are disulfide bonds and highlighted in red are potential post-transcriptional modifications: **Y** represent putative NH₂-linked glycosylation sites; **-PO₃** represent PKC and PKA phosphorylation sites. (Adapted from Miller and Gao, 2008).

(Cain et al 2003). Moreover, such distinction may have physiological significance. Shorter forms in the brain may allow a fast degradation of the peptide after release, while larger forms from the intestine might be more difficult to be degraded by the kidney and therefore enable a longer half-life in circulation (Beinfeld 2003a).

Among these several forms of the CCK peptide, the best known are: caerulein (CCK-10), octapeptide (CCK-8), pentagastrin (CCK-5) and tetrapeptide (CCK-4), the last one being the shorter amino-acid sequence necessary for binding central CCK-receptors (Brownstein & Rehfeld 1985) and CCK-8s (C-terminal sulfated octapeptide), as mentioned before, the most abundant fragment in the brain (Vanderhaeghen et al 1975).

2. Receptors and signal transduction

Analyses of the binding properties of CCK peptides and gastrin (a peptide which shares the same carboxyl terminal sequence) have provided evidence of the existence of two G protein-coupled receptor (GPCR) types, CCK₁ and CCK₂, belonging to the Family A (or Class I) of GPCRs, the rhodopsin- β adrenergic receptor family. These receptors evolve from a common gene precursor, and share high homology and ~50% of identity, especially in the transmembrane domains; but they differ in terms of detailed molecular structure, distribution, and molecular binding affinity, exhibiting remarkable functional differences (Miller & Gao 2008). Moreover, based on pharmacological and biochemical studies, the existence of splice and polymorphic variants of both receptors has been postulated (Dauge & Lena 1998; Korner & Miller 2009).

The amino acid sequences of CCK₁ and CCK₂ are depicted in [Figure 15](#). Notable features of these molecular structures are the sites of glycosylation on the external loop and tail regions, which have been postulated to display critical roles for proper folding and trafficking to the cell surface. Besides, serine and threonine residues phosphorylation has also been described and are indicated on the diagrams. These biochemical modifications of the receptors provide a rapid and often reversible mechanism for their regulation that occurs either in response to agonist stimulation (homologous activation) or by heterologous activation of other receptors that activate PKC and PKA enzymes. The final functional impact of such phosphorylation is to desensitize the receptors by interfering with their coupling to the G protein (Mazzocchi et al 2004). Apart from these translational modifications, a cellular receptor regulation takes place through two main mechanisms: *i*) Internalization pathways have been reported for the CCK₁ receptor. Tarasova et al (1997)

have taken advantage of the green fluorescent protein to describe and evaluate these pathways, postulating that both ligand-induced and spontaneous (constitutive) internalization may exist for CCK receptors, and one pathway can prevail over the other depending on the cell type. *ii)* Similarly, coupling between receptor and G protein requires lateral mobility in the plasma membrane and access for the two molecules to meet each other. In this sense, a novel mechanism of CCK₁ receptor desensitization was described in which the receptor becomes immobilized in specialized plasma membrane domains (Roettger et al 1999).

In terms of distribution and naturally-occurring ligand binding, CCK₁ receptors were previously known as CCK_A (“alimentary”) due to their abundant presence in the gastrointestinal tract. Nevertheless, they have also been reported in a limited number of brain regions (Moran et al 1986) (See [Table 3](#)). CCK₁ receptor requires the carboxyl-terminal heptapeptide-amide that includes the sulfated tyrosine, found in CCK-8s peptides, for high affinity binding and biological activity (Miller & Gao 2008). In contrast, CCK₂ receptors were previously known as CCK_B (“brain”) for being expressed predominantly and with a large distribution in the CNS (Moran et al 1986). For biological activity they require only the carboxyl-terminal tetrapeptide-amide that is shared by all CCK and gastrin peptides. CCK₂, therefore, displays high affinity for both CCK-4 and CCK-8s molecular forms occurring in the brain (Miller & Gao 2008).

The mode of action of CCK receptors has been extensively explored, with a major focus on the signal-transduction cascade for CCK₁. In this frame, it has been reported that CCK₁ receptors, coupled to the G_q family of G proteins, activate arachidonic acid pathways via the phospholipase-C(PLC)-dependent cascades as well as throughout phospholipase-A₂ (PLA₂) activation. In addition to these activation of PLC and PLA₂ signal-transduction pathways, CCK₁ receptors stimulation can also lead to an increase in adenylyl cyclase signal transduction cascade. Although it was first believed that this effect results from G protein βγ-subunits activation of an isotope of adenylyl cyclase, later evidence from chimeric receptors reported that CCK₁ is directly couple to both G_q and G_s proteins. For CCK₂ receptors, the signal-transduction cascade has been less characterized. Nevertheless, evidence has also linked this receptor to the G_q family of G proteins, causing activation of PLC/IP₃ and PLA₂/arachidonic acid pathways throughout two different coupling states (Noble et al 1999; Pommier et al 1999; Pommier et al 2003). Moreover, recent studies reported the activation of the adenylyl cyclase/protein kinase A signaling cascade acting

through CCK₂ receptors. Altogether, it is currently accepted that G protein-coupled CCK receptors activate both adenylate cyclase- and PLC-dependent cascades (Mazzocchi et al 2004).

3. Intestinal distribution and major effects as a gastrointestinal hormone

In the intestine, CCK is secreted by enteroendocrine cells (I cells) located in the mucosa of the duodenum, jejunum, and proximal ileum, as well as by specialized neurons in the myenteric plexus (Chandra & Liddle 2007). At this level CCK exerts a number of biological actions that together maximize nutrient absorption and mediate the control of meal size. Such actions include: regulation of gut motility, pancreatic secretion, inhibition of gastric emptying and distension, gallbladder contractions and an important feedback signal for satiety (Moran & Kinzig 2004). On this last effect, experimental evidence suggested mediation by the vagal afferent pathway. Specifically, CCK is secreted by duodenal and ileal cells when nutrients enter the lumen and binds to specific CCK₁ receptors located on vagal sensory terminals in the wall of the gastrointestinal tract. This activation reaches the nucleus of the tractus solitarius in the caudal brainstem, and projects from there to the arcuate nucleus, where satiety signals are integrated with adiposity signals (leptin and insulin), and with several hypothalamic and supra-hypothalamic inputs (Valassi et al 2008). Moreover, CCK also inhibits expression of orexigenic peptides (i.e. orexin A and B) of the hypothalamus and prevents stimulation of specialized neurons by ghrelin (Chandra & Liddle 2007). Altogether, this neural circuit creates a complex network which finally elaborates the individual response to a meal intake. Dockray (2009) reported that low plasma concentrations of CCK vagal afferent neurons exhibit increased capacity for appetite-stimulation, while post-prandial concentrations of CCK lead to enhanced capacity for satiety signalling. Thus, he proposed a gatekeeper function of CCK on this complex neural circuit, in that its presence or absence influences the capacity of vagal afferent neurons to respond to other neurohormonal signals.

In support to the hypothesis that CCK-induced inhibition of food intake is mediated by CCK₁ receptors, CCK₁ receptor-deficient mice showed no change in food consumption after administration of CCK-8s, as compared with wild-type control animals (Noble & Roques 2002). Moreover, Otsuka-Long-Evans-Tokushima Fatty (OLETF) rats, that have been shown to be naturally deficient in CCK₁ receptors, present hyperphagia, obesity and the development of non-insulin dependent diabetes mellitus (NIDDM) (Moran & Bi 2006).

Brain region	Peptide		Innervation		Receptors			
	CCK-mRNA	CCK-LI	fibers-LI	terminals-LI	CCK1 radioligand	CCK1 mRNA	CCK2 radioligand	CCK2 mRNA
Olfactory bulb	+++					+	++	++
Olfactory nuclei	+++					+		+
Cortex	+++	++	++	++		+	+++	+++
Cingulate cortex	+++	++	+++	+++		+	+++	+++
Piriform cortex	+++	++	+++	+++		+	+++	+++
Corpus callosum			+++					
Clastrum	++	++	+++	+++		+		+
Septum		++	++	++			+	+
Caudate-Putamen	+	+					++	++
Nucleus accumbens	-	-	+++	+++	(+)		+++	++
Globus Pallidus		++					+	
Ventral Pallidus		-	++	++			+	
Bed nucleus of the stria terminalis		+	++	++		+	+	
Preoptic nuclei		++	++	+		+		+
Thalamus nuclei	+++	+++	+++	++		+	++	++
Habenula					+	+	+	
Hypothalamus nuclei	+	+	+++	++	+		++	++
Basolateral amygdala nuclei	+++	+++	++	++	+		+	+++
Amygdala medial nuclei	++		+++	+++		+	+	+
Central amygdala nuclei	-	-			+		+	+
Hippocampus	+++	++	++	++		+	++	++
Dental gyrus	+		++				++	
Substantia nigra	+++	+					+	+
Ventral tegmental area	+++	+						
Raphe nuclei	+	++			(+)		+	
Tractus solitarius					+		+	
Area postrema					+			
Interpeduncular nuclei					+			+

Table 3: CCK neural components distribution in the adult rodent brain. List (non-exhaustive) of the main peptides, innervations and receptors location determined using *in situ* hybridization (mRNA expression levels), immunohistochemical (-LI: like-immunoreactivity), and radioligand techniques. Levels of reported expression are represented as following: +++, high level; ++, moderate level; +, low level. (+) represent immunoreactivity study. (From: Schiffmann and Vanderhaeghen, 1991; Ingram et al, 1999; Mezaine et al, 1997; Noble et al, 1999; Cain et al, 2003; and Wang et al, 2005).

4. Brain distribution and central systems

As mentioned before, CCK is one of the most abundant neuropeptides in the mammalian brain (Beinfeld et al 1981a) and its mRNA expression has shown a wide distribution from the developing mouse brain (Giacobini & Wray 2008). The central locations of CCK neural components in the adult rodent brain are summarized in [Table 3](#). First studies on mRNA staining reported CCK containing cells in the olfactory bulb and nuclei, the cerebral cortex, clastrum, amygdala, dental gyrus and hippocampal proper, ventral tegmental area, sustantia nigra, raphe nuclei, several nuclei of the thalamus and few cells in some nuclei of the hypothalamus (Ingram et al 1989; Schiffmann & Vanderhaeghen 1991). Later, these localizations were confirmed by Cain et al (2003) who further detailed CCK distribution in the brain. They reported expression in all the layers of the neocortex and stronger staining in Cingulate and Piriform cortices. Abundant number of cells were found in most of the CA subfields of the hippocampus with the major intensity in the pyramidal cell layer of the CA1, and comparative less positive cells in the dental gyrus. For the amygdala, the most abundant CCK containing neurons were present in the BLA and medial nuclei, while any staining was revealed in the CeA. Ventral tegmental area and sustantia nigra positive cells were very heavily labeled and tightly packed. Finally, also very few labeled neurons were reported in the caudate-putamen.

Although some discrepancies were observed, the above presented *in situ* hybridization studies correlates CCK mRNA expression distribution with a previous immunohistochemical study developing a complete CCK mapping in the mouse forebrain (Meziane et al 1997). Such study reported CCK-like immunoreactive cells in cortical areas (cingulate and piriform cortices), clastrum, septum, preoptic nuclei, basal ganglia (caudate-putamen and globus pallidus), thalamus, hypothalamus, bed nucleus of the stria terminalis, amygdaloid complex (especially BLA), hippocampus, sustantia nigra, ventral tegmental area and raphe nuclei. Moreover, the CCK-IR also revealed numerous axons and terminals along the mouse brain that were in agreement with the reported receptors distribution. CCK₂ receptor mRNA is strongly expressed throughout the cortex, nucleus accumbens and several amygdaloid nuclei while CCK₁ receptor expression, initially reported in the gastrointestinal tract, is also found in the CNS mainly at the level of interpeduncular nucleus, area postrema, tractus solitarius, habenular nuclei, hypothalamus and central amygdala (Noble et al 1999; Wang et al 2005).

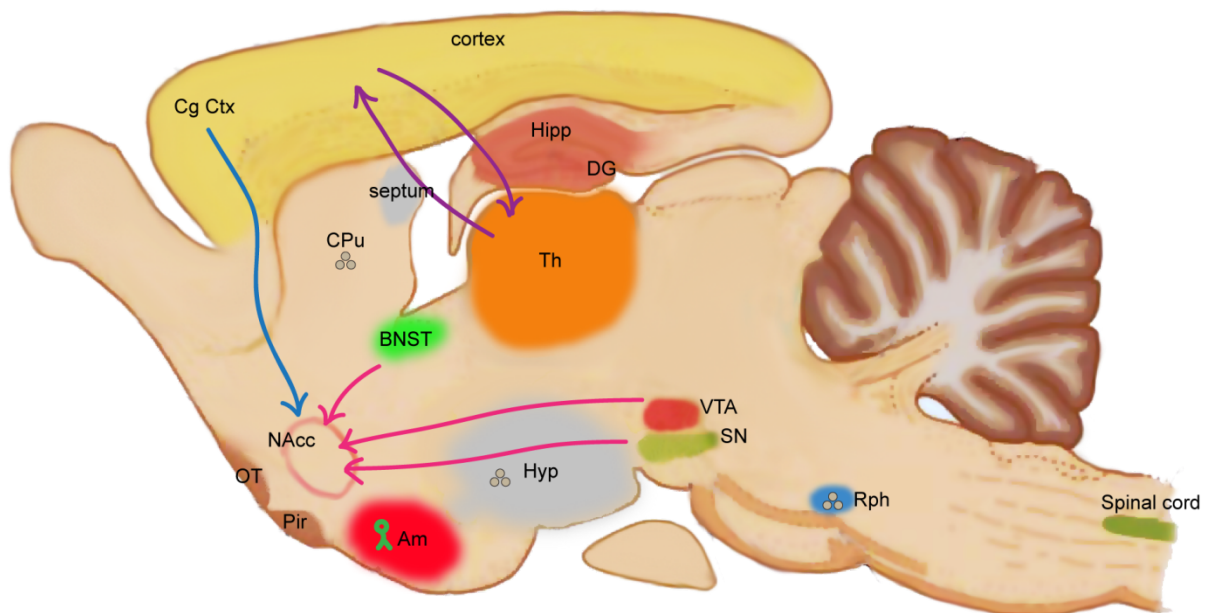


Figure 16: Anatomical distribution of the main CCK-containing neurons and major CCKergic systems. Schematic representation of a rodent brain sagittal section depicting the distribution of CCK-containing neurons in colored areas (non-exhaustive) and the projections forming the main CCKergic pathways summarized by Hokfelt et al (2002): cortico-striatal glutamatergic pathway in blue; thalamo-cortical glutamatergic pathway in violet; nigro-striatal dopaminergic pathway in pink; and amygdalar GABAergic interneurons in green. The symbol $\circ\circ$ represent regions with very low CCK expression levels.

Across the described neuroanatomical distribution, CCK has been reported to be mostly co-localized with classic neurotransmitters as follows (Ghijsen et al 2001):

- In mesolimbic and mesocortical neurons (ex.: Striatum; NAcc; EA) = = with **Dopamine**
- In dorsal Raphe and its ascending projections = = with **Serotonin**
- In pyramidal cells of cerebral cortex = = with **Glutamate**
- In cortex, hippocampal formation and BLA = = with **GABA**

Histochemical evidences demonstrate the presence of three main forebrain CCKergic systems within these co-localized pathways (Hokfelt et al 2002): a nigro-striatal in dopaminergic neurons; a cortico-striatal in glutamatergic neurons; and a thalamo-cortical also presumably in glutamatergic neurons. Among this systems, the CCKergic projections, arising from the substantia nigra and prefrontal cortex to the accumbal core and from the ventral tegmental area and the extended amygdala to the accumbal shell (Lanca et al 1998), has been the most extensively analyzed due to their antagonistic effects on dopamine function and on positively motivated behaviors (Rotzinger et al 2002). Modulation of dopamine receptors binding affinity and GABAergic transmission on the NAcc has been postulated as the mechanisms underlying the regulatory action of CCK (Beinfeld 2003b; Tanganelli et al 2001).

More recently, a CCKergic system in GABAergic interneurons of the basolateral amygdala has also been reported (Chung & Moore 2009; Jasnow et al 2009). This system was involved in the anxiogenic activity of CCK (Chung & Moore 2007; 2009) as well as in the modulation of an endocannabinoid system underlying extinction of fear conditioned memories (Chhatwal et al 2009).

[Figure 16](#) schematically represent the major mentioned CCK-containing neurons and the main projections comprising the CCKergic systems.

5. Major effects as a neuromodulatory peptide

CCK fulfills the criteria of neurotransmitter in the CNS: *i)* is synthesized and stored in cell bodies and nerve terminals, respectively; *ii)* is released by depolarization of the plasma membrane; *iii)* has specific receptors and antagonists; and *vi)* influences the firing rate of other central neurons (Fink et al 1998). But, as mentioned before in part C, this peptide present also some functional differencesa with the classical NT with which it co-localizes (GABA, DA, 5-HT, and glutamate). CCK exerts modulatory functions of the synapses through

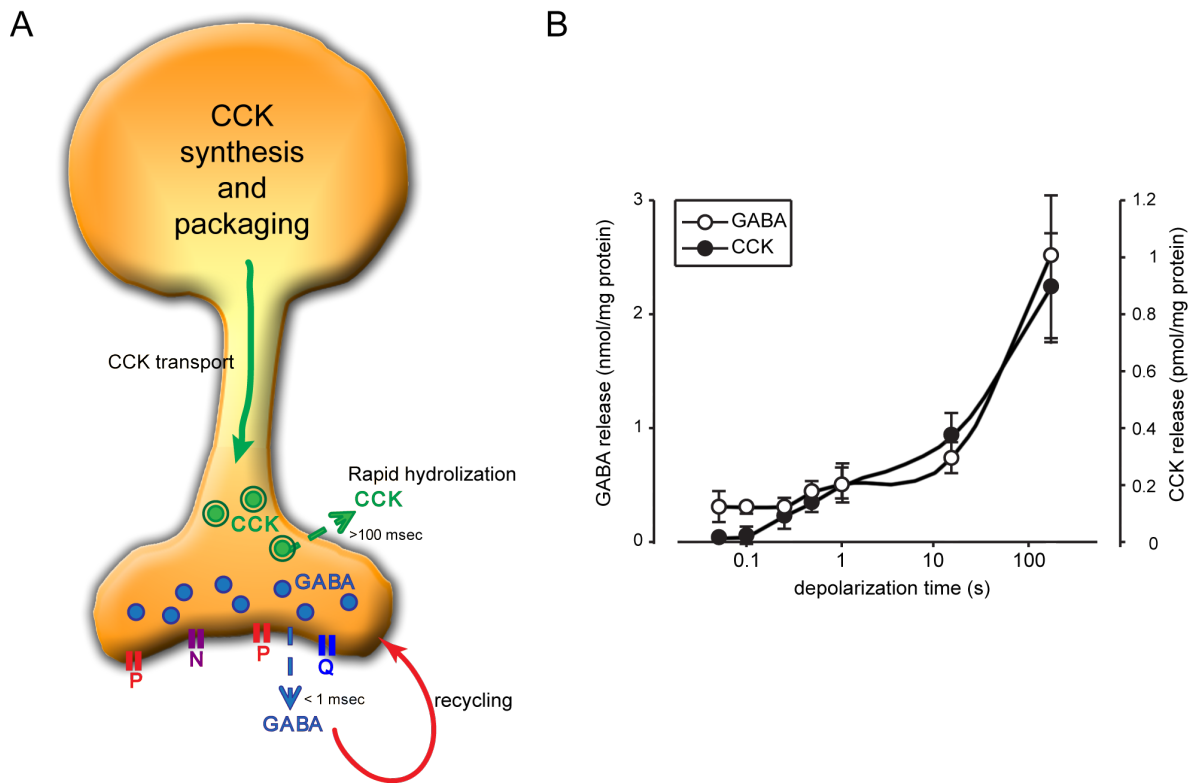


Figure 17: Schematic representation of the neuromodulatory criteria for CCK. (A) Hypothetical scheme of a neuron depicting the main regulatory mechanisms of CCK release as compared to GABA release. See text for detailed explanation. (B) Dynamics of CCK and GABA release from rat cortex synaptosomes. (Adapted from Ghijsen et al, 2001).

a co-release only under conditions that lead to high frequency firing (Rotzinger & Vaccarino 2003). This occurs by a differential release regulation based on the following characteristics summarized by Ghijsen et al (2001), and also schematically presented in [Figure 17](#):

✓ Vesicle storage: CCK peptides are packaged in the cell soma on larger and core-dense vesicles that travel all along the axon toward the nerve terminals, while classic neurotransmitters are produced in the terminals and packaged in small and clear synaptic vesicles.

✓ Pre-synaptic localization: CCK vesicles are stored at remote sites of the membrane, while classic neurotransmitters vesicles are found close to the site of release in the nerve terminals.

✓ Release dynamics: CCK peptide release is more delayed (visible 0.25sec after depolarization) as compared to classic neurotransmitters (ex: GABA visible 50msec after depolarization), and continuously increased during at least 3min of depolarization, while classic neurotransmitters as GABA normally reach a plateau during the first half second of depolarization (see [Figure 17B](#)).

✓ Calcium regulation: Apparently CCK vesicles have a much higher Ca^{2+} sensitivity of secretion than the small transmitters, and response to different high-voltage channels. While CCK uses P/Q channels which show synergism, GABA, for instance, uses P, Q and N channels, without any additive effect.

✓ Recycling: CCK peptides are rapidly hydrolyzed by extracellular peptidases after release, therefore, to save the nerve terminal from depletion, massive stimulation induces release of only a fraction of the total CCK vesicles-pool. In contrast, classic neurotransmitters are recycled back into the terminal by specific transporters after their release.

Functional studies of biologically active CCK in the CNS, have implicated this peptide in a wide range of physiological processes, including cardio-respiratory control, thermoregulation, locomotor activity, nociception, emotional and motivational states, and learning abilities (review in Beinfeld 2001). Among these effects, the main focus has been placed in relation to the facilitatory effects in cognitive processes, as well as the anxiogenic-like effects. While decreased CCK levels within PFC, amygdala and hippocampus has been

associated with learning and memory deficits, high levels of CCK in prefrontal cortex, amygdala and VTA have been related with motivational loss, anxiety and panic disorders (Hebb et al 2005). Consistent with this data, a role has been proposed for CCK in the induction of anxiety and major depression (Berna et al 2007; Shindo & Yoshioka 2005).

Pharmacological evidence has reported the CCK₂ receptors as the main effectors of anxiogenic and cognitive properties of the peptide and hypothesized the existence of two binding sites, CCK-B1 and CCK-B2, which could correspond to different activation states of a single molecular entity. CCK-B1 appears to be responsible for the effects on anxiety levels, while CCK-B2 was involved in the improvement of attention and/or memory processes (Dauge & Lena 1998). Recent studies further confirm the importance of these receptors. In this sense, specific CCK₂ agonists administration have shown anxiogenic effects in several behavioral paradigms, including the elevated plus-maze (EPM), acoustic startle and open field tests (Rotzinger et al 2010). Moreover, systemic administration of specific CCK₂ antagonist attenuated the increased anxiety-like behavior of mice subjected to immobilization restrain stress as examined in the EPM (Wang et al 2011). Importantly, these anxiolytic effects often are not seen unless the system is potentiated, supporting the role of the peptide as a neuromodulator (Hebb et al 2005). In addition, CCK₂ antagonists have been also analyzed for their antidepressant potential in preclinical models (Rotzinger et al 2010). Chronic blockade of CCK₂ receptors was effective normalizing high immobility time in the force swim test and preventing HPA axis hyperactivity, which were both elicited by repeated social defeat-induced stress (Becker et al 2008).

Genetic approaches targeting CCK receptors further investigated these effects. CCK₂-receptor deficient mice presented impaired environmental habituation and retention of spatial recognition as compared to WT animals (Noble & Roques 2002). However, they did not show behavioral modifications in the motility conditioned suppression test for despair-like behavior and results on anxiety studies were controversial. CCK₂-receptor KO induced an anxiolytic-like action in the light-dark test, but not in the EPM or in conditioned models of anxiety such as the fear conditioning test (Dauge et al 2001; Raud et al 2005); indicating that compensatory mechanisms likely occur following receptor invalidation. In addition, inducible forebrain-specific CCK₂ receptor transgenic mice showed enhanced anxiety-like behavior, impaired spatial and recognition memories, and prolonged activation of adrenocorticotrophic hormone and glucocorticoids following acute stress (Chen et al 2010).

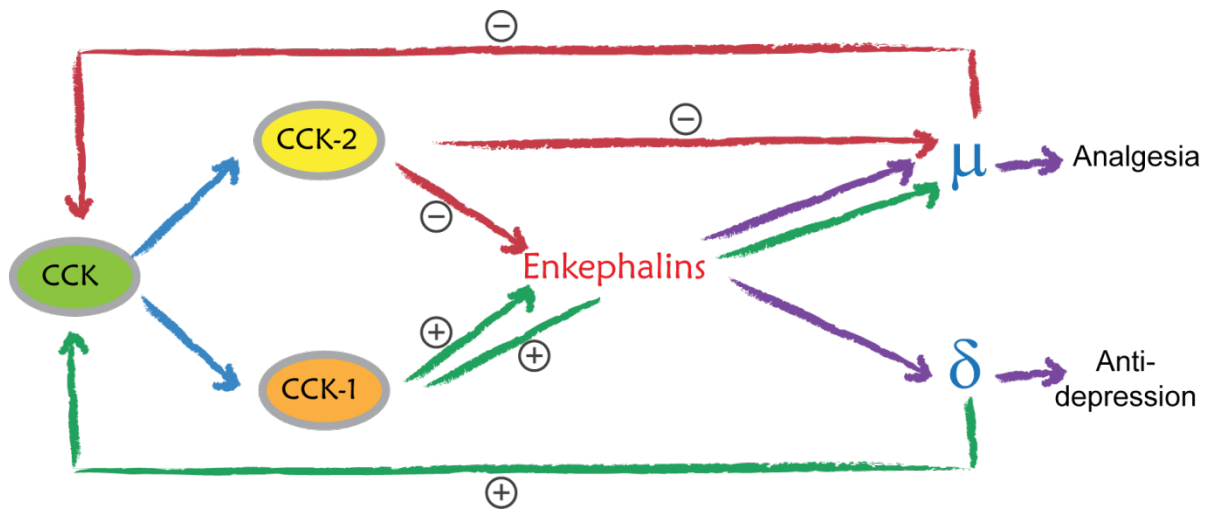


Figure 18: Regulatory loops between opioidergic and CCKergic systems. Hypothetical model of the supraspinal interactions between CCK, via CCK₁ and CCK₂ receptors, and the opioid system, via μ - and δ -receptors. According with this model, CCK₁ and CCK₂ receptors have distinct activatory and inhibitory influences, respectively, over the opioid system. CCK receptor agonists, endogenous or exogenous, can modulate the enkephalinergic systems either directly influencing opioids receptor binding affinity or indirectly via the release of endogenous enkephalins. In addition, activation of μ -opioid receptors, which leads to anti-nociceptive responses, can negatively modulate the release of endogenous CCK, whereas δ -opioid receptor activation, which leads to anti-depressive responses, may enhance it. (Adapted from Noble et al, 1999).

6. CCK and opioid system interactions

Over the last years, there was an increasing interest in the role of CCK in addictive processes due to the referred interactions between the peptide and classical transmission systems in neurons of the rewarding and motivational pathways (Rotzinger & Vaccarino 2003). CCK was shown to exert antagonistic opioid properties for opioid-induced analgesic and antidepressant-like effects. Specifically, on the one hand, CCK₂ antagonist potentiated the antidepressant effect of RB101 (a systemically active inhibitor that protects endogenous enkephalins from peptidase inactivation), and delta-receptor antagonist blocked this potentiation (Hernando et al 1996). On the other hand, increased CCK levels were related with the reduced response to opioids during neuropathic pain after injury in the peripheral or central nervous systems (Wiesenfeld-Hallin et al 2002). Such anti-opioid effects could also contribute to the withdrawal syndrome. Pharmacological studies showed that CCK₂ receptor antagonists were effective in decreasing both somatic and motivational aspects of morphine (Kayser et al 1998; Valverde & Roques 1998) and ethanol withdrawal (Wilson et al 1998). Moreover, CCK₂-receptor knockout mice presented lowest nociceptive threshold and less sensitivity to opioid analgesic drugs, as well as a more severe withdrawal syndrome after chronic morphine treatment, all evidences for an up-regulation of the endogenous opioid system (Pommier et al 2002). In contrast, other pharmacological studies have also positively involved CCK with opioids rewarding properties. The peptide was reported to be necessary for both acquisition and expression of morphine conditioned place preference (CPP) (Higgins et al 1992; Mitchell et al 2006) as well as for the reactivation of extinguished morphine and cocaine CPP (Lu et al 2001; Lu et al 2002).

In view of these contradictions, the previously mentioned effects of CCK on nociception and emotional processes were further evaluated based on the overlapping distributions of the CCKergic and opioidergic systems in the SNC. Noble and Roques (Noble & Roques 2003; Noble et al 1999) proposed the existence of regulatory loops between both peptide systems. In their model, schematically represented in [Figure 18](#), the potentiating of pharmacological effects of exogenous (morphine) or endogenous (enkephalins) opioids occurs through activation of CCK₁ receptors. Thus, antidepressant-like effects of RB-101 were suppressed by CCK₁ antagonist, while CCK-8s and analogs have shown analgesic properties in the hot plate and tail flick tests. In contrast, negative modulation of the opioidergic system may be dependent of CCK₂ receptors. Therefore, co-administration of CCK₂ antagonists with morphine or RB-101 led to an enhancement of analgesic or

antidepressant-like opioid effects. Altogether, the authors postulated that a dysfunction in the balance between the two peptidergic systems involved in rewarding and emotional processes could participate in the neurobiological mechanisms underlying vulnerability to drug addiction.

7. Characterization of CCK peptide-deficient mice

Lo et al (2008) have characterized the CCK-KO mice regarding to the peripheral functions of the peptide in satiety and its central functions in the modulation of exploratory activity, anxiety and cognitive processes. Compared with wild-type (WT) controls, CCK-KO mice had normal food intake, fat absorption, body weight, and body mass, but they had slightly altered meal patterns over the day-night cycle. Moreover, the running wheel activity of CCK-KO mice and WT mice did not differ on any parameter. Therefore, the lack of CCK was not a factor in regulating total food intake or energy expenditure, and such results may suggest that the functions of CCK related to energy homeostasis are likely redundant with other signals. Additionally, CCK-KO mice exhibited attenuated performance in a passive avoidance task and required more time to locate the escape platform in the Morris water maze test than WT controls, suggesting that CCK-KO mice have impaired spatial memory. Intriguingly was the result on the exploratory activity in the elevated plus-maze on this study, where CCK-deficient mice were more anxious than WT controls.

E. Aims of the thesis

In our laboratory, the role of the opioid system in drug abuse is largely investigated in an attempt to understand genetic bases of drug dependence in the brain. This neuronal system plays a key role underlying the effects of drugs of abuse and neuroadaptations to drug dependence. Particularly, the mu-opiate receptor has been proposed as a molecular gateway to drug addiction in the brain (Contet et al 2004).

Within this frame, genome-wide expression analysis was performed in our laboratory using wild-type and mu-opioid receptor knockout mice. This study was conducted on the central EA, a neuroanatomical entity comprising the BNST and the CeA, and strongly implicated in drug seeking, craving and relapse (Koob 2008). We identified a collection of 132 genes whose transcription was specifically regulated by the activation of the mu-opioid receptor upon a morphine chronic treatment (Befort et al 2008). The expression of these mu-dependent genes was further evaluated following chronic treatment with different drugs of abuse (ethanol, THC, nicotine) and after a period of abstinence (Le Merrer et al, submitted). Among the commonly dysregulated genes over these treatments, the cholecystinin (CCK) mRNA showed remarkable modifications in its expression. Particularly, a significant down-regulation was observed after chronic morphine treatment with a rebound up-regulation following 4 weeks of abstinence.

As was developed in the introduction, CCK was first known as a gastrointestinal peptide and more recently described as a neuromodulatory peptide (Rotzinger et al 2010). The major biological actions of CCK are the reduction of food intake, the induction of anxiety-related behavior and the modulation of memory processes (Fink et al 1998). Furthermore, CCK shares a close neuroanatomical distribution with classic neurotransmitters in reward and motivation pathways of the limbic system (Hebb et al 2005). Although a wide range of processes has been described involving interactions of CCK with endogenous opioid peptides, the precise brain regions involved in these effects remain unclear.

The first aim of my thesis was to further investigate CCK transcriptional regulation in response to morphine in other brain regions. We focused on two brain structures where mRNA distribution studies reported high CCK transcript density (Cain et al 2003; Ingram et al 1989; Schiffmann & Vanderhaeghen 1991): the Cg Ctx and BLA. Both structures are

implicated in the processing of emotional states (Devinsky et al 1995; Gallagher & Chiba 1996) and have been also related to drug dependence, particularly in the development of withdrawal syndrome (Frenois et al 2005; Lowe et al 2002) and the processing of primed induced reinstatement (Kalivas & McFarland 2003).

In this study, we performed radioactive *in situ* hybridization with [³⁵S]-labeled probes and developed a quantitative autoradiographic mapping methodology. We quantified changes in the expression pattern of CCK mRNA within the Cg Ctx and BLA following an escalating chronic morphine treatment, and after a 4 weeks period of abstinence. We also included the BNST in the analysis, as a control to compare with our previous study.

In the second part of my thesis, I focused on the possible implication of amygdalar CCK in emotional responses. In this brain region, CCK is expressed in GABAergic interneurons (Jasnow et al 2009) and electrophysiological studies have led to propose an involvement of this nucleus in anxiogenic effects of the peptide (Chung & Moore 2007). Brain sites where CCK modifies emotional states have not been investigated by genetic approaches; therefore we decided to take advantage of the shRNA technology and the viral delivery approach to down-regulate the CCK mRNA in the BLA. We designed a rAAV-eGFP-shRNA viral vector and investigated whether local treatment with the recombinant virus would silence the *mcck* gene and alter emotional responses. We used several tests designed to evaluate anxiety-like behavior, despair-like behavior, naloxone-induced CPA and the withdrawal syndrome to chronic morphine.

This work is presented in part II, which includes the following manuscript in preparation:

- "Genetic silencing of cholecystokinin mRNA in the basolateral amygdala has anxiolytic and antidepressant effects in mice". Del Boca C, Le Merrer J, Lutz PE, Koebel P, Kieffer BL.

I also contributed to two other studies of our laboratory. This work has been published and is briefly presented in an ANNEX part:

- "RSK2 signaling in brain habenula mediates place learning". Darcq E, Koebel P, Del Boca C, Pannetier S, Kirstetter AS, Garnier JM, Hanauer A, Befort K and Kieffer BL. 2011. Submitted.

- “Deletion of the delta-opioid receptor gene impairs place conditioning but preserves morphine reinforcement”. Le Merrer J, Plaza-Zabala A, Del Boca C, Matifas A, Maldonado R and Kieffer BL. *Biol Psychiatry*. 2010.

My contribution to both projects consisted in the development of lithium-induced conditional place aversion in mice. This place conditioning paradigm evaluates ability of the animal to associate a specific context with an aversive stimulus. I tested delta receptor knockout mice and data from this behavioral task completed morphine-induced conditioned place preference in the first paper, demonstrating that delta receptors facilitate contextual learning rather than drug reinforcement. I also tested knockout mice for RSK2, a kinase responsible for the Coffin-Lowry syndrome, and demonstrated that this RSK2 kinase is essential for place learning.

II. PART I

“CCK mRNA regulation during morphine dependence in the mouse brain”

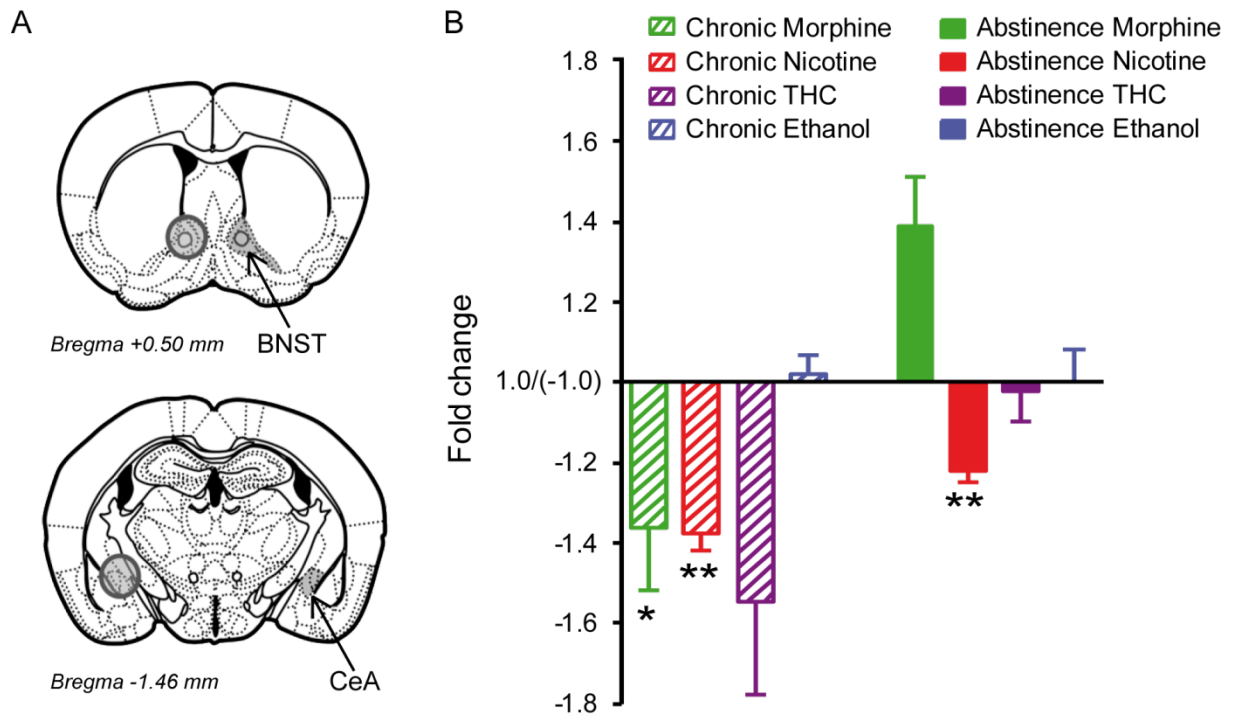


Figure 19: Regulation of CCK mRNA expression in central EA after chronic drug treatments and abstinence. (A) Images from the Mouse Brain Atlas of Paxinos and Franklin (2001) showing brain areas collected for this study: bilateral punches were taken from mouse brain coronal slices (1 mm thick) to collect the bed nucleus of stria terminalis (BNST, +0.5 to -0.5) and the Central nucleus of the Amygdala (CeA, -0.5 to -1.5). BNST and CeA punches were pooled and corresponded to central Extended Amygdala (EAc) samples (from Becker et al 2008). (B) qRT-PCR studies developed in 4 independent drug treatments. Results are expressed as fold change respect to vehicle groups \pm SEM. One-way ANOVA (Statistica 8.0) with treatment (drug or vehicle) as between subject factor, * $p < 0.05$, ** $p < 0.01$ ($n = 12-18$ mice/group for drug and vehicle groups on each treatment) (from Le Merrer, in revision).

A. Introduction

Drug addiction develops when recreational drug intake progressively evolves towards uncontrolled drug-taking. This transition involves a gradual adaptation of the brain to chronic drug use possibly by a restructuration of neural circuits. These modifications involve transcriptional reprogramming within neurons, leading to modifications of neuronal connectivity, cell signaling and synaptic plasticity (McClung & Nestler 2008; Rhodes & Crabbe 2005). Several studies have addressed the modifications in gene expression profiles triggered by chronic treatment with drugs of abuse within the dopaminergic mesocortical system (VTA, NAcc and PFC). To expand this knowledge, our laboratory carried out a genome-wide transcriptional study on the central extended amygdala. As mentioned in the general introduction, this neuroanatomical entity has been involved in positive reinforcing effects of drugs of abuse as well as stress responses associated with protracted abstinence and drug reinstatement (Koob & Kreek 2007; Lu et al 2003; Shaham et al 2003; Waraczynski 2006). We have focused these studies on the mu-opioid receptor, a key molecular target for drug reward in the brain (Contet et al 2004). The study led to the identification of a collection of 132 genes modulated by excessive activation of this receptor upon a chronic morphine treatment (Befort et al 2008). Altogether, these mu-dependent genes potentially contribute to drug-induced neuronal plasticity underlying drug craving and relapse. Among them, CCK showed an interesting pattern of regulation upon morphine exposure. Specifically, CCK mRNA was down-regulated after chronic morphine treatment and a rebound up-regulation was observed after 4 weeks of abstinence (Figure 19). Therefore, to better understand the implication of this peptide in the development of drug dependence, we further examined CCK transcriptional regulation after a morphine treatment in other brain structures, including the cingulate cortex (Cg ctx) and the basolateral nucleus of the amygdala (BLA). Data from these studies are presented below in Part I of the thesis.

1. Involvement of Cg Ctx and BLA in drug dependence

The cingulate cortex (Figure 20) is part of the "grand lobe limbique" of Broca (1898) and is divided in an anterior part, forming a large region around the rostrum of the corpus callosum (with ventral and dorsal areas), and a more posterior part. This region has been

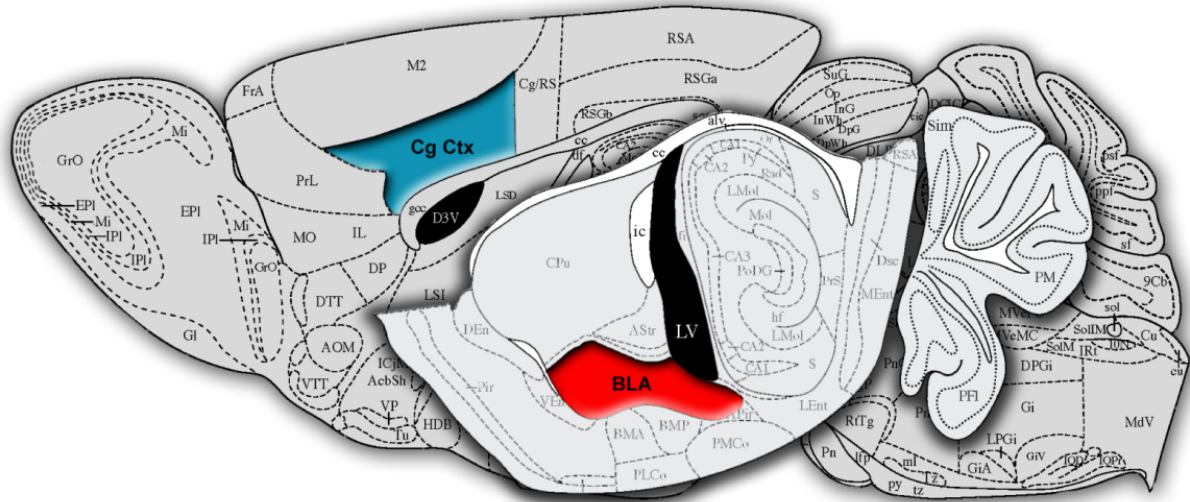


Figure 20: Schematic representation of Cg Ctx and BLA regions location in the mouse brain. Sagittal representation of mouse brain sections showing the location of the cingulate cortex region in blue (from bregma lateral 0.36mm) and the basolateral amygdala region in red (from bregma lateral 3mm).

proposed to be a specialization of the neocortex (Allman et al 2001) playing crucial roles in the initiation of goal-directed behaviors (Devinsky et al 1995). Studies on rats using a cost/benefit T-maze task and excitotoxic lesions of the prefrontal cortex (including prelimbic, infralimbic, and cingulate cortices) have demonstrated that these structures are critical for effort-based decision making, leading the animals to work harder in order to obtain greater rewards (Walton et al 2002). In addition, human studies on reward-based motor decision task were performed together with event-related fMRI (functional magnetic resonance imaging) in an attempt to elucidate the mechanism underlying Cg Ctx roles in cognition and motor control. Significant activation was observed in discrete groups of cells during the performance of the task, proving an initial support for the existence of heterogeneity in the Cg Ctx. The results suggested that distinct cells within this region are variously involved in anticipation and detection of targets, indication of novelty, motor responses, encoding of reward values, and signaling of errors (Bush et al 2002).

The basolateral amygdala is part of the amygdaloid complex, which is a heterogeneous group of subcortical nuclei located in the medial temporal lobe (Figure 20). Anatomy and function of this region has been previously described in the general introduction. Briefly, functional studies have long considered the amygdala as a structure specialized in mediating emotions, emphasizing roles in aversive processing associated with fear and anxiety. Within this line, stress has been postulated to induce amygdalar plasticity, affecting learning and memory processes (Roosendaal et al 2009). Moreover, BLA lesion studies in rats correlate this region with the storage of fear memory as measured by the fear-contextual conditioning paradigm (Gale et al 2004), and with increased anxiety-like behaviors as measured by the SI box and EPM tests (Truitt et al 2009). In the last years, however, evidence has also linked this complex to appetitive processing and positive emotions (Robbins et al 2008). Specifically, the BLA has a key role in the formation and storage of pavlovian learning (Maren 2001) and such role has been extended to the acquisition and retrieval of emotional memories in the context of drug addiction (Frenois et al 2005; Hellemans et al 2006; Wang et al 2008).

Together, the anterior Cg Ctx and the amygdaloid complex link drugs of abuse to motivational and drug relapse systems in the brain. Studies on animal models have involved the BLA in reward associative processes (Baxter & Murray 2002) and rat fMRI analyses have shown activation of the Cg Ctx during opioid precipitated withdrawal (Lowe et al 2002). Further analysis demonstrated that, as was presented in the general

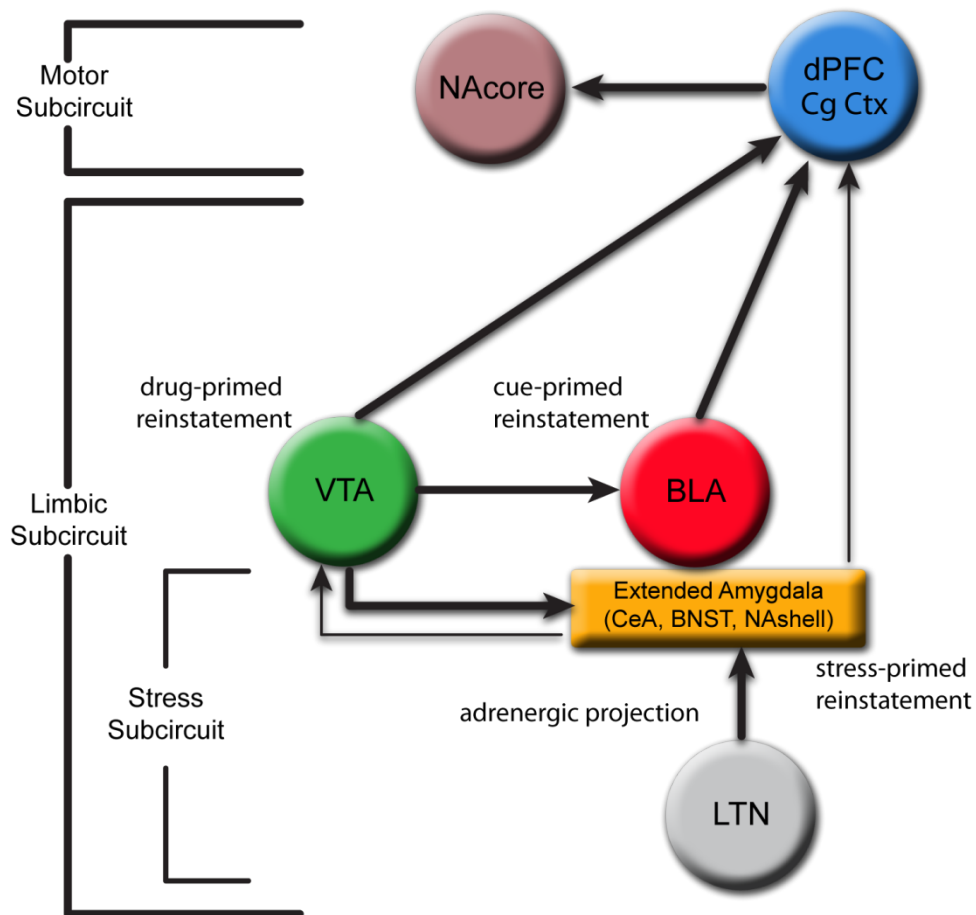


Figure 21: Involvement of Cg Ctx and BLA in drug-seeking. Schematic representation of the brain circuitry proposed by Kalivas and McFarland (2003) summarizing the structures and anatomical connections involved in drug-seeking behavior. **Abbreviations:** NAcore, nucleus accumbens core; dPFC, dorsal prefrontal cortex; Cg Ctx, cingulate cortex; VTA, ventral tegmental area; BLA, basolateral nucleus of the amygdala; CeA, central amygdala; BNST, bed nucleus of the stria terminalis; NAshell, nucleus accumbens shell; LTN, lateral tegmental nucleus. Lighter lines represent theoretical links not experimentally confirmed.

introduction, both regions are involved in the neuronal circuitry associated with the preoccupation/anticipation stage of the addiction cycle (Koob 2009). This stage involves the processing of conditioned reinforcement in the BLA while the executive control depends on the prefrontal cortex (orbital, medial and cingulate) and includes representation of contingencies and subjective states associated with drugs (i.e., craving) (See [Figure 3](#) General Introduction). Indeed, human neuroimaging studies (fMRI technique) have shown that the prefrontal cortex (orbitofrontal, medial prefrontal, prelimbic/cingulate) and the BLA are critical structures in cue- and drug-induced craving (Franklin et al 2007; Goldstein et al 2007). Consistent with these results, studies on animal models of cocaine self-administration have proposed the amygdala as a key regulator of relapse evoked by contextual or discrete stimulus-reinforcer associations, while the anterior cingulate and orbitofrontal cortices are critical regulators of contextual drug-conditioned stimuli as well as drug-primed relapse (Fuchs et al 2005; See 2002). Kalivas and McFarland (2003) propose a hypothetical circuitry to explain these distinct but partially overlapping neural substrates mediating drug reinstatement. As represented in [Figure 21](#), in their model, the BLA was associated with cue-primed reinstatement, the ventral tegmental area with drug-primed reinstatement and the adrenergic innervations of the extended amygdala with stress-primed reinstatement. Also, they postulated that all three priming modes may converge on the anterior Cg Ctx and have a final common output through the nucleus accumbens, another brain region critically involved in the rewarding properties of drugs of abuse and the relapse to drug-seeking behavior.

2. The autoradiographic film quantification technique

For this study we have developed a quantitative autoradiographic (QAR) mapping methodology, which conjugates *in situ* hybridization (ISH) with radioactive labeled-probes, film autoradiographic development, and densitometric image analysis.

Densitometric principles were described in the 16th century by Bouguer and Lambert who analyzed the loss of radiation (or light) in passing through a medium. Later on this field, in 1852, Beer established the physic law of exponential absorption of solutions conforming the fundamental concept for understanding QAR. Beer's law states that the absorption of light by different concentrations of a solute is an exponential function of that concentration (Ingle & Crouch, 1988). However, as is well described by Baskin and Stahl (1993), in the case of QAR such conditions are only approximated ([Figure 22A](#)). Given an

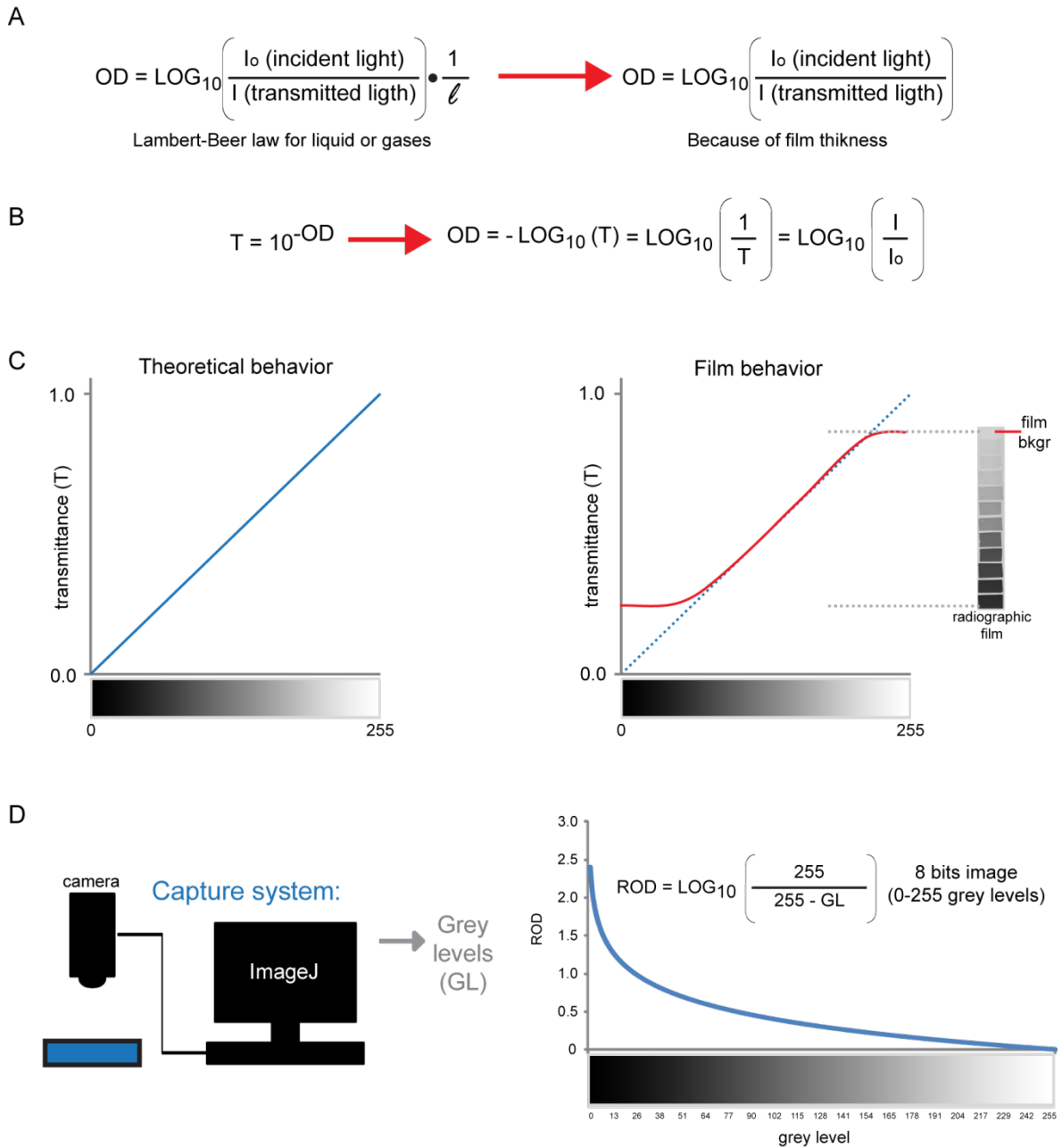


Figure 22: Fundamentals of densitometric image analyses. (A) Lambert-Beer’s law for light absorption and its adaptation for radiographic films. (B) Relation of Transmittance and Optical density. (C) Curves showing grey levels (256: 8-bits) vs Transmittance, left panel: ideal behavior, right panel: film behavior. (D) Left panel: scheme of the image acquisition system, right panel: “uncalibrated” transformation of grey levels into Relative Optical Density (ROD).

autoradiographic image, the absorption of light occurs through the autoradiographic film and the concentration is referred to the amount of radioactive probe present in the tissue rather than in the image itself. Consequently, the concentrations of interest are an indirect function of the light absorption and will depend on the image acquisition and the film response. Regarding to the image acquisition system, it is not possible to measure Optical Density (DO) values directly and the frame grabber pixel values are linear with respect to Transmission (T) (Figure 22B). In reference to film response, the increasing concentrations of radioactivity result in increasing grey level but his film's response is not completely linear, it approaches linearity only over small ranges of radioactivity, as observed in Figure 22C. Moreover, the density of autoradiographic film depends on the isotope used, tissue properties, section thickness, time of exposition, type of film, and film processing. Therefore, a fundamental problem in QAR is to relate the film density of the autoradiographic image to calibrated units that are biologically meaningful.

Consequently, developing the correct calibration method for quantification is a key step of radioactive ISH analysis. To achieve this objective two possibilities of processing are available in computer densitometry: *i*) conversion of the grey levels obtained by the digitized images into optical density values, either by formulas of relative (uncalibrated) optical density (Figure 22D) or by calibration against a standard optical density tablet; or *ii*) conversion of grey levels into units of radioactivity by calibrating against brain paste or membrane standards scales of known amounts of radioactivity concentration (Lazic 2009). Besides, other crucial step in QAR methodology is the sampling problem. The autoradiographic image is often relatively faint and the anatomic landmarks indistinct. Therefore, the definition of regions of interest (ROIs) and background are critically for ISH quantification. In this sense, different techniques have been summarized by Lazic (2009), including image segmentation by setting thresholds based on pixel intensity, and outline methods using hand drawing, template size selection or magic drawing tools of computer software. The selection of these two main parameters, calibration and sampling methods, depend on the size and shape of the structures to analyze, the level of expression of the interested gen in these structures, the characteristics of the image analyzers used (e.i., densitometric measure, spatial and grey scale resolution and processing speed) (Mize et al 1988), and the experimental design of the ISH procedure. The best compromise of all the characteristics will allow the more reliable quantification and comparative analysis,

making the autoradiographic mapping methodology a powerful tool for the study of gene expression regulation by the quantification of mRNA levels.

Altogether, the major advantages of the QAR methodology are the precise anatomical localization of the regions of interest and the delimited quantification of labeling intensity. Therefore, we used this particular technique for this study in order to measure changes in the expression pattern of CCK mRNA within the Cg Ctx and BLA upon a chronic morphine treatment.

B. Materials and Methods

Animals

Male C57BL/6J mice provided by Charles River (Lyon, France) were used for all the experiments. Mice were aged 8 weeks old at the beginning of the experiments and they were housed 3-4 per cage in a 12h dark/light cycle (light from 7am to 7pm), under controlled conditions of temperature and humidity. Food and water were available *ad libitum* except during the behavioral observations. Experimental procedures were conducted in accordance with the European Communities Council Directive of 24 November 1986 (86/609/EEC) and approved by the "Comité Régional d'éthique en matière d'expérimentation animale de Strasbourg" (CREMEAS, 2003-10-08-[1]-58).

Drugs

Morphine hydrochloride (Francopia) was dissolved in sterile isotonic saline (NaCl 0.9%). The doses refer to salt weight and were administered in a volume of 10 ml/kg.

Morphine treatment

Chronic morphine treatment was performed as previously described by Befort et al (2008). Briefly, mice were intraperitoneal (i.p.) injected twice daily (8am and 6pm) either with saline or escalating doses of morphine from 20mg/kg to 100mg/kg over 5 days. On day 6 in the morning, a last single administration of morphine (100mg/kg) was performed. Mice were sacrificed either 20 minutes after the last injection to analyze the morphine-dependent state, or left in their home cages for a 4-weeks drug-free period before sacrificed them to analyze the morphine-abstinent state.

CCK-cRNA probes preparation

DNA template for CCK cRNA-probes (258-600, 343bp) was generated by RT-PCR (Sigma, forward primer: 5'-CTGTACCCAAGCTTGATACATCCAGCAGGTCCGCAA-3', reverse primer: 5'-TTTCCTTGGAATTCAGGAAACACTGCCTTCCGACCAC-3') using total mouse brain RNA extracted by TRIzol reagent (Invitrogen, Cergy Pontoise, France) according to the manufacturer's instructions. The template was cloned into pcDNA3 (Invitrogen) and verified by sequencing. Sequence probe alignment was confirmed with BLASTN 2.2.18 software (<http://blast.ncbi.nlm.nih.gov>, NCBI). Next, CCK-cDNA plasmid (20µg) was linearized by enzymatic digestion of EcoRI for sense probe and HindIII for anti-sense probe, and linearized DNA (1µg) was transcribed using T7 or Sp6 RNA polymerases (Promega) for sense and anti-sense probes production respectively. For Dig-labeled probes, DIG RNA labeling mix 1X (Roche) was used according to manufacturer's specifications. Quality of the RNA was evaluated by agarose gel electrophoresis (RiboRuler Low Range RNA ladder, Fermentas) and concentration determined by spectrophotometry (Nanodrop Labtech ND-1000). For radiolabeled-probes, CTP- α ³⁵S radionucleotides (PerkinElmer) were added to the synthesizing mix. [³⁵S]-probes were purified by gravity-flow chromatography on illustra NICK Columns (GE Healthcare) and specific activity was measured using a topcount apparatus (Packard).

Tissue preparation

For histological analysis, mice were sacrificed by cervical dislocation and brains were rapidly removed and frozen in OCT (optimal Cutting Temperature medium, Thermo Scientific). The OCT-embedded brain blocks were stored at -80°C until use. Coronal brain sections (20µm) covering the whole brain were obtained using a cryostat microtome (Leica CM3500) at -20°C. Slides were mounted in Superfrost slides (Thermo Scientific), air-dried and stored at -80°C to be further processed by non-radioactive and radioactive *in situ* hybridization (see below).

***In situ* hybridization (ISH)**

Dig- and [³⁵S]-labeled RNA probes were used for ISH, following the methods previously described by Chotteau-Lelievre et al (2006). Briefly, fixed brain sections kept at -80°C were thawed at RT for 30 min and rehydrated in 1x PBS for 10 min. Sections were

then incubated at 65°C for 16h in a hybridization mix [formamide 50% (molecular biology grade, Sigma-Aldrich); dextran sulfate 10%; Denhardt's 1x; tRNA 1mg/ml (from Baker's yeast, Sigma-Aldrich); NaCl 300mM; Tris-HCl 20mM pH 6.8; EDTA 5mM; Na₂HPO₄ 5.4mM; Na₂HPO₄ 4.6mM; plus 10 mM DTT for radioactive ISH] with either Dig- or S³⁵-labeled RNA probes at the concentrations of 1.5ng/μl or 20,000 cpm/μl, respectively. DIG-labeled brain sections were afterward incubated with an alkaline phosphatase-labeled anti-DIG antibody (1:1500, Roche) in blocking solution [2% Roche blocking; 20% heat inactivated goat serum, MABT 1x]. Staining was performed with Nitroblue tetrazolium and bromo-chloro-indolyphosphate (NBT/BCIP) as color substrates by incubating the slides in staining solution [polyvinyl alcohol 0.5% (Sigma-aldrich); NaCl 100mM; Tris-HCl 100mM pH 9.5; MgCl₂ 50mM; Tween20 0.1%; NBT 0.35% (Roche); BCIP 0.35% (Roche)] at RT under light-protected conditions until the signal becomes visible (12h). Next, slides were washed 2x10 min (PBS 1x, 1mM EDTA), air-dried and mounted with Eukitt (VWR). To generate autoradiograms, [³⁵S]-labeled brain sections were exposed simultaneously with a [¹⁴C] standard (ARC 0146; American Radiolabeled Chemicals) to Kodak Biomax MR films (Sigma-Aldrich) at -80°C for either 3, 5 or 7 days. Films were developed with a Kodak MIN-R Processor (Carestream Health).

Image analysis

After ISH processing, Dig-labeled brain sections were observed on brightfield under a Leica microscope and images were recorded using a CCD camera (CoolSNAP, Roper Scientific). For atutoradiograms images, the analysis was performed as follows:

Autoradiographic film quantification

The quantification of autoradiographic signal was performed in a darkroom facility using a computerized image processing system including: a light box, a CDD camera, the CoolSNAP software and ImageJ software (<http://imagej.nih.gov>). Brain sections on film were individually captured at high resolution (600 dpi) generating 8-bit (256 grey level) digitized images. Regions of interest (ROIs) were bilaterally outlined using a polygone template tool of ImageJ. Mean gray values were measured within each ROI and transformed into relative radioactive counts by calibration with the co-exposed [¹⁴C] standard using a Rodbard non-linear regression curve (see below). The mean relative value was obtained referring the treated mice to the saline ones. Previously, background value of

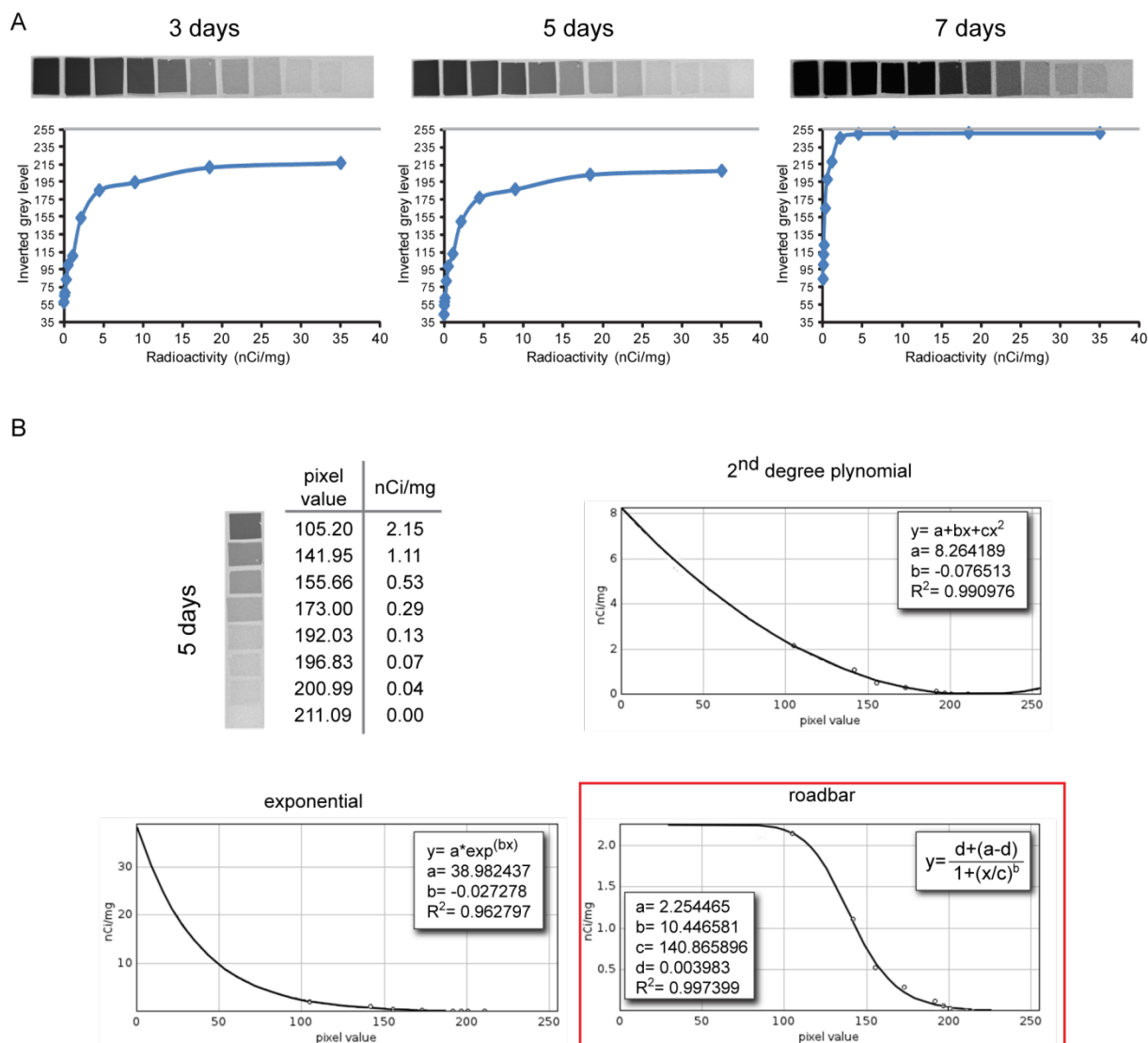


Figure 23: Calibration of densitometric curves of [¹⁴C]-standards scales. (A) Representative autoradiographic images of membrane [¹⁴C] scales and regression analyses evaluated after 3, 5, and 7 days of exposition to the Kodak Biomax MR films. (B) Standard regression curves for the 5 days exposure time point calculated using ImageJ software (<http://imagej.nih.gov>) covering a range of ~0.00-2.15 nCi/mg. Red square highlight the select 'best fit' rodbard non-linear curve (correlation coefficient of $r^2=0.9978$).

a same-size and shape area in the striatum of the same sections was subtracted from each ROI.

Calibration of imaging system and standard scale

For the conversion of grey level values into area-specific radioactivity values, membrane microscales of C^{14} were used. First, it was assumed that identical concentrations of radioactivity in brain sections labeled with $[^{35}S]$ -probes and in membrane scales resulted in identical grey level values in their digitized images (Vizi et al 2001). Thus, in order to allow reliable comparison of image signal between subjects, brain slices of treated and control mice were exposed together with the $[^{14}C]$ microscales in the same sheet of X-ray film, and 3 different exposure times (3, 5 and 7 days) were evaluated (Figure 23). Standard regression functions of measured grey values vs. the corresponding radioactivity values resulted in the densitometric curves, represented in Figure 23A (specific for the image system and conditions analyzed). An exposure time of 5 days was selected as optimal because it generates the best analytical range that maximize signal to noise ratio, preventing at the same time the optical density to reach the saturation limits. Afterward, we determined that grey levels from $[^{35}S]$ -labeled brain microsections at 5 days were included within the analytical range of ~ 0.00 - 2.15 nCi/mg and we evaluated different non-linear regression functions among this range using the ImageJ software (Figure 23B). The 'best fit' curve was the rodbard regression with a correlation coefficient of $r^2=0.9978$, therefore it was selected for accurate conversions of grey levels into nCi/mg radioactive concentration values.

Statistical analysis

Statistical analyses were performed with Graph-Pad Prism software v5 (www.graphpad.com) using unpaired Student's t-test (two-tailed) to compare morphine-treated vs. saline-treated mice in autoradiographic film quantification. Two mice were used for each experimental condition and for each mouse 10 to 12 adjacent brain sections were exposed to quantify CCK mRNA levels into Cg Ctx (given a total of 20-24 ROIs per mouse - bilaterally-), 8 to 10 were used for the BLA ($n=16-20$), and 4 to 5 for the BNST ($n=8-10$). All data are expressed as mean group value \pm S.E.M. and statistical significance was defined as $p \leq 0.05$.

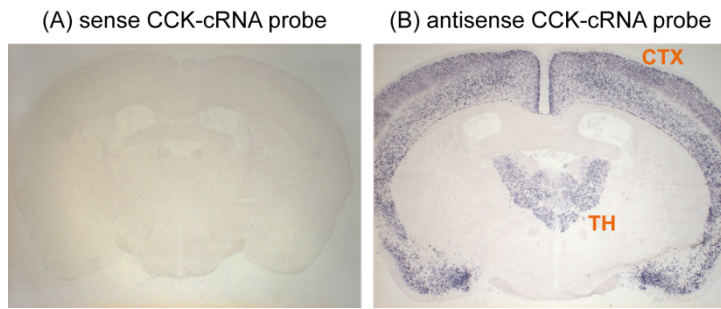


Figure 24: Validation of CCK cRNA probes specificity.

Representative brain microsections processed by nonradioactive-ISH showing Dig-labeling with either (A) sense CCK cRNA probe (no labeling detected) or (B) antisense CCK cRNA probe (labeling on CTX-Cortex and TH-Thalamus nuclei) on brightfield. Images from bregma -0.58/-0.70mm according to the Mouse Brain Atlas of Paxinos and Franklin (2001).

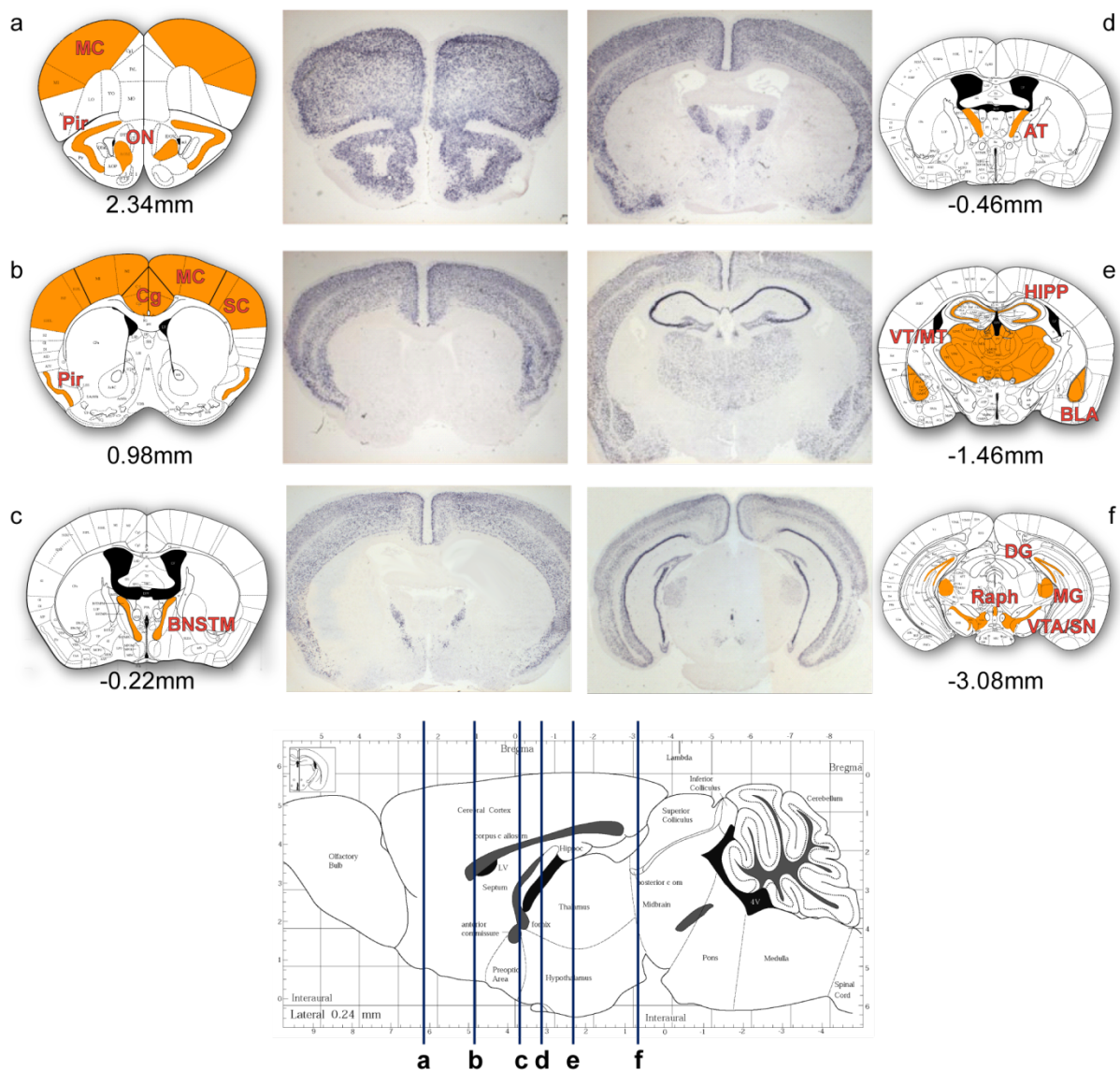


Figure 25: Mapping of CCK-mRNA distribution throughout the mouse brain. Representative brain microsections processed by nonradioactive-ISH showing dig-labeled CCK mRNA together with the corresponding images from the Mouse Brain Atlas of Paxinos and Franklin (2001) located in a schematic Sagittal section (from a to f). **Abbreviations:** ON, Olfactory Nucleus; MC, Motor Cortex; Pir, Piriform Cortex; SC, Somatosensory Cortex; Cg, Cingulate Cortex; BNSTM, Medial division of Bed Nucleus of the Stria Terminalis; AT, Anterior Thalamus nuclei; VT, Ventral Thalamus nuclei; MT, Medial Thalamus nuclei; HIPP, hippocampus; BLA, basolateral amygdala nuclei; DG, dentate gyrus; MG, medial geniculate nucleus; VTA, ventral tegmental area; SN, Substantia Nigra, Raph, Rostral linear nucleus of the Raphe.

C. Results

1. Mapping of CCK-mRNA expression in the mouse brain by *in situ* hybridization (ISH)

In order to confirm the *mcck* expression pattern in mouse brain reported by Jones et al (2009) on the Allen Brain Atlas (<http://www.brain-map.org/>), we first performed nonradioactive *in situ* hybridization (ISH) on brain sections of adult untreated mice. Previously, control experiments were carried out with both sense and anti-sense Dig-labeled probes. The results represented in [Figure 24](#) showed an intense and specific pattern of labeling on ISH of the tissue with the anti-sense *mcck* probe ([Figure 24B](#)) compared to that seen with the sense probe, where no labeling was detected on equivalent coronal brain sections ([Figure 24A](#)). Moreover, sense-slices showed similar background intensity than brain sections of negative control slides where no probe was added to the hybridization mix during the procedure ([data not shown](#)).

Representative images of the complete mapping of *mcck* expression revealed in the mouse brain are depicted in [Figure 25](#). A large number of cells that expressed moderate to high levels of CCK mRNA were observed in the olfactory nucleus, cerebral cortex, bed nucleus of the stria terminalis (medial division), several thalamic nuclei, hippocampus, dental gyrus, and basolateral amygdala nuclei. Less intense labeling was detected in the ventral tegmental area and only few cells were observed in the substantia nigra and rostral linear nucleus of the raphe. No signal was detected in the CeA. Therefore, the BNST region was included in the quantitative analysis, as a control to compare with our previous study carried out in the EA ([Figure 19](#) - Introduction).

2. CCK-mRNA expression pattern regulation upon morphine treatment

The effect of chronic morphine treatment on CCK mRNA levels was examined either immediately after the treatment or following 4 weeks of abstinence. Transcripts levels were quantified in the Cg Ctx, BNST and BLA regions by radioactive ISH and autoradiographic film analyzes based on the regions of interest (ROIs) showed in [Figure 26A](#). Relative *mcck* expression on saline and morphine treated mice are represented in [Figure 26B](#) for chronic treatment and [Figure 26C](#) for abstinent state. These experiments failed to confirm the regulation of the transcript detected in the BNST by previous studies on qRT-PCR. Although no statistical differences were found between groups in any of the

conditions or regions of interest, trends to an up-regulation of CCK mRNA expression were found after the abstinent period both in Cg Ctx ($p=0.0804$) and BLA regions ($p=0.0744$) (Figure 26C).

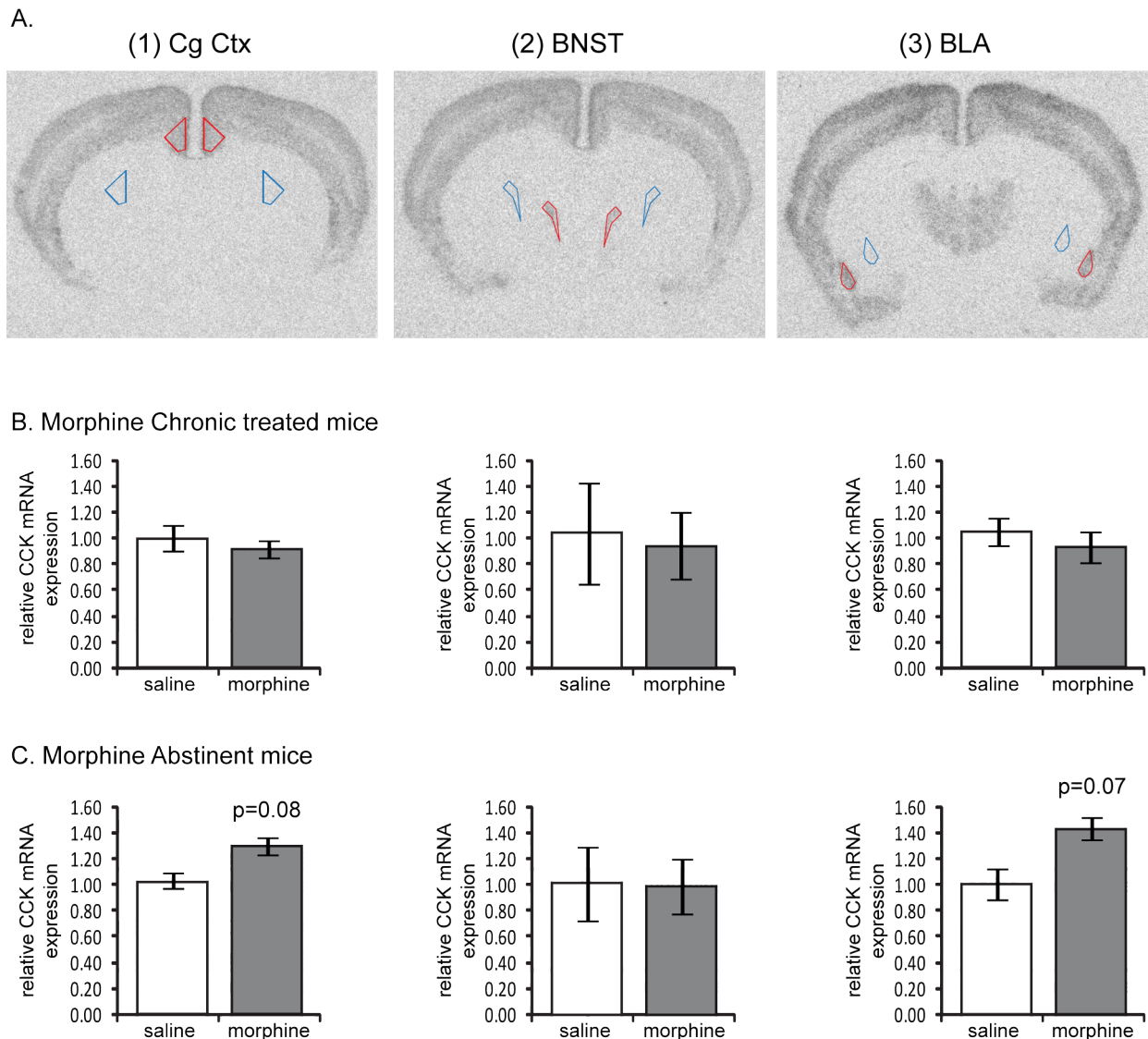


Figure 26: CCK mRNA expression is reduced 4 weeks after termination of a morphine treatment in Cg Ctx and BLA. (A) Representative autoradiographic images of brain microsections processed by radioactive-ISH showing drawing ROIs in red lines: (1) Cingulate Cortex region (from bregma 1.1mm), (2) Bed nucleus of the stria terminalis (from bregma -0.22mm), and (3) Basolateral nucleus of the amygdala (from bregma -1.22mm). In blue striatum background regions. (B-C) Relative mckk expression over these regions in saline control mice (white bars) and morphine treated mice (grey bars) sacrificed either (B) immediately after a chronic escalating morphine treatment (20 to 100 mg/kg, over 6 days) or (C) following a period of 4 weeks of abstinence. Quantification was performed using ImageJ software and a calibration curve of [14 C]-standards (ARC0146; American Radiolabeled Chemicals). A rodbard non-linear regression function was used to convert grey levels into counts of radioactivity (nCi/mg). Results are expressed in normalized mean values (ROI - Striatum background) \pm SEM. Student's t-test revealed no significant differences ($n=2$ mice/condition; ~ 20 ROIs for Cg Ctx, 5 ROIs for BNST and 8-10 ROIs for BLA).

D. Discussion

1. Methodological issues

In the course of the quantitative study we have experienced technical challenges mainly due to signal detection variability on the autoradiographic films and system calibration for reliable quantification.

Unspecific signal variability could be arise for several reasons in X-ray film quantification: overall signal intensity variation across different hybridized slides due to technical issues during the ISH procedure, heterogeneity of different parts of the film due to the exposition procedure, and preanalytic inconsistency due to the quality of the image acquisition system (Ambesi-Impiombato et al 2003). In order to diminish such variability, several technical considerations were carried out as following: *i)* During the ISH procedure, the hybridization mix was continuously homogenized to avoid unequal distribution of the probe over the tissue; *ii)* the hybridization step was perform in chambers humidify with 50% formamide (Fluka) in 1xPBS and vapors saturation was carefully verified to avoid unspecific probe binding in the tissue; *iii)* exposure cassettes were kept at -80°C during the exposition time to optimize the response by reducing latent image fading of the film, as recommended by the manufacturer; *iv)* before acquiring the autoradiogram images, the CDD camera and the light box were pre-warmed during approximately 30 minutes to stabilize light intensity; *v)* 8-bit (256 gray level) digitized images were captured at high resolution (600 dpi).

Moreover, special considerations need to be taken into account during the measurement procedures. On the one hand, we used polygone selection of the ROIs instead of image segmentation based on thresholding, which has been reported to be subject to floor-effects leading to biased results due to the exclusion of pixels with low values within the structure, reducing the range of the data. In addition, mean grey values were measured within each ROI without including its area in the calculation of gene expression given that this integrated values lead to a large loss of precision and can also introduce bias (Lazic 2009). On the other hand, we noted that the film background behave equally among different experiments, however, the background in brain sections can be easily affected, for instance, by the time of exposition. Therefore, we referred the mean ROI grey levels against the striatum because we have not detected CCK labeling in this brain region during

nonradioactive ISH mapping and previous studies on CCK mRNA expression on rat brains have reported only few positive cells in this region (Cain et al 2003).

Regarding the system calibration, given that multiple films are required to reach a significant number of brain microsections to evaluate, a common reference with [¹⁴C] standard microscaler was used to perform reliable comparisons. In this sense, we demonstrated the importance of the exposure time by evaluating 3 different time points. As developed in the methods description, five days of exposition together with roadbar function were finally selected to accurately convert grey level values into area-specific radioactivity values. This procedure allowed us to optimize the system by maximizing signal to noise ratio and preventing the optical density to reach the saturation limits.

2. CCK mRNA distribution in the mouse brain

Overall, the neuroanatomical distribution of CCK mRNA as determined here by non-radioactive ISH is in agreement with previous studies (Cain et al 2003; Ingram et al 1989; Jones et al 2009; Schiffmann & Vanderhaeghen 1991) where *mccr* was principally found in neocortex, piriform cortex, olfactory bulb, lateral and basolateral amygdala (BLA), dental gyrus, hippocampus, several nuclei of the thalamus, ventral tegmental area (VTA), and substantia nigra (SN).

For the cerebral cortex and thalamus, strongly-labeled positive cells were also detected by previous immunohistochemical studies which have suggested that CCK expression in these nuclei occurs in local interneurons as well as in projecting glutamatergic neurons (Meziane et al 1997). Such projections are thought to connect these two regions forming the thalamo-cortical CCKergic pathway and also project from the cortex to the striatum forming the cortico-striatal CCKergic pathway (Hokfelt et al 2002).

We also detected high expression levels of CCK mRNA in the hippocampus and BLA regions, which have been proposed to be located mainly in GABAergic neurons (Ghijssen et al 2001; Jasnow et al 2009).

The absence of labeling detection in the nucleus accumbens (NAcc) was concordant with the lack of reports of ISH data in this region and with Meziane et al (1997) studies, reporting the NAcc as devoid of CCK cell soma immunoreactivity (CCK-IR). These studies as well as radioligand studies (summarized by Noble et al 1999) have considered NAcc as a main target of CCKergic projections arising from VTA and SN and conforming the dopaminergic nigro-striatal CCKergic pathway (Hokfelt et al 2002).

Other regions where we did not observe any labeling were the hypothalamus and caudate-putamen. Although first studies on CCK mapping reported mRNA containing cells in hypothalamic nuclei and caudate-putamen (Ingram et al 1989; Schiffmann & Vanderhaeghen 1991), these findings were not further confirmed by more recent analyses (Cain et al 2003; Jones et al 2009) which detected very few positive cells in such regions.

Finally, our results show strong CCK mRNA expression in the medial division of the bed nucleus of the stria terminalis (BNST) and few positive cells in the rostral linear nucleus of the raphe, structures also observed on the Allen Brain Atlas (<http://www.brain-map.org/>) of Jones et al (2009). Interestingly, these two brain regions reported CCK-IR only provided when peptide transport was blocked prior to immunohistochemical study (Meziane et al 1997).

Altogether, the CCK transcript mapping presented in this study is in fully agreement with previous studies on mRNA and peptide distribution, reporting Cg Ctx, and BLA as two main expression sites for the peptide.

3. CCK mRNA regulation upon morphine treatment

In the second part of this study, we quantified changes in the expression pattern of CCK mRNA within the mouse brain after chronic morphine treatment, and found a trend for CCK mRNA up-regulation after 4 weeks abstinence in the Cg Ctx and BLA regions.

The regulation observed in previous qRT-PCR analyses on the BNST region was not confirmed by this study. This may be due to the difficulty in delimiting ROIs within this region. While for large and strongly labeled structures the technique used provides low between-sections variability, in the narrow area of BNST such variability was considerable increased. In addition, this structure covers a smaller number of brain microsections (4-5 sections *per* mouse), so that a greater number of mice may be necessary to achieve results comparable to the Cg Ctx (10-12 sections *per* mouse) and BLA (8-10 sections *per* mouse) regions. Thus, these results need to be confirmed with an increased number of mice.

The trend for CCK regulation in Cg Ctx and BLA is consistent with an earlier study in our laboratory, which established the existence of depressive-like symptoms in morphine-abstinent mice (Goeldner et al 2011). In addition, CCK receptor antagonists have reported antidepressant-like effects (Rotzinger et al 2010) and both Cg Ctx and BLA regions have been proposed as neural substrates for relapse behavior (See 2002). Therefore, CCK expressed in these structures may be involved on the development of the depressive

syndrome we observed in abstinent animals, facilitating the reinstatement to drug-seeking behavior (see Part II).

Noteworthy is the fact that the increased *mccck* expression seems detectable only after 4 weeks of abstinence, consistent with our previous data (Goeldner et al 2011) and the notion of “incubation” of the negative affective state in drug abstinence.

E. Conclusion and Perspectives

Altogether, we qualitatively confirmed the reported pattern of CCK mRNA expression in the mouse brain, and optimized a quantitative autoradiographic mapping methodology that allowed us to detect CCK transcript up-regulation in Cg Ctx and BLA regions on morphine abstinent mice. This methodology provides accurate measurements of gene expression in specific structures that could facilitate the understanding of modifications in gene expression profiles triggered by drugs of abuse throughout the mouse brain.

Our data from morphine treatment need to be confirmed by a larger number of samples. Moreover, in our previous study, CCK mRNA regulation was observed by qRT-PCR on nicotine studies as well. The transcript showed a down-regulation after chronic nicotine treatment using osmotic minipumps that was maintained following 4 weeks of abstinence (Figure 19 – Introduction). Therefore, we will perform a study to map and quantify changes in the CCK mRNA expression pattern upon chronic nicotine treatment through sites of CCK location. Very little is known about the role of this peptide in nicotine dependence. Previous data reported that CCK antagonist significantly decreased the symptoms of nicotine spontaneous withdrawal in rats by measured in the acoustic-startle test (Rasmussen et al 1996). Besides, polymorphism of the CCK gene have been postulated as one of the risk factors for smoking behavior (Iwahashi & Aoki 2009; Takimoto et al 2005). Therefore, it would be of great interest to assess CCK expression levels along the different stages of nicotine addiction in order to improve our understanding of the possible CCK roles on nicotine dependence.

III. PART II

“Emotional behavioral responses after AAV₂-shCCK-mediated knock-down in the mouse brain”

Summary

For this second part of my thesis, we designed a recombinant AAV-eGFP-shRNA viral vector to silence the *mcck* gene in the mouse BLA and investigate whether this local silencing would alter emotional responses. For this aim, I first optimized the viral delivery and local knockdown methodology in two brain regions; the BLA and the Cg Ctx. Here I will present analyses of the effects of CCK mRNA down-regulation into the BLA along several behavioral tests. The behavioral consequences of *mcck* gene silencing into the cortex would be characterized in future experiments. Therefore, this chapter is organized as follows:

1. Introduction.
2. Detailed methodology.
3. Technical optimization of the AAV-shCCK knock-down strategy and preliminary results targeting Cg Ctx and BLA brain regions.
4. Manuscript 1: “Genetic silencing of cholecystokinin mRNA in basolateral amygdala has anxiolytic and antidepressant effects in mice”. Del Boca C, Le Merrer J, Lutz PE, Koebel P, Kieffer BL.
5. Conclusions and perspectives.

1. Introduction

The possibility of increased *mcck* expression in cingulate cortex (Cg Ctx) and basolateral nucleus of the amygdala (BLA) of abstinent animals showed in the first part of this thesis is consistent with an earlier study in our laboratory, which established the existence of despair-like behavior in morphine-abstinent mice, when the physical signs of withdrawal have dissipated (Goeldner et al 2011). According with previous studies and this data, therefore, protracted abstinence is characterized by a global negative emotional state closely related with stress processing by expressing anxiety (Edwards & Koob 2010) and depressive-like symptoms. This negative state is classically alleviated by reinstatement to drug seeking, a major problem for drug abusers. Consequently, improved understanding of the neuronal mechanisms and emotional alterations involved in protracted abstinence and relapsing episodes consists an important step toward the treatment of drug addiction.

The anatomy and function of the amygdala, a main structure in emotional processing, has been addressed in the general introduction and Part I of this thesis. Previous studies

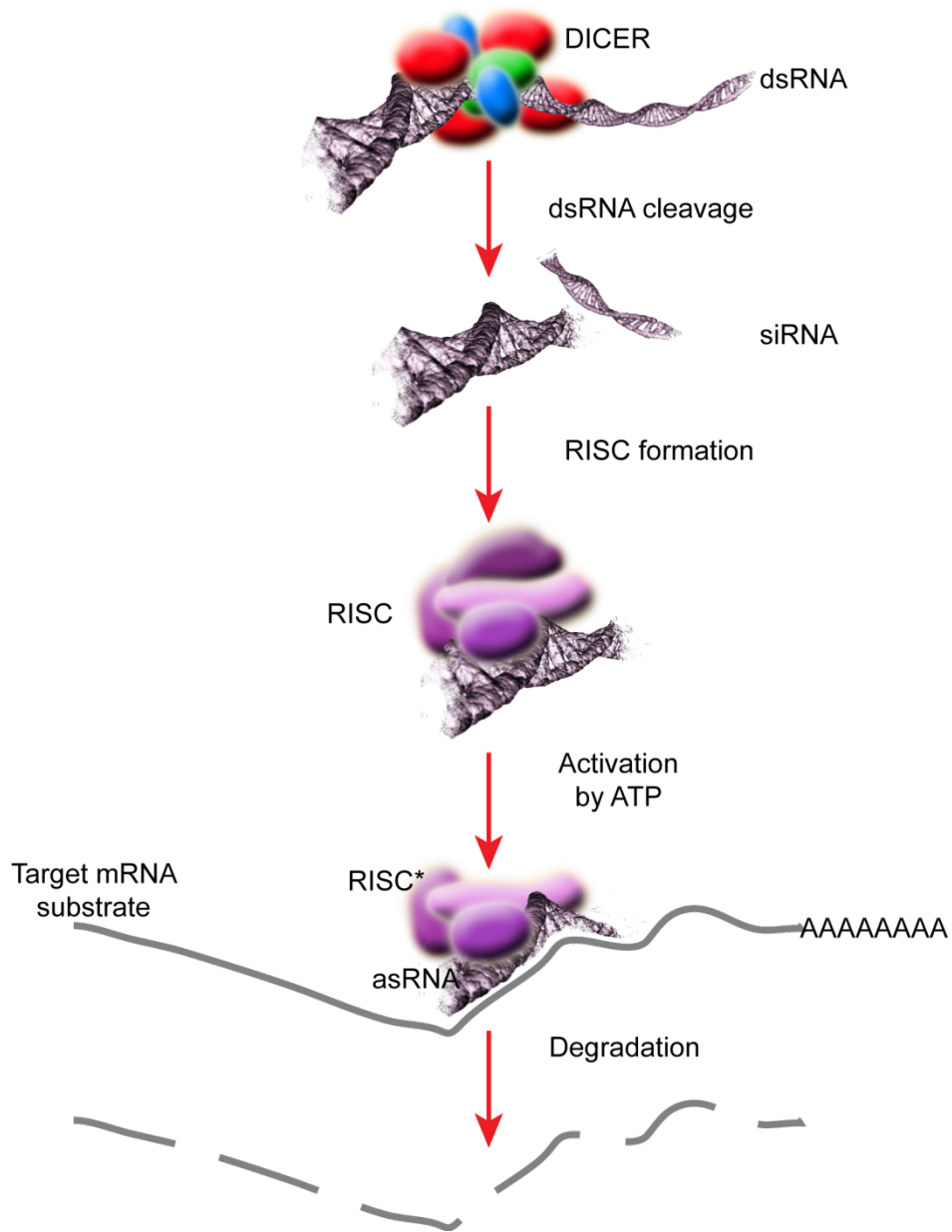


Figure 27: Molecular mechanism of RNA interference. 1°- RNase III enzyme DICER (a functional dimer containing helicase, dsRNA binding site and PAZ domains -Piwi, Argonata and Zwillie proteins-) binds to the dsRNA and cleaves into short fragments of ~21-23 nucleotides (siRNA). 2°- The RISC complex (a RNA-Induced Silencing Complex with endo- and exonuclease components) guide the siRNA to recognize homologous mRNA and degraded. (Adapted from Mocellin and Provenzano, 2004)

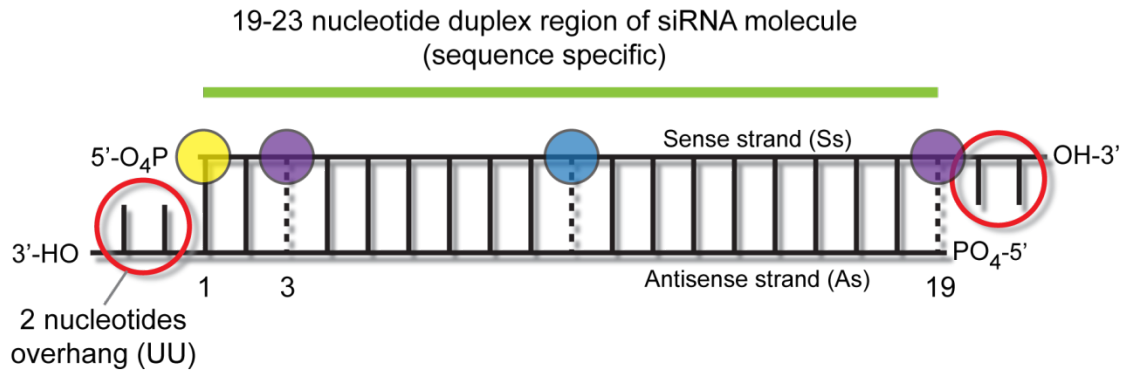
have reported this region, as an important part of the corticolimbic circuit underlying relapse to drug-seeking behavior (See et al 2003). Furthermore, Castro et al (2010) have shown that BLA lesions exerted anti-depressive behavioral effects on rats. It is well possible, therefore, and given the knowledge of CCK as an anxiogenic and depressant-like neuropeptide, that its increased mRNA expression particularly at the level of BLA, may contribute to the development of the depressive syndrome we observed in abstinent animals. Because the role of amygdalar CCK in emotional responses remains unclear, in this study we characterized the behavioral consequences of local CCK knockdown in the mouse BLA.

a) The shRNA knock-down technology

RNA interference (RNAi) is a conserved biological mechanism of post-transcriptional silencing of gene expression in eukaryotes. This process is related with the suppressing expression of potentially harmful segments of the genome, as well as the protection against invasion by transposons and viruses. The phenomenon was first observed by plant biologists in the late 1980s and ten years later, the underlying processing was elucidated by Fire et al (1998) in the nematode *Caenorhabditis elegans*. Afterward, the process was also experimentally documented in Zebra fish (*D. rerio*) (Wargelius et al 1999) and fruit fly (*D. melanogaster*) (Clemens et al 2000).

In the studies performed to elucidate molecular mechanisms of RNAi, two distinct steps were observed as is schematically represented in [Figure 27](#). Briefly, in the first step the RNase III enzyme DICER cleaves long dsRNA into short interfering RNA (siRNA) fragments of around 21-23 nucleotides, with 2 nucleotide 3'-overhangs. In the second step, a multicomponent RNA-induced silencing complex, containing endo- and exo-nucleases, is responsible for guiding the antisense-strand of the siRNA to recognize homologous mRNA and triggers its degradation (Mocellin & Provenzano 2004). In addition to these two steps, plants, worms and insects presented an amplification loop with an additional enzyme complex (RdRp: RNA-dependent RNA-polymerase). In this loop, the siRNA provides sequence-specific primers and the target mRNA is used as the template to produce large quantities of siRNA acting as an additional defense mechanism (Agrawal et al 2003).

The discovery that RNAi natural processes are capable to produce sequence-specific cleavage of a target mRNA converted this phenomenon in a powerful tool for artificial gene "silencing" in research. However, when testing the mechanism in mammalian cells,



- High stability of Ss at 5'-end prevents Ss entry to RISC hence inducing off-target effect
- "Adenosine" confers low stability to the nucleotide duplex
In position 3 that increase the efficacy of the siRNA
At the 5'-end promotes separation of As and Ss and As entry into RISC
- "Uridine" also confers low stability and in the middle of the sequence promotes the RISC-As mediated cleavage of mRNA
- CG ratio content between 45 and 55%

Figure 28: Basic structure of an effective synthetic siRNA. (Design adapted from Leung and Whittaker, 2005).

experimental studies showed that, unlike other organisms, accumulation of very small amounts of dsRNA results in an interferon (IFNs) response capable of producing a vigorous nonspecific shutdown of transcription and an overall block of translation, ultimately leading to apoptosis (Gil & Esteban 2000). In attempts to avoid this problem, Elbashir et al (2001) discovered that RNAi can be induced in mammalian cell lines through the introduction of synthetic dsRNAs sequences of 21-23 nucleotides long. These siRNAs avoid provoking the IFNs responses by being incorporated into the RNAi pathway further downstream, mimicking the products of the DICER enzyme. As a sequence-specific phenomenon, the effectiveness of siRNA silencing is dependent on the structure of these synthetic molecules, hence, the basic construction of effective siRNAs has been extensively analyzed and summarized by Leung and Whittaker (2005) as depicted in [Figure 28](#).

However, suppression of gene expression by siRNA is generally a transient phenomenon in mammalian cells due to the short half-life of these molecules. Degradation processes as well as dilution lead to recovery of gene expression usually after 96 to 120 hours or 3 to 5 cell divisions following transfection (Mocellin & Provenzano 2004). Gene silencing is, therefore, dependent on the number of molecules transfected. An optimization of the technology was obtained by the construction of short hairpin RNAs (shRNA). In this small double-stranded RNA, sense and antisense strands are connected by a short loop sequence, giving more stability to the molecule (Paddison et al 2002).

Altogether, the potency and flexibility exhibited by RNAi in experimental systems has stimulated efforts to use RNAi-based reagents in the clinic as “molecular targeting” therapeutics to shut down disease-associated genes such as viral infections, cancer, and neurodegenerative disorders (Grimm & Kay 2007).

b) The viral delivery approach

The critical factor of *in vivo* RNA interference is the delivery of the siRNAs/shRNAs molecules into the system. A number of different approaches have been developed in this field, including rapid infusion by hydrodynamic injection, lipid based formulations, intravascular delivery, electroporation and intradermal administration (Leung & Whittaker 2005). Recently, several vector-based systems have been developed for siRNAs/shRNAs constructs delivery. These vector-constructs present several advantages. First, they allow a smoother synthesis of siRNA/shRNA in the cell compared to the transfection of numerous siRNA molecules necessary for other delivery systems. Secondly, the time of action of the

Viral vector	structure	size of DNA deliver	properties	drawbacks	principal uses	
Retrovirus	Retroviral vectors	single-stranded RNA	7-8kb of foreign DNA	<ul style="list-style-type: none"> Based on Murine stem cells virus Infect dividing cells Stable genomic integration 	<ul style="list-style-type: none"> Risk of mutagenesis and carcinogenesis 	Suppress gene expression in stem cells
	Lentiviral vectors	two copies of a single-stranded RNA	9kb of foreign DNA	<ul style="list-style-type: none"> Based on HIV-1 human virus Infect dividing a non-dividing cells Stable genomic integration (without risk of insertional mutagenesis) 		Generate transgenic animals
Adenovirus	Adenoviral vectors	double-stranded DNA	8 up to 30kb of foreign DNA	<ul style="list-style-type: none"> Infect dividing cells Robust expression Ease and effectiveness vector production 	<ul style="list-style-type: none"> Strong immunogenicity Short gene/siRNA expression duration Don't integrate into the genome 	Gene therapies of cancer
Parvovirus	Adeno-associated viral vectors	single-stranded DNA	5kb of foreign DNA	<ul style="list-style-type: none"> Infect dividing and non-dividing cells Mediates persistent gene/siRNA expression Integrates specifically 		<i>in vitro</i> and <i>in vivo</i> silencing

Table 4: Vector-based systems for RNAi delivery. Characteristics of different viral vector used to facilitate an efficient delivery and stable expression of siRNA/shRNA constructs in mammalian cells (From: Dillon et al, 2005; Grimm and Kay, 2007; and Leung and Whittaker, 2005).

RNAi lasts much longer since the vectors can be stably integrated into the genome of recipient cells (Yu et al 2002). Finally, expression of these vectors can be controlled by inducible elements, such as that used on CRE-lox-based strategy, to achieve temporally and spatially control knockdown of genes of interest (Gao & Zhang 2007). From a molecular point of view, vector-based systems contain RNA polymerase III promoters that express either sense and antisense strands separately (siRNA tandem type) or stem-loop constructs encoding shRNAs that are later cleaved by DICER to produce siRNAs into the cells (shRNA type) (Leung & Whittaker 2005). Although both techniques have demonstrated to be useful, a comparative analysis reported by Miyagishi and Taira (2002) has suggested that shRNA system is more effective than tandem system in gene silencing activity.

Within this frame, several recombinant viral vectors have been evaluated as vector-based systems for RNAi delivery (Table 4). Among them, the Adeno-Associated Viral (AAV) vectors are relatively new members with interesting advantages.

AAV are replication-deficient parvoviruses, which have traditionally required co-infection with helper adenovirus or herpes simplex virus for productive infection and replication. Consequently, despite high seroprevalence in the human population, AAV virus has not been linked with any human disease (Goncalves 2005). Two of the attractive advantages of this system on animal experimentation and gene therapy are these biosafety features and the demonstrated capability of transducing both dividing and nondividing cells *in vitro* and *in vivo*. Although vectors based on AAV can persist as episomes, its integration into the host cell genome often occurs at sites of actively transcribed genes and double-strand breaks (Mingozzi & High 2011; Russell 2003). Besides, the risk of integration-mediated mutagenesis is minimal possible due to the high probability of these integration events to occur into a specific region of chromosome 9 (McCarty et al 2004). Combining this advantage of potential integration with the lack of viral genes, rAAV vector offers a long-term transduction with minimal risk of immune response. Therefore, construction of recombinant AAV is emerging as one of the leading gene therapy vectors owing to its nonpathogenicity and low immunogenicity, stability and the potential to integrate site-specifically without known side-effects (Buning et al 2008). In this sense, the adeno-associated viral technology has been used for expressing non-coding RNAs in several tissues including brain, muscle or liver, as summarized by Danos (2008).

Following the establishment of the first infectious clone of AAV serotype 2 in 1982 (Samulski et al), exponential progress of AAV-based vectors has been made possible by the

Hierarchy of transduction efficiency in major tissues of AVV serotype vectors	
Tissue	Optimal serotype(s)
Liver	AVV1, AVV2, AVV6, AVV8, AVV9
Skeletal muscle	AVV1, AVV6, AVV7, AVV8, AVV9
CNS	AVV1, AVV2, AVV4, AVV5
Eye	
RPE	AVV4, AVV5
Photoreceptor cells	AVV5
Lung	AVV2, AVV5, AVV6, AVV9
Heart	AVV8
Pancreas	AVV8
Kidney	AVV2

Table 5: Tissue tropism of distinct AAV serotype vectors. Summary of main target tissues for optimal transduction efficiency of different AAV viral vector capsid serotypes. (Adapted from Wu et al, 2006).

isolation of several naturally occurring AAV variants. These serotypes differ in their viral capsid structure and, therefore, in the target cell surface receptors and intracellular processing. Wu et al (2006) have summarized the main features of AAV serotypes and established a general hierarchy of transduction efficiency as represented in [Table 5](#). Along the broad cell tropism of the AAV virus, several serotypes have revealed distinct patterns of transduction within the CNS. In general, while AAV4 appears to transduce specific cell types such as ependyma and astrocytes (Davidson et al 2000), AAV1, 2 and 5 vectors transduce mainly neurons with differences in local spread (Burger et al 2004). Markakis et al (2010) have demonstrated that AAV5 has the greatest efficiency among six AAV serotypes (from AAV1 to AAV6) analyzed in nonhuman primate brain. In these studies, AAV5 infected the most cells over the largest volume, and effectively transduced glial cells as well as neurons, whereas AAV2 showed greater tropism for neurons. Moreover, this latest serotype presented no-toxicity in studies performed on primary cortical cultures derived from rat embryos (Howard et al 2008).

Altogether, the development of efficient, stable and inducible viral vectors driving the expression of shRNAs has further expanded the application of RNAi both in tissue culture and animal models. Although RNAi-mediated gene knockdown cannot replace gene knockout approaches because the expression of endogenous genes is not completely repressed, this technology represents a powerful tool for functional gene studies. AAV-based vector delivery of shRNAs allows regional targeted studies in the CNS to uncover transcript regulation effects. Therefore, as mentioned before, we take advantage of this methodology to investigate the amygdalar CCK role in emotional responses.

2. Detailed Methodology

Animals

Male C57BL/6J mice provided by Charles River (Lyon, France) were used for all the experiments. See Methods on Part 1 for further details.

a) General procedure

- **Technical optimization of the AAV-shRNA strategy in Cg Ctx and BLA**

Experiment 1. Naïve mice were unilaterally injected with Chinese ink solution into either the Cg Ctx or the BLA regions in order to establish the stereotaxical coordinates to accurately reach the target regions.

Experiment 2. A total number of 30 naïve mice were unilaterally injected with AAV₂-eGFP into either the Cg Ctx or the BLA in order to determine the different conditions of the microinjection procedure (volume of injection, speed of injection, and latency to withdrawal the cannulae).

Experiment 3. 20 naïve mice were bilaterally injected into the Cg Ctx and BLA (left and right hemispheres, respectively) with either AAV₂-shCCK292 (n=8), AAV₂-shCCK601 (n=8) or AAV₂-eGFP (n=4) to analyze the silencing activity of the viral vector construction by a qualitative methodology (*in situ* hybridization with Dig-labeled cRNA probes). Two different time points were evaluated to confirm the stability of the produced CCK-knockdown (2 and 6 weeks following surgery; n=4/time point for the shCCK and n=2/time point for the negative control).

Experiment 4. 8 naïve mice were bilaterally injected with AAV₂-eGFP and AAV₅-eGFP into either the Cg Ctx or the BLA in order to evaluate and select the best viral serotype to target each region of interest.

Experiment 5. 2 naïve mice were unilaterally injected into the BLA with either AAV₂-shCCK601 or AAV₂-eGFP in order to preliminary evaluate the silencing activity of the viral vector construction by a quantitative methodology (*in situ* hybridization with [³⁵S]-labeled cRNA probes). Of each mouse 10 adjacent brain sections were exposed to the autoradiographic films and quantification of amygdalar CCK mRNA levels was performed using ImageJ software analyzer.

- **Evaluation of the effects of AAV2-shCCK-mediated knock-down in the BLA on emotional behavioral responses (Manuscript 1)**

Experiment 6. 56 mice (2 independent cohorts) were bilaterally injected into the BLA with either AAV₂-shCCK or AAV₂-shScramble (Cohort 1, n=16 mice/group; Cohort 2, n=12 mice/group) and 5 weeks later analyzed for emotional responses. Animals from the second cohort were processed only throughout tests for which a reliable trend for an effect was observed in the first cohort. 24 hours after the last behavioral experiment, all mice were sacrificed and brains analyzed for injection accuracy and viral spread.

Experiment 7. After behavioral testing, five mice for each experimental group (shCCK and shScramble) were used for quantitative validation of the AAV₂-shCCK silencing activity (*in situ* hybridization with [³⁵S]-labeled cRNA probes). Of each mouse, amygdalar CCK mRNA levels were quantified on 10 adjacent brain sections (autoradiographic image analyzes). Other 3 mice of each experimental group were processed for qualitative observation of the obtained down-regulation at this 9 weeks time point.

b) Materials and Methods

Drugs

Morphine hydrochloride (Francopia) and Naloxone hydrochloride (Sigma) were dissolved in sterile isotonic saline (NaCl 0.9%). For surgeries mice were anaesthetized using ketamine/xylazine (Virbac/Bayer, 100/10 mg/kg). All the doses refer to salt weight and were administered in a volume of 10 ml/kg.

- **AAV-shCCK vector-based strategy**

CCK-shRNA design

For the shRNA design, two target sequences were selected in the *mccck* gene by the SureSilencing™ shRNA designer (SuperArray) using accession number NM_031161. One of these selected sequences was inside the coding region of *mccck* gene: sh292 (5'-GCCGCATGTCCGTTCTTAAGA-3'), while the other one was in the untranslated region of the gene: sh601 (5'-TCAGTGACTCCCAGACCTAATGTT-3'). Recombinant AAV-eGFP-shCCK viral vectors expressing eGFP (enhanced Green Fluorescent Protein) and shRNA (short hairpin RNA) under the control of CMV (CytomégaloVirus) and mU6 (mouse U6) promoters

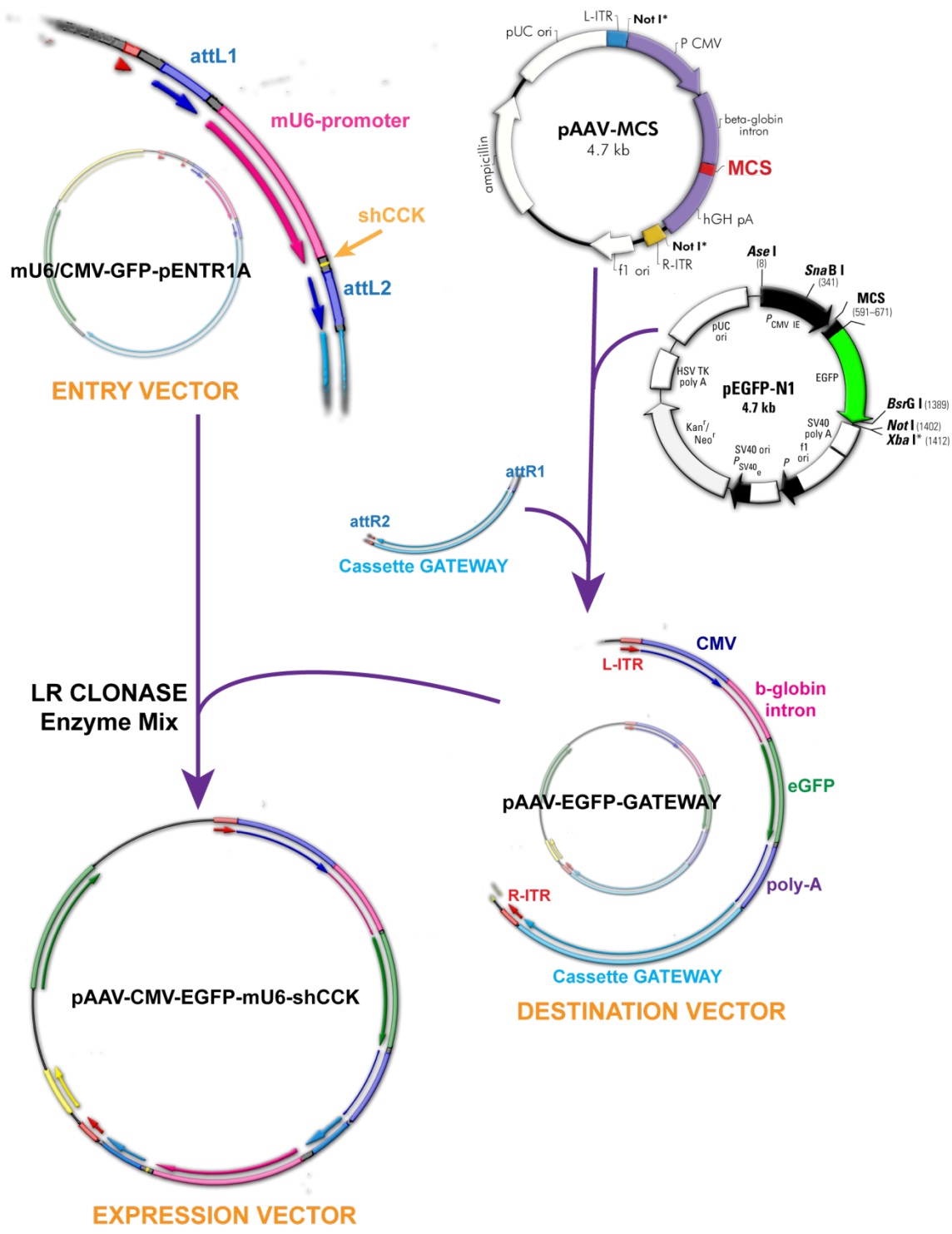


Figure 29: The Gateway cloning technology. Schematic representation of the recombination between an ENTRY vector, carrying the shRNA cassette, and a DESTINATION vector, carrying the eGFP cassette together with the ITR AAV DNA, leading to obtain the double CMV-U6 promoter-based EXPRESSION vector (see text for details)

respectively were generated in the IGBMC genetic engineering unit. Control vectors encode either for eGFP alone (AAV₂-eGFP) or for eGFP and a scramble shRNA (AAV₂-shScramble). The shScramble sequence (5'-GTTGGCTCCTAGCAGATCCTA-3') selected (<http://www.sirnowizard.com>, InvivoGen) has no match *in silico* in the mouse genome. The Gateway technology, schematically represented in [Figure 29](#), was used for the cloning strategy: On the one hand, the mU6 promoter and the sequence coding for the shRNAs were successively introduced into an entry vector pENTR1A (Invitrogen), flanked by the 2 attL recombination sites (attL1 and attL2). On the other hand, a pAAV-eGFP-Gateway destination vector was obtained by cloning eGFP from pEGFP-N1 vector (Clontech) downstream the CMV promoter and β -globin intron in pAAV-MCS vector (Stratagene). Afterward, the Gateway reading frame cassette A (Invitrogen) flanked by the 2 attR recombination sites (attR1 and attR2) was introduced downstream the poly-A sequence on the same vector. Then, the entry vector pENTR-shCCK was recombined with the destination vector pAAV-eGFP-Gateway by using the Gateway LR Clonase II system (Invitrogen).

Viral vector production and purification

rAAV2/2 and rAAV2/5 vectors were generated by triple vector transfection of AAV-293 cell line (Stratagene). Briefly, cells were transfected with pAAV-eGFP or pAAV-eGFP-shRNA containing all the *cis*-acting elements necessary for the replication and packaging (ITR) and 2 auxiliary plasmids. The first auxiliary plasmid contained *rep* (replication) and *cap* (capsid) genes of the adeno-associated virus provided *in trans*: pAAV-RC (Stratagene) provided the AAV genes of serotype-2 and pXR5 (a gift of R. Jude Samulski, PhD, UNC Vector Core) provided the AAV genes of serotype-5. The second auxiliary plasmid was a pHelper (Stratagene) that contains the adenoviral E2A, E4 and VA helper genes, while the fourth adenoviral helper gene E1 is provided by the cell line AAV-293 stably transfected. Following 2 days after transfection, cells were collected, lysed by three freeze/thaw cycles in dry ice-ethanol and 37°C baths, further treated with Benzonase (50U/ml, sigma) for 30 minutes at 37°C and clarified by centrifugation. Viral vectors were then purified by Iodixanol gradient ultracentrifugation (Zolotukhin et al 2002) followed by dialysis and concentration against Dulbecco PBS using centrifugal filters (Amicon Ultra-15 Centrifugal Filter Devices 50K). Physical particles were quantified by real time PCR using a plasmid standard pAAV-eGFP.rAAV. rAAV-shRNA titers in viral genomes *per ml* (vg/ml) were:

AAV₂-eGFP 1.5×10^{12} , AAV₅-eGFP 5.5×10^{12} , AAV₂-shCCK292 1×10^{11} , AAV₂-shCCK601 6×10^{11} , AAV₂-shScramble 3×10^{11} . To achieve comparable working concentrations viruses were diluted in Dulbecco-PBS buffer.

Stereotaxic surgery delivery

For the surgery procedures, mice were anesthetized with ketamine/xylazine (100/10 mg/kg) administered i.p. in a volume of 10ml/kg. The skull was exposed and incisor bar adjusted such that bregma and lambda were at the same height. Unilateral and bilateral injections were performed according to the Mouse Brain Atlas of Paxinos and Franklin (2001). For this aim, a 5 μ l microsyringe (SGE Analytical Science, Australia) was mounted to a micro-drive pump (Harvard apparatus, France) and connected by a PE-10 polyethylene tubing (Harvard apparatus, France) to a stainless-steel injector needle (0.28mm external diameter).

- **AAV-shCCK silencing activity evaluation by *In situ* hybridization (ISH)**

CCK-cRNA probes preparation

DNA template for CCK cRNA-probes (258-600, 343bp) was generated by RT-PCR (Sigma, forward primer: 5'-CTGTACCCAAGCTTGATACATCCAGCAGGTCCGCAA-3', reverse primer: 5'-TTTCCTTGGAATTCAGGAAACACTGCCTTCCGACCAC-3') as previously described in Part I.

Tissue preparation

For histological analysis, mice were sacrificed by cervical dislocation and brains were rapidly removed and frozen fresh in OCT (Optimal Cutting Temperature medium, Thermo Scientific). Afterward, OCT-embedded brain blocks were stored at -80°C until use. Coronal brain sections (20 μ m) were obtained by a cryostat microtome (Leica CM3500) at -20°C., using the Mouse Brain Atlas of Paxinos and Franklin (2001) as an anatomical reference (approx. from bregma 1.54mm to -0.22mm to cover the Cg ctx and from bregma -0.58mm to -1.82mm to cover the BLA). For Chinese ink solution injections, slides were mounted in Superfrost slides (Thermo Scientific) and processed by a cresyl violet acetate staining. For rAAV viral vector injections, slides were mounted onto Superfrost slides (Thermo Scientific), immediately fixed with 4% paraformaldehyde (PFA), air-dried and stored at -80°C until use. In the case of rAAV-shCCK injections for sequence selection, slides were

further processed by *in situ* hybridization (ISH) using digoxigenin(Dig)-labeled RNA probes.

***In situ* hybridization (ISH)**

Dig- and [³⁵S]-labeled RNA probes were used for ISH, following the methods previously described by Chotteau-Lelievre et al (2006) as previously described in Part I.

For autoradiographic film quantification, [³⁵S]-labeled brain sections were exposed either alone or simultaneously with a [¹⁴C] standard (ARC 0146; American Radiolabeled Chemicals) to Kodak Biomax MR films (Sigma-Aldrich) at -80°C for five days. Films were developed with a Kodak MIN-R Processor (Carestream Health).

Image analysis

For the determination of the stereotaxical coordinates, Chinese ink injection accuracy was examined on brain sections under a light microscope (Leica). For viral vector injections, fixed cryostat brain sections were analyzed using a Leica epifluorescent microscopy to analyze injection accuracy and viral spread. After ISH processing, Dig-labeled brain sections were observed on brightfield under microscope (Leica) and autoradiograms under bright lighting. All the images were recorded using a CCD camera (CoolSNAP, Roper Scientific).

Autoradiographic film quantification

For the quantification of autoradiographic signal, brain sections were individually captured at high resolution (600 dpi) generating 8-bit (256 gray level) digitized images. Regions of interest (ROIs) were bilaterally outlined with an oval template tool of ImageJ software (<http://imagej.nih.gov>) located in the basal part of the BLA, where the GFP signal was previously detected.

In a first pilot experiment where unilateral injections of AAV₂-shCCK and AAV₂-eGFP virus were performed, injected BLA was compared to non-injected contralateral BLA. For this, mean gray values (GL) were measured within each ROI and converted into relative (uncalibrated) optical density (ROD) (see also [Figure 22D PartI](#)) values by the following:

$$ROD = \text{Log}_{10} \left(\frac{255}{255 - GL} \right)$$

Background ROD values were subtracted from each ROI using a same-size and shape delimited area in the striatum of the same sections, because we have not detected CCK labeling in this brain region during nonradioactive ISH mapping and previous studies on CCK mRNA expression on rat brains have reported only few positive cells in this region (Cain et al 2003).

In next experiments, where bilateral injections of AAV₂-shCCK and AAV₂-shScramble virus were performed, comparisons were made between groups of injected mice. For this, mean gray values were measured within each ROI and transformed into relative radioactive counts by calibration with the co-exposed [¹⁴C] standard using a Rodbard non-linear regression curve. As recommended by Ambesi-Impombato et al (2003), other brain reference regions were analyzed within the same microsections and with the same size-shape oval template: *i)* a non-virally injected region, the retrosplenial agranular cortex (RSA), where CCK mRNA expression level was not affected by viral injection in the BLA (shScramble group: 0.0921 ± 0.0118 nCi/mg; sh-cck: 0.0942 ± 0.0087 nCi/mg) and, *ii)* a region lacking CCK mRNA expression, the striatum. Therefore, normalized values were obtained from mean radioactive measures by the following:

$$= \frac{BLA - \text{Striatum background}}{Cortex - \text{Striatum background}}$$

- **Behavioral testing**

Experimental design. We evaluated the effects of local shRNA injections into BLA in 4 categories of behaviors: anxiety-like behavior, despair-like behavior, aversive place conditioning, and withdrawal syndrome, starting 5 weeks after surgery. The design of the behavioral test battery represented in [Figure 30](#) was adapted from previous reports (Duangdao et al 2009; McIlwain et al 2001) and test were ordered from less to most stressful test as follows: elevated plus-maze (EPM), open field, light/dark box, forced swim, tail suspension, naloxone-induced CPA, and naloxone-induced withdrawal. Elevated plus-maze was placed at the beginning of the battery as recommended by Voikar et al (2004) since it is our most reliable test to measure anxiety and also a very susceptible test to the handling effects. The inter-test intervals were selected to allow the mice to fully recover between test and reduce the likelihood of previous test experience (Paylor et al 2006). A spaced 3-days interval was chosen between tests of the same category. Among categories, a

5-days interval was chosen to separate anxiety from despair behaviors while 7-days intervals were placed before and after the naloxone-induced CPA. The paradigm of place conditioning involves cognitive learning and depends on motivational state of the animals; both parameters could be sensitive to the test history (Voikar et al 2004). Moreover, this test implicates the injection of an aversive drug (naloxone); therefore, mice need more time to recover afterwards. All behavioral sessions were performed between 8am and 1pm.

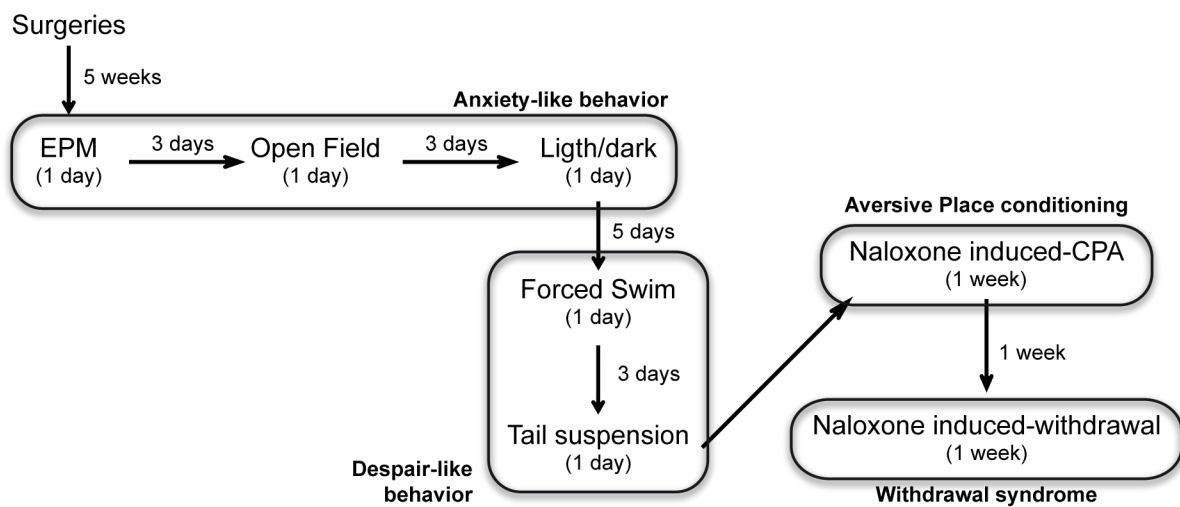


Figure 30: Behavioral testing. Schematic representation of the general procedure used to evaluate the effect of local shRNA-CCK injections into mouse BLA over emotional responses on two independent cohorts of mice.

For detailed description of each behavioral paradigm see Manuscript 1.

c) Statistical analysis

Statistical analysis were performed with Statistica software v8 (www.statsoft.com) and Graph-Pad Prism software v5 (www.graphpad.com). All data are expressed as mean group value \pm S.E.M. and statistical significance was defined as $p < 0.05$. Unpaired Student's t-test (two-tailed) was used to compare BLA injected side vs. BLA non-injected side and AAV₂-shCCK vs. AAV₂-shScramble injected mice in autoradiographic film quantification. As regards to behavioral experiments, a two-way ANOVA was used for EPM with Cohort and shRNA as between-group factors, and time spent in and number of entries to the open and closed arms as within-group factors. A one-way ANOVA was used in the forced swim test for Cohort 1 to compare immobility and latency time between injected mice, and a two-way ANOVA with

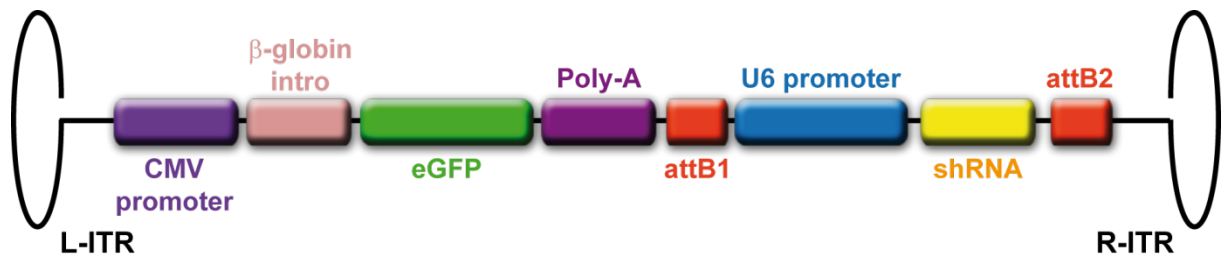


Figure 31: rAAV-expression vector. Schematic representation of the recombinant Adeno-Associated Viral vector constructed to down-regulate CCK-mRNA in the mouse brain. This vector contains an eGFP (enhanced Green Fluorescent Protein) cassette under the control of CMV (CytomégaloVirus) promoter and a shRNA (short hairpin RNA) cassette under the control of mU6 (mouse U6) promoter. The eGFP cassette has a β -globin intron to provide a better GFP expression and a Poly-A tail to end the protein transduction. The shRNA cassette is flanked by *attB1* and *attB2* sites remaining from the recombination procedure. Finally, the vector contains the inverted terminal repeats (L-ITR and R-ITR) from the adeno-associated viral DNA, which gives the secondary structure necessary for viral replication.

repeated measures for bin comparisons. In cohort 2, a two-way ANOVA with repeated measures was used with shRNA as a between-group factor and days/bins as a within-group factor. For both cohorts, significant main effects were followed by post-hoc test (Newman Keules). Place conditioning data were analyzed using a three-way ANOVA with Cohort, shRNA and treatment as between-group factors and session (pre- vs. post-conditioning) as within-group factor. Data from the scoring of somatic signs of withdrawal were analyzed using two-way ANOVAs with treatment and shRNA as group factors. One-way ANOVA were also used to analyze the data from the open field, light/dark box and tail suspension tests. Extreme studentized deviate (ESD) method was used to determine significant ($p < 0.05$) outliers.

3. Technical optimization of the AAV-shCCK knock-down strategy and preliminary results targeting Cg Ctx and BLA regions

- Double CMV-U6 promoter-based vector strategy

As has been developed in the introduction, vector-based systems are able to introduce *in vivo* stable siRNA promoter-driven expression in mammalian cells (Leung & Whittaker 2005). For the present study, we have designed rAAV vectors containing individual cassettes that codify for both eGFP and shRNA expression (Figure 31). In this double promoter system, the eGFP, allowing for detection of infected neurons, is under the control of cytomegalovirus immediate-early (CMV) promoter; while the shRNA, inducing post-translational gene silencing, is under the control of mouse U6 (mU6) promoter.

CMV is a RNA polymerase II promoter which synthesizes precursors of mRNAs. This promoter has demonstrated the ability to give strong expression of target genes in a variety of mammalian cell types (Cheng et al 2004). Most of the *in vivo* studies that have been performed using AAV₂ vectors containing CMV promoter have showed high efficiency and long-term gene expression (up to 1 year) (Tenenbaum et al 2000). Moreover, several studies converged to conclude that rAAV₂-based vectors using the CMV promoter almost exclusively transduce neurons when delivered into the rodent CNS (Tenenbaum et al 2004). Howard et al (2008) have examined the tropism (by GFP expression) of different AAV serotypes at 2 time points and demonstrated that 2 days post-transduction, for all serotypes the infection was predominantly glia, however, by 6 days post-transduction, the

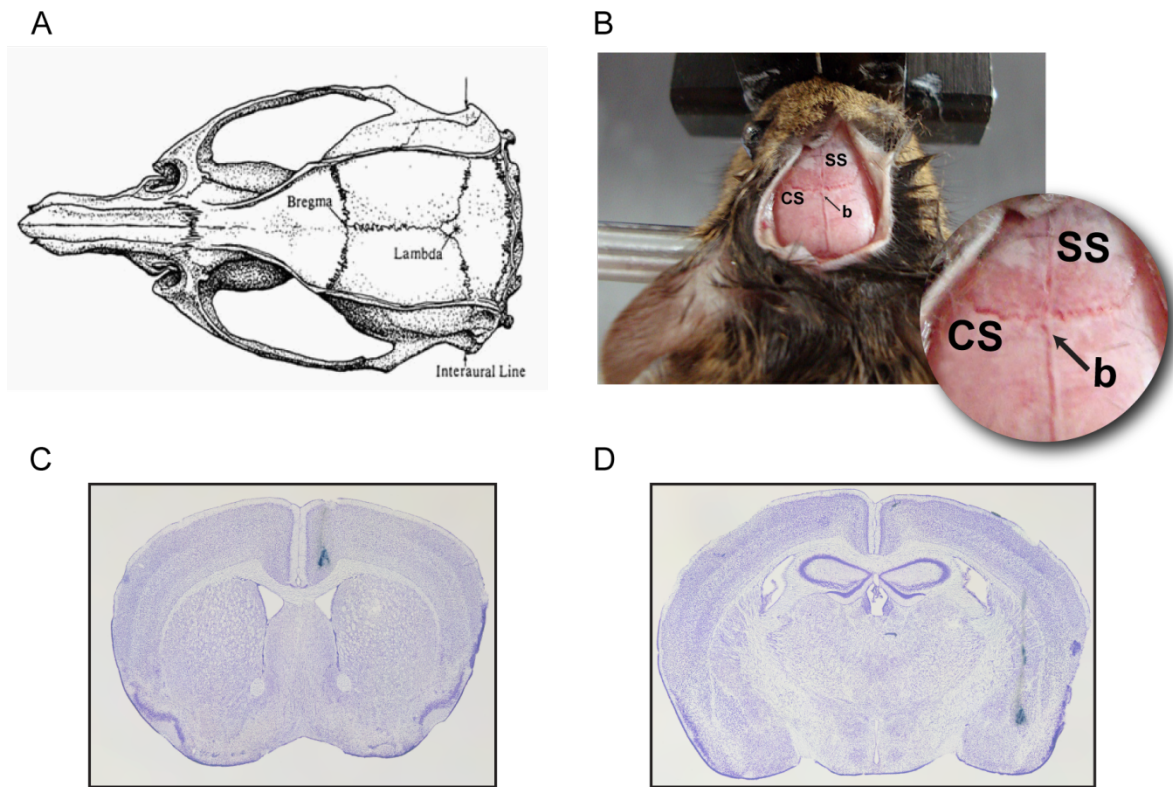


Figure 32: Selection of stereotaxical coordinates to target Cingulate cortex (Cg Ctx) and basolateral nucleus of the amygdala (BLA) of the mouse brain. (A) Diagram of the dorsal surface of the mouse skull showing the horizontal plane reference points: bregma, lambda and interaural line. (B) Picture of the head of a mouse during a stereotaxic surgery showing the Coronal (CS) and Sagittal Sutures (SS) of the skull and the Bregma (b) referent point. (C-D) Coronal brain microsections stained with cresyl violet acetate showing stereotaxical injections of Chinese ink solution. (C) Cg Ctx -from bregma: AP, 1.3mm; ML, ± 0.32 mm; DV, 2mm- and (D) BLA -from bregma: AP, -0.64mm; ML, ± 3.1 mm; DV, 5.15mm-.

Structure	Volume of injection (μ l)	Speed of injection (μ l/min)	Latency time to withdrawal the cannulae (min)	Number of mice	Representative image
Cingulate cortex	1.2	0.1	10	2	(undetected GFP)
	3	1.5	5	2	Fig 8. A1
	0.5	0.1	5	2	Fig 8. A2
	0.5	0.05	15	2	Fig 8. A3
	1	0.05	20	4	(excessive time surgery)
	2*	0.1*	10*	3	Fig 8. C
Basolateral Amygdala	0.25	0.05	10	2	(undetected GFP)
	0.5	0.05	10	2	Fig 8. B1
	1.0	0.1	5	2	Fig 8. B2
	1.0	0.2	15	2	Fig 8. B3
	0.5	0.05	20	4	(excessive time surgery)
	1.5*	0.1*	10*	3	Fig 8. C

Table 6: Evaluation of stereotaxic injection parameters. Different conditions for stereotaxic injections parameters tested with an AAV₂-eGFP viral vector (1×10^{11} vg/ml) in order to optimize the surgery procedure in Cingulate cortex and basolateral nucleus of the amygdala. The final selected conditions are indicated by a star (*).

GFP expression was largely located in NeuN-IR cells. Besides, mU6 is a RNA polymerase III promoter that naturally produces a variety of small and stable RNA species and has demonstrated high activity in mammalian cells (Paule & White 2000). Viral-vector based constitutive expression of shRNA by U6 has been shown to result in stable and efficient suppression of target genes (Gupta et al 2004). Moreover, it has been demonstrated that U6 promoter is more efficient compared to other small nuclear promoters such as H1, leading to a more powerful knockdown persistent in the mouse brain for at least 9 months (Makinen et al 2006).

- **Setting up of the stereotaxic surgery procedure**

In order to establish the experimental conditions to reach regions of interest within the mouse brain, we first selected the appropriate target points in the mouse brain atlas of Paxinos and Franklin (2001). This atlas is based on a flat position of the mouse skull with three reference points (Figure 32A): Bregma, defined as the midpoint of the curve of best fit along the coronal suture; Lambda, defined as the point of intersection of the projection of lines of best fit through the sagittal and lambdoid sutures; and the midpoint of the interaural line, an hypothetical line that runs right between the ears. The coordinates to target Cg Ctx and BLA were adjusted according to our experimental determination of the bregma. This main stereotaxic reference point was located at the exact intersection of the coronal and the sagittal sutures (Figure 32B). Thus, in *experiment 1*, male C57BL/6J mice (weight range 24-29g) were injected unilaterally with Chinese ink solution into either Cg Ctx or BLA. Animals were sacrificed immediately after the surgery and the accuracy of the injections was evaluated in cryostat brain microsections. The selected coordinates are showed in Figure 32C-D.

When stereotaxic coordinates were optimized, AAV₂-eGFP (enhanced Fluorescent Protein) viral vectors were used on *experiment 2* to determine conditions of the microinjection procedure. The different parameters evaluated on this step were: the volume of injection (μ l), the speed of injection (μ l/min) and the latency time to withdrawal the cannulae after delivery was completed (min). Several technical considerations were taken into account as suggested by Peterson (1998). First, the spread of a microinjected drug solution in the brain is dependent on both the volume administered and the speed of administration. On the one hand, a large injection volume leads to large spread of the solution, and this extend of viral spread depends on the volume size of the structure

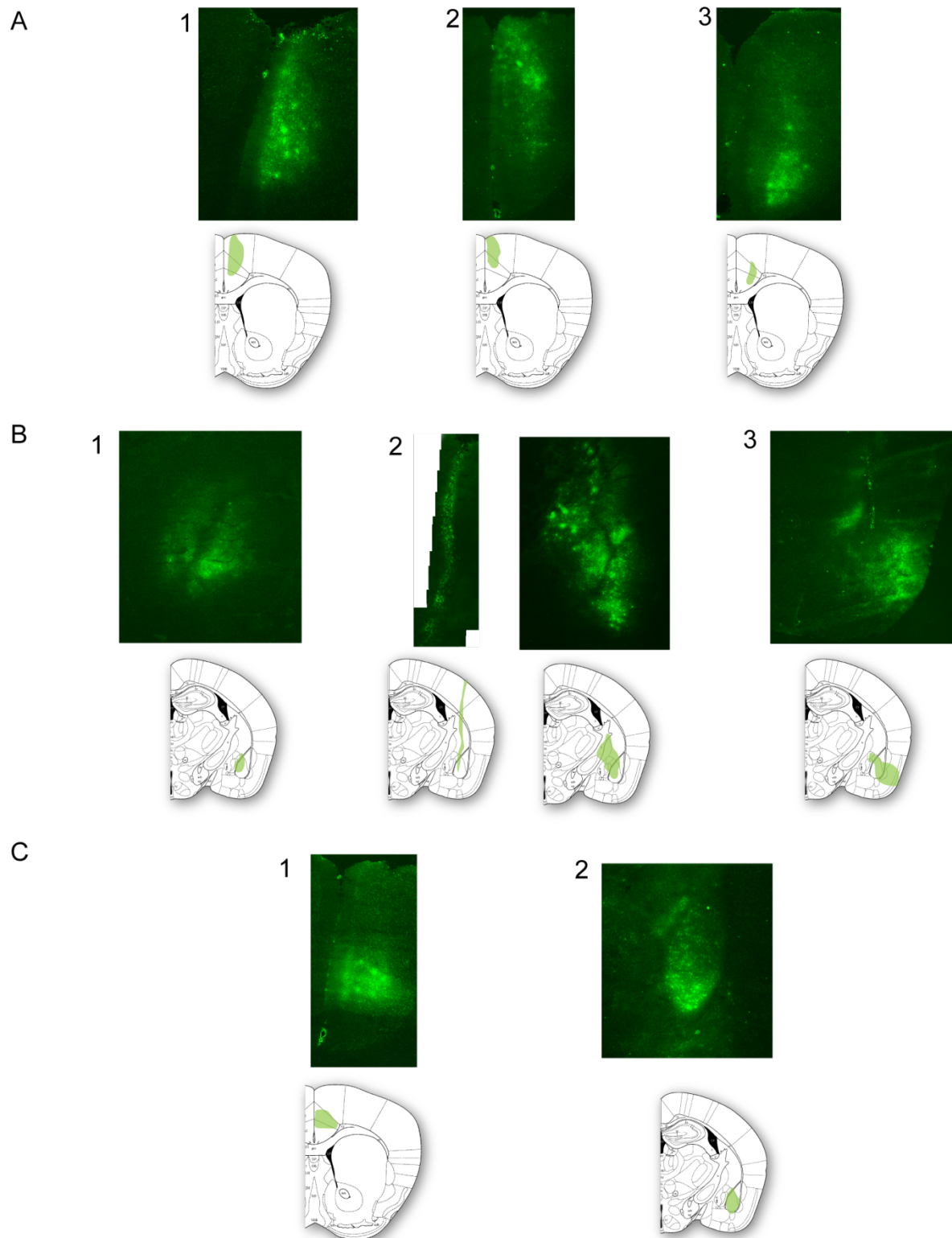


Figure 33: Evaluation of stereotaxic injection parameters. Representative pictures of coronal brain microsections showing eGFP expression illustrating the evaluated conditions from Table 6: (A) Cg Ctx (1) large injection volume and short latency time to cannula withdrawal, resulting in leaking of the viral suspension through the cannula tract, (2) small injection volume and short latency time to cannula withdrawal, also resulting in leaking of the viral suspension liquid, (3) small injection volume does not cover the target region. (B) BLA (1) small injection volume does not cover the target region, (2) small injection volume and short latency time to cannula withdrawal, resulting in the liquid leaking through the cannula tract, (3) small injection volume and fast speed of injection, resulting in the liquid spreading out of the target region. (C) Representative images of final selected conditions for the two target regions.

(Malpeli 1999). On the other hand, a fast injection speed leads to large spread, and also tend to distend and disrupt the target tissue. Finally, the latency to withdrawal the cannulae following injection impact on the treatment spread accuracy. Short latency times could result in solution leaking through the cannula tract, but long latency times may affect animals' health due to a long duration of the surgery and anesthesia. Therefore, different experimental conditions (Table 6) were tested on male C57BL/6J mice (weight range 24-29g) and GFP expression was analyzed after viral vector injection by fluorescent microscopy. Figure 33 illustrates the major problems evaluated in this step of the experimental design, and depicts also the best compromise between tested parameters leading to the best coverage of the target regions and avoiding infection of surrounding areas (Figure 33C).

- Selection of the shCCK sequence producing the best silencing activity

The efficiency of a small interfering RNA (siRNA) to down-regulate specific gene expression *in vivo* is variable depending on a number of sequence-governed and structural parameters of the siRNA duplex (Overhoff et al 2005). Several considerations have been proposed to increase the probability of producing an effective siRNA. The first critical variable is the gene target site. Generally, it is recommended to choose target sites located at least 100-200 nucleotides from the AUG initiation codon and to avoid targets within 50-100 nucleotides of the termination codon (Mocellin & Provenzano 2004). The 5' and 3' untranslated regions (UTRs) represent a controversial point, some authors strongly recommend to avoid target sites within these sequences since associated regulatory proteins might compromise the efficiency of the siRNA (Schubert et al 2005). Despite that, other reports have shown effective RNA interference targeting UTRs sequences (Anthony et al 2009; Tschuch et al 2008). As is currently impossible to predict the degree of gene knockdown produced by a particular siRNA, the next step of our optimization was to test 2 different target sites according with the previous recommendations. One of these selected sequences was inside the coding region of *mccK* gene on nucleotide position: 292-311 (named AAV₂-shCCK292), while the other one was in the untranslated region of the gene on nucleotide position: 601-624 (named AAV₂-shCCK601) (Figure 34A). In order to avoid cross reaction with unwanted genes, specificity of both siRNAs was confirmed by performing sequence alignment using BLASTN 2.2.18 software (<http://blast.ncbi.nlm.nih.gov>, NCBI).

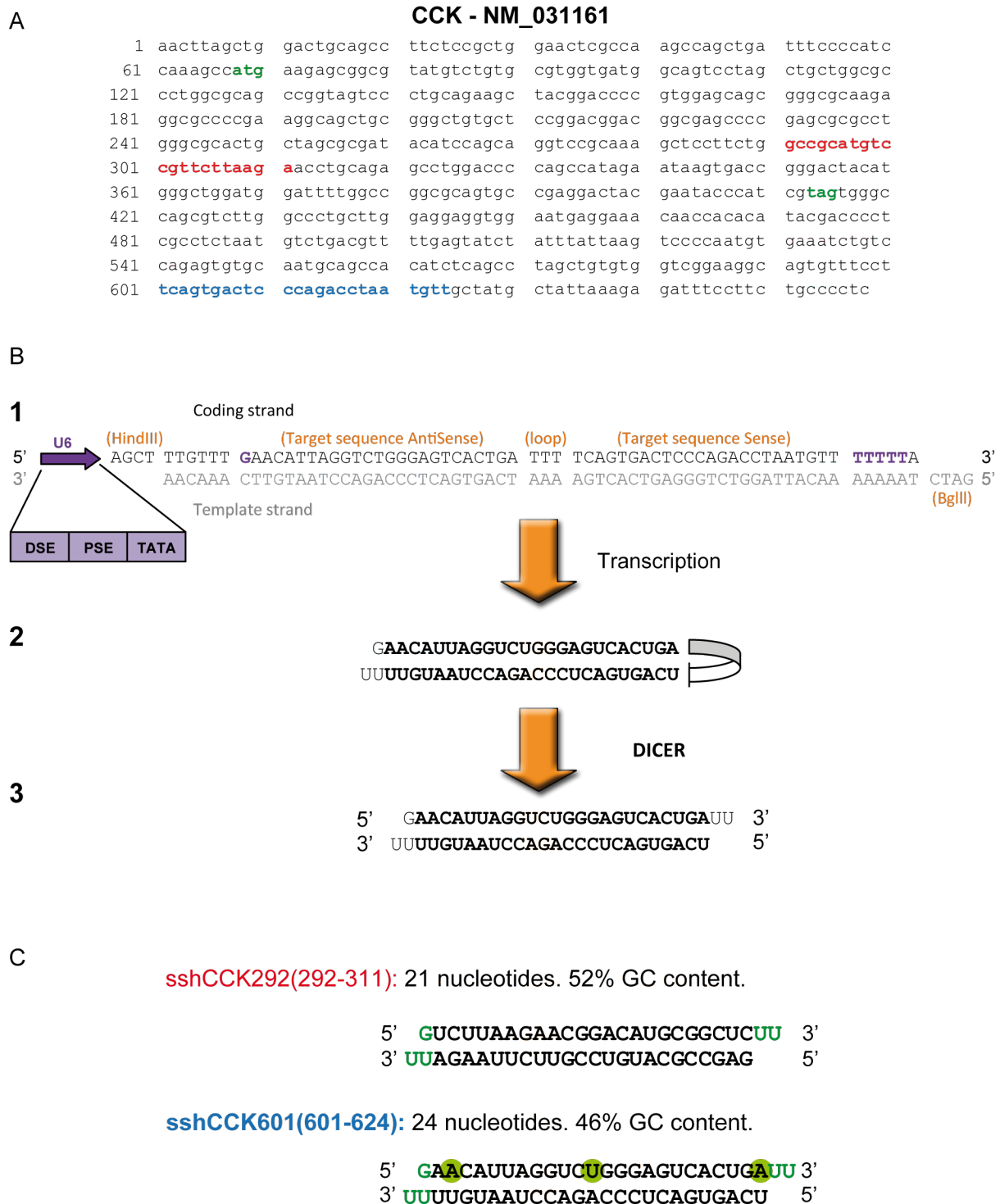


Figure 34: Sequence structure design of shCCK. (A) *mcck* gene sequence -accession number NM_031161- showing the nucleotide position of the two target sites. AAV₂-shCCK292 in red and AAV₂-shCCK601 in blue. In green initiation and termination codons. (B) Flow diagram of the shCCK processing: (1) Sequence map of shCCK contained within the rAAV₂ vector, (2) shCCK transcript, (3) double stranded siRNA. (C) shCCK sequences highlighting in green the structural characteristics concordant with Leung and Whittaker (2005) recommendations, namely: 3'-d(UU) overhangs to increase efficiency; -d(A) in position 3 and at the 5'-end of the SS to increase efficacy and promote separation of the strands getting AS entry into the RISC complex; -d(U) in the middle of the SS sequence to promote the RISC-AS mediated degradation of mRNA.

Additionally, even though AAV viral vectors have shown to maintain gene expression over long periods of time (Kaplitt et al 1994; McCown et al 1996), it is necessary to determine onset and duration of siRNA induced mRNA knock-down for any given siRNA. The construct design used for this study (CMV-GFP, mU6-shRNA) has demonstrated silencing activity at 12 but not 6 days following delivery in the mouse brain (Hommel et al 2003). Therefore, on *experiment 3* we evaluated the efficiency of AAV₂-shCCK292 and AAV₂-shCCK601 viral vectors at 2 weeks after surgery and at the time point we plan to start future behavioral studies (6 weeks following surgery) in order to confirm the stability of gene silencing activity.

Male C57BL/6J mice (weight range 24-29g) were bilaterally injected into Cg Ctx (Figure 35) and BLA (Figure 36) (of left and right hemispheres, respectively) with either AAV₂-shCCK292, AAV₂-shCCK601 or AAV₂-eGFP viral vectors (1×10^{11} vg/ml). Animals were sacrificed either 2 or 6 weeks after the surgery. Viral gene expression was verified by fluorescence microscopy and CCK mRNA down-regulation was qualitative-analyzed by *in situ* hybridization with Dig-labeled probes. Both viral vectors were clearly effective in down-regulating CCK mRNA two weeks after the surgery (Figure 35A-B and Figure 36A-B, left panels) and this silencing activity was equally maintained six weeks following surgery (Figure 35A-B and Figure 36A-B, right panels). Nevertheless, at this later time point the AAV₂-shCCK292 vector seemed less efficient compared to the AAV₂-shCCK601 vector, particularly in the BLA as shown in Figure 35Aright. Importantly, although other studies have reported dose dependent toxicity of shRNAs (Ehlert et al 2010), in our studies DAPI staining shows cellular integrity within the target regions in both AAV₂-shCCK292 and AAV₂-shCCK601 injected brains. Finally, intact pattern of CCK mRNA expression was observed with negative control injections of AAV₂-eGFP (Figure 35C and Figure 36C).

Although we have not quantified the degree of down-regulation obtained with each vector in these pilot experiments, we considered that the two shCCK sequences showed comparable efficiencies to down-regulate CCK mRNA into Cg Ctx and BLA after 2 weeks, and that AAV₂-shCCK601 showed stable efficacy up to the 6 weeks time point. Based on these qualitative results and the theoretical knowledge on synthetic siRNA design, we selected the AAV₂-shCCK601 viral to further pursue our study.

Cingulate Cortex

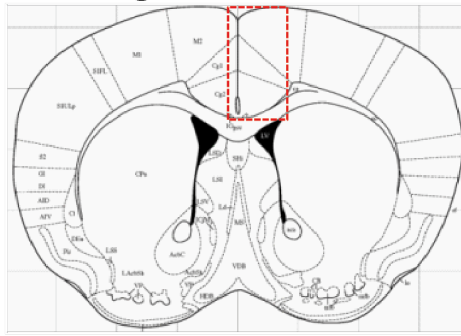


Figure 24 (Paxinos and Franklin atlas, 2001)

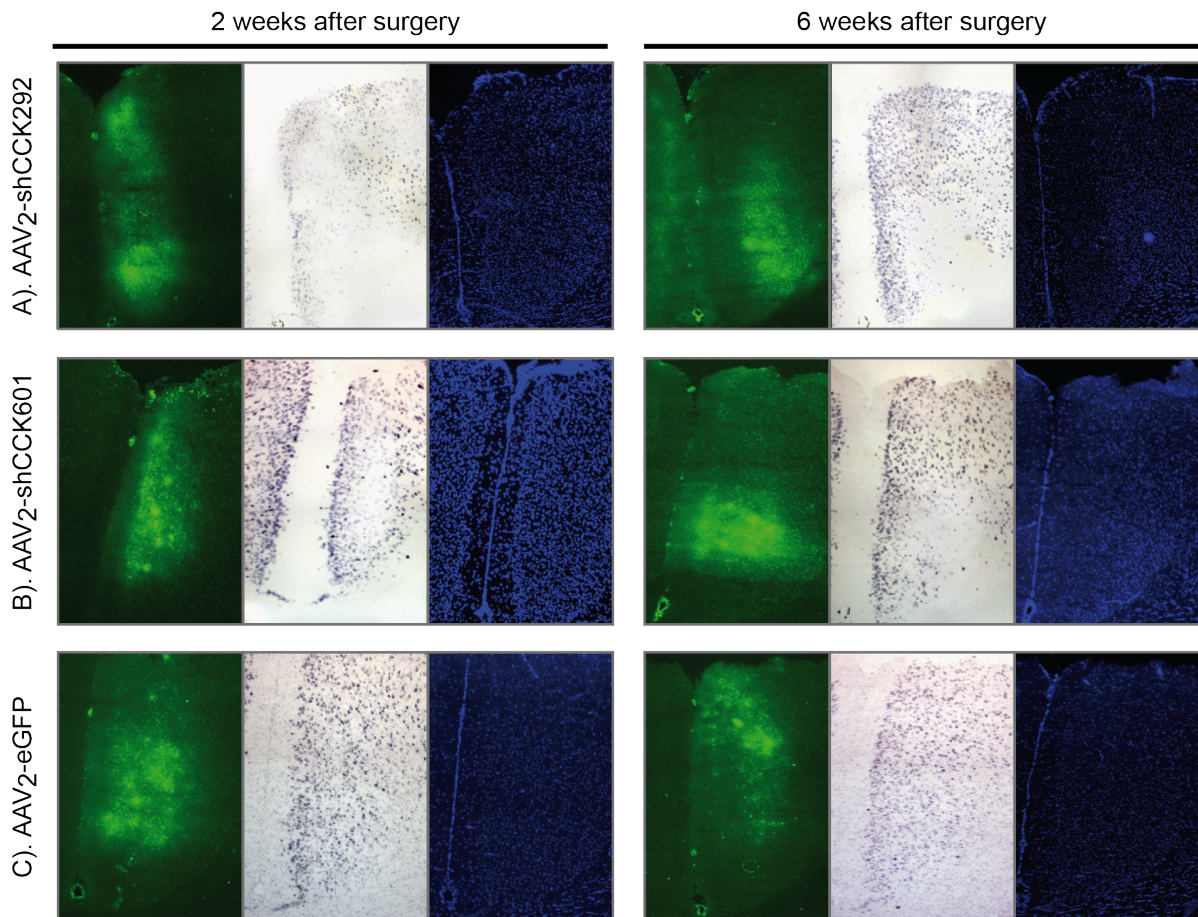


Figure 35: CCK-mRNA down-regulation into mouse Cingulate Cortex (Cg Ctx) produced by shRNAs designed against two different target sequences of *mcck*. Representative coronal brain microsections showing stereotaxical injections of 2 μ l (1 \times 10¹¹ vg/ml) of different viral vectors into the Cg Ctx region. (A) AAV₂-shCCK292, (B) AAV₂-shCCK601, (C) AAV₂-eGFP. Left: eGFP expression, middle: dig-labeled CCK-mRNA, right: DAPI staining. For time course study, mice were sacrificed for tissue collection either 2 (left panels) or 6 (right panels) weeks after surgery.

Basolateral Amygdala

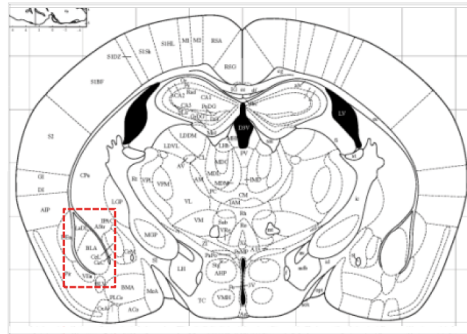


Figure 41 (Paxinos and Franklin atlas, 2001)

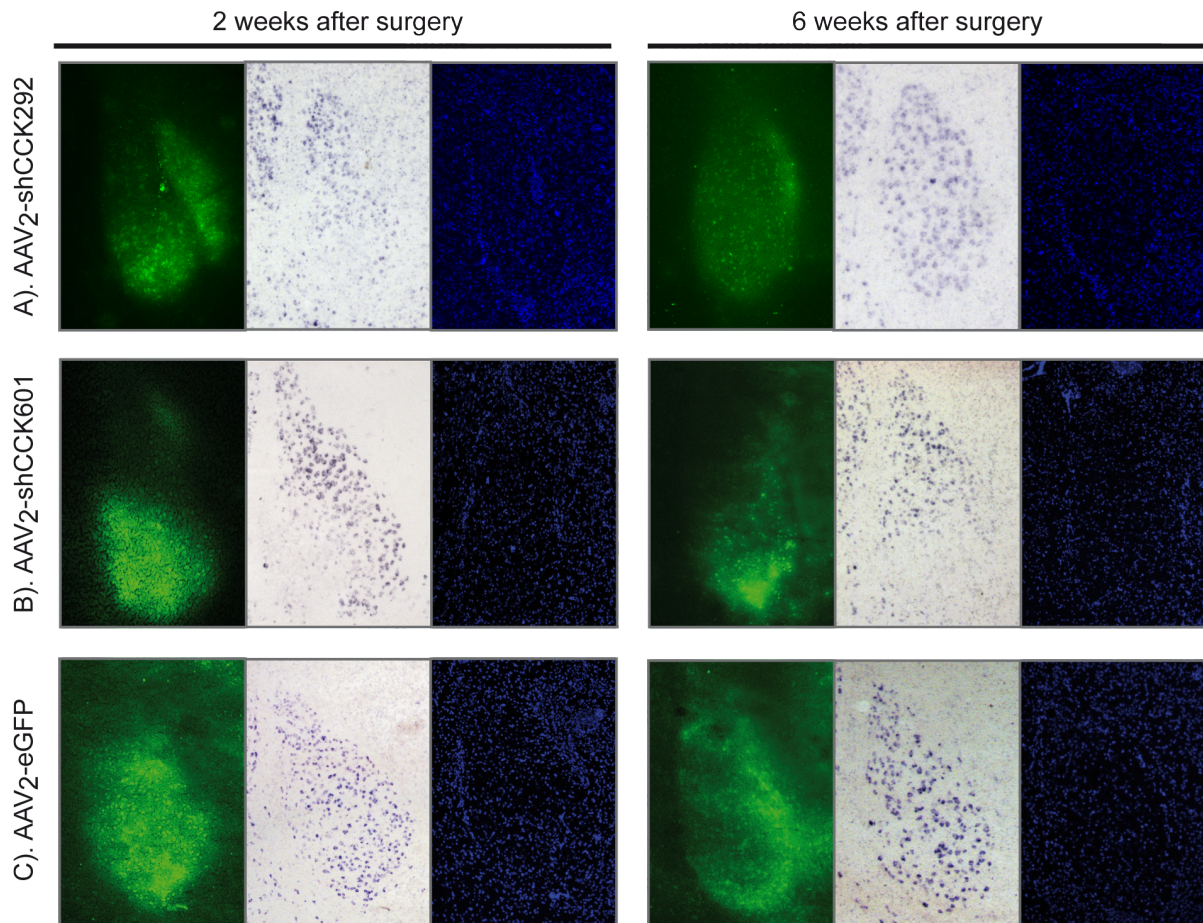


Figure 36: CCK-mRNA down-regulation into basolateral nucleus of the mouse amygdala (BLA) produced by shRNAs designed against two different target sequences of *mcck*. Representative coronal brain microsections showing stereotaxical injections of 1.5 μ l (1×10^{11} vg/ml) of different viral vectors into the BLA. (A) AAV₂-shCCK292, (B) AAV₂-shCCK601, (C) AAV₂-eGFP. Left: eGFP expression, middle: dig-labeled CCK-mRNA, right: DAPI staining. For time course study, mice were sacrificed for tissue collection either 2 (left panels) or 6 (right panels) weeks after surgery.

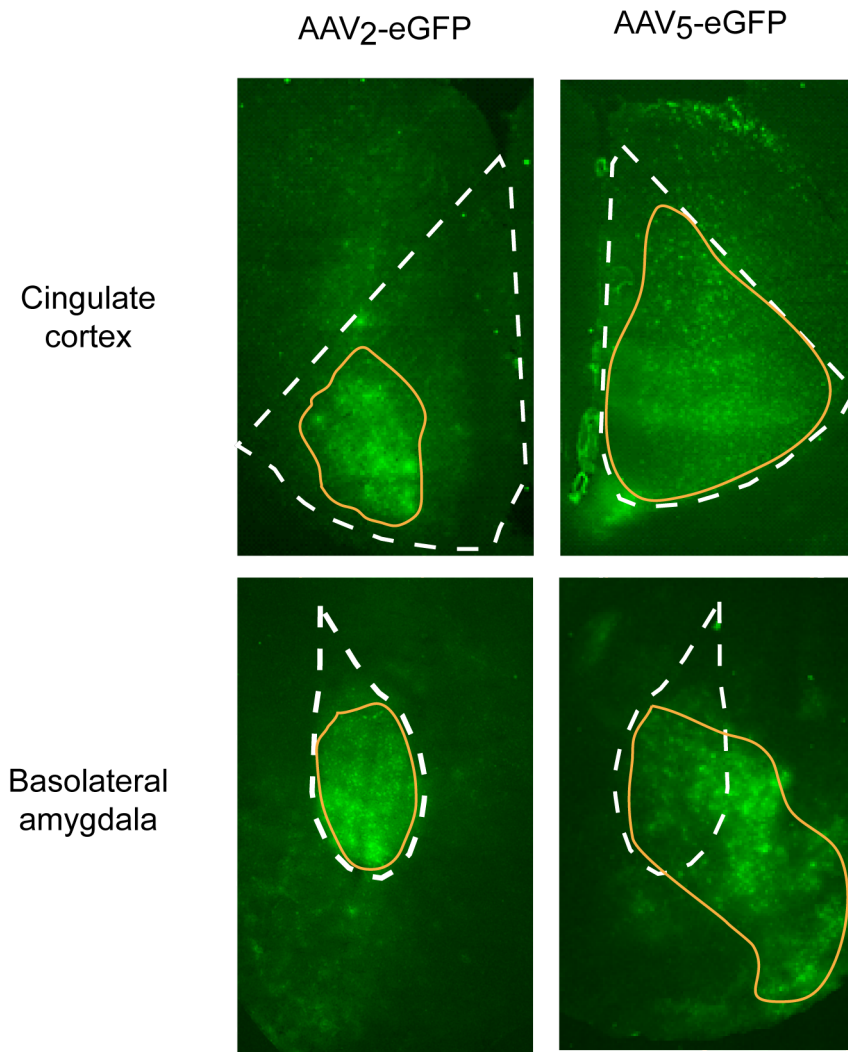


Figure 37: Viral vector spread of AAV-serotype 2 and AAV-serotype 5 into Cingulate Cortex (Cg Ctx) and basolateral nucleus of the amygdala (BLA) of the mouse brain. Representative coronal brain microsections showing eGFP expression of AAV₂-eGFP (left panels) and AAV₅-eGFP (right panels) viral vectors (1.5×10^{12} vg/ml) stereotaxically injected into Cingulate Cortex ($2 \mu\text{l}$; upper panels) and BLA ($1.5 \mu\text{l}$; bottom panels) as Fig. 1. Yellow lines delimiting the area affected for the viral infection.

- Selection of the best viral serotype to target each region of interest

Recombinant adeno-associated viral vectors can be engineered based on capsid DNA from different viral serotypes. As mentioned earlier in the introduction, AAV serotypes have distinct efficiencies and cell tropisms over a wide variety of tissues (Wu et al 2006). Among the rAAV revealing diverse patterns of transduction within the mammalian nervous system, AAV-serotype 2 and AAV-serotype 5 have been reported to preferentially infect neurons (Burger et al 2004). However, the two serotypes display distinct spread properties over those studies. Therefore, as we were not satisfied by the viral spread obtained with AAV₂-eGFP in the Cg Ctx region, we decided to test different viral vector engineering on *experiment 4* in order to select the best viral serotype to target each region of interest. Male C57BL/6J mice (weight range 24-29g) were bilaterally injected with AAV₂-eGFP and AAV₅-eGFP viral vectors (on right and left hemispheres, respectively) either into Cg Ctx or BLA (Figure 37). As mentioned in the detail description of the methods, to achieve comparable working concentrations viruses were diluted in Dulbecco-PBS buffer and the same quantity of viral genome particles was injected for each viral vectors in the two evaluated regions, allowing reliable comparisons of spread between the two serotypes. Animals were then sacrificed one week after the surgery and the regional pattern of viral transduction was evaluated in cryostat brain microsections by fluorescent microscopy. As is presented in Figure 37, the AAV-serotype 5 showed clearly infect a larger brain area as compared to the AAV-serotype 2. These results are fully concordant with previous reports showing that AAV5 vectors transduce both a greater number of cells and a larger volume of tissue compared with AAV2 vectors (Burger et al 2004; Davidson et al 2000; Shevtsova et al 2005; Tenenbaum et al 2004). In conclusion, based on our results and volumetric studies on this brain structures (Mozhui et al 2007; Wolf et al 2002), we selected the AAV-serotype 2 vector to target BLA and the AAV-serotype 5 to target Cg Ctx.

- Pilot experiment on AAV₂-shCCK knock-down quantification

For preliminary analyses of shCCK silencing activity quantification, a pilot experiment (*experiment 5*) was developed using an autoradiographic film methodology. Male C57BL/6J mice (weight range 24-29g) were unilaterally injected into BLA with either AAV₂-shCCK601 or AAV₂-eGFP viral vectors (1×10^{11} vg/ml). Animals were sacrificed 5 weeks after surgery and brains removed in order to analyze cryostat microsections for eGFP fluorescence, and further process them by *in situ* hybridization using S³⁵-labeled probes.

We then performed quantification of autoradiographic signal using the ImageJ software and determined the effect of viral injections over the CCK mRNA expression by comparing injected vs. non-injected BLAs within the brain. On [Figure 38A-B upper panels](#) representative autoradiographic images of brain microsections are depicted showing injected and non-injected sides. Student's t-test revealed a significant difference on mRNA expression between BLAs on the AAV₂-shCCK injected mouse (***p*<0.001) but no statistical difference was found in the AAV₂-eGFP injected mouse ([Figure 38A and B bottom graphics](#)).

These observations indicate a potent reduction of *mccck* expression upon AAV₂-shCCK viral vector infection in BLA. A result that was later confirmed with a larger number of mice and a more appropriate control, i.e. viral vector expressing shSramble sequences with no similarity among the mouse genome instead of AAV₂-eGFP (See manuscript below).

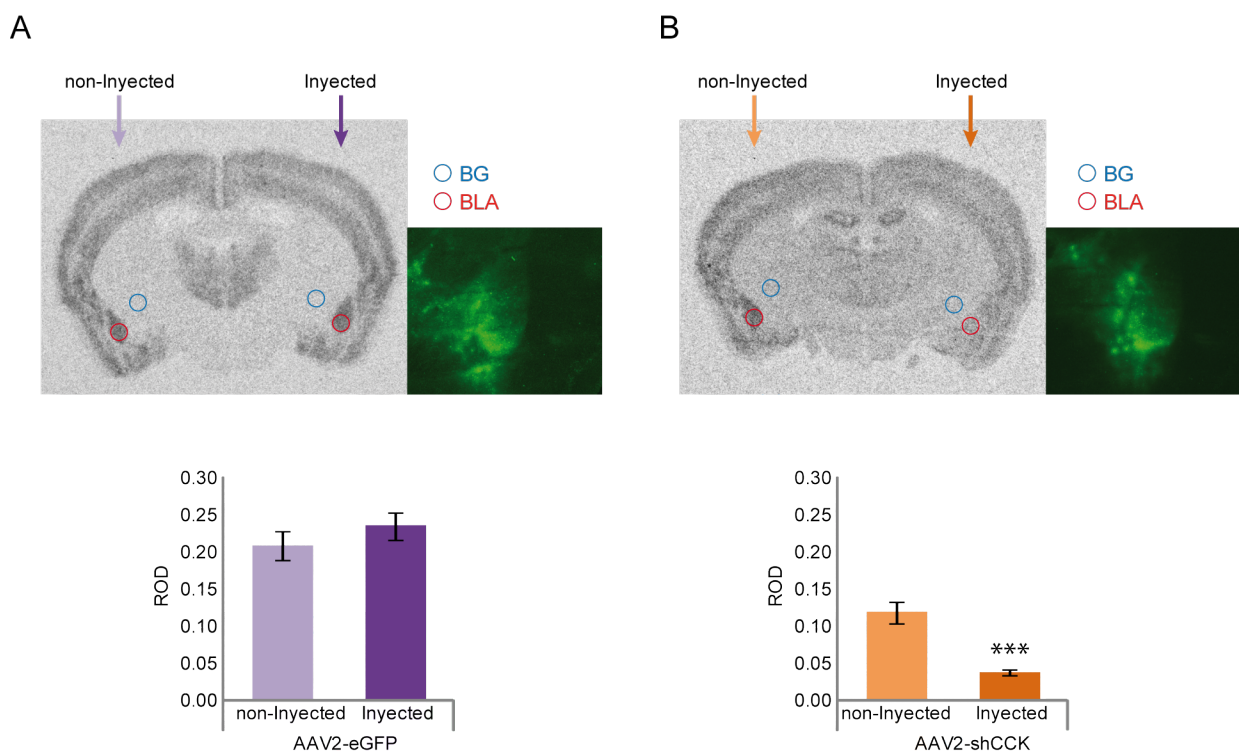


Figure 38: Quantification of AAV₂-shCCK knock-down into the mouse BLA. Unilateral stereotaxical injections of 1.5 μ l (1 \times 10¹¹ vg/ml) of (A) AAV₂-eGFP and (B) AAV₂-shCCK601 viral vectors into the BLA. Upper panels showing representative autoradiographic images of coronal brain microsections showing drawing ROIs (BG, Striatum BackGround; BLA, BasoLateral nucleus of the Amygdala), and fluorescent microscopy pictures of BLA-eGFP expression. Bottom bar graphics showing quantification of mRNA CCK expression on BLA of injected and non-injected sides. Results are expressed relative optical density mean \pm SEM. Student's t-test ***p*<0.001 (n=1mouse/condition, 10sections/BLA). Mice were sacrificed for tissue collection 6 weeks after surgery.

4. Manuscript 1:

Genetic silencing of cholecystokinin mRNA in the basolateral amygdala has anxiolytic and antidepressant effects in mice

Del Boca C¹, Le Merrer J¹, Lutz PE¹, Koebel P¹, Kieffer BL¹.

1. Institut de Génétique et de Biologie Moléculaire et Cellulaire (IGBMC), Centre National de Recherche Scientifique/Institut National de la Santé et de la Recherche Médicale/Université de Strasbourg, 1 Rue Laurent Fries, F-67404 Illkirch-Graffenstaden, France.

Corresponding author:

Pr. Brigitte L KIEFFER

IGBMC

Parc d'innovation 1 rue Laurent Fries BP 10142

67404 Illkirch Cedex, France

Telephone : +33 (0)8 65 56 93

Fax : +33 (0)8 65 56 04

e-mail address : briki@igbmc.fr

Abstract

CCK is a neuromodulatory peptide widely distributed in the mammalian brain. This peptide has been related to a variety of physiological functions such as feeding behavior, cardio-respiratory control, thermoregulation, nociception, anxiety and depression, memory processes and motivational responses. CCK-expressing brain regions involved in all these effects remain unclear and their identification represents an important step towards understanding CCK function in the brain. In this study we focused on the basolateral amygdala, which is strongly involved in the generation of emotional states and expresses high levels of CCK. Thus, we examined the role of amygdalar CCK in emotional responses in the mouse. We found that virally-mediated shRNA-CCK knockdown in the basolateral amygdala strongly reduces levels of anxiety and despair behavior, as evidenced in the elevated plus-maze and forced swim test, respectively. Moreover, shCCK mice showed a reduction in naloxone-induced conditioned-place aversion, another paradigm involving negative emotional responses. Altogether, our data indicate that CCK produced at the level of the basolateral amygdala represents a key substrate for anxiogenic and depressant effects of neural CCK, and strongly suggest that amygdalar CCK contributes to the well-known CCK-associated panic disorders and major depression.

Introduction

Cholecystokinin (CCK) was first identified as a gastrointestinal hormone (Mutt & Jorpes 1968) and is present at high levels in the brain (Meziane et al 1997). This peptide has been implicated in a wide range of physiological processes both at the periphery and in the central nervous system, including digestion, cardiovascular and respiratory function, thermoregulation, nociception, emotional and motivational states, and cognition (for a review see Beinfeld 2001). Neural CCK is mostly co-localized with classic neurotransmitters (dopamine, glutamate, GABA and serotonin) (Ghijsen et al 2001; Hokfelt et al 2002) and acts as a neuromodulatory peptide (Rotzinger et al 2010). The transcript occurs in several forms of varying aminoacid length and CCK-8s (C-terminal sulfated octapeptide) represents the most abundant CCK fragment in the brain. This peptide produces its broad biological activities by activating with two closely related G protein coupled receptors, CCK₁ and CCK₂, the latter being predominant in the brain (Noble et al 1999).

High levels of CCK have been associated with motivational loss, anxiety and panic disorders (Hebb et al 2005), and a role has been proposed for CCK in the induction of anxiety and major depression (Berna et al 2007; Shindo & Yoshioka 2005). CCK₂ receptors are main effectors of anxiogenic properties of the peptide (Bradwejn & Koszycki 2001; Eser et al 2011). In rodents, CCK₂ agonist administration increased levels of anxiety in several behavioral paradigms, including the elevated plus-maze (EPM), acoustic startle and open field tests (for a review see Rotzinger et al 2010). Moreover, systemic CCK₂ antagonist treatment attenuated anxiety-like behavior in mice subjected to immobilization restrain stress as examined in the EPM (Wang et al 2011). In addition, CCK₂ antagonists showed

antidepressant properties in preclinical models (for a review see Rotzinger et al 2010). In particular, systemic administration of these compounds produced antidepressant responses in the forced swim test, and their effects were synergistic with the activity of the antidepressant compound RB101 (Hernando et al 1996). Furthermore, chronic blockade of CCK₂ receptors normalized high immobility time in the force swim test and prevented HPA axis hyperactivity, which were both elicited by repeated social defeat-induced stress (Becker et al 2008). Genetic approaches using CCK₁ and CCK₂ receptor deficient mice have also investigated CCK receptor implication in physiological functions of the peptide (for a review see Noble & Roques 2002). Regarding emotional responses, CCK₂-receptor knockout mice displayed decreased levels of anxiety in the light-dark test, and presented increased function of the GABAergic system in the brain, concordant with the pharmacology (Raud et al 2005). In another study, CCK₂-receptor knockout mice showed a phenotype in learning and memory processes, however no deficit was detected in the elevated plus maze and conditioned suppression of motility, possibly due to the development of compensatory mechanisms in the knockout animals (Dauge et al 2001). Moreover, transgenic mice over-expressing CCK₂ receptors showed increased levels of anxiety, as well as prolonged activation of adrenocorticotrophic hormone and glucocorticoids following acute stress (Chen et al 2010). Finally, antagonistic interactions between CCK and opioid systems have been established in the modulation and expression of stress-related behaviors, opposing memory-enhancing and anxiogenic effects of CCK to amnesic, analgesic and anxiolytic effects of opioid peptides (see Hebb et al 2005). Further data on this field also implicate CCK in reward, motivation and addictive behaviors (Lu et al 2002; Mitchell et al 2006; Pommier et al 2002).

Anatomically, CCK systems are widely distributed in the rodent brain since early development (Giacobini & Wray 2008). Immunohistochemical analyses and *in situ* hybridization studies have reported CCK positive cells at high density in olfactory bulb, cerebral cortex, hippocampus, amygdala, thalamus, substantia nigra and ventral tegmental area (Cain et al 2003; Meziane et al 1997). CCK₂ receptor mRNA is strongly expressed throughout the cortex, nucleus accumbens and several amygdaloid nuclei; while CCK₁ receptor expression, initially reported in the gastrointestinal tract, is also found in the CNS mainly at the level of interpeduncular nucleus, area postrema, tractus solitarius, habenular nuclei, hypothalamus and central amygdala (Noble et al 1999; Wang et al 2005). Together therefore, the CCK system may modulate cognitive, emotional and motivational behaviors at several brain sites.

The amygdalar complex is implicated in the generation of emotional states, stress coding and associative learning (LeDoux 2000), as well as the retrieval of aversive memories (Frenois et al 2005). Local pharmacological studies have suggested a role for CCK₂ receptors expressed at the level of basolateral amygdala (BLA) in anxiogenic effects of the peptide (Rotzinger & Vaccarino 2003). Moreover, electrophysiological studies have reported CCK and CCK₂ receptor expression in GABAergic interneurons of the BLA (Chung & Moore 2009; Jasnow et al 2009). To our knowledge, however, the role of CCK and its receptors in this brain structure has not been investigated by local genetic approaches. Thus, here we used an mRNA knock-down strategy to examine the implication of

amygdalar CCK on emotional responses. To this aim, we induced local CCK mRNA silencing in the mouse BLA using a rAAV2-eGFP-shCCK viral vector, and investigated whether local CCK knock-down alters behavioral responses in several models involving emotional negative affective states. These include levels of anxiety and depressive-like behavior, naloxone-induced conditioned place aversion and naloxone-precipitated withdrawal in morphine-dependent mice. Our data demonstrate for the first time that CCK produced by BLA increases anxiety, despair behavior and aversive memory.

Materials and Methods

1. AAV₂ viral vectors construction

A short hairpin (sh) RNA was designed to target the *mcck* gene (shCCK) in the sequence nucleotide position 601-624 (NM_031161:5'-TCTTAAGAACGGACATGCGGC-3'). Recombinant AAV₂-shCCK viral vectors were generated expressing eGFP and shCCK under the control of CMV and mU6 promoters respectively. Control vectors encode either for eGFP alone (AAV₂-eGFP) or for eGFP and a scramble shRNA (AAV₂-shScramble). The shScramble sequence (5'-GTTGGCTCCTAGCAGATCCTA-3') selected (<http://www.sirnawizard.com>, InvivoGen) has no match *in silico* in the mouse genome. AAV₂ vectors were then generated by triple transfection of AAV-293 cell line (Stratagene) using (i) either pAAV-eGFP, pAAV-eGFP-shScramble or pAAV-eGFP-shCCK, (ii) pAAV-RC (Stratagene) containing *rep* and *cap* genes of the adeno-associated virus serotype-2 and (iii) pHelper (Stratagene) encoding for the adenoviral helping functions. Following 2 days cells were collected, lysed and treated with Benzonase (50U/ml, sigma, 30mn, 37°C). Viral vectors were then purified by Iodixanol gradient ultracentrifugation (Zolotukhin et al 2002) followed by dialysis and concentration against Dulbecco PBS using centrifugal filters (Amicon Ultra-15 Centrifugal Filter Devices 50K). Viral particles were quantified by real time PCR using a plasmid standard pAAV-eGFP. To achieve comparable working concentrations viruses were diluted in Dulbecco-PBS buffer to a final concentration of 3x10¹¹ viral genomes *per* ml (vg/ml) and finally stored at -80°C until use.

2. Behavioral experiments

Animals. Male C57BL/6J mice provided by Charles River (Lyon, France) were used for all the experiments. Mice were aged 8 weeks at the beginning of the experiments and they were housed 3-4 per cage in a 12h dark/light cycle (light from 7am to 7pm), under controlled conditions of temperature and humidity. Food and water were available *ad libitum*. Experimental procedures were conducted in accordance with the European Communities Council Directive of 24 November 1986 (86/609/EEC) and approved by the "Comité Régional d'éthique en matière d'expérimentation animale de Strasbourg" (CREMEAS, 2003-10-08-[1]-58).

Drugs. Morphine hydrochloride (Francopia) and Naloxone hydrochloride (Sigma) were dissolved in sterile isotonic saline (NaCl 0.9%). For surgery mice were anaesthetized using ketamine/xylazine (Virbac/Bayer, 100/10 mg/kg). All the doses refer to salt weight and were administered in a volume of 10ml/kg.

Experimental procedure

Experiment 1. 12 naïve mice were unilaterally injected into the BLA with either AAV₂-shCCK (n=4) or AAV₂-eGFP (n=4) to qualitatively assess the silencing activity of the viral vector by *in situ* hybridization (ISH), using Dig-labeled cRNA probes. To confirm the stability of CCK-knockdown over time, Dig-ISH was performed either 2 or 6 weeks following surgery (n=2mice/time point).

Experiment 2. 56 mice (2 independent cohorts) were bilaterally injected into the BLA with either AAV₂-shCCK or AAV₂-shScramble (Cohort 1, n=16 mice/group; Cohort 2, n=12 mice/group) and 5 weeks later analyzed for emotional responses. Animals from the second cohort were processed only throughout tests for which a reliable trend for an effect was observed in the first cohort. 24 hours after the last behavioral experiment, all mice were sacrificed and brains analyzed for injection accuracy and viral spread. Finally, we used Dig-ISH to qualitatively confirm the patten of down-regulation (n=3 mice/condition) and [³⁵S]-ISH to quantify the intensity of CCK knock-down in both shCCK- and shScramble-injected mice (n=5 mice/condition).

Surgery and virus delivery. Anesthetized mice were placed in a stereotaxic frame (Unimécanique, France). The skull was exposed and incisor bar adjusted such that bregma and lambda were at the same height. Bilateral stereotaxic injections were performed according to the Mouse Brain Atlas of Paxinos and Franklin (2001). For this aim, a 5µl microsyringe (SGE Analytical Science, Australia) was mounted to a micro-drive pump (Harvard apparatus, France) and connected by a PE-10 polyethylene tubing (Harvard apparatus, France) to a stainless-steel injector needle (0.28mm external diameter). 1.5µl of purified AAV₂ viral vectors were delivered into the BLA uni- or bilaterally in experiment 1 and 2, respectively. Injection speed was 0.1µl/min, and the needle was slowly withdrawn 10min after delivery. Following surgery, mice were single housed for 48 hours to recover and then placed back in their original home cages.

Behavioral testing. We evaluated the effects of local shRNA injections into BLA in 4 categories of behaviors: anxiety-like behavior, despair-like behavior, aversive place conditioning, and withdrawal syndrome, starting 5 weeks after surgery. The design of the behavioral test battery was adapted from previous reports (Duangdao et al 2009; McIlwain et al 2001) and tests were ordered from less to most stressful as follows: elevated plus-maze (EPM), open field, light/dark box, forced swim, tail suspension, naloxone-induced conditioned place aversion (CPA), and naloxone-induced withdrawal. Elevated plus-maze was placed at the beginning of the battery as recommended by Voikar et al (2004). The inter-test intervals were selected to allow the mice to fully recover between tests. A spaced

3-days interval was chosen between tests of the same category. Among categories, a 5-days interval was chosen to separate anxiety from despair behaviors while 7-days intervals were placed before and after the naloxone-induced CPA. All behavioral sessions were performed between 8am and 1pm.

Elevated Plus-Maze. The EPM was a plus-shaped maze elevated 52cm from base, with black Plexiglas floor, consisting of two open and two closed arms (37x6cm each) connected by a central platform (6x6cm). The walls of the closed arms were made of 18 cm-high clear acrylic. The experiments were conducted under low-intensity light (10 Lx). The apparatus was placed over an infrared-lit platform. The movement and location of the mice were analyzed by an automated tracking system equipped with an infrared-sensitive camera (Videotrack; View Point, Lyon, France). All sessions were videotaped for further analyses. The test started when the mouse was placed on the central platform facing a closed arm and lasted 5 minutes. Anxiety-like behavior was assessed by measures of the time spent and number of entries in closed and open arms of the maze (automated counting), and related to time and activity ratios (time spent -number of entries in open arms/total time spent -number of entries in arms). Risk-taking was evaluated by time spent in the distal part of the open arms (1/3 last part of the arm) and number of head dips (total number of head dips and head dips from the distal part of the open arms). Finally, the distance traveled in the maze (automated counting) was used as measure of locomotor activity.

Open Field. The apparatus consisted of 4 equal square arenas (50x50cm) separated by 35cm-high opaque grey Plexiglas walls. Light intensity of the room was set at 50 Lx. The floor was a white Plexiglas infrared-lit platform. The movement and location of the mice were analyzed by an automated tracking system equipped with an infrared-sensitive camera (Videotrack; View Point, Lyon, France). All sessions were videotaped for further analyses. The test started when the mouse was introduced in an arena facing a corner, and lasted 30 minutes. The following parameters were measured to assess anxiety levels: percentage of time spent in a center zone (12x12cm from the outer edge) and episodes of complete immobility. Total distance traveled in the arena (automated counting) and numbers of rearing and grooming episodes were used as measures of general activity.

Light/dark box. The apparatus consisted of two compartments (Panlab, Barcelona, Spain). The light-side compartment (25x25x27cm), with white Plexiglas walls and floor, was brightly illuminated by a white lamp (1500 Lx) placed 25 cm above the entrance of the compartment. The dark-side compartment (25x16x27cm), with black Plexiglas walls and floor, was illuminated by a red lamp (37 Lx) placed 25cm above the entrance. Both compartments were connected through an open door located in the middle of the dividing wall. The test started by placing the mouse in the dark compartment facing the wall opposite to the door and lasted 5 minutes. Total time spent in each compartment, latency to first enter the light compartment and number of entries into this compartment were recorded as anxiety parameters.

Forced swim test. Mice were individually forced to swim for 6 minutes in an open glass cylindrical container (diameter, 18cm; height, 27cm) containing 20cm of water. Total duration of immobility, climbing and swimming episodes were scored in 2-minute bins and results were expressed as percentage of total time. Latency to first immobility episode was also quoted. Each mouse was judged to be immobile when it ceased struggling and remained floating motionless in the water, making only those movements necessary to keep its head above water. Experimental conditions slightly differed between the two cohorts of experimental animals. For the first cohort, light intensity of the experimental room was set at 30 Lx and temperature of water at 19°C. For the second cohort, light intensity was set at 20 Lx and temperature of water at 22°C; moreover, the experiment was repeated on the next day. At the end of the behavioral session, mice were dried with paper towel and placed under a heating lamp for 10min before being returned to their home cage.

Tail suspension. This test was carried out in an automated device (MED associates Inc, St Albans, VT) consisting of 6 black boxes (14x14x25cm). Mice were suspended 4cm above the floor by an adhesive tape placed approximately 1cm from the tip of the tail. Total duration of immobility was monitored during 6-minute test sessions. An upper and a lower threshold defined struggling (active) and immobility (passive) behaviors, respectively. The latency to the first episode of immobility was also scored.

Naloxone-induced conditioned place aversion. Place conditioning experiments were performed in unbiased computerized boxes (Imetronic, Pessac, France) formed by two Plexiglas chambers (15.5x16.5cm) separated by a central alley (6x16.5cm). Two sliding doors (3x20cm) connected the alley with the chambers. Two triangular parallelepipeds of transparent polycarbonate were arranged in one chamber, and one square parallelepiped in the other to form different shape patterns (covering the same surface). Distinct textured floors of translucent polycarbonate provide additional contextual cues. The activity location of mice was recorded using five photocells located throughout the apparatus. Behavioral data were collected by an interface connected to a PC. Dim light (30 Lx) was used in the room to minimize levels of anxiety. Place conditioning consisted of three phases. On day 1, shCCK and shScramble injected mice were placed in the central alley and permitted to freely explore the apparatus for 15 minutes. Based on the results of this pretest, the drug-paired chambers were assigned in such way that saline and naloxone groups were counterbalanced and unbiased toward contextual cues. Conditioning phase lasted 3 days. On the mornings of days 2, 3 and 4 (8.30am) all mice received a subcutaneous (s.c.) injection of saline and were confined to the “vehicle-paired” chamber for 30 minutes. On the afternoons of the same days (4 hours later, 12:30pm), mice received an injection of either naloxone (1mg/kg s.c.) or saline and were confined to the “drug-paired” chamber for 30 minutes. The testing phase was conducted on day 5, 24 hours after the last conditioning session. The mice were placed in the neutral central alley and permitted to explore the apparatus for 15 minutes. Number of entries and time spent in each chamber were recorded. Results were expressed as percentage of number of entries to or time spent in the drug-paired compartment [% time spent in the drug-paired

compartment = (time spent in the drug-paired compartment)/(time spent in both compartments)x100].

Naloxone precipitated-withdrawal. shCCK and shScramble injected mice were daily injected (8.00am) with either morphine (30mg/kg i.p.) or saline during 7 days. On day 7, withdrawal was precipitated two hours after the last morphine administration by injecting the opioid antagonist naloxone (1mg/kg s.c.). Each mouse was immediately placed into a Plexiglas transparent box (15x15x30cm) and observed individually during 20 minutes to score somatic signs of withdrawal (Frenois et al 2002; Matthes et al 1996). Numbers jumps, front paw tremors, scratches, rearings, groomings, and genital lick episodes were counted. Body tremor, ptosis, mastication, and piloerection were scored 1 for appearance or 0 for nonappearance within 5 min bins. Locomotor activity over 5 min periods was rated from 0 for inactivity to 2 for increased activity. A global score of withdrawal was calculated for each mouse taking into account the relative weight of each sign (adapted from Berrendero et al 2003): (horizontal activity + rearings + scratches + genital licks + groomings)x0.5 + (jumps + front paw tremors + sniffings)x1 + (body tremors + ptosis + teeth hattering + piloerection)x1.

3. In situ hybridization

CCK-cRNA probes preparation. DNA template for CCK cRNA-probes (258-600, 343bp) was generated by RT-PCR (Sigma, forward primer: 5'-CTGTACCCAAGCTTGATACATCCAGCAGGTCCGCAA-3', reverse primer: 5'-TTTCCTTGGAATTCAGGAAACACTGCCTTCCGACCAC-3') using total mouse brain RNA extracted by TRIzol reagent (Invitrogen, Cergy Pontoise, France) according to the manufacturer's instructions. The template was cloned into pcDNA3 (Invitrogen) and verified by sequencing. Sequence probe alignment was confirmed with BLASTN 2.2.18 software (<http://blast.ncbi.nlm.nih.gov>, NCBI). Next, CCK-cDNA plasmid (20µg) was linearized by enzymatic digestion of EcoRI for sense probe and HindIII for anti-sense probe, and linearized DNA (1µg) was transcribed using T7 or Sp6 RNA polymerases (Promega) for sense and anti-sense probes production respectively. For Dig-labeled probes, DIG RNA labeling mix 1X (Roche) was used according to manufacturer's specifications. Quality of the RNA was evaluated by agarose gel electrophoresis (RiboRuler Low Range RNA ladder, Fermentas) and concentration determined by spectrophotometry (Nanodrop Labtech ND-1000). For radiolabeled-probes, CTP- α S³⁵ radionucleotides (PerkinElmer) were added to the synthesizing mix. S³⁵-probes were purified by gravity-flow chromatography on illustra NICK Columns (GE Healthcare) and specific activity was measured using a topcount apparatus (Packard).

Tissue preparation. Mice were sacrificed by cervical dislocation, brains rapidly removed, frozen in OCT (Optimal Cutting Temperature medium, Thermo Scientific) and stored at -80°C until use. Coronal brain sections (20µm) were obtained for BLA (-0.8 to -1.8 mm

from bregma) according to the mouse brain atlas (Paxinos and Franklin, 2001) using a cryostat microtome (Leica CM3500) at -20°C. Slides were mounted onto Superfrost slides (Thermo Scientific) and immediately fixed at room temperature (RT) for 15 minutes with 4% paraformaldehyde (PFA), 0.1M phosphate buffer (PB, pH 7.4). Fixed sections were then washed in 0.1M PB for 15 minutes, air-dried and stored at -80°C until use.

***In situ* hybridization (ISH).** Dig- and [³⁵S]-labeled RNA probes were used for ISH, following the methods previously described by Chotteau-Lelievre et al (2006). Briefly, fixed brain sections kept at -80°C were thawed at RT for 30min and rehydrated in 1xPBS for 10min. Sections were then incubated at 65°C for 16h in a hybridization mix [formamide 50% (molecular biology grade, Sigma-Aldrich); dextran sulfate 10%; Denhardt's 1x; tRNA 1mg/ml (from Baker's yeast, Sigma-Aldrich); NaCl 300mM; Tris-HCl 20mM pH 6.8; EDTA 5mM; NaH₂PO₄ 5.4mM; Na₂HPO₄ 4.6mM; plus 10 mM DTT for radioactive ISH] with either Dig- or S³⁵-labeled RNA probes at the concentrations of 1.5ng/μl or 20,000 cpm/μl, respectively. DIG-labeled brain sections were afterward incubated with an alkaline phosphatase-labeled anti-DIG antibody (1:1500, Roche) in blocking solution [2% Roche blocking; 20% heat inactivated goat serum, MABT 1x]. Staining was performed with Nitroblue tetrazolium and bromo-chloro-indolyphosphate (NBT/BCIP) as color substrates by incubating the slides in staining solution [polyvinyl alcohol 0.5% (Sigma-aldrich); NaCl 100mM; Tris-HCl 100mM pH 9.5; MgCl₂ 50mM; Tween20 0.1%; NBT 0.35% (Roche); BCIP 0.35% (Roche)] at RT under light-protected conditions until the signal becomes visible (12h). Next, slides were washed 2x10 min (PBS 1x, 1mM EDTA), air-dried and mounted with Eukitt (VWR). To generate autoradiograms, [³⁵S]-labeled brain sections were exposed simultaneously with a [¹⁴C] standard (ARC 0146; American Radiolabeled Chemicals) to Kodak Biomax MR films (Sigma-Aldrich) at -80°C for seven days. Films were developed with a Kodak MIN-R Processor (Carestream Health).

Image analysis. Brain sections were observed under epifluorescent microscopy (Leica) and autoradiograms under a macroscope and bright lighting. In both cases, images were acquired with a CCD camera (CoolSNAP, Roper Scientific). For autoradiograms, 10 brain sections of each mouse were individually captured as high resolution (600 dpi) 8-bit images. In each section ImageJ was used to draw bilaterally regions of interest (ROI, see Figure 7C) and measure mean grey levels in (i) the BLA, where the GFP signal was previously detected, (ii) in the striatum, a region lacking CCK expression (Meziane et al 1997; Schiffmann & Vanderhaeghen 1991) and (iii) in the retrosplenial agranular cortex (RSA). Grey level values were then transformed into relative radioactive counts by calibration with the co-exposed [¹⁴C] standard using a Rodbard non-linear regression curve. As recommended by Ambesi-Impimbato et al (2003), radioactive value in the striatum, corresponding to non specific hybridization, was subtracted to both BLA and RSA. As CCK mRNA expression level in RSA was not affected by viral injections in the BLA (shScramble group: 92.1 ± 11.8 nCi/g; sh-cck: 94.2 ± 8.7 nCi/g), normalized BLA radioactive values were calculated by dividing BLA value by that in the RSA of the same section.

4. Statistical analysis

Statistical analysis were performed with Statistica software v8 (www.statsoft.com) and Graph-Pad Prism software v5 (www.graphpad.com). All data are expressed as mean group value \pm S.E.M. and statistical significance was defined as $p \leq 0.05$. Unpaired Student's *t*-test (two-tailed) was used to compare AAV₂-shCCK vs. AAV₂-shScramble injected mice in autoradiographic film quantification. As regards to behavioral experiments, a two-way ANOVA was used for EPM with Cohort and shRNA as between-group factors, and time spent in and number of entries to the open and closed arms as within-group factors. A one-way ANOVA was used in the forced swim test for Cohort 1 to compare immobility and latency time between injected mice, and a two-way ANOVA with repeated measures for bin comparisons. In cohort 2, a two-way ANOVA with repeated measures was used with shRNA as a between-group factor and days/bins as a within-group factor. For both cohorts, significant main effects were followed by post-hoc test (Newman Keules). Place conditioning data were analyzed using a three-way ANOVA with Cohort, shRNA and treatment as between-group factors and session (pre- vs. post-conditioning) as within-group factor. Data from the scoring of somatic signs of withdrawal were analyzed using two-way ANOVAs with treatment and shRNA as group factors. One-way ANOVA were also used to analyze the data from the open field, light/dark box and tail suspension tests. Extreme studentized deviate (ESD) method was used to determine significant ($p < 0.05$) outliers.

Results

CCK down-regulation in the BLA *in vivo*

In *experiment 1* we evaluated the efficacy of the AAV₂-shCCK viral vector *in vivo*. Animals were injected unilaterally in the BLA with the AAV₂-shCCK or control AAV₂-eGFP vectors. Two or 6 weeks following surgery, brain sections at the level of the BLA were analyzed for cellular integrity, eGFP fluorescence and CCK mRNA expression. Representative images are shown in [Figure 1](#). For all animals, we found intact DAPI staining and a strong expression of eGFP, confirming the absence of toxicity due to surgery or viral infection and robust transgene expression, respectively. Using AAV₂-eGFP, CCK mRNA levels were comparable between injected and contra-lateral non-injected BLAs ([data not shown](#)), indicating that surgery and viral infection have no unspecific effect on CCK expression. On the contrary, 2 or 6 weeks after the surgery, the *mcck* transcript was barely detectable on the basal part of the BLA of AAV₂-shCCK injected mice. This pattern, consistent with the viral spread revealed by eGFP detection, demonstrates the stability of shRNA-induced CCK down-regulation in the BLA over time.

Behavioral effects of CCK down-regulation in the BLA

In *experiment 2*, we investigate whether *mcck* gene silencing in BLA influences emotional responses. The effects of local injections of AAV₂-shRNA into BLA were evaluated across various behavioral tests as schematically represented in Figure 2A-B.

Anxiety like-behavior

We first performed an elevated plus-maze test to examine whether CCK mRNA down-regulation in BLA influences anxiety levels in the two independent cohorts of injected mice. As no statistical differences were revealed between cohorts, they were pooled together and results are shown in Figure 3. AAV₂-shCCK injections resulted in decreased anxiety-like behavior in the EPM (Figure 3A), as revealed by increased time spent (Cohort: $F_{(1,40)}=3.92$, NS; shRNA: $F_{(1,40)}=1.89$, NS; arms: $F_{(1,40)}=25.19$, $p<0.001$; shRNA x arms interaction $F_{(1,40)}=8.44$, $p<0.01$) and number of entries (Cohort: $F_{(1,40)}=3.58$, NS; shRNA: $F_{(1,40)}=0.93$, NS; arms: $F_{(1,40)}=24.04$, $p<0.001$; shRNA x arms interaction $F_{(1,40)}=19.04$, $p<0.001$) in open arms in AAV₂-shCCK treated mice as compared to shScramble-injected controls. Accordingly, time (Cohort: $F_{(1,40)}=0.69$, NS; shRNA: $F_{(1,40)}=8.50$, $p<0.01$) and entry (Cohort: $F_{(1,40)}=3.99$, NS; shRNA: $F_{(1,40)}=16.63$, $p<0.001$) ratios were increased in AAV₂-shCCK injected mice. Total distance traveled in the maze was similar between groups (Cohort: $F_{(1,40)}=3.03$, NS; shRNA: $F_{(1,40)}=0.11$, NS), suggesting that shCCK treatment had no effect on locomotor activity.

AAV₂-shCCK injected mice also showed increased risk-taking behavior, as illustrated in Figure 3B. These mice displayed increased total number of head-dips (Cohort: $F_{(1,40)}=0.075$, NS; shRNA: $F_{(1,40)}=7.39$, $p<0.01$), increased number of head-dips made from the distal part of the open arms (Cohort: $F_{(1,40)}=2.67$, NS; shRNA: $F_{(1,40)}=9.47$, $p<0.01$) and increased time spent in the distal part of the open arms (Cohort: $F_{(1,40)}=0.51$, NS; shRNA: $F_{(1,40)}=5.40$, $p<0.05$) compared to AAV₂-shScramble.

Animals from Cohort 1 were further tested for anxiety-like behavior in the open field and the light/dark box tests. No significant differences were found in these paradigms (Suppl. Figure 1A and B respectively).

Despair-like behavior

We next evaluated the effects of CCK mRNA down-regulation in BLA on despair behavior in the forced swim test. As illustrated in Figure 4A, AAV₂-shCCK injected mice from Cohort 1 presented a reduction of despair behavior, showing less immobility as compared to AAV₂-shScramble injected mice ($F_{(1,19)}=17.87$, $p<0.001$). When split in 2-min time bins, differences in immobility time appeared significant during the last two bins (shRNA: $F_{(1,19)}=17.87$, $p<0.001$; Bins: $F_{(2,38)}=81.52$, $p<0.001$; Newman Keuls: Bin 1, NS; Bin 2, $p<0.01$; Bin 3, $p<0.05$). No significant difference between groups was detected for latency to the first immobility episode ($F_{(1,19)}=0.68$, NS).

In cohort 2 and under less stressful conditions (Figure 4B), repeated measure ANOVA revealed decreased immobility in the shCCK-treated mice as compared to shScramble-treated animals on the second day of testing, and a significant effect of test repetition only

in AAV₂-shScramble injected mice (shRNA: $F_{(1,17)}=9.68$, $p<0.01$; Days: $F_{(1,17)}=17.98$, $p<0.001$; Newman Keuls: shScramble day1 vs. day2, $p<0.01$; shCCK day1 vs. day2, NS; Day 1 shScramble vs. shCCK, NS; Day 2 shScramble vs. shCCK, $p<0.001$). When split in 2-min time bins, differences in immobility time appeared significant on the second day of testing (Day 1 shRNA: $F_{(1,17)}=3.75$, NS; Bins: $F_{(2,34)}=90.66$, $p<0.001$; Day 2 shRNA: $F_{(1,17)}=11.34$, $p<0.01$; Bins: $F_{(2,34)}=16.07$, $p<0.001$). Latency to the first immobility episode was increased in shCCK-injected mice on day 1 (shRNA: $F_{(1,17)}=4.54$, $p<0.05$; Days: $F_{(1,17)}=121.76$, $p<0.001$; Newman Keuls: shScramble day1 vs. day2, $p<0.001$; shCCK day1 vs. day2, $p<0.001$; Day 1 shScramble vs. shCCK, $p<0.05$; Day 2 shScramble vs. shCCK, NS). Altogether, these results suggest that down-regulating CCK expression in the amygdala decreases despair-like behavior.

Animals from Cohort 1 were further tested in the tail suspension paradigm. No statistical difference was detected for behavioral parameters of despair in this test (Suppl. Figure 2).

Aversive place conditioning

The ability of AAV₂-shCCK injected mice to acquire conditioned place aversion (CPA) was evaluated in both cohorts of injected mice. As no statistical differences were revealed between cohorts, they were pooled together and results are shown in Figure 5. Animals injected with AAV₂-shCCK or AAV₂-shScramble both acquired a CPA induced by naloxone (cohort: $F_{(1,36)}=0.39$, NS; shRNA: $F_{(1,36)}=1.45$, NS; treatment: $F_{(1,36)}=7.20$, $p<0.01$; session $F_{(1,36)}=11.57$, $p<0.001$; session x treatment interaction $F_{(1,36)}=9.08$, $p<0.01$). No statistical differences were detected between groups for the activity during drug-paired conditioning sessions neither for the number of entries in the compartments during test sessions (Suppl. Figure 3).

Physical dependence to morphine

Finally, we examined the effects of CCK mRNA down-regulation in BLA on somatic signs of withdrawal to morphine. A significant incidence of behavioral signs of withdrawal was observed after naloxone administration in both AAV₂-shCCK and AAV₂-shScramble injected mice (Horizontal activity: shRNA $F_{(1,12)}=0.00$, NS; treatment $F_{(1,12)}=8.54$, $p<0.01$; Rearing: shRNA $F_{(1,12)}=2.18$, NS; treatment $F_{(1,12)}=30.93$, $p<0.001$; Jumping: shRNA $F_{(1,12)}=1.17$, NS; treatment $F_{(1,12)}=26.34$, $p<0.001$; Front paw tremors: shRNA $F_{(1,12)}=1.40$, NS; treatment $F_{(1,12)}=42.46$, $p<0.001$; Scratches: shRNA $F_{(1,12)}=0.04$, NS; treatment $F_{(1,12)}=12.94$, $p<0.01$; Genital licks: shRNA $F_{(1,12)}=0.45$, NS; treatment $F_{(1,12)}=2.17$, NS; Grooming: shRNA $F_{(1,12)}=0.08$, NS; treatment $F_{(1,12)}=13.25$, $p<0.01$; Body tremor: shRNA $F_{(1,12)}=0.33$, NS; treatment $F_{(1,12)}=8.33$, $p<0.01$; Ptosis: shRNA $F_{(1,12)}=0.20$, NS; treatment $F_{(1,12)}=88.20$, $p<0.001$; Mastication: shRNA $F_{(1,12)}=0.00$, NS; treatment $F_{(1,12)}=338.00$, $p<0.001$; Piloerection: shRNA $F_{(1,12)}=0.00$, NS; treatment $F_{(1,12)}=450.00$, $p<0.001$) (see Table 1). The results of the global withdrawal analysis (Figure 6) showed a significant effect of treatment ($F_{(1,12)}=10.10$, $p<0.001$) but no effect of shRNA injection ($F_{(1,12)}=0.17$, NS). Thus the viral treatment had no effect on the somatic signs of morphine-induced withdrawal.

Accuracy and efficiency of CCK down-regulation in the BLA in behaviorally tested animals

In *experiment 2*, after the last behavioral experiment, we checked for stereotaxic injection accuracy in the BLA (Figure 7A). Animals showing absent or misplaced eGFP expression were excluded from statistical analysis (Cohort 1: 7 mice; Cohort 2: 3 mice). Qualitative *in situ* hybridization procedures were performed to confirm *mcck* down-regulation; representative pictures are depicted in Figure 7B. In addition, [³⁵S]-ISH allowed quantifying CCK mRNA level (Figure 7D). CCK binding showed a significant ~35% reduction in the BLA (Unpaired Student's t-test, $t=3.17$, $**p<0.01$) of AAV₂-shCCK injected mice, as compared to controls (AAV₂-shScramble). Together with *experiment 1*, our results clearly demonstrate that AAV₂-shCCK viral vector injection enabled potent down-regulation of CCK expression in the BLA throughout the whole period of behavioral analysis.

Discussion

The aim of the present study was to examine the role of CCK expressed at the level of the basolateral nucleus of the amygdala in negative emotional responses. We used a local shRNA approach to evaluate the implication of amygdalar CCK in several behavioral responses, including anxiety and despair-like behaviors, aversive place conditioning and the withdrawal syndrome to chronic morphine.

CCK has been largely implicated in anxiety-related behaviors as demonstrated in human studies (Berna et al 2007; Eser et al 2011), as well as animal models using either pharmacological (Rotzinger et al 2010; Wang et al 2011) or genetics approaches (Chen et al 2010; Dauge et al 2001; Raud et al 2005). In the open field and the light/dark box tests, we found no genotype effect, possibly due to stressful lighting conditions during testing (Prut & Belzung 2003) or to handling and test history effects, as previously reported by Voikar et al (2004). Remarkably, data from the EPM experiments showed a significant enhancement of exploration in the open arms and increased risk-taking behavior in two independent cohorts of AAV₂-shCCK injected mice. Because shRNA treatment produced no change in total locomotor activity in this test, the observed effects are not attributable to general activity changes. This result clearly indicates that CCK down-regulation decreases levels of anxiety, in agreement with the well-established anxiogenic role of CCK in previous reports. Most importantly, the strong effect of local CCK down-regulation at the level of BLA, while CCK mRNA expression was intact in other brain areas, reveals a main role for amygdalar CCK in the regulation of anxiety. This is consistent with the notion that high CCK activity in the amygdala is associated with high levels of anxiety. Sherrin et al (2009) demonstrated that both CCK mRNA expression levels and CCK₂ receptor immunoreactivity were elevated in BLA of mice presenting anxiogenic responses in the open field and EPM tests, both elicited by pretreatment with a corticotrophin-releasing factor agonist. Also, studies in rats showed that local activation of amygdalar CCK₂ receptors reduced time spent in open arms of the plus-maze (Belcheva et al 1994) and potentiated the startle response in the acoustic startle test (Frankland et al 1997). The latter studies together with our data suggest that

CCK acting at local CCK₂ receptors of the BLA increases levels of anxiety. This mechanism is in accordance with anatomical and electrophysiological studies indicating that CCK is mainly expressed in GABAergic interneurons of the BLA (Chung & Moore 2009; Jasnow et al 2009). Altogether therefore, the data suggest that a large part of anxiogenic activity of the CCK system operates via local mechanisms within the BLA. We cannot exclude, however, that CCK possibly expressed at the level of glutamatergic BLA neurons (Mascagni & McDonald 2003) and acting at receptors in BLA projections areas may also be involved, and this will be investigated in future studies.

The CCK system has been also involved in depressive-related behaviors, although this aspect of CCK function is less-well documented than its role in anxiety. Polymorphisms of the CCK gene were associated with susceptibility for suicidal behavior (Berna et al 2007; Shindo & Yoshioka 2005). In preclinical studies, systemic administration of CCK₂-antagonists decreased immobility in the forced swim test, with synergistic effects of the enkephalinase inhibitor RB101 (Hernando et al 1996), and reduced despair behavior after restraint stress (Becker et al 2008). In agreement with these previous reports, our data show a reduction of despair-like behavior upon AAV₂-shCCK treatment in the forced swim test. The antidepressant effect of CCK down-regulation was not detected in the tail suspension test. Although the two tests share common theoretical bases and behavioral measures (Kulkarni & Dhir 2007), differences in sensitivity were reported in response to experimental manipulations and environmental factors (handling, age, sex, previous behavioral testing) (Miller et al 2010). Importantly again, modifications in the forced swim test were detected following local CCK mRNA down-regulation specifically in the BLA, whereas CCK mRNA was expressed elsewhere in the brain. This result demonstrates for the first time a key role for amygdalar CCK in despair behavior. To our knowledge, no previous pharmacological manipulation has provided evidence for this. As for anxiety-related behaviors, the modulation of depressive states by CCK expressed at the level of the BLA may recruit local mechanisms, which requires further investigation.

Finally CCK has been also involved in appetitive/aversive responses, and this was evidenced in both the expression of morphine-induced place preference (Mitchell et al 2006) and morphine withdrawal-induced place aversion (Valverde & Roques 1998). Therefore, we also evaluated the effect of local CCK mRNA down-regulation in the BLA using two aversive situations, i.e. place aversion induced by naloxone and the physical consequences of morphine withdrawal. On one hand, we observed that AAV₂-shCCK injected mice show a trend toward reduced place aversion in the naloxone-induced CPA paradigm. This suggests that CCK either mediates aversive properties of naloxone, at least partially, or contributes to place learning (Le Merrer et al 2011). Further investigations will be necessary to confirm this result. Experiments using different place conditioning paradigms, such as morphine-conditioned place preference and lithium-induced CPA will clarify whether decreased naloxone-CPA may reflect a role of amygdalar CCK in cognition or hedonic homeostasis. On the other hand, our analysis of the morphine withdrawal syndrome shows no effect of amygdalar CCK down-regulation in somatic signs of withdrawal. Pommier et al (2002) reported increased prevalence of physical withdrawal in CCK₂ receptor deficient mice, implicating the CCK system in morphine withdrawal. Physical

withdrawal, however, engages many transmitter systems throughout the brain (Koob & Volkow 2010), and it is therefore not surprising that the local deletion of CCK in a highly restricted brain region does not influence the withdrawal syndrome. In addition, motivational signs of withdrawal were not measured in this experiment, and CCK contributes only partially to the physical signs of withdrawal.

In conclusion, this study establishes for the first time that CCK produced at the level of amygdala increases levels of anxiety and favors despair behavior, possibly via local activity. This neural mechanism likely contributes to mood homeostasis and dysregulation of CCK expression in the amygdala may be a causal factor in panic disorders and major depression.

Bibliography

- Ambesi-Impiombato A, D'Urso G, Muscettola G, de Bartolomeis A. 2003. Method for quantitative in situ hybridization histochemistry and image analysis applied for Homer1a gene expression in rat brain. *Brain Res Brain Res Protoc* 11:189-96
- Becker C, Zeau B, Rivat C, Blugeot A, Hamon M, Benoliel JJ. 2008. Repeated social defeat-induced depression-like behavioral and biological alterations in rats: involvement of cholecystokinin. *Mol Psychiatry* 13:1079-92
- Beinfeld MC. 2001. An introduction to neuronal cholecystokinin. *Peptides* 22:1197-200
- Belcheva I, Belcheva S, Petkov VV, Petkov VD. 1994. Asymmetry in behavioral responses to cholecystokinin microinjected into rat nucleus accumbens and amygdala. *Neuropharmacology* 33:995-1002
- Berna MJ, Tapia JA, Sancho V, Jensen RT. 2007. Progress in developing cholecystokinin (CCK)/gastrin receptor ligands that have therapeutic potential. *Curr Opin Pharmacol* 7:583-92
- Berrendero F, Castane A, Ledent C, Parmentier M, Maldonado R, Valverde O. 2003. Increase of morphine withdrawal in mice lacking A2a receptors and no changes in CB1/A2a double knockout mice. *Eur J Neurosci* 17:315-24
- Bradwejn J, Koszycki D. 2001. Cholecystokinin and panic disorder: past and future clinical research strategies. *Scand J Clin Lab Invest Suppl* 234:19-27
- Cain BM, Connolly K, Blum A, Vishnuvardhan D, Marchand JE, Beinfeld MC. 2003. Distribution and colocalization of cholecystokinin with the prohormone convertase enzymes PC1, PC2, and PC5 in rat brain. *J Comp Neurol* 467:307-25
- Chen Q, Tang M, Mamiya T, Im HI, Xiong X, et al. 2010. Bi-directional effect of cholecystokinin receptor-2 overexpression on stress-triggered fear memory and anxiety in the mouse. *PLoS One* 5:e15999
- Chotteau-Lelievre A, Dolle P, Gofflot F. 2006. Expression analysis of murine genes using in situ hybridization with radioactive and nonradioactively labeled RNA probes. *Methods Mol Biol* 326:61-87
- Chung L, Moore SD. 2009. Cholecystokinin excites interneurons in rat basolateral amygdala. *J Neurophysiol* 102:272-84
- Dauge V, Sebret A, Beslot F, Matsui T, Roques BP. 2001. Behavioral profile of CCK2 receptor-deficient mice. *Neuropsychopharmacology* 25:690-8
- Duangdao DM, Clark SD, Okamura N, Reinscheid RK. 2009. Behavioral phenotyping of neuropeptide S receptor knockout mice. *Behav Brain Res* 205:1-9
- Eser D, Uhr M, Leicht G, Asmus M, Langer A, et al. 2011. Glyoxalase-I mRNA expression and CCK-4 induced panic attacks. *J Psychiatr Res* 45:60-3

- Frankland PW, Josselyn SA, Bradwejn J, Vaccarino FJ, Yeomans JS. 1997. Activation of amygdala cholecystokininB receptors potentiates the acoustic startle response in the rat. *J Neurosci* 17:1838-47
- Frenois F, Cador M, Caille S, Stinus L, Le Moine C. 2002. Neural correlates of the motivational and somatic components of naloxone-precipitated morphine withdrawal. *Eur J Neurosci* 16:1377-89
- Frenois F, Stinus L, Di Blasi F, Cador M, Le Moine C. 2005. A specific limbic circuit underlies opiate withdrawal memories. *J Neurosci* 25:1366-74
- Ghijzen WE, Leenders AG, Wiegant VM. 2001. Regulation of cholecystokinin release from central nerve terminals. *Peptides* 22:1213-21
- Giacobini P, Wray S. 2008. Prenatal expression of cholecystokinin (CCK) in the central nervous system (CNS) of mouse. *Neurosci Lett* 438:96-101
- Hebb AL, Poulin JF, Roach SP, Zacharko RM, Drolet G. 2005. Cholecystokinin and endogenous opioid peptides: interactive influence on pain, cognition, and emotion. *Prog Neuropsychopharmacol Biol Psychiatry* 29:1225-38
- Hernando F, Fuentes JA, Fournie-Zaluski MC, Roques BP, Ruiz-Gayo M. 1996. Antidepressant-like effects of CCK(B) receptor antagonists: involvement of the opioid system. *Eur J Pharmacol* 318:221-9
- Hokfelt T, Blacker D, Broberger C, Herrera-Marschitz M, Snyder G, et al. 2002. Some aspects on the anatomy and function of central cholecystokinin systems. *Pharmacol Toxicol* 91:382-6
- Jasnow AM, Ressler KJ, Hammack SE, Chhatwal JP, Rainnie DG. 2009. Distinct subtypes of cholecystokinin (CCK)-containing interneurons of the basolateral amygdala identified using a CCK promoter-specific lentivirus. *J Neurophysiol* 101:1494-506
- Koob GF, Volkow ND. 2010. Neurocircuitry of addiction. *Neuropsychopharmacology* 35:217-38
- Kulkarni SK, Dhir A. 2007. Effect of various classes of antidepressants in behavioral paradigms of despair. *Prog Neuropsychopharmacol Biol Psychiatry* 31:1248-54
- Le Merrer J, Plaza-Zabala A, Del Boca C, Matifas A, Maldonado R, Kieffer BL. 2011. Deletion of the delta Opioid Receptor Gene Impairs Place Conditioning But Preserves Morphine Reinforcement. *Biol Psychiatry* 69:700-3
- LeDoux JE. 2000. Emotion circuits in the brain. *Annu Rev Neurosci* 23:155-84
- Lu L, Zhang B, Liu Z, Zhang Z. 2002. Reactivation of cocaine conditioned place preference induced by stress is reversed by cholecystokinin-B receptors antagonist in rats. *Brain Res* 954:132-40
- Mascagni F, McDonald AJ. 2003. Immunohistochemical characterization of cholecystokinin containing neurons in the rat basolateral amygdala. *Brain Res* 976:171-84

- Matthes HW, Maldonado R, Simonin F, Valverde O, Slowe S, et al. 1996. Loss of morphine-induced analgesia, reward effect and withdrawal symptoms in mice lacking the mu-opioid-receptor gene. *Nature* 383:819-23
- McIlwain KL, Merriweather MY, Yuva-Paylor LA, Paylor R. 2001. The use of behavioral test batteries: effects of training history. *Physiol Behav* 73:705-17
- Meziane H, Devigne C, Tramu G, Soumireu-Mourat B. 1997. Distribution of cholecystokinin immunoreactivity in the BALB/c mouse forebrain: an immunocytochemical study. *J Chem Neuroanat* 12:191-209
- Miller BH, Schultz LE, Gulati A, Su AI, Pletcher MT. 2010. Phenotypic characterization of a genetically diverse panel of mice for behavioral despair and anxiety. *PLoS One* 5:e14458
- Mitchell JM, Bergren LJ, Chen KS, Fields HL. 2006. Cholecystokinin is necessary for the expression of morphine conditioned place preference. *Pharmacol Biochem Behav* 85:787-95
- Mutt V, Jorpes JE. 1968. Structure of porcine cholecystokinin-pancreozymin. 1. Cleavage with thrombin and with trypsin. *Eur J Biochem* 6:156-62
- Noble F, Roques BP. 2002. Phenotypes of mice with invalidation of cholecystokinin (CCK(1) or CCK(2)) receptors. *Neuropeptides* 36:157-70
- Noble F, Wank SA, Crawley JN, Bradwejn J, Seroogy KB, et al. 1999. International Union of Pharmacology. XXI. Structure, distribution, and functions of cholecystokinin receptors. *Pharmacol Rev* 51:745-81
- Pommier B, Beslot F, Simon A, Pophillat M, Matsui T, et al. 2002. Deletion of CCK2 receptor in mice results in an upregulation of the endogenous opioid system. *J Neurosci* 22:2005-11
- Prut L, Belzung C. 2003. The open field as a paradigm to measure the effects of drugs on anxiety-like behaviors: a review. *Eur J Pharmacol* 463:3-33
- Raud S, Innos J, Abramov U, Reimets A, Koks S, et al. 2005. Targeted invalidation of CCK2 receptor gene induces anxiolytic-like action in light-dark exploration, but not in fear conditioning test. *Psychopharmacology (Berl)* 181:347-57
- Rotzinger S, Lovejoy DA, Tan LA. 2010. Behavioral effects of neuropeptides in rodent models of depression and anxiety. *Peptides* 31:736-56
- Rotzinger S, Vaccarino FJ. 2003. Cholecystokinin receptor subtypes: role in the modulation of anxiety-related and reward-related behaviours in animal models. *J Psychiatry Neurosci* 28:171-81
- Schiffmann SN, Vanderhaeghen JJ. 1991. Distribution of cells containing mRNA encoding cholecystokinin in the rat central nervous system. *J Comp Neurol* 304:219-33

- Sherrin T, Todorovic C, Zeyda T, Tan CH, Wong PT, et al. 2009. Chronic stimulation of corticotropin-releasing factor receptor 1 enhances the anxiogenic response of the cholecystokinin system. *Mol Psychiatry* 14:291-307
- Shindo S, Yoshioka N. 2005. Polymorphisms of the cholecystokinin gene promoter region in suicide victims in Japan. *Forensic Sci Int* 150:85-90
- Valverde O, Roques BP. 1998. Cholecystokinin modulates the aversive component of morphine withdrawal syndrome in rats. *Neurosci Lett* 244:37-40
- Voikar V, Vasar E, Rauvala H. 2004. Behavioral alterations induced by repeated testing in C57BL/6J and 129S2/Sv mice: implications for phenotyping screens. *Genes Brain Behav* 3:27-38
- Wang H, Spiess J, Wong PT, Zhu YZ. 2011. Blockade of CRF1 and CCK2 receptors attenuated the elevated anxiety-like behavior induced by immobilization stress. *Pharmacol Biochem Behav* 98:362-8
- Wang H, Wong PT, Spiess J, Zhu YZ. 2005. Cholecystokinin-2 (CCK2) receptor-mediated anxiety-like behaviors in rats. *Neurosci Biobehav Rev* 29:1361-73
- Zolotukhin S, Potter M, Zolotukhin I, Sakai Y, Loiler S, et al. 2002. Production and purification of serotype 1, 2, and 5 recombinant adeno-associated viral vectors. *Methods* 28:158-67

Legends to figures

Figure 1: Qualitative validation of AAV₂-shCCK knockdown into the mouse BLA. Representative brain microsections showing DAPI staining (left), dig-labeled CCK mRNA (middle), and eGFP expression (right) of mice unilaterally injected into BLA with either (A) AAV₂-eGFP (intact *mcck* expression), or (B) AAV₂-shCCK (reduced *mcck* expression) viral vectors (1.5 μ l, 3x10¹¹ vg/ml), and sacrificed for tissue collection either 2 or 6 weeks following surgery.

Figure 2: Behavioral testing. Schematic representation of the general procedure used to evaluate the effects of local AAV₂-shCCK injections into mouse BLA over emotional responses on two independent cohorts of mice. (A) Set of behaviors evaluated in cohort 1. (B) Set of behaviors evaluated in cohort 2. *For the forced swim test experimental conditions were slightly different between cohorts. Cohort 1; 1 day of test - room light intensity: 30Lx - temperature of the water: 19°C. Cohort 2; 2 days of test - room light intensity: 20Lx - temperature of the water: 22°C.

Figure 3: CCK knockdown in mouse BLA reduces anxious behavior in the Elevated Plus-Maze. Emotional responses in EMP test of mice stereotaxically injected into BLA with either AAV₂-shCCK (grey bars) or AAV₂-shScramble (white bars) viral vectors (1.5 μ l, 3x10¹¹ vg/ml). (A) AAV₂-shCCK-injected mice showed reduced anxiety levels as evaluated by: Total time spent in the arms (seconds); Total number of entries in the arms; Ratio of time spent in and number of entries to the open arms ((open arm)/(open arm + closed arms)); Total distance traveled in the maze (cm). (B) AAV₂-shCCK-injected mice showed increased risk-taking behavior as determined by: Total number of head dips in the open arms; Number of head dips made and Percentage of time spent (seconds) in the distal part of the open arms (last 1/3 of the arm). All results are expressed as mean \pm SEM. Statistical differences were detected between treatments but not in cohort comparisons, thus data of cohort 1 and 2 are pooled together. White stars, comparisons between arms; asterisks, comparisons between shRNA. ☆☆☆p<0.001, *p<0.05, **p<0.01, ***p<0.01 (two-way ANOVA) (n=22 mice/group).

Figure 4: CCK knockdown in mouse BLA reduces despair-like behavior in the Forced Swim test. Emotional responses in forced swim test of mice stereotaxically injected into BLA with either AAV₂-shCCK (grey bars and circles) or AAV₂-shScramble (white bars and circles) viral vectors (1.5 μ l, 3x10¹¹ vg/ml). AAV₂-shCCK-injected mice showed reduced despair behavior both in Cohort 1 (A) and Cohort 2 (B) as evaluated by: Time course of immobility in 2min bins (seconds); Percentage of immobility time during the 6min test; Latency to the first immobility episode (seconds). In Cohort 2 data shows results on both day 1 and day 2 of testing. All results are expressed as mean \pm SEM. Asterisks, individual comparisons between shRNA; black stars, global time courses comparisons between shRNAs; white stars, comparisons between days. On cohort 1 (A), ★★p<0.001, two-way

ANOVA; * $p < 0.05$, ** $p < 0.01$, post-hoc conditioning test; *** $p < 0.001$, one-way ANOVA; (n=10-11 mice/group). On cohort 2 (B), ★★ $p < 0.01$, two-way ANOVA; * $p < 0.05$, ** $p < 0.01$, *** $p < 0.001$, ☆☆ $p < 0.01$, ☆☆☆ $p < 0.001$, post-hoc conditioning test; (n=9-10 mice/group).

Figure 5: CCK knockdown in mouse BLA reduces naloxone-induced place aversion.

CPA paradigm of mice stereotaxically injected into BLA with either AAV₂-shCCK (grey bars) or AAV₂-shScramble (white bars) viral vectors (1.5 μ l, 3x10¹¹ vg/ml). Place preference data is shown as mean \pm SEM of time spent in the drug-paired chamber (expressed as a percentage of time spent in the two compartments) during the 15min pre-conditioning (full bars) and post-conditioning (striped bars) test sessions. Three-way ANOVA showed differences in treatments and conditioning sessions but not in Cohorts or shRNA injections. Thus data of cohort 1 and 2 are pooled together. Individual analysis within the naloxone treated mice showed differences between pre- and post-conditioning test only in the shScramble group. *** $p < 0.001$, Unpaired Student's t-test (n=11 mice/group).

Figure 6: CCK knockdown in mouse BLA has no effect over naloxone-precipitated withdrawal after morphine-chronic treatment.

Behavioral evaluation of withdrawal syndrome of mice stereotaxically injected into BLA with either AAV₂-shCCK (grey bars) or AAV₂-shScramble (white bars) viral vectors (1.5 μ l, 3x10¹¹ vg/ml). Global withdrawal score data ((activity + rearings + scratches + genital licks + head shakes + wet dog shakes + grooming)x0.5 + (jumps + front paw tremors + sniffings)x1 + (body tremors + ptosis + teeth chattering + piloerection)x1) is expressed as mean \pm SEM. Two-way ANOVA showed differences in treatments but not in shRNA comparisons, *** $p < 0.01$ (n=4 mice/group).

Figure 7: Quantitative validation of AAV₂-shRNA-CCK knockdown into the mouse BLA.

(A) Images from the Mouse Brain Atlas of Paxinos and Franklin (2001) showing histological reconstruction of injection sites into BLA. Black circles: correct injections of shCCK and shScramble vectors, red circles: misplaced injections. (B) Representative brain microsections showing eGFP expression (up), Dig-labeled CCK mRNA (middle) and DAPI staining (bottom) from mice bilaterally injected into BLA with either AAV₂-shScramble (intact *mcck* expression, left), or AAV₂-shCCK (reduced *mcck* expression, right) viral vectors (1.5 μ l, 3x10¹¹ vg/ml). (C) Representative autoradiographic image of a brain microsection processed by radioactive-ISH showing drawing ROIs (Ctx, RAS cortex region; BG, Striatum BackGround; BLA, BasoLateral nucleus of the Amygdala). (D) Relative *mcck* expression within BLA showing a ~35% reduction in AAV₂-shCCK respect to AAV₂-shScramble injected mice. Quantification was performed using ImageJ software and a calibration curve of C¹⁴standards (ARC0146; American Radiolabeled Chemicals). A rodbard non-lineal regression function was used to convert grey levels into counts of radioactivity (nCi/mg). Results are expressed in normalized values obtained from mean radioactive measures by the formula: (BLA - Striatum background)/(RAS Cortex - Striatum background) \pm SEM. Unpaired Student's t-test ** $p < 0.01$ (n=5mice/condition). Mice were sacrificed for tissue collection 9 weeks after surgery.

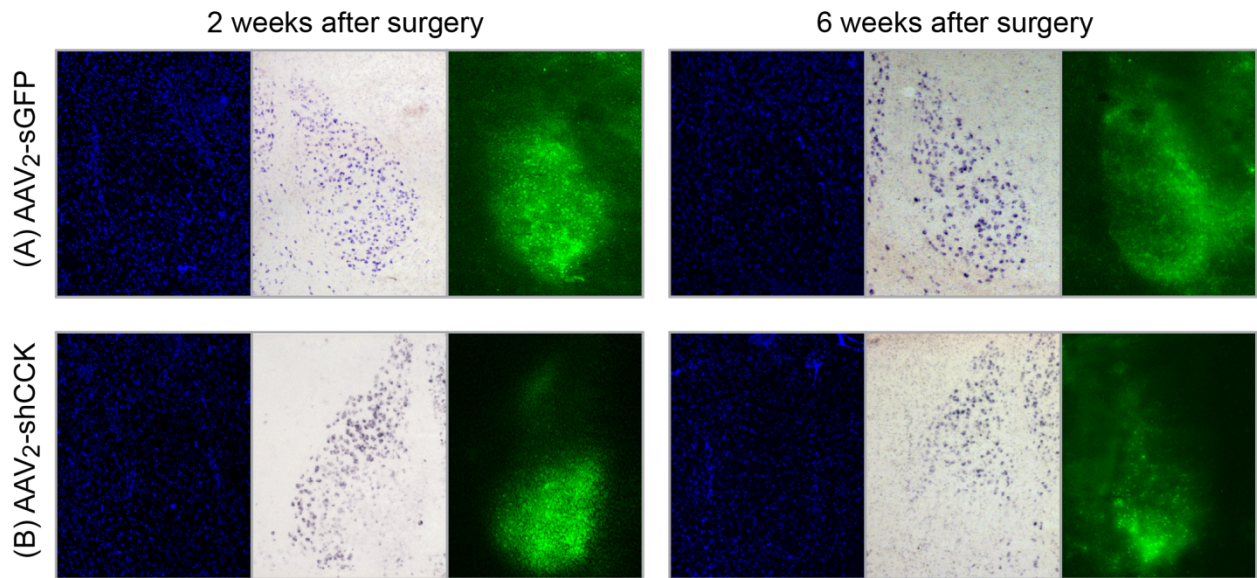
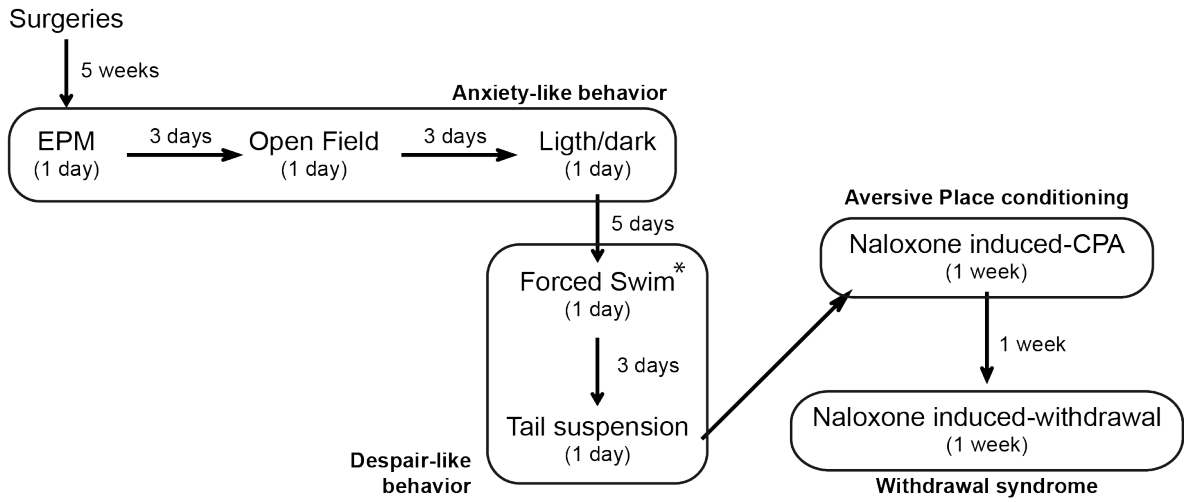


Figure 1

(A) Cohort 1



(B) Cohort 2

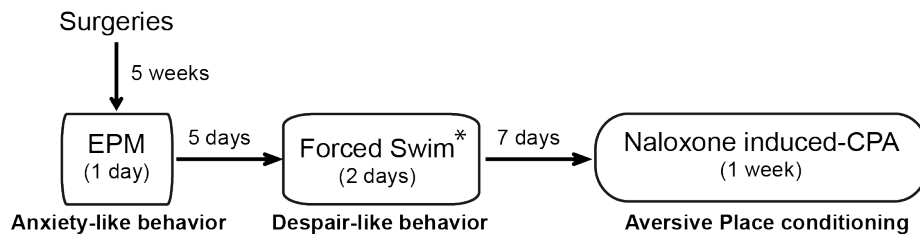


Figure 2

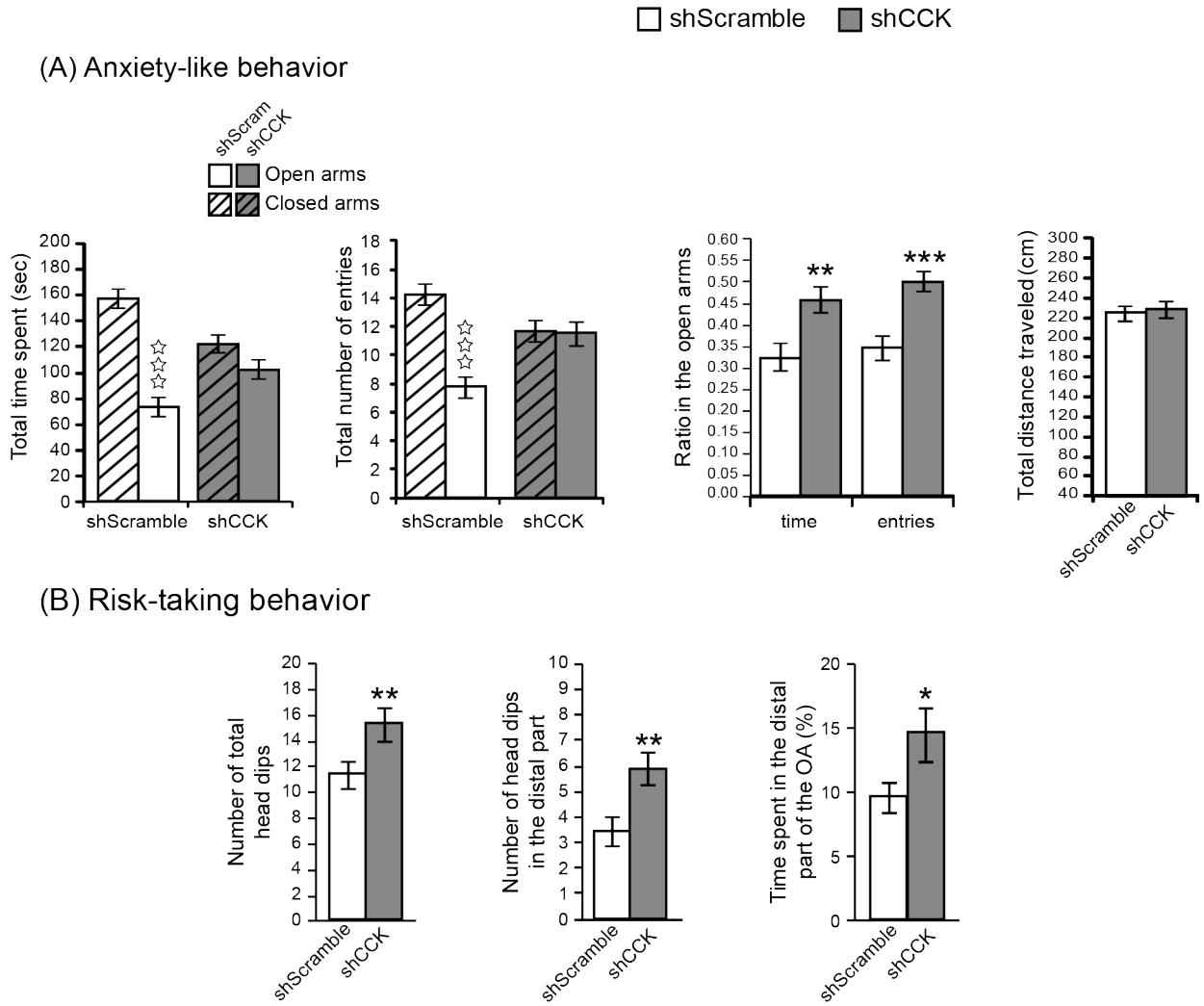
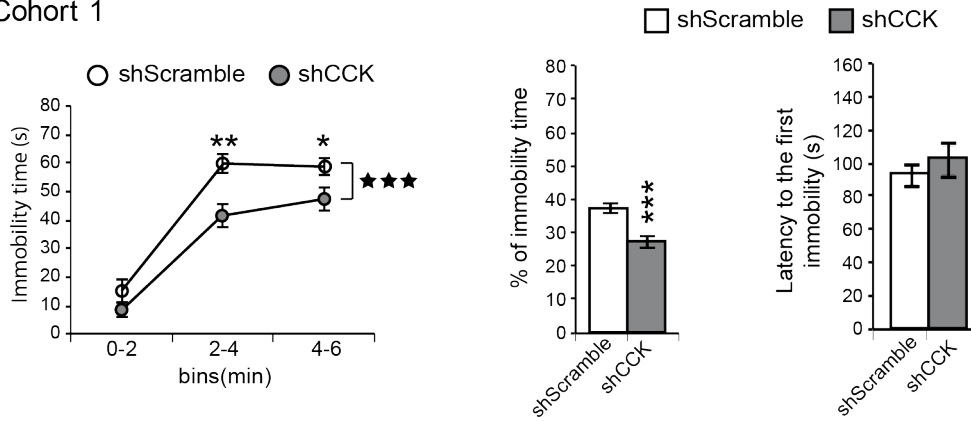


Figure 3

(A) Cohort 1



(B) Cohort 2

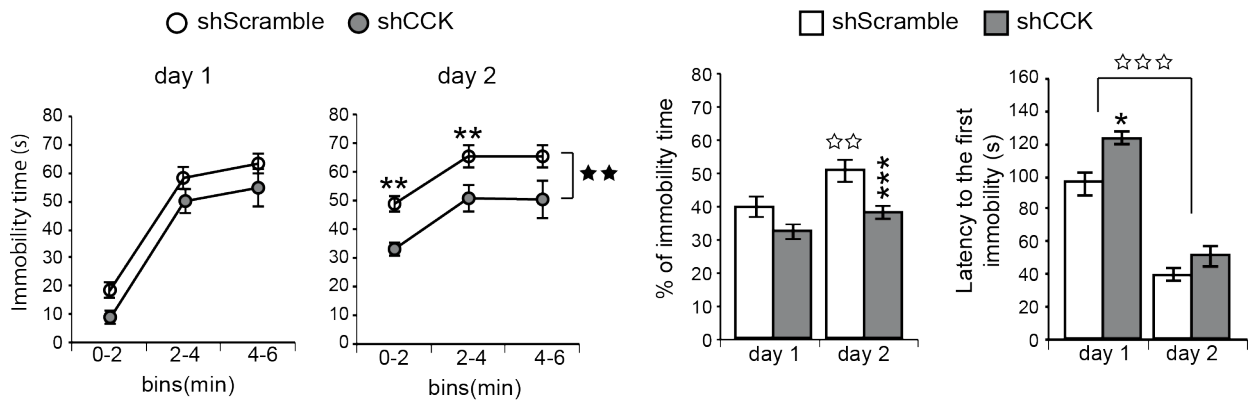


Figure 4

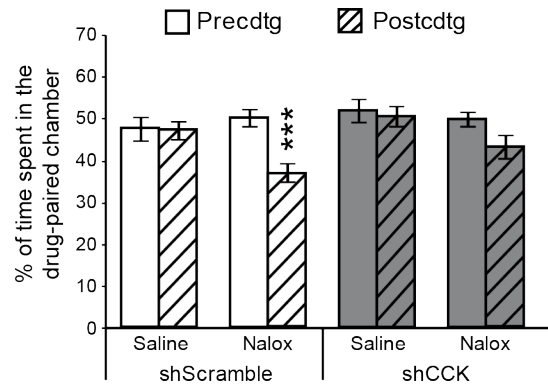


Figure 5

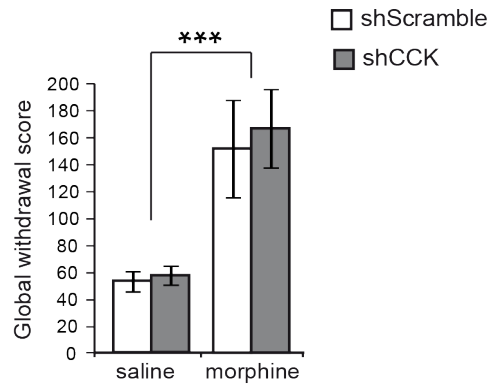


Figure 6

Table 1: Individual signs of naloxone precipitated-withdrawal in AAV₂-shCCK and AAV₂-shScramble injected mice after a morphine-chronic treatment. Data expressed in mean \pm SEM

Somatic Signs of Withdrawal					One-way ANOVA			
	shScramble		shCCK		Treatment comparison in shScramble		Treatment comparison in shCCK	
	saline	morphine	saline	morphine	F _(1,12)	P	F _(1,12)	P
Horizontal activity	5.50 \pm 0.20	3.75 \pm 0.63	5.13 \pm 0.52	4.13 \pm 0.43	7.00	0.05	2.23	NS
Rearings	80.75 \pm 6.86	45.00 \pm 6.75	91.75 \pm 9.03	53.75 \pm 1.32	13.81	0.01	17.34	0.01
Jumpings	0.00	51.75 \pm 12.34	0.00	33.75 \pm 11.19	15.59	0.01	9.09	0.05
Front paw tremors	1.25 \pm 0.75	64.00 \pm 18.22	1.50 \pm 0.87	91.50 \pm 14.70	11.83	0.01	37.35	0.00
Scratches	4.50 \pm 2.10	0.00	4.00 \pm 1.08	0.00	4.58	NS	13.17	0.05
Genital licks	2.50 \pm 1.50	0.75 \pm 0.75	1.50 \pm 0.65	0.50 \pm 0.50	1.09	NS	1.50	NS
Groomings	10.00 \pm 2.45	3.25 \pm 1.44	9.00 \pm 0.91	3.25 \pm 1.70	5.65	NS	8.86	0.05
Body tremor	0.00	1.5 \pm 0.71	0.00	1.00 \pm 0.58	5.40	NS	3.00	NS
Ptosis	0.00	2.5 \pm 0.29	0.00	2.75 \pm 0.48	75.00	0.001	33.00	0.001
Mastication	0.00	3.25 \pm 0.25	0.00	3.25 \pm 0.25	169.00	0.001	169.00	0.001
Piloerection	0.00	3.75 \pm 0.25	0.00	3.75 \pm 0.25	225.00	0.001	225.00	0.001

(n= 4 mice/group).

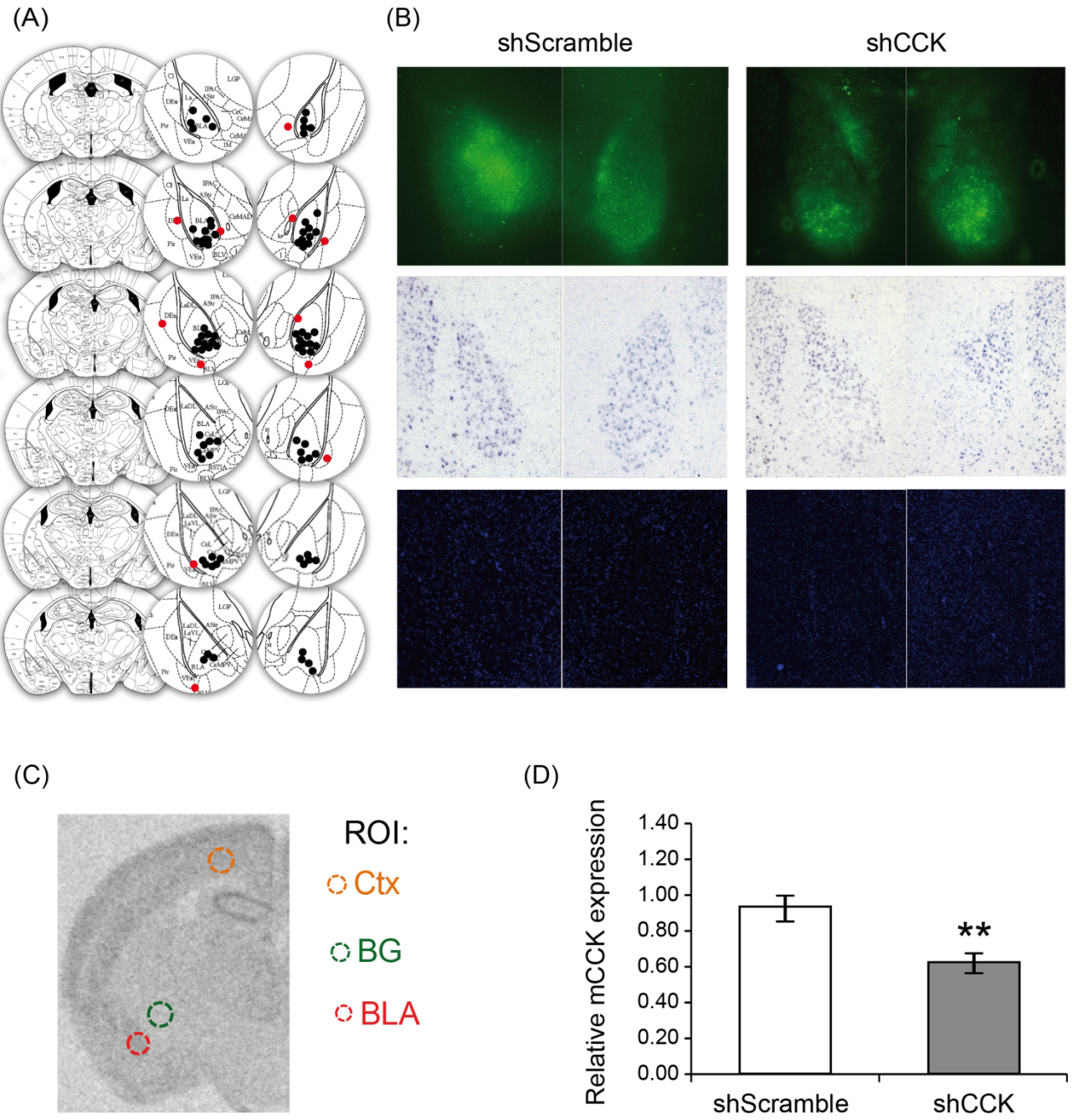


Figure 7

Supplementary information

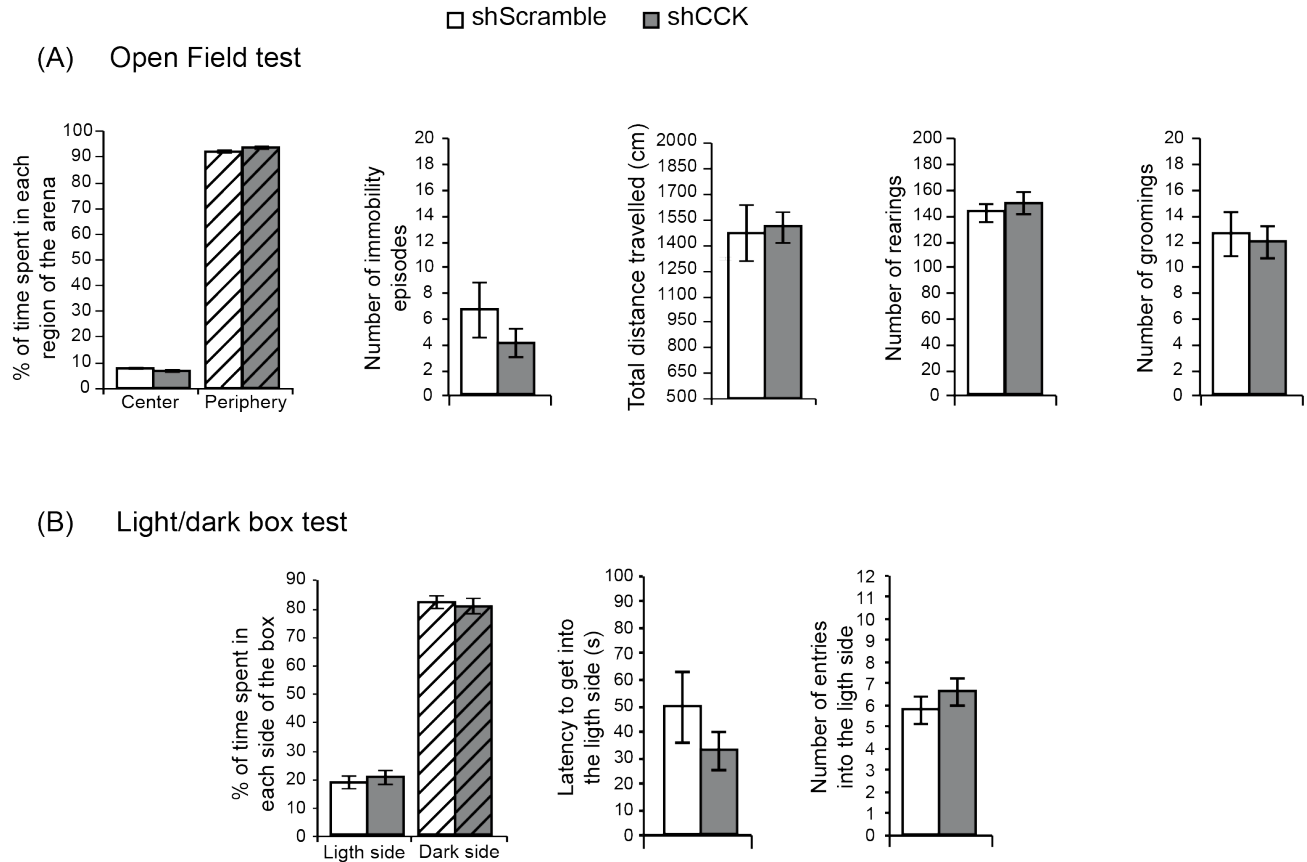


Figure S1: Anxiety responses in Open Field and Light/dark box test was not modified by CCK knockdown in mouse BLA. Emotional responses of mice stereotaxically injected into BLA with either AAV2-shCCK (grey bars) or AAV2-shScramble (white bars) viral vectors ($1.5\mu\text{l}$; 3×10^{11} vg/ml) were evaluated for the following parameters in the Open Field test (A): Percentage of time spent in each region of the arena (center vs. periphery); Number of immobility episodes during the 30min test; Total distance travelled in the arena (cm); Number of rearings and number of grooming during the 30min test. And the light/dark box test (B): Percentage of time spent in each side of the box (light side vs. dark side); Latency to get into the light side (seconds); Number of entries in the light side during the 6 min test. All results are expressed as mean \pm SEM ($n = 12-13$ mice/group).

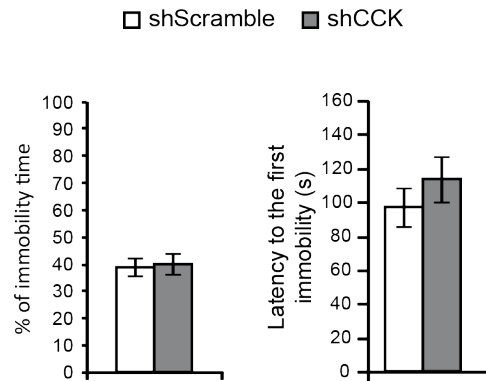


Figure S2: Tail suspension test response was not modified by CCK knockdown in mouse BLA. Emotional responses in tail suspension test of mice stereotaxically injected into BLA with either AAV2-shCCK (grey bars) or AAV2-shScramble (white bars) viral vectors ($1.5\mu\text{l}$; 3×10^{11} g/ml) were evaluated by the percentage of immobility time during the 6 min test and the latency to the first episode of immobility (seconds). All results are expressed as mean \pm SEM (n= 12-13 mice/group).

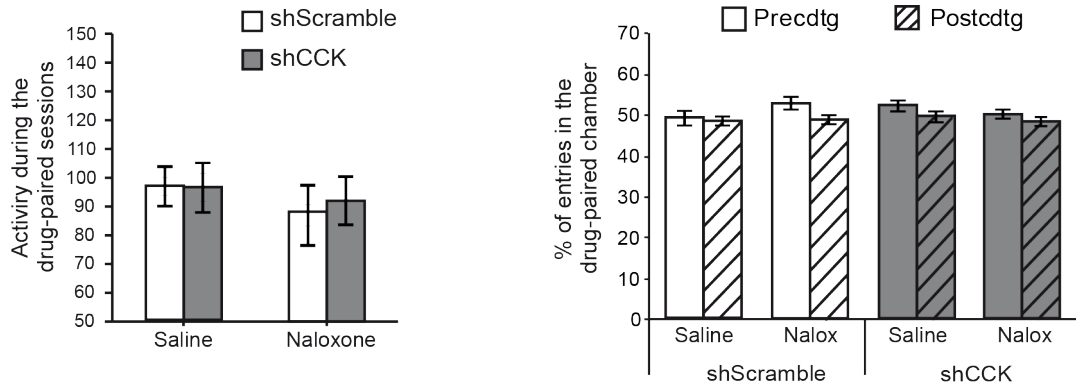


Figure S3: Activity signs evaluated during the naloxone-induced place aversion (CPA).

Conditioned place aversion paradigm of mice stereotaxically injected into BLA with either AAV2-shCCK (grey bars) or AAV2-shScramble (white bars) viral vectors ($1.5\mu\text{l}$; 3×10^{11} vg/ml) showed no differences in the total activity scored during drug-paired conditioning sessions, nor in the percentage of entries into the drug-paired chamber during the 15min pre-conditioning (full bars) and post-conditioning (striped bars) test sessions. All results are expressed as mean \pm SEM. (n= 11 mice/group).

5. Conclusions and perspectives

We designed a double promoter-based rAAV-eGFP(CMV)-shRNA(mU6) viral vector to target the CCK mRNA *in vivo* and demonstrated that this system provides efficient, long-lived (up to 3 months) and non-toxic shRNA expression in the mouse brain. During stereotaxic surgery delivery, after the viral injection, the extent of the transduced area depends on both the specific brain region targeted and the viral serotype used. In this sense, we showed that rAAV-serotype 5 presents a considerably increased spread as compared to the rAAV-serotype 2. Finally, we optimized the experimental conditions in order to effectively and stable down-regulate the CCK transcript in specific brain regions. Particularly, we successfully silenced *mccck* expression locally in the mouse Cg Cxt and BLA.

Using this genetic approach, we have demonstrated that CCK mRNA down-regulation in BLA has significant anxiolytic and antidepressant effects in the elevated plus-maze and forced swim test, respectively. On the one hand, the result observed on anxiety testing is agreement with previous pharmacological evidence showing the implication of amygdalar CCK on the anxiogenic-like effects of the peptide (Rotzinger & Vaccarino 2003; Sherrin et al 2009). On the other hand, our study uncovers an effect of amygdalar CCK on despair behavior. This evidence is in accordance with the demonstrated depressant properties of the peptide (Becker et al, 2008; Hernando et al 1996), as well as with previous studies showing that BLA lesions exerted anti-depressive behavioral effects on rats (Castro et al 2010). Moreover, rAAV₂-shCCK injected mice showed an apparent reduction in the performance of the naloxone-induced CPA. This result need to be confirmed with a larger number of mice and further analysis of place conditioning paradigms will be complete to elucidate whether this effect reflects a role of CCK in conditioned learning or in hedonic homeostasis. Finally, no effect of AAV₂-shCCK delivery into BLA was found on the naloxone-precipitated withdrawal to chronic morphine, reflecting the fact that many brain regions and complex circuits are involved in this aversive state (Koob & Volkow 2010).

In conclusion, the present study establishes for the first time a role of amygdalar CCK in the modulatory effect of the peptide on anxiety and depressive-like behaviors.

In this frame, as mentioned before, we have also set up the experimental conditions to target the mouse Cg Ctx region, another brain area where *mccck* appear to be modulated during protracted abstinence (see Part I). The Cg Ctx has been postulated as a critical region on the modulation of drug relapse evoked by conditioned stimuli, and has been also implicated in withdrawal syndrome (Goldstein & Volkow 2002; Lowe et al 2002).

Therefore, in future experiments we will characterize behavioral consequences of CCK silencing into Cg Ctx, particularly over the negative emotional state emergent during withdrawal and after prolonged drug-free periods.

IV. GENERAL DISCUSSION AND PERSPECTIVES

The aim of my thesis was to identify brain sites from which CCK could modulate emotional related behaviors and drug dependence. Thus, we investigated CCK transcriptional regulation in response to morphine treatment throughout the mouse brain, with focus in Cg Ctx and BLA; and we examined a possible implication of amygdalar CCK in emotional processing. In particular, we studied the role played by CCK expressed at the level of the BLA on negative emotional responses.

CCK is one of the major neuromodulatory peptides in the mammalian brain. Both peptides and receptors (especially CCK₂ receptor) present a wide distribution in the CNS co-localizing with classic neurotransmitters (dopamine, glutamate, GABA and serotonin) in neurons of rewarding, motivational and emotional pathways. The CCKergic system modulates a broad variety of physiological functions, including feeding behavior, cardio-respiratory control, thermoregulation, nociception, anxiety, depression, memory processes, and motivational responses. A previous study in our laboratory identified CCK as a mu-dependent gene which mRNA was significant modulated in the central extended amygdala upon morphine and nicotine treatments.

In this study, we first mapped the pattern of CCK mRNA distribution in the mouse brain and found that *mcck* was principally expressed in neocortex, piriform cortex, olfactory bulb, BNST, BLA, dental gyrus, hippocampus, several nuclei of the thalamus, ventral tegmental area, substantia nigra, and Raphe nuclei. This neuroanatomical distribution is in fully agreement with previous studies on mRNA and peptide localization (Cain et al 2003; Ingram et al 1989; Jones et al 2009; Schiffmann & Vanderhaeghen 1991). Next, we focused on two brain structures implicated in the processing of emotional states and drug dependence, both showing high CCK transcript density: the Cg Ctx and the BLA. We evaluated the consequences of an escalating chronic morphine treatment and a period of 4 weeks of abstinence over CCK mRNA expression in these regions. Our results show a trend for *mcck* up-regulation after 4 weeks abstinence in both Cg Ctx and BLA. Although these results need to be confirmed with an increased number of mice, the presented trends, detectable only in the abstinent mice, are consistent with an earlier study in our laboratory which examined both physical withdrawal and emotional alterations during protracted

abstinence and demonstrated a time-dependent dichotomy in the two processes (Goeldner et al 2011). This study, established the existence of depressive-like symptoms in morphine-abstinent mice emergent when the physical signs of withdrawal have dissipated; giving the notion of “incubation” of the negative affective state in drug abstinence. Such incubation would involve gradual restructuration of neural circuits as occurs for the neuronal adaptation involved in the transition from drug use to drug abuse (McClung & Nestler 2008; Rhodes & Crabbe 2005). Thus, the possibility of CCK up-regulation in the Cg Ctx and BLA after 4 weeks of drug-free period in morphine dependent mice suggests that CCK expressed in these structures may be involved in the development of the negative state characterizing protracted abstinence.

In the second part of this project, I developed an AAV-shCCK knock-down strategy and effectively down-regulated the CCK transcript in the mouse Cg Cxt and BLA. Taking advantage of this technology, we focused on the BLA region to examine the role of CCK in negative emotional responses in the mouse. We found that virally-mediated shCCK knockdown in this brain structure strongly reduces levels of anxiety and despair behavior, as evidenced in the elevated plus-maze and forced swim test, respectively. Moreover, AAV-shCCK injected mice showed a reduction in naloxone-induced conditioned-place aversion, another paradigm involving a negative emotional state.

This phenotype and the mechanism involved need to be further investigated. We first wish to confirm the result obtained in the naloxone-induced CPA and to further extend our knowledge of the amygdalar CCK role in this paradigm. In this sense, special care should be paid to the theoretical interpretation of the place conditioning results because, as a pavlovian task, this paradigm involves both learning processes and affective valuation of the tested drug through rewarding mechanisms (see review in Sanchis-Segura & Spanagel, 2006). Therefore, conditioned place preference to rewarding drugs, such as morphine, and conditioned place aversion to lithium, which exclude motivational circuits, will help to separate the tight intertwining of reward and cognitive processes (see ANNEX) and better elucidate the effect of amygdalar CCK over these responses. Furthermore, we will also complete the analysis of the morphine withdrawal syndrome. In the present study we show that local shCCK knockdown in BLA has no effect on the physical consequences of naloxone-precipitated withdrawal in morphine dependent mice. In future experiments we will evaluate the motivational component of morphine withdrawal syndrome, since

previous studies reported that systemic administration of CCK₂ receptor antagonist impair place aversion induced by naloxone in morphine dependent mice (Valverde & Roques 1998).

On the other hand, further molecular characterization of the shCCK BLA induced anxiogenic manifestations would help to understand the underlying mechanism through which CCK influence emotional responses. In this sense, different functional pathways are possible. The amygdalar CCK system could be operating via a local mechanism within the BLA. In support to this hypothesis, previous reports showed that local CCK₂ receptor agonist administration into BLA produce increased anxiety responses on rats as evaluated in the EPM and the acoustic startle test (Belcheva et al 1994; Frankland et al 1997). Nevertheless, the same local administration of CCK₂ receptor antagonist did not affect baseline acoustic startle response (Josselyn et al 1995). Systemic studies on mice have correlated an elevated CCK mRNA expression and CCK₂ receptor immunoreactivity in the BLA with anxiety responses induced by corticotrophin-releasing factor as evaluated in the EPM and the open field test (Sherrin et al 2009). In the same direction, i.p. injections of CCK₂ receptor antagonist attenuated anxiety-like behavior in animals subjected to immobilization restrain stress as examined in the EPM (Wang et al 2011). Interestingly, other studies using restrain protocols on rats reported that this stress decreased GABAergic inhibitory control in the BLA as well as increased anxiety in the EPM (Martijena et al 2002). Furthermore, this behavioral consequence of restrain stress was mimicked by administration of GABA_A receptor antagonist both systemic and locally into BLA (Rodriguez Manzanares et al 2005). These pharmacological data is concordant with data from CCK₂-receptor knockout mice whose displayed decreased levels of anxiety in the light-dark test, and presented increased function of the GABAergic system in the brain (Raud et al 2005). In contrast, electrophysiological studies are controversial with the previous results. Chung & Moore (2007) reported that local CCK application on rat BLA slices stimulates intrinsic GABAergic neurons acting with CCK₂ receptors, but the mechanism underlying this effect remains unclear. Besides, other study in periaqueductal gray region proposed a mechanism in which CCK induces suppression of GABAergic transmission by activation of CCK₁ receptors in both GABAergic and glutamatergic neurons (Mitchell et al 2011). Finally, CCK was shown expressed in a heterogeneous population of GABAergic BLA interneurons (Jasnow et al 2009) and, as presented in the general introduction, this co-localization shows a differential release modulation where CCK is co-released with GABA only under

conditions that lead to high frequency firing (Ghijsen et al 2001). Therefore, together with our results of anxiolytic responses obtained by AAV₂-shCCK mediated knock-down in BLA, we suggest a modulatory action between GABAergic transmission inducing anxiolytic responses and the CCKergic system inducing anxiogenic states occurring locally into BLA.

We cannot exclude, however, an involvement of CCK in projecting areas since immunohistochemical studies have also reported low levels of CCK immunoreactivity in pyramidal glutamatergic neurons of the BLA (Mascagni & McDonald 2003). The amygdaloid complex has widespread connections with other brain regions, and particularly, the BLA has major projections to the nucleus accumbens (NAcc) and the prefrontal cortex (PFC) regions (Sah et al 2003) (see [Figure 7](#) introduction). On one hand, pharmacological studies have involved Anterior and Posterior parts of NAcc in the depressant and anxiogenic effects of CCK, respectively (Dauge et al 1990; Smadja et al 1997). On the other hand, PFC has been related to processing of depression and mediation of anxiety-like responses (Blanco et al 2009; Koenigs et al 2008). Although there is no evidence concerning specific the role of cortical CCK in such behaviors, radioligand studies have shown high densities of CCK-binding sites on this area (Wang et al 2005), and amygdaloid nuclei has been linked to PFC in central circuits regulating depressive disorders and emotion (Bennett 2011; Davidson 2002).

Therefore, given the complexity of the amygdalar CCK system, a main step to follow this study will be to determine the brain localization of the peptide and its receptors in the local CCK knock-down mice. Immunohistochemical mapping of CCK (Meziane et al 1997) will enable to identify whether CCK mRNA down-regulation in the BLA affect peptide levels inside this structure and/or in projecting areas. Moreover, the receptor location in specific neuronal populations would help to better describe the molecular mechanism. A possible method to address this question is the use of immunofluorescence coupled with confocal microscopy for CCK receptors and specific neuron markers, such as GAD-67, specific marker for GABAergic neurons (Buddhala et al 2009), and v-glut, specific marker for glutamatergic neurons (Santos et al 2009).

Taken together, our data on this first local genetic approach of CCK role in emotional responses represents an important step towards understanding the peptide function in the brain. We clearly identify BLA as a main site for anxiogenic and depressant effects of neural CCK, and strongly suggest that amygdalar CCK contributes to mood homeostasis and

dysregulation of CCK expression in this region may be a causal factor in panic disorders and major depression. Besides, in the context of drug abuse, our results combined with preliminary data obtained in our laboratory, suggest that CCK in BLA may contribute to the depressive state that characterizes abstinence.

V. ANNEX

“Contributions to other projects in the laboratory. The lithium-conditioned place aversion paradigm”

A. Introduction

Conditioned place preference and aversion paradigms (CPP and CPA) are the most popular models to study the motivational effects of drugs treatments in experimental animals (Tzschentke 2007). In these procedures, the drug's effects (acting as unconditioned stimulus, US) are repeatedly paired with an initially neutral context, which will, therefore, acquire the ability to act as a conditioned stimulus (CS). Subsequently, the single exposure to the context is able to predict the effects of the drug and trigger a response of approach/avoidance behavior depending on the nature of such drug (appetitive or aversive, respectively). Therefore, place conditioning paradigms are useful tools to evaluate emotional and physiological properties of drugs treatments. Noteworthy, as a pavlovian conditioning task, these paradigms also involves environment recognition and discrimination, learning of the hierarchical relationships among events and cognitive establishment of the US-CS association (Maren 2001). Accordingly, many brain structures have been implicated in drug-induced place conditioning, involving main sites of reward pathways, such as ventral tegmental area, nucleus accumbens, and prefrontal cortex, but also the ventral pallidum, amygdala, hippocampus and pedunculo pontine tegmental nucleus (Silva et al 1998; Tzschentke 1998). Altogether, CPP and CPA paradigms implicated both high/order cognitive integration of contextual cues and emotional processing of the drug stimulus, which together contribute to setting of the drug/context association.

Among the drugs that have been tested in these conditioned paradigms, during this part of the thesis I will focus in the lithium chloride.

Experimental contribution

Lithium has long been a primary drug used for the treatment of bipolar disorder due to its established role as mood stabilizer, and additional main effects as neuroprotective and anti-apoptotic drug have been also reported (Chiu & Chuang 2010). Besides, in animal models, LiCl-induced conditioned place aversions have been found for a wide range of doses (Tenk et al 2005). For instance, Skoubis et al (2005) have used naloxone- and lithium-induced CPA to evaluate mice deficient of endogenous opioids and demonstrated that lithium aversion is not related to the endogenous opioid tone regulating hedonic state, since pro-enkephalin knockout mice failed to show aversion to naloxone but showed a

normal LiCl-CPA. In addition, although the mechanism underlying lithium place aversion is unclear, this behavioral task has been used to assess the nauseogenic properties of experimental drugs and it was reported that different antiemetic treatments either attenuate or completely block LiCl-CPA. Thus, the place avoidance produced by LiCl has been proposed as consequence of an emesis-related illness response in rodents (Frisch et al 1995; Rinaman et al 2009). Peripheral noradrenergic and serotonergic neurons located within the dorsomedial medulla and vagal afferents, respectively, appear to contribute importantly, mediating LiCl-induced hypophagia, nausea and vomiting effects (Parker & Limebeer 2006; Rinaman & Dzmura 2007).

During my thesis I established a lithium-induced-CPA paradigm in our laboratory as a useful tool to perform reliable studies on associative pavlovian learning as well as comparisons with drug-reinforced place conditioning paradigms, facilitating the distinction between rewarding and cognitive effects of specific treatments. Particularly, the paradigm was used to answer two questions:

1. Is the protein kinase RSK2 involved in place conditioned learning?
2. Is the impairment on morphine induced-CPP of δ -knockout mice related to the reinforcing properties of this drug or to an alteration on place learning processing?

This work lead to the publication of the following two manuscripts.

B. Manuscript 2:

RSK2 signaling in brain habenula mediates place learning

Darcq E¹, Koebel P¹, **Del Boca C¹**, Pannetier S¹, Kirstetter AS¹, Garnier JM¹, Hanauer A¹, Befort K¹ and Kieffer BL¹.

Submitted.

¹. Département de Neurobiologie et Génétique, Institut de Génétique et de Biologie Moléculaire et Cellulaire (IGBMC), Illkirch-Graffenstaden, France.

Corresponding author:

Pr. Brigitte L KIEFFER

IGBMC, Parc d'innovation 1 rue Laurent Fries BP 10142, 67404 Illkirch Cedex, France

Telephone: +33 (0)8 65 56 93, Fax: +33 (0)8 65 56 04, e-mail address: briki@igbmc.fr

Here, we used *mrsk2* gene knock-out mice (RSK2-KO) to investigate the role of the kinase, in the ability of the mice to associate a specific context with an aversive stimulus. RSK2 is a Ser/Thr kinase acting in the Ras/MAPK pathway, which deficiency leads to the Coffin-Lowry Syndrome characterized by cognitive deficit (Pereira et al 2010; Trivier et al 1996). Because of uncovered significant RSK2 mRNA expression in the habenular complex, we then further used a functional shRNA-viral approach to produce a local habenular *mrsk2* knockdown and investigate the impact of this modification on conditioned learning. In both parts of the study (RSK2-KO and RSK2-Knockdown) we used lithium-induced place aversion as a cognitive task to evaluate conditioned place learning.

Our results show that both RSK2 receptor KO and local RSK2 habenular-knockdown mice fail to demonstrate lithium place-aversion. Therefore, our study reveals a novel role of RSK2 signaling in cognitive processes and also uncovers the critical implication of the habenular complex on this behavioral task.

Abstract

RSK2 is a Ser/Thr kinase acting in the Ras/MAPK pathway. *Rsk2* gene deficiency leads to the Coffin-Lowry Syndrome, notably characterized by cognitive deficits. We found that *mrsk2* knockout mice are unable to associate an aversive stimulus with context, in a place-learning task requiring both high-order cognition and emotional processing. Virally-mediated shRNARSK2 knockdown in the habenula, whose involvement in cognition receives increasing attention, also ablated contextual conditioning. RSK2 signaling in habenula, therefore, is essential for this task. Our study reveals a novel role for RSK2 in cognitive processes, and uncovers the critical implication of an intriguing brain structure in place learning.

Introduction

The 90kDa ribosomal S6 kinases (RSKs) constitute a family of four homologous Ser/Thr kinases (RSK1-4) that are activated by extracellular-regulated kinases 1 and 2 (ERK1/2) in response to growth factors, hormones, chemokines and neurotransmitters. RSKs, in turn, phosphorylate several cytosolic and nuclear targets, and regulate a variety of cellular processes implicated in cell survival, growth, proliferation and migration (Anjum and Blenis, 2008). Many aspects of RSK function have been clarified at the level of cellular signaling, but the implications of RSK signaling *in vivo* remain largely unknown.

The important physiological role of RSK2 was uncovered by the discovery of *rsk2* gene defects in the Coffin-Lowry Syndrome (CLS) (Trivier et al., 1996). This X-linked disorder is characterized by psychomotor retardation, digit and facial dysmorphisms and progressive skeletal deformations (Hanauer and Young, 2002; Pereira et al., 2010). CLS is highly heterogeneous and mental retardation is variable, but most male patients show severe cognitive impairment. *mrsk2* knockout (KO) mice show some of the common features of CLS and altered glycogen metabolism in skeletal muscle (Dufresne et al., 2001) or lipodystrophy (El-Haschimi et al., 2003) have been reported. At the behavioral level, *mrsk2* KO mice show normal motor function and emotional responses, but display deficits in working and long-term spatial memory, as well as learning impairments in exploratory behavior (Poirier et al., 2007). Together therefore, both the human syndrome and the mouse phenotype reveal a role for RSK2 in learning and memory processes, in accordance with the reported brain distribution of this kinase in neocortex and hippocampus that are essential for cognitive function (Zeniou et al., 2002).

Here we investigated the role of RSK2 in the ability to associate a specific context with an aversive stimulus. This cognitive task involves place learning, which is essential for species survival (Silva et al., 1998). We examined *mrsk2* KO mice in a lithium-conditioned place aversion paradigm, and found that mutant mice are unable to express lithium place conditioning. Further, our investigation of RSK2 distribution in the mouse brain led us to uncover significant RSK2 expression in the habenular complex (Hb), a highly conserved brain

structure whose function is attracting increasing interest (Hikosaka, 2010; Lecourtier and Kelly, 2007). We then targeted RSK2 expression specifically in Hb, using virally-mediated RSK2 shRNA knockdown. We found a similar lack of lithium-conditioned place aversion in treated animals, demonstrating that RSK2 signaling in Hb is essential for the formation of drug/context associations.

Results

RSK2 knockout reduces conditioned place learning

We submitted *mrsk2* KO mice and their wild-type (WT) counterparts to a conditioned place aversion paradigm (CPA). Mutant mice and WT controls were conditioned to receive either saline or lithium (3 mE/kg) and tested for CPA (Figure 1). Three-way ANOVA showed a main effect of treatment [$F(1,56)=9.27$, $p=0.004$] but no effect of genotype [$F(1,56)=1.74$, $p=0.193$]. There were significant genotype x treatment ([$F(1,56)=4.672$, $p=0.035$), session x treatment ([$F(1,56)=11.76$, $p=0.001$), and session x genotype x treatment ([$F(1,56)=5.131$, $p=0.027$) interactions. Post-hoc comparisons of the post-conditioning session revealed no effect of genotype following saline, however the mutant mice had significantly decreased CPA compared to the WT group following 3mEq LiCl. These results show that lithium CPA is impaired in *mrsk2* KO mice, indicating that the ability to form the drug/context association is altered in these animals. RSK2 signaling, therefore, contributes to place learning.

RSK2 is expressed in medial habenula

RSK2 is expressed during embryogenesis (Dugani et al., 2010; Kohn et al., 2003) and postnatally. In the adult, strongest expression of RSK2 was reported in skeletal muscle, heart and pancreas. In the brain RSK2 was found at the level of the neocortex, hippocampus and purkinje cells of the cerebellum in both mouse and human (Zeniou et al., 2002). To fine map RSK2 expression throughout the adult mouse brain, we hybridized a digoxigenin-labeled *mrsk2* RNA probe to coronal brain sections from WT mice (Figure 2A). Our data confirm expression of the *mrsk2* transcript in the cortex and hippocampus, with strongest expression in the CA3 field. Interestingly, we also observed substantial *mrsk2* expression in Hb (Figure 2A). Labeling was prominent in the medial subdivision of Hb (MHb), indicating a transcript distribution restricted to Hb neurons receiving inputs from the limbic system and sending outputs to the interpeduncular nucleus projecting to the raphe (Hikosaka, 2010). We further confirmed expression of RSK2 protein in the Hb complex by Western blot analysis (Figure 2B). The 90 KDa immunolabelled protein was detectable at similar levels in microdissected cortex and Hb samples and staining was absent in samples from *mrsk2* KO mice. Expression of RSK2 in the Hb has not been reported earlier. RSK2 may therefore contribute to cognitive processing

via its broad expression in cortical and hippocampal neural networks, and also through the modulation of MHb neuronal activity.

RSK2 knockdown in Hb reduces lithium place aversion

We then examined whether RSK2 signaling in Hb contributes to place conditioning. To knock down RSK2 expression locally in the brain, we first designed three shRNA sequences targeting distinct regions of *mrsk2* mRNA (shRSK2-105, shRSK2-1112 and shRSK2-1954) and a shRNA containing scrambled sequence with no similarity with any known gene (shScramble) (see Methods). We compared *in vitro* efficacies of the three shRNAs by cotransfecting COS-1 cells with two plasmids, one over-expressing the RSK2 protein in fusion with the fluorescent reporter dsRed (RSK2-dsRed) and the other expressing the shRNA together with a fluorescent eGFP reporter (see Methods). One irrelevant shRNA was also tested. Following two days post-transfection, we evaluated RSK2 expression levels either by fluorescence-activated cell sorting (FACS) or Western blot analysis. FACS analysis of the red fluorescent signal showed reduced RSK2-dsRed expression in cells expressing each of the three shRNAs, compared to cells expressing either the scramble, irrelevant or no shRNA (Figure 3A). Consistent with this observation, Western blot analysis showed lower RSK2 immunoreactivity in the three *mrsk2* shRNA expressing samples compared with controls (Figure 3A). In both cases, shRSK2-105 showed the best silencing activity and was therefore selected for insertion into the AAV2 viral vector (see Methods).

Next, we tested the AAV2-shRSK2 virus for *in vivo* RSK2 knockdown in Hb. We injected viral particles stereotaxically into the Hb complex, as medially as possible (see Methods). To directly compare the effects of the AAV2-shRSK2 with those of a control scrambled shRNA, several animals were injected bilaterally using AAV2-shRSK2 on one side and AAV2-shScramble on the other side. Three weeks following surgery, brains were removed and sections analyzed for eGFP fluorescence, *mrsk2* mRNA expression and cellular integrity. A representative section is shown in Figure 3B. For all animals (n=4), fluorescence imaging showed strong expression of viral eGFP, and intact DAPI staining on the two sides, confirming efficient viral infection and lack of histological damage following both AAV2-shRSK2 and AAV2-shScramble injections. Importantly, the *mrsk2* transcript was clearly detectable on the control side, while labeling was barely detectable on the AAV2-shRSK2 side. These observations indicate that the stereotaxic injection procedure leads to efficient, accurate and histologically innocuous viral infection in MHb, and that the AAV2-shRSK2 potently reduces *mrsk2* mRNA expression at the injection site.

These experimental conditions were therefore used to generate cohorts of virally infected animals for behavioral analysis. Two independent cohorts of 32 animals were prepared accordingly. For each cohort, animals were injected bilaterally either with AAV2-shRSK2 (n=16) or with AAV2-shScramble (n=16). After 6 weeks, each cohort was subjected to lithium-induced conditioned place aversion, as previously done for RSK2 knockout mice (n=8, per group and per drug). After behavioral testing, brains were removed and analyzed for

correct injection site (Figure 4A) and viral expression (eGFP signal) (Figure 4B). Most animals showed intense eGFP expression in MHb. Few animals showed absent (2 animals) or misplaced (4 animals) eGFP signal at one side and were excluded from the behavioral statistical analysis. In situ hybridization analysis was performed on three animals from each group to confirm *mrsk2* down-regulation (Figure 4B).

Behavioral lithium CPA data from the two independent cohorts were pooled (Figure 4C). A three-way ANOVA showed significant main effects of treatment [$F(1,54)=12.52$, $p=0.001$] and genotype [$F(1,54)=4.33$, $p=0.042$]. There were significant session x treatment ([$F(1,54)=8.53$, $p=0.05$) and session x genotype ([$F(1,54)=9.41$, $p=0.003$) interactions. Posthoc comparisons of the post-conditioning session revealed no effect of shRNA following saline, however the AAV2-shRSK2 injected mice had a significant decrease in CPA compared to AAV2-shScramble treated animals following 3mEq LiCl. This result demonstrates that full expression of RSK2 in MHb is necessary for place learning.

Discussion

Our study demonstrates that RSK2 signaling in MHb is essential for the formation of drug/context associations, and this observation has two important implications. First the data reveal a novel role of RSK2 signaling in cognitive processes, and second, our findings uncover the critical implication of an intriguing brain structure in place learning.

RSK2 is a serine/threonine kinase operating in the Ras/MAPK signaling pathway, which plays an important role in synaptic plasticity and memory (Davis and Laroche, 2006). Mutations in the *rsk2* gene lead to the Coffin-Lowry Syndrome (Pereira et al., 2010), a severe X-linked disorder involving developmental, metabolic and cognitive alterations, and *rsk2* gene KO in the mouse recapitulates some aspects of the syndrome at both peripheral (Dufresne et al., 2001; El-Haschimi et al., 2003; Yang et al., 2004) and central levels (Poirier et al., 2007). Poirier and coll. examined general behavior and cognitive processes in *mrsk2* KO mice through two extensive test batteries. A main finding of their study was a substantial performance impairment of mutant mice in the acquisition of several place navigation tasks, using the water-maze. A slight modification was also observed in the 8-arm radial maze, and these two phenotypes indicate a prominent role of RSK2 in spatial learning and working memory (Poirier et al., 2007). Mutant mice otherwise behaved normally in many other cognitive tasks (habituation of exploratory activity, hole-board task and object exploration), suggesting that RSK2 modulates specific aspects of spatial learning. Behavioral data from Poirier and coll. are consistent with the well-described RSK2 expression in hippocampus, a brain structure strongly implicated in spatial tasks. In this study we examined *mrsk2* KO mice in a different type of cognitive paradigm. Lithium place conditioning is a form of learning that requires both high-order cognitive integration of contextual cues and emotional processing of an aversive stimulus (Silva et al., 1998), which together contribute to the setting of drug/context

association. The lack of lithium CPA in KO mice first demonstrates the importance of RSK2 in integrating contextual elements, consistent with hippocampal RSK2 expression, and the previously reported role of RSK2 in spatial learning. In addition, this finding suggests a role for RSK2 in processing value-based information, and we propose that RSK2 signaling also regulates emotional aspects of learning and memory.

RSK2-mediated emotional learning may operate at non-hippocampal brain sites. Contextual conditioning recruits cortical, hippocampal and amygdalar neural networks (Tzschentke, 1998). Another less-well known and intriguing brain structure possibly involved in contextual conditioning is the habenular complex. Lesion studies, electrophysiology and imaging studies in humans converge to show a role for the Hb in learning, memory and attention, as well as behavioral flexibility (Lecourtier and Kelly, 2007). The Hb is a highly conserved brain structure, and represents a key reciprocal node linking limbic and extrapyramidal systems (Lecourtier and Kelly, 2007). It receives strong input from the basal ganglia (via the entopeduncular nucleus) and regulates ascending monomaminergic and cholinergic transmission throughout the forebrain. As such, the Hb is not only involved in cognitive behaviors, but also in their motoric, motivational and rewarding aspects, and is essential in value-based decision-making (Hikosaka, 2010).

Our observation of discrete and strong RSK2 expression in MHb, in addition to other brain structures involved in cognitive tasks, led us to investigate whether habenular RSK2 could be involved in contextual conditioning. Our data demonstrate that RSK2 signaling in MHb indeed is necessary for this form of learning. Whether RSK2 activity in MHb is sufficient for this remains to be established. At this stage, we cannot exclude that RSK2 acting at other brain sites also contributes to contextual learning, and future studies will determine whether hippocampal or cortical RSK2 signaling is also involved in lithium CPA. Importantly here, our findings showing that both *mrsk2* KO mice and AAV2-shRSK2-treated mice lack lithium CPA demonstrates for the first time that MHb is a critical neural substrate for place learning.

There has been a surge of interest in the Hb network in the last years, however molecular events operating at the level of habenular neurons are largely unknown. The few existing studies have mainly investigated cholinergic transmission, since Hb nuclei (LHb and MHb) express high levels of nicotinic receptors, including $\alpha 2$, $\alpha 5$ and $\beta 4$ subunits. Pharmacological blockage of nicotinic receptors by mecamylamine decreases memory performance in a 16-arm maze upon injection in the LHb (Sanders et al., 2010), and induces nicotine withdrawal after antagonist administration targeting the MHb-interpeduncular system (Salas et al., 2009). Our study identifies RSK2 as a novel important molecular actor of MHb, which regulates neural activity of the Hb complex in contextual conditioning. Upstream RSK2 activators, including cell surface membrane receptors and associated extracellularregulated kinases, and downstream effectors operating in MHb neurons remain to be clarified. Molecular genetics using simpler model organisms (Agetsuma et al., 2010) will further help expanding our knowledge of molecular mechanisms underlying Hb function in the brain.

Methods

Animals. Knockout *mrsk2* mice were described previously (Yang et al., 2004), see Supplementary online for details.

Place conditioning. Mice were tested in the conditioning place-preference paradigm to evaluate the aversive properties of LiCl, as described previously (Le Merrer et al., 2010). Data were computed with the Statistical Program for the Social Sciences (SPSS; V.18.0), and analyzed using three-way analysis of variance (ANOVA), with genotype/shRNA and treatment as between-groups factors and session (pre- versus post-conditioning) as a withingroup factor. See Supplementary online for details.

RSK2-ShRNA design, viral production and delivery. Viral production was carried out using the AAV2 Helper-Free system (Stratagene) with some modifications. See Supplementary online for details.

Drugs, tissue preparation, histology and Western blotting. See Supplementary online for details. Supplementary information is available at EMBO reports online.

Acknowledgements

We wish to thank J. Le Merrer and A. Pradhan for behavioral advice and M. Mahoney and C. Gavériaux-Ruff for careful reading of the manuscript. This work was supported by the Centre National de la Recherche Scientifique, Institut National de la Santé et de la Recherche Médicale, and Université de Strasbourg. We thank the European Union (GENADDICT/FP6 005166) and the National Institutes of Health (NIAAA AA-16658 and NIDA DA-16768), for financial support.

Conflict of interest. None

References

- Agetsuma, M., Aizawa, H., Aoki, T., Nakayama, R., Takahoko, M., Goto, M., Sassa, T., Amo, R., Shiraki, T., Kawakami, K., Hosoya, T., Higashijima, S. and Okamoto, H. (2010) The habenula is crucial for experience-dependent modification of fear responses in zebrafish. *Nat Neurosci*, 13, 1354-1356.
- Anjum, R. and Blenis, J. (2008) The RSK family of kinases: emerging roles in cellular signalling. *Nat Rev Mol Cell Biol*, 9, 747-758.
- Davis, S. and Laroche, S. (2006) Mitogen-activated protein kinase/extracellular regulated kinase signalling and memory stabilization: a review. *Genes Brain Behav*, 5 Suppl 2, 61-72.
- Dufresne, S.D., Bjorbaek, C., El-Haschimi, K., Zhao, Y., Aschenbach, W.G., Moller, D.E. and Goodyear, L.J. (2001) Altered extracellular signal-regulated kinase signaling and glycogen metabolism in skeletal muscle from p90 ribosomal S6 kinase 2 knockout mice. *Mol Cell Biol*, 21, 81-87.
- Dugani, C.B., Paquin, A., Kaplan, D.R. and Miller, F.D. (2010) Coffin-Lowry syndrome: a role for RSK2 in mammalian neurogenesis. *Dev Biol*, 347, 348-359.
- El-Haschimi, K., Dufresne, S.D., Hirshman, M.F., Flier, J.S., Goodyear, L.J. and Bjorbaek, C. (2003) Insulin resistance and lipodystrophy in mice lacking ribosomal S6 kinase 2. *Diabetes*, 52, 1340-1346.
- Hanauer, A. and Young, I.D. (2002) Coffin-Lowry syndrome: clinical and molecular features. *J Med Genet*, 39, 705-713.
- Hikosaka, O. (2010) The habenula: from stress evasion to value-based decision-making. *Nat Rev Neurosci*, 11, 503-513.
- Kohn, M., Hameister, H., Vogel, M. and Kehrer-Sawatzki, H. (2003) Expression pattern of the Rsk2, Rsk4 and Pdk1 genes during murine embryogenesis. *Gene Expr Patterns*, 3, 173-177.
- Le Merrer, J., Plaza-Zabala, A., Boca, C.D., Matifas, A., Maldonado, R. and Kieffer, B.L. (2010) Deletion of the delta Opioid Receptor Gene Impairs Place Conditioning But Preserves Morphine Reinforcement. *Biol Psychiatry*.
- Lecourtier, L. and Kelly, P.H. (2007) A conductor hidden in the orchestra? Role of the habenular complex in monoamine transmission and cognition. *Neurosci Biobehav Rev*, 31, 658-672.
- Pereira, P.M., Schneider, A., Pannetier, S., Heron, D. and Hanauer, A. (2010) Coffin-Lowry syndrome. *Eur J Hum Genet*, 18, 627-633.
- Poirier, R., Jacquot, S., Vaillend, C., Southiphong, A.A., Libbey, M., Davis, S., Laroche, S., Hanauer, A., Welzl, H., Lipp, H.P. and Wolfer, D.P. (2007) Deletion of the Coffin-Lowry syndrome gene Rsk2 in mice is associated with impaired spatial learning and reduced control of exploratory behavior. *Behav Genet*, 37, 31-50.
- Salas, R., Sturm, R., Boulter, J. and De Biasi, M. (2009) Nicotinic receptors in the habenulointerpeduncular system are necessary for nicotine withdrawal in mice. *J Neurosci*, 29, 3014-3018.
- Sanders, D., Simkiss, D., Braddy, D., Baccus, S., Morton, T., Cannady, R., Weaver, N., Rose, J.E. and Levin, E.D. (2010) Nicotinic receptors in the habenula: importance for memory. *Neuroscience*, 166, 386-390.
- Silva, A.J., Giese, K.P., Fedorov, N.B., Frankland, P.W. and Kogan, J.H. (1998) Molecular, cellular, and neuroanatomical substrates of place learning. *Neurobiol Learn Mem*, 70, 44-61.
- Trivier, E., De Cesare, D., Jacquot, S., Pannetier, S., Zackai, E., Young, I., Mandel, J.L., Sassone-Corsi, P. and Hanauer, A. (1996) Mutations in the kinase Rsk-2 associated with Coffin-Lowry syndrome. *Nature*, 384, 567-570.

- Tzschentke, T.M. (1998) Measuring reward with the conditioned place preference paradigm: a comprehensive review of drug effects, recent progress and new issues. *Prog Neurobiol*, 56, 613-672.
- Yang, X., Matsuda, K., Bialek, P., Jacquot, S., Masuoka, H.C., Schinke, T., Li, L., Brancorsini, S., Sassone-Corsi, P., Townes, T.M., Hanauer, A. and Karsenty, G. (2004) ATF4 is a substrate of RSK2 and an essential regulator of osteoblast biology; implication for Coffin-Lowry Syndrome. *Cell*, 117, 387-398.
- Zeniou, M., Ding, T., Trivier, E. and Hanauer, A. (2002) Expression analysis of RSK gene family members: the RSK2 gene, mutated in Coffin-Lowry syndrome, is prominently expressed in brain structures essential for cognitive function and learning. *Hum Mol Genet*, 11, 2929-2940.

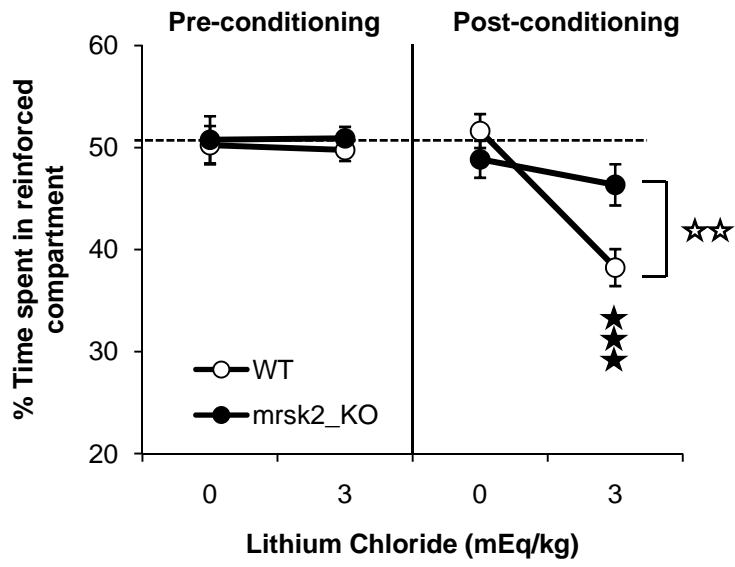
Legends to figures

Fig. 1. Lithium conditioned place aversion is impaired in mice lacking RSK2 gene (*mrsk2* KO). Wild-type (WT) but not *mrsk2* KO animals exhibit a significant place aversion for the compartment associated with LiCl when tested drug-free (WT, n=16 per dose and KO n=14 per dose). Data show mean (\pm SEM) time spent in the drug-paired compartment (expressed as a percentage of time spent in the two compartments) during the 20-min pre- and post-conditioning sessions. ★★★p<0.001 comparison to saline control; ☆☆p<0.05 comparison between genotype.

Fig.2. RSK2 is expressed in medial habenula. (A) In situ hybridization shows *mrsk2* mRNA expression in hippocampus (1), cortex (2) and habenula (3). (B) RSK2 protein is expressed in cortex and habenula of WT mice but not KO mice, as revealed by Western blotting.

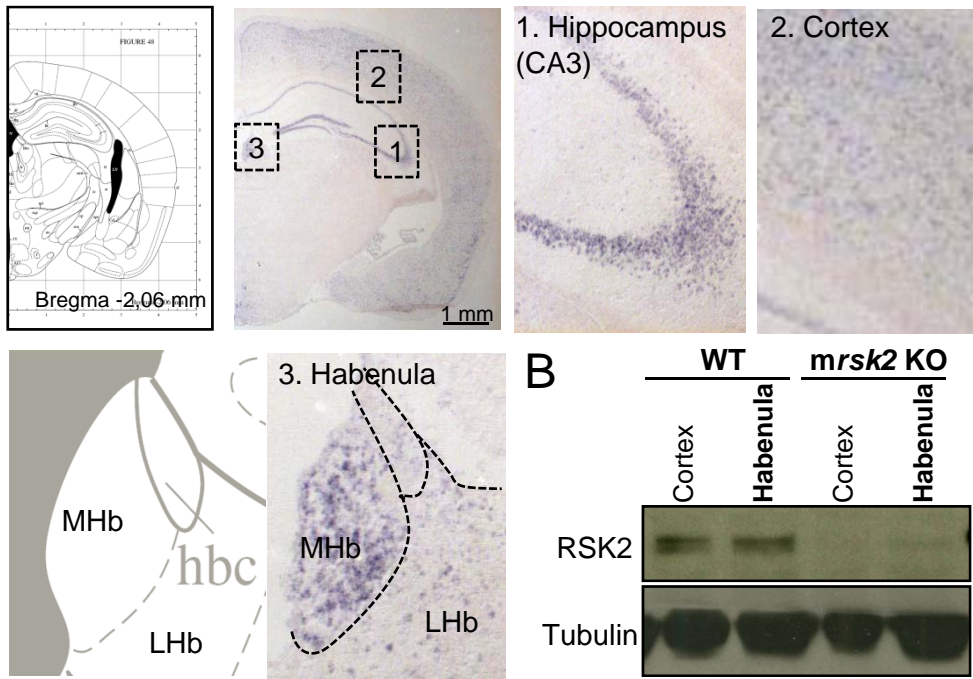
Fig.3. Validation of AAV2-shRNA RSK2 knockdown. (A) *In vitro* validation. Expression level of RSK2-dsRed in COS-1 cells coexpressing *mrsk2*-targeted or control shRNAs, as measured by fluorescence-activated cell sorting (left) and Western blotting (right). shRSK2-105 shows best silencing activity. (B) *In vivo* validation. AAV2-shScramble (right) or AAV2-shRSK2 (left) were injected stereotaxically in Hb (n=4). After three weeks, brain sections were processed for detection of Green fluorescent protein (GFP) (left), *mrsk2* mRNA (middle) and DAPI staining (right). AAV2-shRSK2, but not AAV2-shScramble, reduces *mrsk2* mRNA expression in Hb. A representative image is shown.

Fig.4. RSK2 knockdown in Hb decreases lithium conditioned place aversion. (A) Injection sites in the Hb (dark circle) and outside (red circle) were determined for all mice. Mice with injections visibly outside of MHb were excluded from statistical analysis. (B) Representative images showing viral expression (GFP) and intact (AAV2-shScramble) or reduced (AAV2-shRSK2) *mrsk2* expression (analysis done for n=3 per group/ each cohort). (C) LiCl CPA in mice injected with AAV2-shRSK2 in habenula (shRSK2) and their controls (shScramble). AAV2-shRSK2-injected mice failed to display lithium CPA. Data show mean (\pm SEM) time spent in the drug-paired compartment (expressed as a percentage of time spent in the two compartments) during the 20-min pre- and post-conditioning sessions (AAV2-shRSK2, saline, n=15, lithium, n=14; AAV2-shScramble, saline, n=14, lithium, n=15). ★★★p<0.001 comparison to saline control; ☒☒p<0.05 comparison between shRNA.



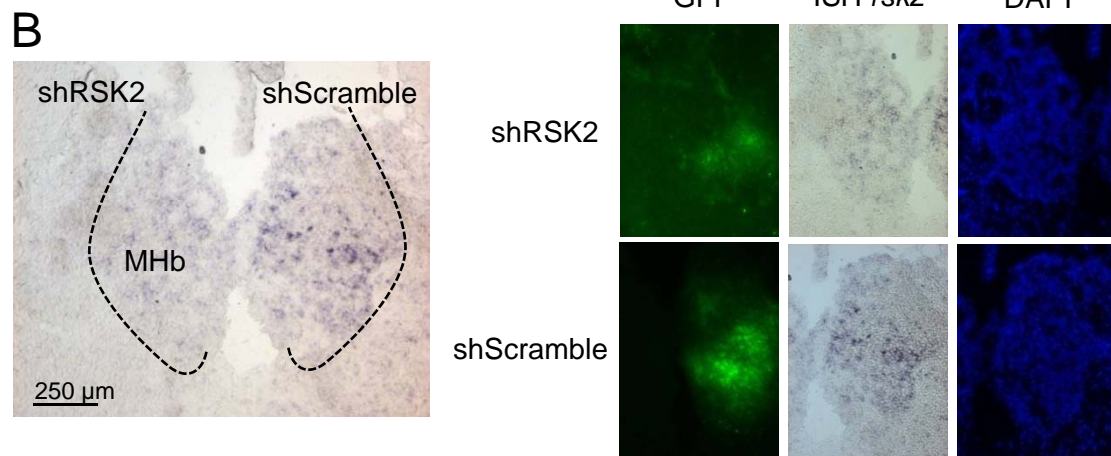
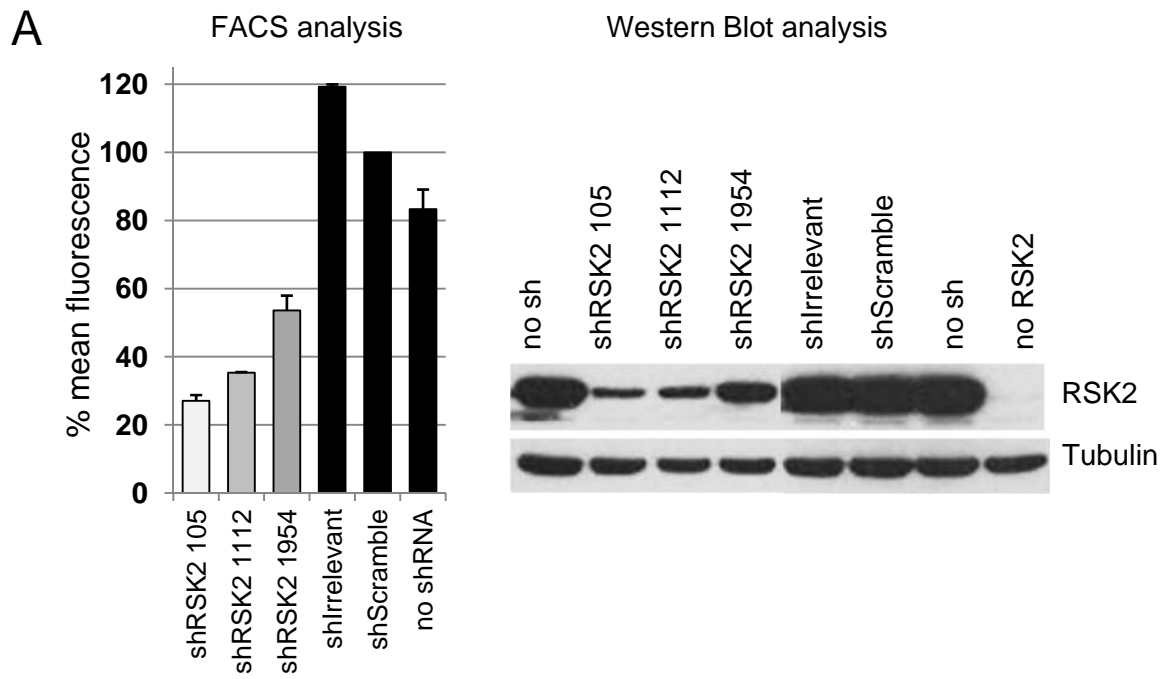
Darcq et al, Figure 1

A



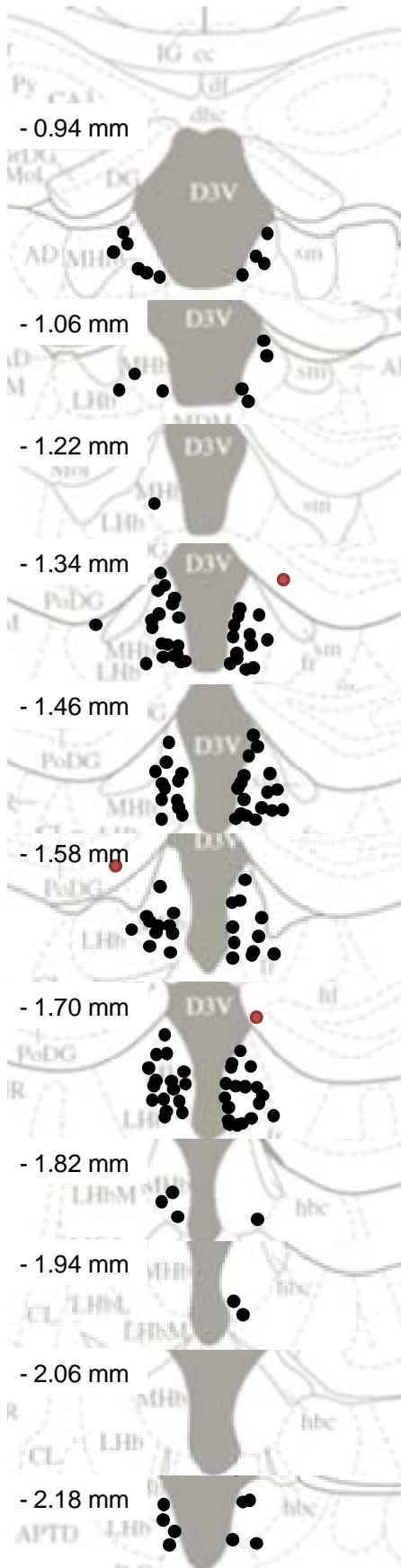
B

Darcq et al, Figure 2

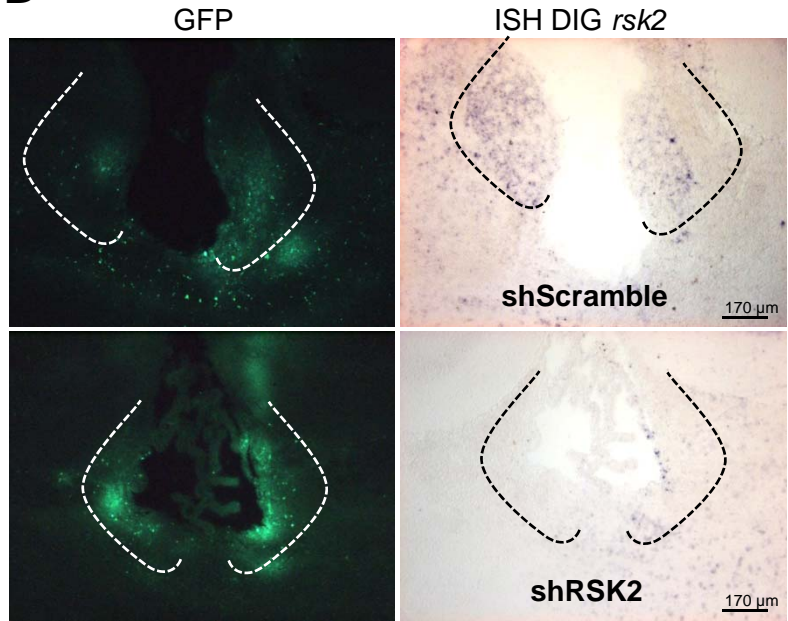


Darcq et al, Figure 3

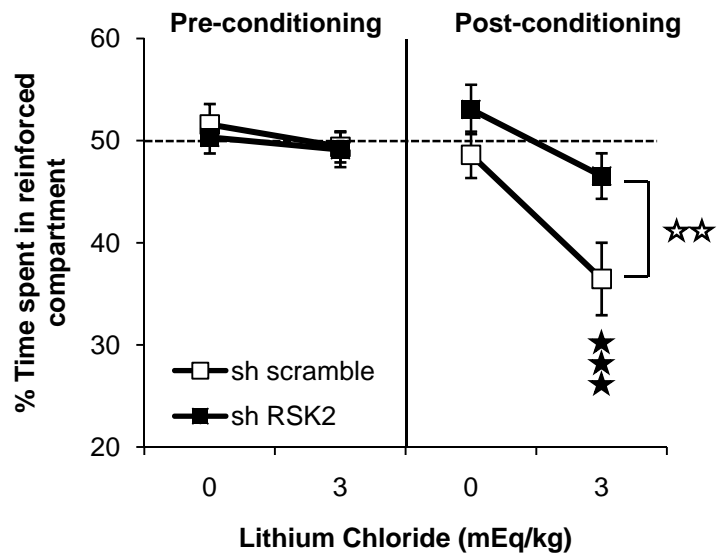
A



B



C



Darcq et al, Figure 4

Supplementary information

Supplementary Methods

Animals. Knockout *mrsk2* mice were generated as described (Yang et al., 2004). Heterozygous females carrying the mutation were crossed with C57BL/6J males for at least 20 generations to obtain a 99.99% C57BL/6J genetic background. Wild-type and knockout animals used in this study were from the same littermates and genotype was verified by PCR for each individual as previously described (Yang et al., 2004). Male mice aged 8 weeks old at the beginning of the experiments were housed 4 per cage in a 12h dark/light cycle (light on from 7 am to 7 pm), under controlled conditions of temperature and humidity. For stereotaxic experiments, we used wild-type C57BL/6J mice (Charles River). Food and water were available *ad libitum* except during behavioral observations. Experimental procedures were conducted in accordance with the European Communities Council Directive of 24 November 1986 (86/609/EEC) and approved by the Comité régional d'éthique en matière d'expérimentation animale de Strasbourg (CREMEAS, 2003-10-08-[1]-58).

Drugs. Lithium chloride (LiCl, Sigma Aldrich, Steinheim, Germany) was dissolved in sterile isotonic saline (NaCl 0.9%). For surgery, mice were anaesthetized using ketamine/xylazine (100/10 mg/kg). Drugs were administered intraperitoneally (LiCl and anaesthetics) in a volume of 10 ml/kg.

Place conditioning. Following 5 days of handling and habituation to subcutaneous saline injection, mice were tested in the conditioning place-preference paradigm to evaluate the aversive properties of lithium chloride (Le Merrer et al., 2010). The apparatus consisted of two Plexiglas chambers with different shape patterns and floors (15.5x16.5x20 cm) separated by a central corridor (6x16.5x20 cm) with sliding doors (3x20 cm) connecting the alley with the chambers (Imetronic, Pessac, France). Activity and location of mice were recorded using five photocells located throughout the apparatus. During the preconditioning phase, naïve mice were placed in the corridor and had free access to both compartments for 20 min, with the time spent in each compartment recorded. Treatments were further counterbalanced between compartments to use an unbiased procedure. No initial place aversion for the different compartments was observed in the experiment. The conditioning phase lasted 3 days with two daily conditioning sessions. Mice were injected morning and afternoon with either saline (vehicle-paired session, 9.00 am) or LiCl (drug-paired session, 4.00 pm, 3mEq/kg, s.c.) and confined in the corresponding-paired chamber for 45 min. Control animals received saline injections mornings and afternoons followed by a 45 min confinement. Testing phase was conducted on the fifth day in a drug-free state, with free access to both chambers for 20 min, and time spent in each chamber was recorded. Data were expressed as percentage of time spent in the drug-paired compartment using the formula: % Time spent in the drug-associated compartment = (Time spent in the drug-associated compartment)/(time spent in both compartments) x 100. Data were computed with the Statistical Program for the Social Sciences

(SPSS; V.18.0), and analyzed using three-way ANOVA with genotype/shRNA and treatment as between-groups factors and session (pre- versus post-conditioning) as a within-group factor. When significant main effects were observed in between-subjects analyses, post hoc tests were performed using a Bonferroni correction. Within-subjects significant main effects were analyzed further with post hoc paired t tests with a α correction for the number of comparisons made. Statistical significance was set at $p < 0.05$ for all tests.

RSK2-ShRNA design and viral production. Viral production and shRNA design were carried out using AAV2-Helper-Free system (Stratagene) as recommended by the manufacturer, with some modifications. Three target sequences were selected in the coding region of *mrsk2* gene by the BLOCK-iT™ RNAi Designer (Invitrogen) using accession number NM_148945.1: sh105 (5'-GGAGGAGATTAACCCACAAAC-3'), sh1112 (5'-GCATTCCACCTAGTGCTAACG-3') and sh1954 (5'-GCAAAGGACCTGGTGTCAAAG-3'). pAAV-eGFP-sh vectors expressing eGFP and shRNA under the control of CMV and mU6 promoters respectively were generated by recombination using the Gateway LR Clonase II (Invitrogen). Control pAAV-eGFP-sh vectors were also generated containing either an irrelevant, a scrambled shRNA sequence or none. For in vitro validation, a plasmid expressing the human RSK2 protein in fusion with dsRed was used (*phrsk2-dsRed*). Silencing efficiency was measured by cotransfection of COS-1 cells with *phrsk2-dsRed* and the pAAV-eGFP-shRNA as previously described (Barth and Volkandt, 2008), for two independent transfections. Briefly, COS-1 cells were plated one day before transfection at 5.10^4 cells per well in a 24-well culture plate. Cells were cotransfected with 0.2ug of *phRSK2dsRed* and 0.02 to 0.2ug of pAAV-eGFP-shRNA plasmids per well. Two days later cells were analyzed by flow cytometry (FACSCalibur flow cytometer, CellQuest Pro software, Becton Dickinson) and Western blotting.

Viral production and purification. rAAV2/2 vectors were generated by a triple transfection of AAV-293 cell line (Stratagene). Briefly, cells were transfected with pAAV-eGFP-RSK2sh105 (see above), pAAV-RC containing rep and cap genes of AAV serotype-2 and with pHelper encoding the adenovirus helper functions. Following 2 days cells were collected, lysed by three freeze/thaw cycles in dry ice-ethanol and 37°C baths, further treated with Benzonase (50U/mL, Sigma) for 30 minutes at 37°C and clarified by centrifugation. Viral vectors were then purified by Iodixanol gradient ultracentrifugation (Zolotukhin et al., 2002) followed by dialysis and concentration against Dulbecco PBS using centrifugal filters (Amicon Ultra-15 Centrifugal Filter Devices 50K). Physical particles were quantified by real time PCR using a plasmid standard pAAV-eGFP. rAAV titers were $1.3 \cdot 10^{11}$ viral genomes per ml (vg/ml) for both AAV2-shRSK2 and AAV2-shScramble. Viruses were aliquoted and stored in light-protected boxes at -80°C until use.

Surgery and Virus delivery. Mice were anesthetized using ketamine/xylazine (100/10 mg/kg). Bilateral stereotaxic injections (Unimecanique, France) of 1.5 μl of purified AAV2 per side were performed according to the atlas of Paxinos and Watson (Paxinos and Franklin, 2001) into the medial habenula (anteroposterior (AP), -1.34mm from bregma; mediolateral (ML), ± 0.3 mm

from midline; dorsoventral (DV), -3.0 mm from dura skull surface) using a 5µl microsyringe (SGE Analytical Science, Australia). Injection speed was 0.1µl/min, and the needle was slowly withdrawn 10min following delivery. Following surgery, mice were single housed for 48 hours and back to their home cage for six weeks before behavioral testing. All mice were handled at least one week prior to behavioral experiments.

Tissue preparation and histology. Following behavioral tests, mice were killed by cervical dislocation and brains were rapidly extracted for microdissection or slicing. A chilled metal matrix (ASI Instruments, Warren, MI, USA) was used for microdissection as previously described (Befort et al., 2008). Briefly, ten chilled razor blades were inserted into the 1-mm-spaced coronal grooves with the first (most rostral) blade being inserted at the ventrocaudal limit of olfactory bulbs, and brain slices were transferred in ice-cold PBS. Cortex was sampled with a scalpel and habenula was dissected using a 2 mm diameter tissue corer (Fine Science Tools, Foster City, CA, USA). Punched samples were rapidly frozen in liquid nitrogen and stored at -80°C until use. For histology, brains were fresh frozen in OCT (Optimal Cutting Temperature medium, Thermo Scientific) and stored at -20 °C until use. Cryostat brain sections (20 µm) were analyzed for injection accuracy in the medial habenula using fluorescent microscopy. Location of GFP fluorescence was determined according to the atlas of Paxinos and Watson (Paxinos and Franklin, 2001). Mice with injection misplacement were excluded from behavioral analysis. Slices were further processed for *in situ* hybridization (ISH) using digoxigenin-labeled RNA probes as previously (Chotteau-Lelievre et al., 2006) with a 276 bp *Rsk2* probe (Zenjou et al., 2002). To identify the location of viral injection (EGFP expression) and DIG positive staining brain sections were mounted and observed using a fluorescence microscope (Leica) with 10x and 20x objectives.

Western blotting. Western blotting was carried out from transfected cells or brain samples using standard procedures. Cotransfected COS-1 cells were lysed in RIPA buffer containing 1%NP40, 0.1%SDS, 0.5% sodium deoxycholate and supplemented with a protease inhibitor cocktail (Complete EDTA-free, Roche Diagnostics) for 30 minutes at 4°C. Total protein content was determined by Bradford assay (Biorad). Ten micrograms of protein were loaded and separated by electrophoresis on a SDS-10% bisacrylamide gel, and transferred to nitrocellulose membranes. For brain samples, punches were homogenized and sonicated in 2% SDS buffer containing 50mM Tris, pH 6.8, 1mM EDTA, 1mM sodium fluoride, 1mM sodium orthovanadate and a complete protease inhibitor mixture (Roche Applied Science, Indianapolis, IN). Homogenates were boiled at 95° for 4 min, and total protein content was determined by Bradford assay. Twenty-five micrograms of protein were loaded on a SDS-10% bisacrylamide gel and further transferred to polyvinylidene difluoride membranes. For detection, the following antibodies were used: a rabbit anti-human RSK2 (1/1000, Santa Cruz Biotechnology #sc-1430-R), a mouse anti-tubulin (1/40000, IGBMC antibody platform). Proteins were then visualized using horseradish peroxidase-conjugated secondary goat antibodies anti-mouse IgG (1/20000,

Biolegend #405306) or anti-rabbit IgG (1/10000, Jackson ImmunoResearch #111-036-046) and the Western lightning plus- enhanced chemiluminescent substrate (ECL, Perkin Elmer).

Supplementary references

- Barth, J. and Volkandt, W. (2008) Evaluation of small hairpin RNA silencing efficiency in live cells by cotransfection of two fluorescent probes. *Anal Biochem*, 379, 133-135.
- Befort, K., Filliol, D., Ghate, A., Darcq, E., Matifas, A., Muller, J., Lardenois, A., Thibault, C., Dembele, D., Le Merrer, J., Becker, J.A., Poch, O. and Kieffer, B.L. (2008) Mu-opioid receptor activation induces transcriptional plasticity in the central extended amygdala. *Eur J Neurosci*, 27, 2973-2984.
- Chotteau-Lelievre, A., Dolle, P. and Gofflot, F. (2006) Expression analysis of murine genes using in situ hybridization with radioactive and nonradioactively labeled RNA probes. *Methods Mol Biol*, 326, 61-87.
- Le Merrer, J., Plaza-Zabala, A., Boca, C.D., Matifas, A., Maldonado, R. and Kieffer, B.L. (2010) Deletion of the delta Opioid Receptor Gene Impairs Place Conditioning But Preserves Morphine Reinforcement. *Biol Psychiatry*.
- Paxinos, G. and Franklin, K. (2001) *The Mouse Brain in Stereotaxic Coordinates*, San Diego.
- Yang, X., Matsuda, K., Bialek, P., Jacquot, S., Masuoka, H.C., Schinke, T., Li, L., Brancorsini, S., Sassone-Corsi, P., Townes, T.M., Hanauer, A. and Karsenty, G. (2004) ATF4 is a substrate of RSK2 and an essential regulator of osteoblast biology; implication for Coffin-Lowry Syndrome. *Cell*, 117, 387-398.
- Zeniou, M., Ding, T., Trivier, E. and Hanauer, A. (2002) Expression analysis of RSK gene family members: the RSK2 gene, mutated in Coffin-Lowry syndrome, is prominently expressed in brain structures essential for cognitive function and learning. *Hum Mol Genet*, 11, 2929-2940.
- Zolotukhin, S., Potter, M., Zolotukhin, I., Sakai, Y., Loiler, S., Fraites, T.J., Jr., Chiodo, V.A., Phillipsberg, T., Muzyczka, N., Hauswirth, W.W., Flotte, T.R., Byrne, B.J. and Snyder, R.O. (2002) Production and purification of serotype 1, 2, and 5 recombinant adeno-associated viral vectors. *Methods*, 28, 158-167.

C. Manuscript 3:

Deletion of the delta-opioid receptor gene impairs place conditioning but preserves morphine reinforcement

Le Merrer J¹, Plaza-Zabala A², **Del Boca C**¹, Matifas A¹, Maldonado R² and Kieffer BL¹.

Biol Psychiatry. 2010.

¹. Département de Neurobiologie et Génétique, Institut de Génétique et de Biologie Moléculaire et Cellulaire (IGBMC), Illkirch-Grattenstaden, France.

². Laboratorio de Neurofarmacología, Departamento de Ciencias Experimentales y de la Salud, Universidad Pompeu Fabra, Barcelona, Spain.

Corresponding author:

Pr. Brigitte L KIEFFER

IGBMC, Parc d'innovation 1 rue Laurent Fries BP 10142, 67404 Illkirch Cedex, France

Telephone: +33 (0)8 65 56 93, Fax: +33 (0)8 65 56 04, e-mail address : briki@igbmc.fr

Here, we investigated the impact of the delta-opioid receptor gene knock-out mice (δ receptor-KO) on reinforced conditioned learning. The aim was to clarify the implication of delta receptors in drug reinforcement by evaluating whether delta inactivation cause deleterious effect on learning or in reward. Therefore, we used different paradigms of drug-context association for either morphine(appetitive)- or lithium(aversive)-induced place conditioning, and an operant intravenous self-administration protocol.

Our results show that δ receptor-KO mice fail to express appetitive morphine-CPP as well as aversive lithium-CPA, and they display intact acquisition of morphine self-administration. Moreover, the impairments observed in context-drug associations were prevented by priming injection of the drugs prior to the test, demonstrating state-dependent place conditioned procedures in both cases. Therefore, our study demonstrates that delta opioid receptors facilitate contextual learning rather than drug reinforcement.

Deletion of the δ Opioid Receptor Gene Impairs Place Conditioning But Preserves Morphine Reinforcement

Julie Le Merrer, Ainhoa Plaza-Zabala, Carolina Del Boca, Audrey Matifas, Rafael Maldonado, and Brigitte L. Kieffer

Background: Converging experimental data indicate that δ opioid receptors contribute to mediate drug reinforcement processes. Whether their contribution reflects a role in the modulation of drug reward or an implication in conditioned learning, however, has not been explored. In the present study, we investigated the impact of δ receptor gene knockout on reinforced conditioned learning under several experimental paradigms.

Methods: We assessed the ability of δ receptor knockout mice to form drug-context associations with either morphine (appetitive)- or lithium (aversive)-induced Pavlovian place conditioning. We also examined the efficiency of morphine to serve as a positive reinforcer in these mice and their motivation to gain drug injections, with operant intravenous self-administration under fixed and progressive ratio schedules and at two different doses.

Results: Mutant mice showed impaired place conditioning in both appetitive and aversive conditions, indicating disrupted context-drug association. In contrast, mutant animals displayed intact acquisition of morphine self-administration and reached breaking-points comparable to control subjects. Thus, reinforcing effects of morphine and motivation to obtain the drug were maintained.

Conclusion: Collectively, the data suggest that δ receptor activity is not involved in morphine reinforcement but facilitates place conditioning. This study reveals a novel aspect of δ opioid receptor function in addiction-related behaviors.

Key Words: Instrumental conditioning, knockout mice, lithium, motivation, opiate, reward

Within the endogenous opioid system, μ opioid receptors are necessary for most drugs of abuse to exert their rewarding properties (1). Pharmacological evidence suggests that δ opioid receptors play a similar role. Delta agonists elicit conditioned place preference (CPP) (2–5), whereas antagonists attenuate CPP to cocaine, methamphetamine, or morphine (6–8) and alter cocaine self-administration (9). In these studies, however, δ compounds might produce their effects via partial activation of μ receptors (10,11). Gene knockout therefore represents a unique approach to tackle the role of δ receptors in vivo. At present however, behavioral characterization of δ receptor knockout mice (*Oprd1*^{-/-}) failed to clarify the implication of δ receptors in drug reinforcement. Although morphine-induced CPP was decreased in *Oprd1*^{-/-} mice (6), cannabinoid-induced CPP (12) and morphine self-administration into the ventral tegmental area (13) were preserved.

A major difficulty when assessing drug reinforcement in animal models lies in the tight intertwining of reward and learning processes. Most animal models used to measure rewarding properties of drugs also assess conditioned learning (14), and pharmacological data point toward a role of δ receptors in learning processes (15,16). Delta receptor blockade or genetic inactivation might cause deleterious effects on learning rather than reward, which might explain the previously observed deficits in drug reinforcement. To challenge this hypothesis, we examined acquisition of either appetitive

(morphine-induced) or aversive (lithium-induced) place conditioning in *Oprd1*^{-/-} mice. We assumed that altered opioid reward in mutant mice would specifically result in decreased morphine-induced CPP, whereas a deficit in learning would impact on aversive as well as appetitive conditioning. To further assess δ receptor contribution to conditioning processes, we tested *Oprd1*^{-/-} mice for operant morphine self-administration. We evaluated morphine efficiency as a positive reinforcer with a fixed ratio 1 (FR1) schedule of reinforcement and motivation to earn morphine injections under a progressive ratio (PR) schedule.

Methods and Materials

Independent groups of *Oprd1*^{-/-} mice (17) and their wild-type (WT) control subjects were trained for morphine-induced (5, 10, 20 mg/kg, 6 days) or lithium-induced (3 mEq/kg, 3 days) place conditioning and tested either drug-free or under drug effects (state-dependency). Other groups of mice were trained to self-administer morphine (.25 or .5 mg/kg/infusion) under an FR1 schedule of reinforcement for 10 days. Animals that completed self-administration criteria were moved to a PR schedule of reinforcement on Day 11. The PR session was performed only once and allowed the determination of a breaking-point for each animal (see Supplement 1 for complete protocols and surgical methods).

Results

Intact Spatial Novelty Discrimination

We first performed a novelty discrimination test to examine whether mutant mice discriminate spatial cues under the same conditions as for place conditioning. During choice session, WT and *Oprd1*^{-/-} mice spent more time [novelty: $F(1,20) = 6.66, p < .05$] and were more active [$F(1,20) = 28.81, p < .0001$] in the novel compartment compared with familiar compartment (Figure 1A). Thus, mice from both lines were similarly able to discriminate between these two environments [gender: $F(1,20) = 4.29$ and $F(1,20) = .12$; genotype: $F(1,20) = .06$ and $F(1,20) = .50$, respectively, $p = \text{ns}$].

From the Département de Neurobiologie et Génétique (JLM, CDB, AM, BLK), Institut de Biologie Moléculaire et Cellulaire, Illkirch, France; and Laboratori de Neurofarmacologia (AP-Z, RM), Departament de Ciències Experimentals i de la Salut, Universitat Pompeu Fabra, Barcelona, Spain.

Address correspondence to Brigitte L. Kieffer, Ph.D., Institut de Biologie Moléculaire et Cellulaire, Département de Neurobiologie et Génétique, 1 rue Laurent Fries, 67 404 Illkirch Cedex, France; E-mail: briki@igbmc.fr.

Received May 11, 2010; revised Oct 4, 2010; accepted Oct 22, 2010.

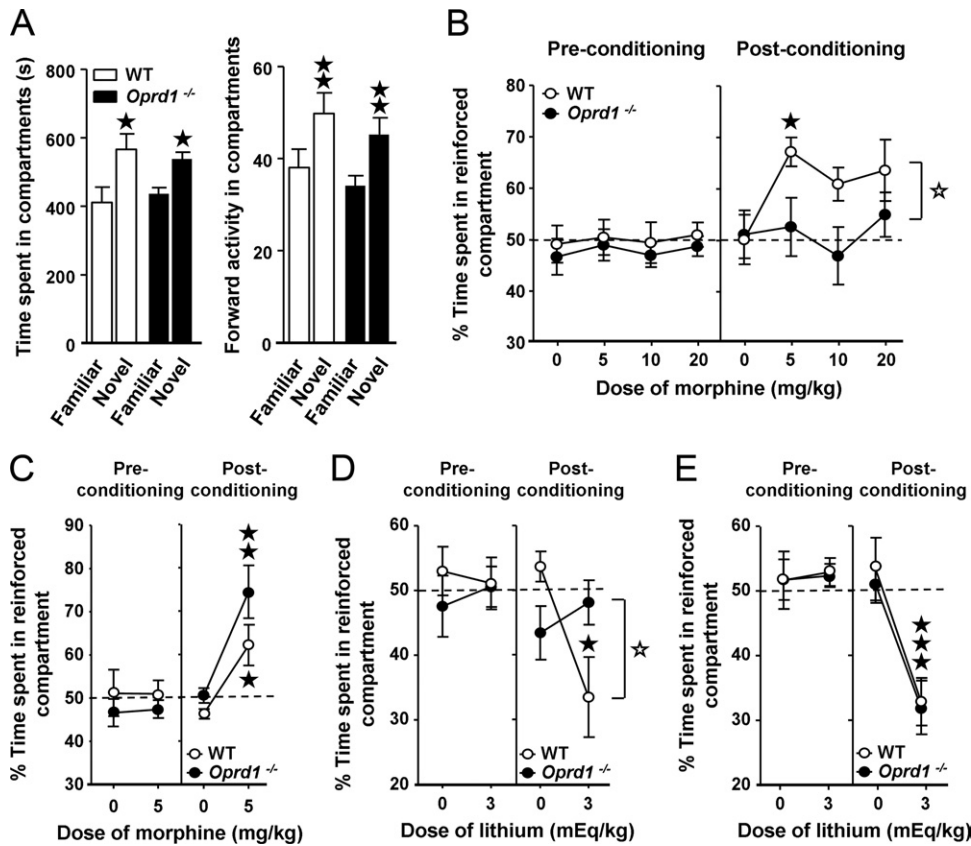


Figure 1. Spatial discrimination and place conditioning in mice lacking the δ opioid receptor gene (*Oprd1*^{-/-}) and their wild-type counterparts (WT). Independent groups of naive animals were used for each set of experiments. **(A)** The WT and *Oprd1*^{-/-} mice spent more time and were more active in the novel versus familiar compartment of the place preference apparatus, showing similar ability to discriminate the two compartments. **(B)** The WT but not *Oprd1*^{-/-} animals exhibited a significant place preference for the compartment associated with morphine injections over a four-time dose range (5–20 mg/kg) when tested drug-free. **(C)** The WT and *Oprd1*^{-/-} animals displayed place preference to morphine (5 mg/kg) when tested under the effects of the drug. **(D)** In contrast to WT animals, drug-free *Oprd1*^{-/-} mice failed to display a place aversion to lithium chloride (3 mEq/kg). **(E)** When tested under the effect of lithium, WT and mutant animals similarly avoided the lithium-paired compartment. Spatial discrimination data are presented as mean (\pm SEM) time spent and forward activity (two consecutive beam breaks) in the familiar and the novel compartments ($n = 5$ –7/gender and genotype). Place preference data show mean (\pm SEM) time spent in the drug-paired compartment (expressed as a percentage of time spent in the two compartments) during the 20-min pre- and post-conditioning sessions ($n = 3$ –5/gender, genotype, and dose). 1 solid star $p < .05$; 2 solid stars $p < .01$; 3 solid stars $p < .001$, comparison with familiar compartment or vehicle control (one-way analysis of variance followed by Dunnett’s test where appropriate). 1 open star $p < .05$, comparison between genotypes (four-way analysis of variance).

Decreased CPP to Both Appetitive and Aversive Stimuli

We submitted *Oprd1*^{-/-} mice to several place conditioning paradigms. First, distinct groups of animals were tested in a drug-free state after conditioning to saline or morphine (5–20 mg/kg). The WT but not mutant mice acquired morphine CPP [gender: $F(1,48) = .14, p = ns$; genotype: $F(1,48) = 5.69, p < .05$; conditioning: $F(1,48) = 15.67, p < .001$] (Figure 1B). Post hoc comparison with the control group performed for postconditioning session detected a significant CPP at 5 mg/kg in WT mice. Second, mice were tested under the effect of morphine (5 mg/kg). Both WT and *Oprd1*^{-/-} mice displayed similar morphine-induced CPP [gender: $F(1,24) = .36, p = ns$; genotype: $F(1,24) = 2.11, p = ns$; treatment: $F(1,24) = 18.00, p < .001$; conditioning: $F(1,24) = 16.26, p < .001$; treatment \times conditioning: $F(1,24) = 17.95, p < .001$] (Figure 1C). State-dependent morphine-induced CPP was not observed in mice lacking the μ opioid receptor (Figure S2 in Supplement 1). Third, mice were tested in a drug-free state for lithium-induced conditioned place aversion (CPA). As for morphine CPP, WT but not *Oprd1*^{-/-} animals avoided the lithium-paired compartment [gender: $F(1,26) = .02, p = ns$; conditioning: $F(1,26) = 5.79, p < .05$; genotype \times treatment: $F(1,26) = 5.52, p < .05$; genotype \times treatment \times conditioning:

$F(1,26) = 4.39, p < .05$] (Figure 1D). In contrast, when tested under the effects of lithium, WT and *Oprd1*^{-/-} mice displayed similar strong aversion for the lithium-paired compartment [gender: $F(1,26) = 2.30, p = ns$; genotype: $F(1,26) = .09, p = ns$; treatment: $F(1,26) = 13.76, p < .001$; conditioning: $F(1,26) = 18.28, p < .001$; treatment \times conditioning: $F(1,26) = 19.92, p < .001$] (Figure 1E). Altogether the data indicate that both morphine CPP and lithium CPA are impaired in *Oprd1*^{-/-} mice.

Maintained Acquisition of Intravenous Morphine Self-Administration and Motivation to Earn Morphine

We evaluated acquisition of operant morphine self-administration and motivation to obtain the drug at two doses (.25 and .5 mg/kg/infusion) in *Oprd1*^{-/-} and WT mice. Under an FR1 schedule of reinforcement, a similar percentage of WT and mutant mice reached the acquisition criteria for self-administration at the two doses tested (.25 mg/kg: 55% and 50%, respectively, $\chi^2 = .125, p = ns$; .5 mg/kg: 66.7% and 53.8% respectively, $\chi^2 = .99, p = ns$). Five-way analysis of variance revealed no effect of gender [$F(1,36) = .70, p = ns$] or genotype [$F(1,36) = .54, p = ns$] but significant discrimination between active and inactive hole

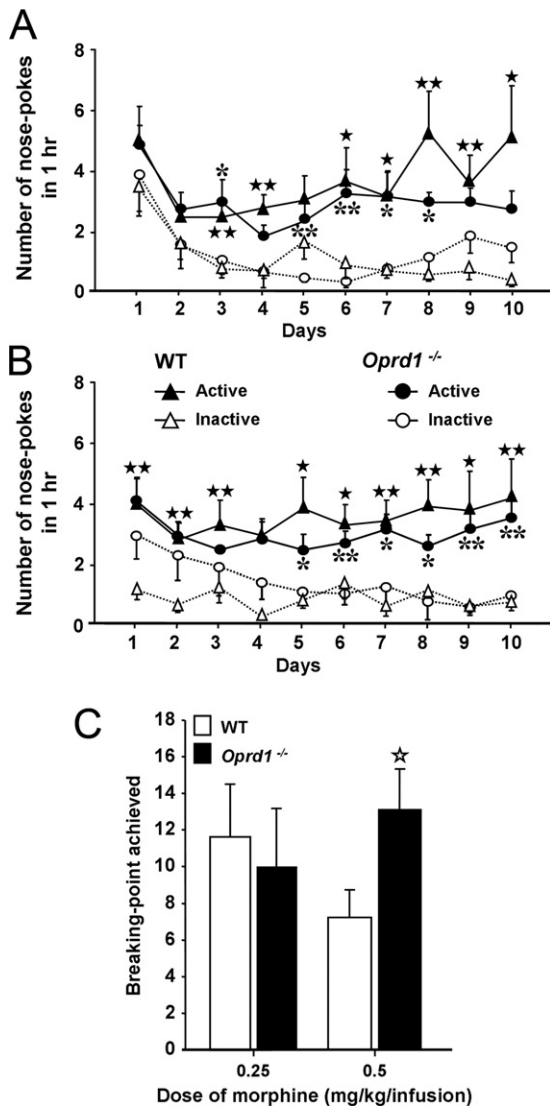


Figure 2. Operant morphine self-administration in mice lacking the δ opioid receptor gene (*Oprd1*^{-/-}) and their wild-type counterparts (WT). Mice from WT and *Oprd1*^{-/-} lines discriminate between the active and the inactive holes and acquire self-administration for intravenous morphine at (A) .25 or (B) .5 mg/kg/infusion. The data represent the number of nose-pokes in each hole/1-hour daily session. Data are expressed as mean \pm SEM (.25 mg/kg/infusion: $n = 3$ –7/gender and genotype; .5 mg/kg/infusion: $n = 6$ –10/gender and genotype). 1 solid star/** $p < .05$; 2 solid stars/** $p < .01$, comparison between holes (one-way analysis of variance). (C) The *Oprd1*^{-/-} mice achieved a similar breaking-point as WT mice under a progressive ratio schedule of reinforcement. Data analysis at each dose separately shows increased breaking-point at the high dose only, 1 open star $p < .05$, comparison between genotypes (one-way analysis of variance).

[$F(1,36) = 36.63, p < .0001$], significant effect of sessions [$F(9,324) = 6.92, p < .0001$], and significant hole \times session interaction [$F(9,324) = 2.39, p < .05$]. Therefore, WT and *Oprd1*^{-/-} mice similarly acquired operant self-administration for morphine (Figures 2A and 2B). Under a PR schedule, *Oprd1*^{-/-} mice achieved a breaking-point similar to WT mice [genotype: $F(1,21) = .85, p = ns$; dose: $F(1,21) = .07, p = ns$] (Figure 2C). These data indicate that acquisition of morphine self-administration and motivation for the drug are preserved in mutant mice.

Discussion

In our study, *Oprd1*^{-/-} mice failed to express morphine CPP over a 5–20-mg/kg dose range. Mutant animals as WT mice, however, were able to discriminate novel from familiar compartment in the place conditioning apparatus. This suggests that decreased morphine CPP in mutant mice does not result from altered recognition of spatial contexts, at least in the CPP apparatus. Furthermore, when tested under the effects of morphine, *Oprd1*^{-/-} mice displayed preference for the morphine-paired context, similar to WT animals. Morphine-induced CPP was thus state-dependent in *Oprd1*^{-/-} mice. Otherwise, state-dependent morphine-induced CPP was not observed in mice lacking μ opioid receptors, consistent with the essential role of μ receptors as the primary target for morphine in vivo. State-dependency qualifies a behavioral response that can only be retrieved when the animal experiences the same (drug) state as during the acquisition of this response (18). Interoceptive drug cues can then function as conditioned stimuli and contribute to contextual information together with external cues. In the present study, *Oprd1*^{-/-} mice and not their WT counterparts needed both internal and external cues to express a morphine-induced CPP. Together, these data suggest that the ability to form drug-context associations and/or retrieve such associations was blunted in *Oprd1*^{-/-} mice.

To challenge this hypothesis, we tested *Oprd1*^{-/-} mice in a place aversion-conditioning paradigm with lithium chloride (3 mEq/kg) as a potent nonopioid aversive stimulus. Knockout mice failed to display lithium-induced CPA when tested drug-free but showed strong aversion for the lithium-paired compartment when tested under the effects of lithium. Thus, as for morphine-induced CPP, lithium-induced CPA was state-dependent in *Oprd1*^{-/-} mice, a finding that strengthens the hypothesis of deficient drug-context associations. Altogether, impaired appetitive and aversive place conditioning demonstrate that reinforced learning is altered in *Oprd1*^{-/-} mice, regardless of the affective value of the stimuli. This is consistent with previously reported decreased morphine CPP in *Oprd1*^{-/-} mice (6) as well as in WT animals injected with δ antagonists before conditioning sessions (6,8). Notably, such effects were not detected in a cannabinoid CPP paradigm (12). In the latter study, increased number of drug-pairings (five sessions vs. three) could have facilitated drug-context associations.

Our place conditioning data provide evidence for impaired drug-context association but do not exclude that drug reward is also reduced in δ receptor knockout mice. Hence we further addressed consequences of the gene knockout on opioid conditioned reinforcement with operant morphine self-administration. The WT and *Oprd1*^{-/-} mice similarly acquired morphine self-administration and reached the acquisition criteria (FR1). This result is consistent with previous studies showing preserved operant responding for food (19) or intra-ventral tegmental area morphine self-administration (13) in *Oprd1*^{-/-} mice. Hence, morphine served as an efficient positive reinforcer in both WT and knockout mice. Moreover, mutant mice achieved a similar or even higher breaking-point than WT control subjects under a PR schedule, strongly suggesting that motivation for morphine reinforcement is preserved in the absence of δ receptors. This result contrasts with the prevailing view of comparable roles of μ and δ opioid receptors in mediating drug reinforcement (see introductory text) and further documents the notion of divergent δ and μ receptor activities previously established for emotional responses (17) and motor impulsivity (19).

In conclusion, the present study demonstrates that δ receptor gene knockout alters place conditioning, whereas morphine reinforcement is maintained. The place conditioning phenotype sug-

gests that δ receptor activation might facilitate drug–context associations, an effect that might influence contextual aspects of addiction-related behaviors. Neural mechanisms through which these receptors influence conditioning, however, remain to be elucidated. Remarkably, these receptors are expressed in all key brain regions controlling conditioned learning processes (1,20), where they can fine-tune reinforced memory processes.

This work was supported by the Centre de la Recherche Scientifique, Institut de la Santé et de la Recherche Médicale, Université de Strasbourg; the Spanish “Ministerio de Ciencia e Innovación” (# SAF2007-64062); and the Catalan Institution for Research and Advanced Studies Foundation (ICREA Academia-2008). We thank the European Union (GENADDICT/FP6 005166) and the National Institutes of Health (NIAAA AA-16658 and NIDA DA-16768/DA-005010) for financial support. The authors report no biomedical financial interests or potential conflicts of interest.

Supplementary material cited in this article is available online.

1. Le Merrer J, Becker JA, Befort K, Kieffer BL (2009): Reward processing by the opioid system in the brain. *Physiol Rev* 89:1379–1412.
2. Longoni R, Cadoni C, Mulas A, Di Chiara G, Spina L (1998): Dopamine-dependent behavioural stimulation by non-peptide delta opioids BW373U86 and SNC 80: 2. Place-preference and brain microdialysis studies in rats. *Behav Pharmacol* 9:9–14.
3. Morales L, Perez-Garcia C, Alguacil LF (2001): Effects of yohimbine on the antinociceptive and place conditioning effects of opioid agonists in rodents. *Br J Pharmacol* 133:172–178.
4. Shippenberg TS, Bals-Kubik R, Herz A (1987): Motivational properties of opioids: Evidence that an activation of delta-receptors mediates reinforcement processes. *Brain Res* 436:234–239.
5. Suzuki T, Tsuji M, Mori T, Ikeda H, Misawa M, Nagase H (1997): Involvement of dopamine-dependent and -independent mechanisms in the rewarding effects mediated by delta opioid receptor subtypes in mice. *Brain Res* 744:327–334.
6. Chefer VI, Shippenberg TS (2009): Augmentation of morphine-induced sensitization but reduction in morphine tolerance and reward in delta-opioid receptor knockout mice. *Neuropsychopharmacology* 34:887–898.
7. Menkens K, Bilsky EJ, Wild KD, Portoghese PS, Reid LD, Porreca F (1992): Cocaine place preference is blocked by the delta-opioid receptor antagonist, naltrindole. *Eur J Pharmacol* 219:345–346.
8. Suzuki T, Yoshiike M, Mizoguchi H, Kamei J, Misawa M, Nagase H (1994): Blockade of delta-opioid receptors prevents morphine-induced place preference in mice. *Jpn J Pharmacol* 66:131–137.
9. Ward SJ, Roberts DC (2007): Microinjection of the delta-opioid receptor selective antagonist naltrindole 5'-isothiocyanate site specifically affects cocaine self-administration in rats responding under a progressive ratio schedule of reinforcement. *Behav Brain Res* 182:140–144.
10. Hutcheson DM, Matthes HW, Valjent E, Sanchez-Blazquez P, Rodriguez-Diaz M, Garzon J, *et al.* (2001): Lack of dependence and rewarding effects of deltorphin II in mu-opioid receptor-deficient mice. *Eur J Neurosci* 13:153–161.
11. Scherrer G, Befort K, Contet C, Becker J, Matifas A, Kieffer BL (2004): The delta agonists DPDPE and deltorphin II recruit predominantly mu receptors to produce thermal analgesia: A parallel study of mu, delta and combinatorial opioid receptor knockout mice. *Eur J Neurosci* 19:2239–2248.
12. Ghozland S, Matthes HW, Simonin F, Filliol D, Kieffer BL, Maldonado R (2002): Motivational effects of cannabinoids are mediated by mu-opioid and kappa-opioid receptors. *J Neurosci* 22:1146–1154.
13. David V, Matifas A, Gavello-Baudy S, Decorte L, Kieffer BL, Cazala P (2008): Brain regional Fos expression elicited by the activation of mu-but not delta-opioid receptors of the ventral tegmental area: Evidence for an implication of the ventral thalamus in opiate reward. *Neuropsychopharmacology* 33:1746–1759.
14. Stephens DN, Duka T, Crombag HS, Cunningham CL, Heilig M, Crabbe JC (2010): Reward sensitivity: Issues of measurement, and achieving consistency between human and animal phenotypes. *Addict Biol* 15:145–168.
15. Jutkiewicz EM, Rice KC, Woods JH, Winsauer PJ (2003): Effects of the delta-opioid receptor agonist SNC80 on learning relative to its antidepressant-like effects in rats. *Behav Pharmacol* 14:509–516.
16. Yang S, Kawamura Y, Yoshikawa M (2003): Effect of rubiscolin, a delta opioid peptide derived from rubisco, on memory consolidation. *Pepptides* 24:325–328.
17. Filliol D, Ghozland S, Chluba J, Martin M, Matthes HW, Simonin F, *et al.* (2000): Mice deficient for delta- and mu-opioid receptors exhibit opposing alterations of emotional responses. *Nat Genet* 25:195–200.
18. Overton DA (1978): Basic mechanisms of state-dependent learning. *Psychopharmacol Bull* 14:67–68.
19. Olmstead MC, Ouagazzal AM, Kieffer BL (2009): Mu and delta opioid receptors oppositely regulate motor impulsivity in the signaled nose poke task. *PLoS ONE* 4:e4410.
20. White NM, McDonald RJ (2002): Multiple parallel memory systems in the brain of the rat. *Neurobiol Learn Mem* 77:125–184.

VI. REFERENCES

- Agrawal N, Dasaradhi PV, Mohmmmed A, Malhotra P, Bhatnagar RK, Mukherjee SK. 2003. RNA interference: biology, mechanism, and applications. *Microbiol Mol Biol Rev* 67:657-85
- Akil H, Owens C, Gutstein H, Taylor L, Curran E, Watson S. 1998. Endogenous opioids: overview and current issues. *Drug Alcohol Depend* 51:127-40
- Alexander GE, Crutcher MD, DeLong MR. 1990. Basal ganglia-thalamocortical circuits: parallel substrates for motor, oculomotor, "prefrontal" and "limbic" functions. *Prog Brain Res* 85:119-46
- Allman JM, Hakeem A, Erwin JM, Nimchinsky E, Hof P. 2001. The anterior cingulate cortex. The evolution of an interface between emotion and cognition. *Ann N Y Acad Sci* 935:107-17
- Ambesi-Impiombato A, D'Urso G, Muscettola G, de Bartolomeis A. 2003. Method for quantitative in situ hybridization histochemistry and image analysis applied for Homer1a gene expression in rat brain. *Brain Res Brain Res Protoc* 11:189-96
- Anthony KG, Bai F, Krishnan MN, Fikrig E, Koski RA. 2009. Effective siRNA targeting of the 3' untranslated region of the West Nile virus genome. *Antiviral Res* 82:166-8
- Aroniadou-Anderjaska V, Qashu F, Braga MF. 2007. Mechanisms regulating GABAergic inhibitory transmission in the basolateral amygdala: implications for epilepsy and anxiety disorders. *Amino Acids* 32:305-15
- Baskin DG, Stahl WL. 1993. Fundamentals of quantitative autoradiography by computer densitometry for in situ hybridization, with emphasis on 33P. *J Histochem Cytochem* 41:1767-76
- Baxter MG, Murray EA. 2002. The amygdala and reward. *Nat Rev Neurosci* 3:563-73
- Becker A, Grecksch G, Kraus J, Loh HH, Schroeder H, Hollt V. 2002. Rewarding effects of ethanol and cocaine in mu opioid receptor-deficient mice. *Naunyn Schmiedebergs Arch Pharmacol* 365:296-302
- Becker C, Zeau B, Rivat C, Blugeot A, Hamon M, Benoliel JJ. 2008. Repeated social defeat-induced depression-like behavioral and biological alterations in rats: involvement of cholecystokinin. *Mol Psychiatry* 13:1079-92
- Befort K, Filliol D, Ghate A, Darcq E, Matifas A, et al. 2008. Mu-opioid receptor activation induces transcriptional plasticity in the central extended amygdala. *Eur J Neurosci* 27:2973-84
- Beinfeld MC. 2001. An introduction to neuronal cholecystokinin. *Peptides* 22:1197-200
- Beinfeld MC. 2003a. Biosynthesis and processing of pro CCK: recent progress and future challenges. *Life Sci* 72:747-57
- Beinfeld MC. 2003b. What we know and what we need to know about the role of endogenous CCK in psychostimulant sensitization. *Life Sci* 73:643-54
- Beinfeld MC, Meyer DK, Brownstein MJ. 1981a. Cholecystokinin in the central nervous system. *Peptides* 2 Suppl 2:77-9
- Beinfeld MC, Meyer DK, Eskay RL, Jensen RT, Brownstein MJ. 1981b. The distribution of cholecystokinin immunoreactivity in the central nervous system of the rat as determined by radioimmunoassay. *Brain Res* 212:51-7

- Belcheva I, Belcheva S, Petkov VV, Petkov VD. 1994. Asymmetry in behavioral responses to cholecystokinin microinjected into rat nucleus accumbens and amygdala. *Neuropharmacology* 33:995-1002
- Bennett MR. 2011. The prefrontal-limbic network in depression: Modulation by hypothalamus, basal ganglia and midbrain. *Prog Neurobiol* 93:468-87
- Berna MJ, Tapia JA, Sancho V, Jensen RT. 2007. Progress in developing cholecystokinin (CCK)/gastrin receptor ligands that have therapeutic potential. *Curr Opin Pharmacol* 7:583-92
- Berrendero F, Robledo P, Trigo JM, Martin-Garcia E, Maldonado R. 2010. Neurobiological mechanisms involved in nicotine dependence and reward: participation of the endogenous opioid system. *Neurosci Biobehav Rev* 35:220-31
- Biederman J, Faraone SV. 2005. Attention-deficit hyperactivity disorder. *Lancet* 366:237-48
- Blanco E, Castilla-Ortega E, Miranda R, Begega A, Aguirre JA, et al. 2009. Effects of medial prefrontal cortex lesions on anxiety-like behaviour in restrained and non-restrained rats. *Behav Brain Res* 201:338-42
- Bodnar RJ. 2010. Endogenous opiates and behavior: 2009. *Peptides* 31:2325-59
- Boeree CG. 2006. *The basal ganglia*. Shippensburg University Website. <http://webpace.ship.edu/cgboer/basalganglia.html>
- Bonelli RM, Cummings JL. 2007. Frontal-subcortical circuitry and behavior. *Dialogues Clin Neurosci* 9:141-51
- Brownstein MJ, Rehfeld JF. 1985. Molecular forms of cholecystokinin in the nervous system. *Ann N Y Acad Sci* 448:9-10
- Buning H, Perabo L, Coutelle O, Quadt-Humme S, Hallek M. 2008. Recent developments in adeno-associated virus vector technology. *J Gene Med* 10:717-33
- Burger C, Gorbatyuk OS, Velardo MJ, Peden CS, Williams P, et al. 2004. Recombinant AAV viral vectors pseudotyped with viral capsids from serotypes 1, 2, and 5 display differential efficiency and cell tropism after delivery to different regions of the central nervous system. *Mol Ther* 10:302-17
- Bush G, Vogt BA, Holmes J, Dale AM, Greve D, et al. 2002. Dorsal anterior cingulate cortex: a role in reward-based decision making. *Proc Natl Acad Sci U S A* 99:523-8
- Cain BM, Connolly K, Blum A, Vishnuvardhan D, Marchand JE, Beinfeld MC. 2003. Distribution and colocalization of cholecystokinin with the prohormone convertase enzymes PC1, PC2, and PC5 in rat brain. *J Comp Neurol* 467:307-25
- Castro JE, Varea E, Marquez C, Cordero MI, Poirier G, Sandi C. 2010. Role of the amygdala in antidepressant effects on hippocampal cell proliferation and survival and on depression-like behavior in the rat. *PLoS One* 5:e8618
- Clemens JC, Worby CA, Simonson-Leff N, Muda M, Maehama T, et al. 2000. Use of double-stranded RNA interference in Drosophila cell lines to dissect signal transduction pathways. *Proc Natl Acad Sci U S A* 97:6499-503
- Contet C, Kieffer BL, Befort K. 2004. Mu opioid receptor: a gateway to drug addiction. *Curr Opin Neurobiol* 14:370-8
- Chandra R, Liddle RA. 2007. Cholecystokinin. *Curr Opin Endocrinol Diabetes Obes* 14:63-7

- Cheetham A, Allen NB, Yucel M, Lubman DI. 2010. The role of affective dysregulation in drug addiction. *Clin Psychol Rev* 30:621-34
- Chen Q, Tang M, Mamiya T, Im HI, Xiong X, et al. 2010. Bi-directional effect of cholecystokinin receptor-2 overexpression on stress-triggered fear memory and anxiety in the mouse. *PLoS One* 5:e15999
- Cheng T, Xu CY, Wang YB, Chen M, Wu T, et al. 2004. A rapid and efficient method to express target genes in mammalian cells by baculovirus. *World J Gastroenterol* 10:1612-8
- Chhatwal JP, Gutman AR, Maguschak KA, Bowser ME, Yang Y, et al. 2009. Functional interactions between endocannabinoid and CCK neurotransmitter systems may be critical for extinction learning. *Neuropsychopharmacology* 34:509-21
- Chiu CT, Chuang DM. 2010. Molecular actions and therapeutic potential of lithium in preclinical and clinical studies of CNS disorders. *Pharmacol Ther* 128:281-304
- Chotteau-Lelievre A, Dolle P, Gofflot F. 2006. Expression analysis of murine genes using in situ hybridization with radioactive and nonradioactively labeled RNA probes. *Methods Mol Biol* 326:61-87
- Chow TW. 2000. Personality in frontal lobe disorders. *Curr Psychiatry Rep* 2:446-51
- Chung L, Moore SD. 2007. Cholecystokinin enhances GABAergic inhibitory transmission in basolateral amygdala. *Neuropeptides* 41:453-63
- Chung L, Moore SD. 2009. Cholecystokinin excites interneurons in rat basolateral amygdala. *J Neurophysiol* 102:272-84
- Danos O. 2008. AAV vectors for RNA-based modulation of gene expression. *Gene Ther* 15:864-9
- Dauge V, Bohme GA, Crawley JN, Durieux C, Stutzmann JM, et al. 1990. Investigation of behavioral and electrophysiological responses induced by selective stimulation of CCKB receptors by using a new highly potent CCK analog, BC 264. *Synapse* 6:73-80
- Dauge V, Lena I. 1998. CCK in anxiety and cognitive processes. *Neurosci Biobehav Rev* 22:815-25
- Dauge V, Sebret A, Beslot F, Matsui T, Roques BP. 2001. Behavioral profile of CCK2 receptor-deficient mice. *Neuropsychopharmacology* 25:690-8
- Davidson BL, Stein CS, Heth JA, Martins I, Kotin RM, et al. 2000. Recombinant adeno-associated virus type 2, 4, and 5 vectors: transduction of variant cell types and regions in the mammalian central nervous system. *Proc Natl Acad Sci U S A* 97:3428-32
- Davidson RJ. 2002. Anxiety and affective style: role of prefrontal cortex and amygdala. *Biol Psychiatry* 51:68-80
- Devinsky O, Morrell MJ, Vogt BA. 1995. Contributions of anterior cingulate cortex to behaviour. *Brain* 118 (Pt 1):279-306
- Dillon CP, Sandy P, Nencioni A, Kissler S, Rubinson DA, Van Parijs L. 2005. *Rnai as an experimental and therapeutic tool to study and regulate physiological and disease processes*. *Annu Rev Physiol* 67:147-73
- Dockray GJ. 2009. Cholecystokinin and gut-brain signalling. *Regul Pept* 155:6-10

- Duangdao DM, Clark SD, Okamura N, Reinscheid RK. 2009. Behavioral phenotyping of neuropeptide S receptor knockout mice. *Behav Brain Res* 205:1-9
- Edwards S, Koob GF. 2010. Neurobiology of dysregulated motivational systems in drug addiction. *Future Neurol* 5:393-401
- Ehlert EM, Eggers R, Niclou SP, Verhaagen J. 2010. Cellular toxicity following application of adeno-associated viral vector-mediated RNA interference in the nervous system. *BMC Neurosci* 11:20
- Elbashir SM, Harborth J, Lendeckel W, Yalcin A, Weber K, Tuschl T. 2001. Duplexes of 21-nucleotide RNAs mediate RNA interference in cultured mammalian cells. *Nature* 411:494-8
- Everitt BJ, Robbins TW. 2005. Neural systems of reinforcement for drug addiction: from actions to habits to compulsion. *Nat Neurosci* 8:1481-9
- Feltenstein MW, See RE. 2008. The neurocircuitry of addiction: an overview. *Br J Pharmacol* 154:261-74
- Filliol D, Ghozland S, Chluba J, Martin M, Matthes HW, et al. 2000. Mice deficient for delta- and mu-opioid receptors exhibit opposing alterations of emotional responses. *Nat Genet* 25:195-200
- Fink H, Rex A, Voits M, Voigt JP. 1998. Major biological actions of CCK--a critical evaluation of research findings. *Exp Brain Res* 123:77-83
- Fire A, Xu S, Montgomery MK, Kostas SA, Driver SE, Mello CC. 1998. Potent and specific genetic interference by double-stranded RNA in *Caenorhabditis elegans*. *Nature* 391:806-11
- Franklin TR, Wang Z, Wang J, Sciortino N, Harper D, et al. 2007. Limbic activation to cigarette smoking cues independent of nicotine withdrawal: a perfusion fMRI study. *Neuropsychopharmacology* 32:2301-9
- Fredriksson R, Lagerstrom MC, Lundin LG, Schioth HB. 2003. The G-protein-coupled receptors in the human genome form five main families. Phylogenetic analysis, paralogon groups, and fingerprints. *Mol Pharmacol* 63:1256-72
- Frenois F, Stinus L, Di Blasi F, Cador M, Le Moine C. 2005. A specific limbic circuit underlies opiate withdrawal memories. *J Neurosci* 25:1366-74
- Frisch C, Hasenohrl RU, Mattern CM, Hacker R, Huston JP. 1995. Blockade of lithium chloride-induced conditioned place aversion as a test for antiemetic agents: comparison of metoclopramide with combined extracts of *Zingiber officinale* and *Ginkgo biloba*. *Pharmacol Biochem Behav* 52:321-7
- Fuchs RA, Evans KA, Ledford CC, Parker MP, Case JM, et al. 2005. The role of the dorsomedial prefrontal cortex, basolateral amygdala, and dorsal hippocampus in contextual reinstatement of cocaine seeking in rats. *Neuropsychopharmacology* 30:296-309
- Fudge JL, Emiliano AB. 2003. The extended amygdala and the dopamine system: another piece of the dopamine puzzle. *J Neuropsychiatry Clin Neurosci* 15:306-16
- Gale GD, Anagnostaras SG, Godsil BP, Mitchell S, Nozawa T, et al. 2004. Role of the basolateral amygdala in the storage of fear memories across the adult lifetime of rats. *J Neurosci* 24:3810-5

- Gallagher M, Chiba AA. 1996. The amygdala and emotion. *Curr Opin Neurobiol* 6:221-7
- Gao X, Zhang P. 2007. Transgenic RNA interference in mice. *Physiology (Bethesda)* 22:161-6
- Gaveriaux-Ruff C, Karchewski LA, Hever X, Matifas A, Kieffer BL. 2008. Inflammatory pain is enhanced in delta opioid receptor-knockout mice. *Eur J Neurosci* 27:2558-67
- Gaveriaux-Ruff C, Kieffer BL. 2002. Opioid receptor genes inactivated in mice: the highlights. *Neuropeptides* 36:62-71
- Ghijssen WE, Leenders AG, Wiegant VM. 2001. Regulation of cholecystokinin release from central nerve terminals. *Peptides* 22:1213-21
- Giacobini P, Wray S. 2008. Prenatal expression of cholecystokinin (CCK) in the central nervous system (CNS) of mouse. *Neurosci Lett* 438:96-101
- Gianoulakis C. 2009. Endogenous opioids and addiction to alcohol and other drugs of abuse. *Curr Top Med Chem* 9:999-1015
- Gil J, Esteban M. 2000. Induction of apoptosis by the dsRNA-dependent protein kinase (PKR): mechanism of action. *Apoptosis* 5:107-14
- Goeldner C, Lutz PE, Darcq E, Halter T, Clesse D, et al. 2011. Impaired emotional-like behavior and serotonergic function during protracted abstinence from chronic morphine. *Biol Psychiatry* 69:236-44
- Goldstein RZ, Tomasi D, Rajaram S, Cottone LA, Zhang L, et al. 2007. Role of the anterior cingulate and medial orbitofrontal cortex in processing drug cues in cocaine addiction. *Neuroscience* 144:1153-9
- Goldstein RZ, Volkow ND. 2002. Drug addiction and its underlying neurobiological basis: neuroimaging evidence for the involvement of the frontal cortex. *Am J Psychiatry* 159:1642-52
- Goncalves MA. 2005. Adeno-associated virus: from defective virus to effective vector. *Virology* 2:43
- Goodman A. 2008. Neurobiology of addiction. An integrative review. *Biochem Pharmacol* 75:266-322
- Grimm D, Kay MA. 2007. RNAi and gene therapy: a mutual attraction. *Hematology Am Soc Hematol Educ Program*:473-81
- Gupta S, Schoer RA, Egan JE, Hannon GJ, Mittal V. 2004. Inducible, reversible, and stable RNA interference in mammalian cells. *Proc Natl Acad Sci U S A* 101:1927-32
- Hebb AL, Poulin JF, Roach SP, Zacharko RM, Drolet G. 2005. Cholecystokinin and endogenous opioid peptides: interactive influence on pain, cognition, and emotion. *Prog Neuropsychopharmacol Biol Psychiatry* 29:1225-38
- Hellemans KG, Everitt BJ, Lee JL. 2006. Disrupting reconsolidation of conditioned withdrawal memories in the basolateral amygdala reduces suppression of heroin seeking in rats. *J Neurosci* 26:12694-9
- Hernando F, Fuentes JA, Fournie-Zaluski MC, Roques BP, Ruiz-Gayo M. 1996. Antidepressant-like effects of CCK(B) receptor antagonists: involvement of the opioid system. *Eur J Pharmacol* 318:221-9
- Higgins GA, Nguyen P, Sellers EM. 1992. Morphine place conditioning is differentially affected by CCKA and CCKB receptor antagonists. *Brain Res* 572:208-15

- Higham JP, Barr CS, Hoffman CL, Mandalaywala TM, Parker KJ, Maestripieri D. 2011. Mu-opioid receptor (OPRM1) variation, oxytocin levels and maternal attachment in free-ranging rhesus macaques *Macaca mulatta*. *Behav Neurosci* 125:131-6
- Hokfelt T, Blacker D, Broberger C, Herrera-Marschitz M, Snyder G, et al. 2002. Some aspects on the anatomy and function of central cholecystokinin systems. *Pharmacol Toxicol* 91:382-6
- Hommel JD, Sears RM, Georgescu D, Simmons DL, DiLeone RJ. 2003. Local gene knockdown in the brain using viral-mediated RNA interference. *Nat Med* 9:1539-44
- Howard DB, Powers K, Wang Y, Harvey BK. 2008. Tropism and toxicity of adeno-associated viral vector serotypes 1, 2, 5, 6, 7, 8, and 9 in rat neurons and glia in vitro. *Virology* 372:24-34
- Hughes J, Smith TW, Kosterlitz HW, Fothergill LA, Morgan BA, Morris HR. 1975. Identification of two related pentapeptides from the brain with potent opiate agonist activity. *Nature* 258:577-80
- Ide S, Sora I, Ikeda K, Minami M, Uhl GR, Ishihara K. 2010. Reduced emotional and corticosterone responses to stress in mu-opioid receptor knockout mice. *Neuropharmacology* 58:241-7
- Ingle JD, Crouch SR. 1988. SPECTROCHEMICAL ANALYSIS, Prentice Hall, New Jersey.
- Ingram SM, Krause RG, 2nd, Baldino F, Jr., Skeen LC, Lewis ME. 1989. Neuronal localization of cholecystokinin mRNA in the rat brain by using in situ hybridization histochemistry. *J Comp Neurol* 287:260-72
- Ishii S, Weintraub N, Mervis JR. 2009. Apathy: a common psychiatric syndrome in the elderly. *J Am Med Dir Assoc* 10:381-93
- Iwahashi K, Aoki J. 2009. A review of smoking behavior and smokers evidence (chemical modification, inducing nicotine metabolism, and individual variations by genotype: dopaminergic function and personality traits). *Drug Chem Toxicol* 32:301-6
- Jackson KJ, Carroll FI, Negus SS, Damaj MI. 2010. Effect of the selective kappa-opioid receptor antagonist JD1c on nicotine antinociception, reward, and withdrawal in the mouse. *Psychopharmacology (Berl)* 210:285-94
- Jasnow AM, Ressler KJ, Hammack SE, Chhatwal JP, Rainnie DG. 2009. Distinct subtypes of cholecystokinin (CCK)-containing interneurons of the basolateral amygdala identified using a CCK promoter-specific lentivirus. *J Neurophysiol* 101:1494-506
- Jones AR, Overly CC, Sunkin SM. 2009. The Allen Brain Atlas: 5 years and beyond. *Nat Rev Neurosci* 10:821-8
- Jutkiewicz EM. 2006. The antidepressant-like effects of delta-opioid receptor agonists. *Mol Interv* 6:162-9
- Kalivas PW, McFarland K. 2003. Brain circuitry and the reinstatement of cocaine-seeking behavior. *Psychopharmacology (Berl)* 168:44-56
- Kaplitt MG, Leone P, Samulski RJ, Xiao X, Pfaff DW, et al. 1994. Long-term gene expression and phenotypic correction using adeno-associated virus vectors in the mammalian brain. *Nat Genet* 8:148-54
- Kayser V, Idanpaan-Hekkila JJ, Christensen D, Guilbaud G. 1998. The selective cholecystokininB receptor antagonist L-365,260 diminishes the expression of

- naloxone-induced morphine withdrawal symptoms in normal and neuropathic rats. *Life Sci* 62:947-52
- Kieffer BL. 1995. *Recent advances in molecular recognition and signal transduction of active peptides: receptors for opioid peptides*. *Cell Mol Neurobiol* 15:615-35
- Koenigs M, Huey ED, Calamia M, Raymont V, Tranel D, Grafman J. 2008. Distinct regions of prefrontal cortex mediate resistance and vulnerability to depression. *J Neurosci* 28:12341-8
- Koob G, Kreek MJ. 2007. Stress, dysregulation of drug reward pathways, and the transition to drug dependence. *Am J Psychiatry* 164:1149-59
- Koob GF. 2008. A role for brain stress systems in addiction. *Neuron* 59:11-34
- Koob GF. 2009. Dynamics of neuronal circuits in addiction: reward, antireward, and emotional memory. *Pharmacopsychiatry* 42 Suppl 1:S32-41
- Koob GF, Ahmed SH, Boutrel B, Chen SA, Kenny PJ, et al. 2004. Neurobiological mechanisms in the transition from drug use to drug dependence. *Neurosci Biobehav Rev* 27:739-49
- Koob GF, Le Moal M. 2005. Plasticity of reward neurocircuitry and the 'dark side' of drug addiction. *Nat Neurosci* 8:1442-4
- Koob GF, Le Moal M. 1997. *Drug abuse: hedonic homeostatic dysregulation*. *Science* 278:52-8
- Koob GF, Volkow ND. 2010. Neurocircuitry of addiction. *Neuropsychopharmacology* 35:217-38
- Korner M, Miller LJ. 2009. Alternative splicing of pre-mRNA in cancer: focus on G protein-coupled peptide hormone receptors. *Am J Pathol* 175:461-72
- Lanca AJ, De Cabo C, Arifuzzaman AI, Vaccarino FJ. 1998. Cholecystokinergic innervation of nucleus accumbens subregions. *Peptides* 19:859-68
- Lazic SE. 2009. Statistical evaluation of methods for quantifying gene expression by autoradiography in histological sections. *BMC Neurosci* 10:5
- LeDoux JE. 2000. Emotion circuits in the brain. *Annu Rev Neurosci* 23:155-84
- Le Merrer J, Plaza-Zabala A, Del Boca C, Matifas A, Maldonado R, Kieffer BL. 2011. *Deletion of the delta Opioid Receptor Gene Impairs Place Conditioning But Preserves Morphine Reinforcement*. *Biol Psychiatry* 69:700-3
- Le Moal M, Koob GF. 2007. *Drug addiction: pathways to the disease and pathophysiological perspectives*. *Eur Neuropsychopharmacol* 17:377-93
- Leung RK, Whittaker PA. 2005. RNA interference: from gene silencing to gene-specific therapeutics. *Pharmacol Ther* 107:222-39
- Lo CM, Samuelson LC, Chambers JB, King A, Heiman J, et al. 2008. Characterization of mice lacking the gene for cholecystokinin. *Am J Physiol Regul Integr Comp Physiol* 294:R803-10
- Lord JA, Waterfield AA, Hughes J, Kosterlitz HW. 1977. Endogenous opioid peptides: multiple agonists and receptors. *Nature* 267:495-9

- Lowe AS, Williams SC, Symms MR, Stolerman IP, Shoaib M. 2002. Functional magnetic resonance neuroimaging of drug dependence: naloxone-precipitated morphine withdrawal. *Neuroimage* 17:902-10
- Lu L, Huang M, Ma L, Li J. 2001. Different role of cholecystokinin (CCK)-A and CCK-B receptors in relapse to morphine dependence in rats. *Behav Brain Res* 120:105-10
- Lu L, Shepard JD, Hall FS, Shaham Y. 2003. Effect of environmental stressors on opiate and psychostimulant reinforcement, reinstatement and discrimination in rats: a review. *Neurosci Biobehav Rev* 27:457-91
- Lu L, Zhang B, Liu Z, Zhang Z. 2002. Reactivation of cocaine conditioned place preference induced by stress is reversed by cholecystokinin-B receptors antagonist in rats. *Brain Res* 954:132-40
- Makinen PI, Koponen JK, Karkkainen AM, Malm TM, Pulkkinen KH, et al. 2006. Stable RNA interference: comparison of U6 and H1 promoters in endothelial cells and in mouse brain. *J Gene Med* 8:433-41
- Malpeli JG. 1999. Reversible inactivation of subcortical sites by drug injection. *J Neurosci Methods* 86:119-28
- Maren S. 1999. Long-term potentiation in the amygdala: a mechanism for emotional learning and memory. *Trends Neurosci* 22:561-7
- Maren S. 2001. Neurobiology of Pavlovian fear conditioning. *Annu Rev Neurosci* 24:897-931
- Markakis EA, Vives KP, Bober J, Leichtle S, Leranath C, et al. 2010. Comparative transduction efficiency of AAV vector serotypes 1-6 in the substantia nigra and striatum of the primate brain. *Mol Ther* 18:588-93
- Martijena ID, Rodriguez Manzanares PA, Lacerra C, Molina VA. 2002. Gabaergic modulation of the stress response in frontal cortex and amygdala. *Synapse* 45:86-94
- Martin M, Matifas A, Maldonado R, Kieffer BL. 2003. Acute antinociceptive responses in single and combinatorial opioid receptor knockout mice: distinct mu, delta and kappa tones. *Eur J Neurosci* 17:701-8
- Martin WR, Eades CG, Thompson JA, Huppler RE, Gilbert PE. 1976. The effects of morphine- and nalorphine- like drugs in the nondependent and morphine-dependent chronic spinal dog. *J Pharmacol Exp Ther* 197:517-32
- Mascagni F, McDonald AJ. 2003. Immunohistochemical characterization of cholecystokinin containing neurons in the rat basolateral amygdala. *Brain Res* 976:171-84
- Mathon DS, Lesscher HM, Gerrits MA, Kamal A, Pintar JE, et al. 2005. Increased gabaergic input to ventral tegmental area dopaminergic neurons associated with decreased cocaine reinforcement in mu-opioid receptor knockout mice. *Neuroscience* 130:359-67
- Mazzocchi G, Malendowicz LK, Aragona F, Spinazzi R, Nussdorfer GG. 2004. Cholecystokinin (CCK) stimulates aldosterone secretion from human adrenocortical cells via CCK2 receptors coupled to the adenylate cyclase/protein kinase A signaling cascade. *J Clin Endocrinol Metab* 89:1277-84
- McCarty DM, Young SM, Jr., Samulski RJ. 2004. Integration of adeno-associated virus (AAV) and recombinant AAV vectors. *Annu Rev Genet* 38:819-45

- McClung CA, Nestler EJ. 2008. Neuroplasticity mediated by altered gene expression. *Neuropsychopharmacology* 33:3-17
- McCown TJ, Xiao X, Li J, Breese GR, Samulski RJ. 1996. Differential and persistent expression patterns of CNS gene transfer by an adeno-associated virus (AAV) vector. *Brain Res* 713:99-107
- McDonald AJ. 1985. Morphology of peptide-containing neurons in the rat basolateral amygdaloid nucleus. *Brain Res* 338:186-91
- McIlwain KL, Merriweather MY, Yuva-Paylor LA, Paylor R. 2001. The use of behavioral test batteries: effects of training history. *Physiol Behav* 73:705-17
- Meziane H, Devigne C, Tramu G, Soumireu-Mourat B. 1997. Distribution of cholecystokinin immunoreactivity in the BALB/c mouse forebrain: an immunocytochemical study. *J Chem Neuroanat* 12:191-209
- Millan MJ. 2003. The neurobiology and control of anxious states. *Prog Neurobiol* 70:83-244
- Miller LJ, Gao F. 2008. Structural basis of cholecystokinin receptor binding and regulation. *Pharmacol Ther* 119:83-95
- Mingozzi F, High KA. 2011. Therapeutic in vivo gene transfer for genetic disease using AAV: progress and challenges. *Nat Rev Genet* 12:341-55
- Mitchell JM, Bergren LJ, Chen KS, Fields HL. 2006. Cholecystokinin is necessary for the expression of morphine conditioned place preference. *Pharmacol Biochem Behav* 85:787-95
- Miyagishi M, Taira K. 2002. Development and application of siRNA expression vector. *Nucleic Acids Res Suppl*:113-4
- Mize RR, Holdefer RN, Nabors LB. 1988. Quantitative immunocytochemistry using an image analyzer. I. Hardware evaluation, image processing, and data analysis. *J Neurosci Methods* 26:1-23
- Mocellin S, Provenzano M. 2004. RNA interference: learning gene knock-down from cell physiology. *J Transl Med* 2:39
- Moeller FG, Barratt ES, Dougherty DM, Schmitz JM, Swann AC. 2001. Psychiatric aspects of impulsivity. *Am J Psychiatry* 158:1783-93
- Moles A, Kieffer BL, D'Amato FR. 2004. Deficit in attachment behavior in mice lacking the mu-opioid receptor gene. *Science* 304:1983-6
- Moran TH, Bi S. 2006. Hyperphagia and obesity in OLETF rats lacking CCK-1 receptors. *Philos Trans R Soc Lond B Biol Sci* 361:1211-8
- Moran TH, Kinzig KP. 2004. Gastrointestinal satiety signals II. Cholecystokinin. *Am J Physiol Gastrointest Liver Physiol* 286:G183-8
- Moran TH, Robinson PH, Goldrich MS, McHugh PR. 1986. Two brain cholecystokinin receptors: implications for behavioral actions. *Brain Res* 362:175-9
- Mozhui K, Hamre KM, Holmes A, Lu L, Williams RW. 2007. Genetic and structural analysis of the basolateral amygdala complex in BXD recombinant inbred mice. *Behav Genet* 37:223-43
- Mutt V, Jorpes JE. 1968. Structure of porcine cholecystokinin-pancreozymin. 1. Cleavage with thrombin and with trypsin. *Eur J Biochem* 6:156-62

- Nadal X, Banos JE, Kieffer BL, Maldonado R. 2006. Neuropathic pain is enhanced in delta-opioid receptor knockout mice. *Eur J Neurosci* 23:830-4
- Nestler EJ. 2005. Is there a common molecular pathway for addiction? *Nat Neurosci* 8:1445-9
- Newman SW. 1999. The medial extended amygdala in male reproductive behavior. A node in the mammalian social behavior network. *Ann N Y Acad Sci* 877:242-57
- Noble F, Roques BP. 2002. Phenotypes of mice with invalidation of cholecystokinin (CCK(1) or CCK(2)) receptors. *Neuropeptides* 36:157-70
- Noble F, Roques BP. 2003. The role of CCK2 receptors in the homeostasis of the opioid system. *Drugs Today (Barc)* 39:897-908
- Noble F, Wank SA, Crawley JN, Bradwejn J, Seroogy KB, et al. 1999. International Union of Pharmacology. XXI. Structure, distribution, and functions of cholecystokinin receptors. *Pharmacol Rev* 51:745-81
- Overhoff M, Alken M, Far RK, Lemaitre M, Lebleu B, et al. 2005. Local RNA target structure influences siRNA efficacy: a systematic global analysis. *J Mol Biol* 348:871-81
- Paddison PJ, Caudy AA, Bernstein E, Hannon GJ, Conklin DS. 2002. Short hairpin RNAs (shRNAs) induce sequence-specific silencing in mammalian cells. *Genes Dev* 16:948-58
- Papaleo F, Kieffer BL, Tabarin A, Contarino A. 2007. Decreased motivation to eat in mu-opioid receptor-deficient mice. *Eur J Neurosci* 25:3398-405
- Parker LA, Limebeer CL. 2006. Conditioned gaping in rats: a selective measure of nausea. *Auton Neurosci* 129:36-41
- Pasternak G, Pan YX. 2011. Mu opioid receptors in pain management. *Acta Anaesthesiol Taiwan* 49:21-5
- Paule MR, White RJ. 2000. Survey and summary: transcription by RNA polymerases I and III. *Nucleic Acids Res* 28:1283-98
- Paylor R, Spencer CM, Yuva-Paylor LA, Pieke-Dahl S. 2006. The use of behavioral test batteries, II: effect of test interval. *Physiol Behav* 87:95-102
- Pereira PM, Schneider A, Pannetier S, Heron D, Hanauer A. 2010. Coffin-Lowry syndrome. *Eur J Hum Genet* 18:627-33
- Peterson SL. 1998. *Drug microinjection in discrete brain regions*. David Kopf instruments 50
- Pommier B, Beslot F, Simon A, Pophillat M, Matsui T, et al. 2002. Deletion of CCK2 receptor in mice results in an upregulation of the endogenous opioid system. *J Neurosci* 22:2005-11
- Pommier B, Da Nascimento S, Dumont S, Bellier B, Million E, et al. 1999. The cholecystokininB receptor is coupled to two effector pathways through pertussis toxin-sensitive and -insensitive G proteins. *J Neurochem* 73:281-8
- Pommier B, Marie-Claire C, Da Nascimento S, Wang HL, Roques BP, Noble F. 2003. Further evidence that the CCK2 receptor is coupled to two transduction pathways using site-directed mutagenesis. *J Neurochem* 85:454-61
- Rasmussen K, Czachura JF, Kallman MJ, Helton DR. 1996. The CCK-B antagonist LY288513 blocks the effects of nicotine withdrawal on auditory startle. *Neuroreport* 7:1050-2

- Raud S, Innos J, Abramov U, Reimets A, Koks S, et al. 2005. Targeted invalidation of CCK2 receptor gene induces anxiolytic-like action in light-dark exploration, but not in fear conditioning test. *Psychopharmacology (Berl)* 181:347-57
- Rehfeld JF. 2004. Clinical endocrinology and metabolism. Cholecystokinin. *Best Pract Res Clin Endocrinol Metab* 18:569-86
- Rhodes JS, Crabbe JC. 2005. Gene expression induced by drugs of abuse. *Curr Opin Pharmacol* 5:26-33
- Rinaman L, Dzmura V. 2007. Experimental dissociation of neural circuits underlying conditioned avoidance and hypophagic responses to lithium chloride. *Am J Physiol Regul Integr Comp Physiol* 293:R1495-503
- Rinaman L, Saboury M, Litvina E. 2009. Ondansetron blocks LiCl-induced conditioned place avoidance but not conditioned taste/ flavor avoidance in rats. *Physiol Behav* 98:381-5
- Robbins TW, Ersche KD, Everitt BJ. 2008. Drug addiction and the memory systems of the brain. *Ann N Y Acad Sci* 1141:1-21
- Robinson TE, Berridge KC. 2008. Review. The incentive sensitization theory of addiction: some current issues. *Philos Trans R Soc Lond B Biol Sci* 363:3137-46
- Roettger BF, Pinon DI, Burghardt TP, Miller LJ. 1999. Regulation of lateral mobility and cellular trafficking of the CCK receptor by a partial agonist. *Am J Physiol* 276:C539-47
- Roosendaal B, McEwen BS, Chattarji S. 2009. Stress, memory and the amygdala. *Nat Rev Neurosci*
- Rotzinger S, Bush DE, Vaccarino FJ. 2002. Cholecystokinin modulation of mesolimbic dopamine function: regulation of motivated behaviour. *Pharmacol Toxicol* 91:404-13
- Rotzinger S, Lovejoy DA, Tan LA. 2010. Behavioral effects of neuropeptides in rodent models of depression and anxiety. *Peptides* 31:736-56
- Rotzinger S, Vaccarino FJ. 2003. Cholecystokinin receptor subtypes: role in the modulation of anxiety-related and reward-related behaviours in animal models. *J Psychiatry Neurosci* 28:171-81
- Russell DW. 2003. AAV loves an active genome. *Nat Genet* 34:241-2
- Sah P, Faber ES, Lopez De Armentia M, Power J. 2003. The amygdaloid complex: anatomy and physiology. *Physiol Rev* 83:803-34
- Salamone JD, Correa M, Farrar A, Mingote SM. 2007. Effort-related functions of nucleus accumbens dopamine and associated forebrain circuits. *Psychopharmacology (Berl)* 191:461-82
- Samulski RJ, Berns KI, Tan M, Muzyczka N. 1982. Cloning of adeno-associated virus into pBR322: rescue of intact virus from the recombinant plasmid in human cells. *Proc Natl Acad Sci U S A* 79:2077-81
- Schiffmann SN, Vanderhaeghen JJ. 1991. Distribution of cells containing mRNA encoding cholecystokinin in the rat central nervous system. *J Comp Neurol* 304:219-33

- Schubert S, Grunweller A, Erdmann VA, Kurreck J. 2005. Local RNA target structure influences siRNA efficacy: systematic analysis of intentionally designed binding regions. *J Mol Biol* 348:883-93
- See RE. 2002. Neural substrates of conditioned-cued relapse to drug-seeking behavior. *Pharmacol Biochem Behav* 71:517-29
- See RE, Fuchs RA, Ledford CC, McLaughlin J. 2003. Drug addiction, relapse, and the amygdala. *Ann N Y Acad Sci* 985:294-307
- Shaham Y, Shalev U, Lu L, De Wit H, Stewart J. 2003. The reinstatement model of drug relapse: history, methodology and major findings. *Psychopharmacology (Berl)* 168:3-20
- Sherrin T, Todorovic C, Zeyda T, Tan CH, Wong PT, et al. 2009. Chronic stimulation of corticotropin-releasing factor receptor 1 enhances the anxiogenic response of the cholecystokinin system. *Mol Psychiatry* 14:291-307
- Shevtsova Z, Malik JM, Michel U, Bahr M, Kugler S. 2005. Promoters and serotypes: targeting of adeno-associated virus vectors for gene transfer in the rat central nervous system in vitro and in vivo. *Exp Physiol* 90:53-9
- Shindo S, Yoshioka N. 2005. Polymorphisms of the cholecystokinin gene promoter region in suicide victims in Japan. *Forensic Sci Int* 150:85-90
- Silberman Y, Bajo M, Chappell AM, Christian DT, Cruz M, et al. 2009. Neurobiological mechanisms contributing to alcohol-stress-anxiety interactions. *Alcohol* 43:509-19
- Silva AJ, Giese KP, Fedorov NB, Frankland PW, Kogan JH. 1998. Molecular, cellular, and neuroanatomical substrates of place learning. *Neurobiol Learn Mem* 70:44-61
- Skoubis PD, Lam HA, Shoblock J, Narayanan S, Maidment NT. 2005. Endogenous enkephalins, not endorphins, modulate basal hedonic state in mice. *Eur J Neurosci* 21:1379-84
- Smadja C, Ruiz F, Coric P, Fournie-Zaluski MC, Roques BP, Maldonado R. 1997. CCK-B receptors in the limbic system modulate the antidepressant-like effects induced by endogenous enkephalins. *Psychopharmacology (Berl)* 132:227-36
- Solomon RL, Corbit JD. 1974. An opponent-process theory of motivation. I. Temporal dynamics of affect. *Psychol Rev* 81:119-45
- Sulzer D. 2011. How addictive drugs disrupt presynaptic dopamine neurotransmission. *Neuron* 69:628-49
- Surratt CK, Adams WR. 2005. G protein-coupled receptor structural motifs: relevance to the opioid receptors. *Curr Top Med Chem* 5:315-24
- Swanson LW, Petrovich GD. 1998. What is the amygdala? *Trends Neurosci* 21:323-31
- Takimoto T, Terayama H, Waga C, Okayama T, Ikeda K, et al. 2005. Cholecystokinin (CCK) and the CCKA receptor gene polymorphism, and smoking behavior. *Psychiatry Res* 133:123-8
- Tanganelli S, Fuxe K, Antonelli T, O'Connor WT, Ferraro L. 2001. Cholecystokinin/dopamine/GABA interactions in the nucleus accumbens: biochemical and functional correlates. *Peptides* 22:1229-34
- Tarasova NI, Stauber RH, Choi JK, Hudson EA, Czerwinski G, et al. 1997. Visualization of G protein-coupled receptor trafficking with the aid of the green fluorescent protein.

- Endocytosis and recycling of cholecystokinin receptor type A. *J Biol Chem* 272:14817-24
- Tekin S, Cummings JL. 2002. Frontal-subcortical neuronal circuits and clinical neuropsychiatry: an update. *J Psychosom Res* 53:647-54
- Tenenbaum L, Chtarto A, Lehtonen E, Velu T, Brotchi J, Levivier M. 2004. Recombinant AAV-mediated gene delivery to the central nervous system. *J Gene Med* 6 Suppl 1:S212-22
- Tenenbaum L, Jurysta F, Stathopoulos A, Puschban Z, Melas C, et al. 2000. Tropism of AAV-2 vectors for neurons of the globus pallidus. *Neuroreport* 11:2277-83
- Tenk CM, Kavaliers M, Ossenkopp KP. 2005. Dose response effects of lithium chloride on conditioned place aversions and locomotor activity in rats. *Eur J Pharmacol* 515:117-27
- Trivier E, De Cesare D, Jacquot S, Pannetier S, Zackai E, et al. 1996. Mutations in the kinase Rsk-2 associated with Coffin-Lowry syndrome. *Nature* 384:567-70
- Truitt WA, Johnson PL, Dietrich AD, Fitz SD, Shekhar A. 2009. Anxiety-like behavior is modulated by a discrete subpopulation of interneurons in the basolateral amygdala. *Neuroscience* 160:284-94
- Tschuch C, Schulz A, Pscherer A, Werft W, Benner A, et al. 2008. Off-target effects of siRNA specific for GFP. *BMC Mol Biol* 9:60
- Tye KM, Prakash R, Kim SY, Fenno LE, Grosenick L, et al. 2011. Amygdala circuitry mediating reversible and bidirectional control of anxiety. *Nature* 471:358-62
- Tzschentke TM. 1998. Measuring reward with the conditioned place preference paradigm: a comprehensive review of drug effects, recent progress and new issues. *Prog Neurobiol* 56:613-72
- Tzschentke TM. 2007. Measuring reward with the conditioned place preference (CPP) paradigm: update of the last decade. *Addict Biol* 12:227-462
- Valassi E, Scacchi M, Cavagnini F. 2008. Neuroendocrine control of food intake. *Nutr Metab Cardiovasc Dis* 18:158-68
- Valverde O, Roques BP. 1998. Cholecystokinin modulates the aversive component of morphine withdrawal syndrome in rats. *Neurosci Lett* 244:37-40
- Vanderhaeghen JJ, Signeau JC, Gepts W. 1975. New peptide in the vertebrate CNS reacting with antigestrin antibodies. *Nature* 257:604-5
- Vizi S, Palfi A, Hatvani L, Gulya K. 2001. Methods for quantification of in situ hybridization signals obtained by film autoradiography and phosphorimaging applied for estimation of regional levels of calmodulin mRNA classes in the rat brain. *Brain Res Brain Res Protoc* 8:32-44
- Voikar V, Vasar E, Rauvala H. 2004. Behavioral alterations induced by repeated testing in C57BL/6J and 129S2/Sv mice: implications for phenotyping screens. *Genes Brain Behav* 3:27-38
- von Bohlen und Halbach O, Dermietzel R. 2006. NEUROTRANSMITTERS AND NEUROMODULATORS. WILEY-VCH Verlag GmbH & Co. KGaA, Weinheim, Germany
- Walton ME, Bannerman DM, Rushworth MF. 2002. The role of rat medial frontal cortex in effort-based decision making. *J Neurosci* 22:10996-1003

- Wang H, Spiess J, Wong PT, Zhu YZ. 2011. Blockade of CRF1 and CCK2 receptors attenuated the elevated anxiety-like behavior induced by immobilization stress. *Pharmacol Biochem Behav* 98:362-8
- Wang H, Wong PT, Spiess J, Zhu YZ. 2005. Cholecystokinin-2 (CCK2) receptor-mediated anxiety-like behaviors in rats. *Neurosci Biobehav Rev* 29:1361-73
- Wang XY, Zhao M, Ghitza UE, Li YQ, Lu L. 2008. Stress impairs reconsolidation of drug memory via glucocorticoid receptors in the basolateral amygdala. *J Neurosci* 28:5602-10
- Waraczynski MA. 2006. The central extended amygdala network as a proposed circuit underlying reward valuation. *Neurosci Biobehav Rev* 30:472-96
- Wargelius A, Ellingsen S, Fjose A. 1999. Double-stranded RNA induces specific developmental defects in zebrafish embryos. *Biochem Biophys Res Commun* 263:156-61
- Wiesenfeld-Hallin Z, Xu XJ, Hokfelt T. 2002. The role of spinal cholecystokinin in chronic pain states. *Pharmacol Toxicol* 91:398-403
- Wilson J, Watson WP, Little HJ. 1998. CCK(B) antagonists protect against anxiety-related behaviour produced by ethanol withdrawal, measured using the elevated plus maze. *Psychopharmacology (Berl)* 137:120-31
- Winstanley CA, Olausson P, Taylor JR, Jentsch JD. 2010. Insight into the relationship between impulsivity and substance abuse from studies using animal models. *Alcohol Clin Exp Res* 34:1306-18
- Wolf OT, Dyakin V, Vadasz C, de Leon MJ, McEwen BS, Bulloch K. 2002. Volumetric measurement of the hippocampus, the anterior cingulate cortex, and the retrosplenial granular cortex of the rat using structural MRI. *Brain Res Brain Res Protoc* 10:41-6
- Wu Z, Asokan A, Samulski RJ. 2006. Adeno-associated virus serotypes: vector toolkit for human gene therapy. *Mol Ther* 14:316-27
- Yu JY, DeRuiter SL, Turner DL. 2002. RNA interference by expression of short-interfering RNAs and hairpin RNAs in mammalian cells. *Proc Natl Acad Sci U S A* 99:6047-52
- Zolotukhin S, Potter M, Zolotukhin I, Sakai Y, Loiler S, et al. 2002. Production and purification of serotype 1, 2, and 5 recombinant adeno-associated viral vectors. *Methods* 28:158-67

VII. RÉSUMÉ EN FRANÇAIS

Cholecystokinine et abus de drogues: régulation du transcript dans la dépendance et conséquences de l'inactivation fonctionnelle dans l'amygdale basolatérale sur des réponses émotionnelles de souris

La dépendance aux drogues est un désordre psychobiologique chronique caractérisé par une recherche et une prise de drogue compulsives en dépit de conséquences négatives. Alors que la prise récréationnelle de drogues évolue de manière graduelle vers une prise incontrôlée, la dépendance s'installe et un syndrome de sevrage apparaît en cas de privation de drogue. Le soulagement de cet épisode aversif par le biais d'une reprise de la consommation de drogue est impliqué dans l'entretien de l'addiction. En outre, les épisodes de rechute ont souvent lieu après des longues périodes sans contact avec la drogue (abstinence prolongée), caractérisées par l'émergence d'un état émotionnel négatif malgré la disparition des symptômes physiques de sevrage (Goeldner et al 2011). Plusieurs systèmes de neurotransmission sont impliqués dans les mécanismes neuroadaptatifs consécutifs à l'abus de drogue. Parmi ces circuits neuronaux, le système opioïde joue un rôle clé et a été largement étudié au sein de notre laboratoire, dans le but de comprendre les bases génétiques de la dépendance aux drogues dans le cerveau. Nous avons montré que le récepteur mu est essentiel pour l'initiation des comportements addictifs, et nous avons identifié une série de gènes régulés par l'activation excessive de ce récepteur suite à un traitement chronique à la morphine (Befort et al 2008). L'expression de ces gènes a ensuite été évaluée après des traitements chroniques utilisant différentes drogues d'abus, telles que l'éthanol, le delta-9-tétrahydrocannabinol (THC) ou la nicotine, ainsi qu'après une période d'abstinence. Parmi l'ensemble des gènes sous-régulés par ces traitements, l'ARN messager (ARNm) de la cholécystokinine (CCK) fait partie de ceux dont les modifications de l'expression sont les plus remarquables. Le but de cette thèse a été d'approfondir nos connaissances sur la régulation transcriptionnelle de la CCK en réponse à la morphine dans l'intégralité du cerveau de souris, et d'examiner l'implication de la CCK exprimée au niveau de l'amygdale basolatérale dans les réponses émotionnelles.

La CCK a été décrite à l'origine comme un peptide gastro-intestinal, et plus récemment pour son rôle de peptide neuromodulateur. Elle a été principalement étudiée pour ses effets facilitateurs dans les processus cognitifs et pour ses effets anxiogéniques (Daugé & Léna

1998). L'intérêt pour le rôle de la CCK dans l'addiction s'est accru au cours de ces dernières années. Dans le cerveau, la CCK est co-localisée avec différents neurotransmetteurs tels que la dopamine, le glutamate et le GABA, dans les neurones des circuits de la récompense et de la motivation. De plus, il a été montré que la CCK exerce une action opposée aux effets analgésiques des opioïdes (Wiesenfeld-Hallin et al 2002), et qu'elle pourrait également contribuer au syndrome de sevrage. Des études pharmacologiques ont montré que les antagonistes des récepteurs CCK_B pouvaient diminuer les aspects somatiques et motivationnels de le sevrage à la morphine (Valverde & Roques 1998; Kayser et al 1998), ainsi qu'à l'éthanol (Wilson et al 1998; Wilson & Little, 1998). Les régions cérébrales dans lesquelles la CCK contribue aux comportements émotionnels et addictifs sont peu connues, et n'ont pas encore été étudiées par des approches génétiques. Leur identification représente une étape importante pour la compréhension du rôle de la CCK dans le cerveau.

Afin de répondre à cette question, mon projet de thèse s'est principalement focalisé sur deux régions cérébrales que nous avons identifiées comme ayant la plus forte expression en ARNm de la CCK: le noyau basolatéral de l'amygdale (BLA) et le cortex cingulaire (Ctx Cg). Ces deux structures sont impliquées dans la modulation des états émotionnels (Devinsky et al 1995; Gallagher & Chiba, 1996). Premièrement, l'amygdale a été étudiée pour son implication dans les réponses au stress et dans l'apprentissage associatif (LeDoux 2000). Dans cette région, la CCK est exprimée dans les interneurons GABAergiques (Jasnow et al 2008) et l'activation du récepteur CCK_B peut être à l'origine de ses effets anxiogéniques (Chung & Moore 2007). De plus, des sous-populations spécifiques de neurones de la BLA sont impliquées dans la formation et le rappel de la mémoire du sevrage (Frenois et al 2005). Il a aussi été proposé que l'activation du cortex cingulaire joue un rôle déterminant dans la rechute induite par la réexposition aux stimuli conditionnés (Ronald 2002). Cette région est activée chez des sujets dépendants au cours de l'intoxication et du désir irrésistible de la drogue (« manque ») et désactivée pendant le sevrage (Goldstein & Volkow, 2002). Enfin, une autre étude chez le rat a montré une activation du Ctx Cg lors d'un sevrage précipité par la naloxone (Lowe et al 2002).

Objectifs de la thèse:

Notre étude avait deux objectifs :

- Examiner les modifications d'expression de l'ARNm de la CCK dans le cerveau de la souris, consécutif à un traitement chronique à la morphine ou à une période d'abstinence, et plus particulièrement dans la BLA et le Ctx Cg.
- Analyser les effets d'une inhibition locale de l'expression de l'ARNm de la CCK dans la BLA sur une batterie complète de test des comportements émotionnels.

Part I. "Régulation de l'ARNm de la CCK dans le cerveau de souris au cours d'une dépendance à la morphine"

Les études effectuées au sein de notre laboratoire ont permis d'établir que l'expression du gène de la CCK est dépendante de l'activation du récepteur mu (Befort et al 2008). Ces études ont été réalisées dans l'amygdale étendue, une entité neuroanatomique impliquée dans la récompense à la drogue, le stress et la rechute. La régulation du transcript CCK s'est avérée particulièrement intéressante. Plus précisément, l'expression de l'ARNm est inhibée suite à un traitement chronique à la morphine, puis re-augmente jusqu'à atteindre un niveau supérieur au basal après quatre semaines d'abstinence. C'est pourquoi, dans la première partie de ma thèse, j'ai réalisé un examen approfondi des niveaux d'expression du transcript CCK, après un traitement chronique à la morphine, dans d'autres structures cérébrales telles que la BLA et le Ctx Cg. Le traitement a été réalisé selon le protocole décrit dans Befort et al (2008). Brièvement, des souris mâles C57BL/6J ont été injectées soit par une solution saline, soit par des doses croissantes de morphine (entre 20 et 100 mg/kg) pendant 6 jours. Puis, les animaux ont été sacrifiés soit 20 minutes après la dernière injection afin d'analyser l'état de dépendance à la morphine, soit 4 semaines plus tard afin d'analyser l'état d'abstinence à la morphine. J'ai évalué l'impact de ces traitements sur l'expression de l'ARNm CCK dans la BLA et le Ctx Cg, en développant une technique d'hybridation *in situ* radioactive quantitative utilisant des sondes marquées au S³⁵. Les coupes de cerveau des animaux traités ont été exposées aux films radiographiques pendant 3, 5 ou 7 jours, et le signal autoradiographique a été quantifié en utilisant le logiciel ImageJ (<http://imagej.nih.gov>). Une courbe de calibration

de la radioactivité (nCi/mg) a été générée avec des standards C¹⁴, et les valeurs des niveaux de gris moyens ont été converties en unité de radioactivité pour toutes les comparaisons. Aucune différence statistique entre les groupes n'a pu être mesurée quelle que soit la condition et la région d'intérêt. Cependant, on a observé une tendance à l'augmentation du niveau d'expression de l'ARNm de la CCK dans le Ctx Cg ($p=0.08$) et dans la BLA ($p=0.12$) après la période d'abstinence. Ces résultats nécessitent d'être confirmés (Figure 1).

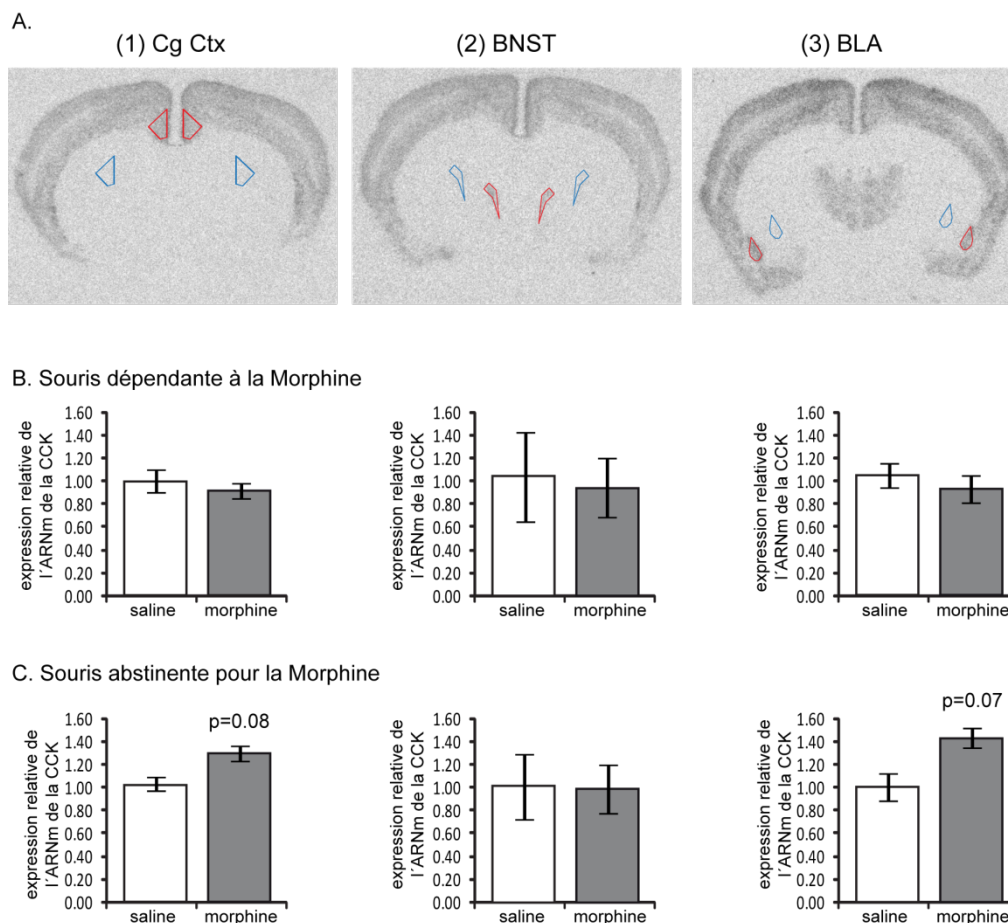


Figure 1: L'expression de l'ARNm de la CCK est diminuée 4 semaines après la fin d'un traitement à la morphine. (A) Autoradiographies de microsections de cerveau traitées par hybridation in situ. Les régions d'intérêt (ROI) sont tracées en rouge. (1) Cortex cingulaire (1.1mm par rapport au bregma), (2) Noyau du lit de la strie terminale (-0.22mm par rapport au bregma), Noyau basolatéral de l'amygdale (-1.22 par rapport au bregma). Les zones délimitées en bleu indiquent les régions du striatum considérées pour mesurer le bruit de fond. (B-C)

Expression relative de la mcck dans ces régions pour les souris contrôle (saline, barres blanches) et pour les souris traitées à la morphine (barres grises), sacrifiées soit (B) immédiatement après un traitement avec des doses croissantes de morphine (de 20 à 100 mg/kg en 6 jours), soit (C) après une période de 4 semaines d'abstinence. La quantification a été faite avec le logiciel ImageJ et une courbe de calibration de standards 14C (ARC0146, American Radiolabeled Chemicals). La conversion des niveaux de gris en mesures de radioactivité (nCi/mg) a été réalisée avec la fonction de régression non-linéaire de Rodbard. Les résultats sont exprimés en valeurs moyennes normalisées (ROI - bruit de fond du striatum) \pm SEM. Un test du t de Student n'a révélé aucune différence significative (n=2 souris/condition; ~20 ROI pour le Ctx Cg et 8 à 10 pour la BLA).

Part II. “Réponses émotionnelles comportementales après inactivation fonctionnelle de la CCK dans la BLA de souris par injection de vecteurs viraux AAV₂-shCCK”

L'expression augmentée (à confirmer) de l'ARNm de la CCK dans la BLA et le Ctx Cg des animaux abstinents est en accord avec une étude précédente obtenus au sein de notre laboratoire. Cette étude a établi un lien direct entre l'abstinence à la morphine et des symptômes de type dépressifs (Goeldner et al 2010). Par ailleurs, d'autres études ont montré qu'une lésion de la BLA provoquait un effet antidépresseur sur le comportement des rats (Castro et al 2010). Il est donc possible que l'augmentation de CCK, en particulier au niveau de la BLA, contribue au développement du syndrome dépressif que nous avons observé chez les animaux de l'abstinence. Étant donné que le rôle de la CCK exprimée au niveau de la BLA dans les réponses émotionnelles est peu connu, j'ai caractérisé les conséquences de l'inactivation fonctionnelle de la CCK dans la BLA lors de la **deuxième partie de ma thèse**. J'ai induit une diminution locale de l'ARNm de la CCK dans la BLA en utilisant des vecteurs viraux rAAV₂-eGFP-shCCK. Ces vecteurs contiennent deux cassettes exprimant l'eGFP (enhanced Green Fluorescent Protein) et un shCCK (short hairpin RNA, ciblant spécifiquement le gène *mcck*), sous le contrôle des promoteurs CMV (Cytomégalo virus) et mU6 (mouse U6) respectivement. J'ai confirmé l'expression du gène viral par microscopie à fluorescence, et quantifié la diminution de l'expression de l'ARNm CCK par d'hybridation *in situ*. J'ai optimisé les conditions expérimentales pour inhiber du transcript CCK de façon efficace et stable dans Cg Ctx et BLA (Figure 2 et 3).

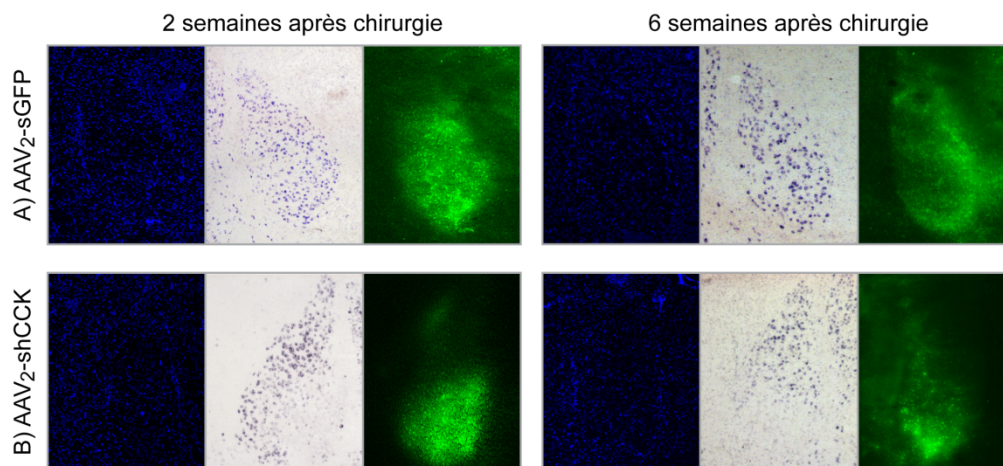


Figure 2: Validation qualitative de l'inactivation fonctionnelle de la CCK par injection d'AAV2-shCCK dans la BLA de souris, évaluée à 2 temps différents. Microphotographies de coupes de cerveau marquées pour le DAPI (à gauche), pour l'ARNm de la CCK (marquage dig, au centre) et pour l'expression de l'eGFP (à droite), chez des souris ayant subi une injection dans la BLA de vecteurs viraux (30x10¹¹) de type (A) AAV2-eGFP (expression de mcck intacte), ou (B) AAV2-shCCK (expression de mcck réduite). Les souris ont été sacrifiées 2 ou 6 semaines après la chirurgie.

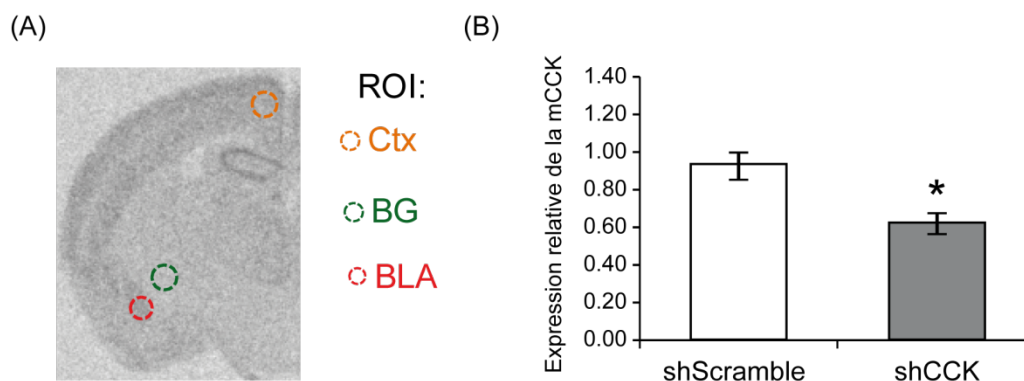


Figure 3: Validation quantitative de l'inactivation fonctionnelle de la CCK dans la BLA de souris avec des AAV2-shCCK. (A) Autoradiographie d'une coupe de cerveau traitée par HIS radioactive. Les ROI sont représentées en pointillés (Ctx, cortex; BG: bruit de fond (BackGround) du striatum; BLA, Noyau Basolatéral de l'Amygdale). (B) Expression relative de la mcck dans la BLA, montrant une diminution de ~35% chez les souris injectées avec l'AAV2-shCCK par rapport à celles injectées avec l'AAV2-shScramble. La quantification a été réalisée avec le logiciel ImageJ et une courbe de calibration de standards ¹⁴C (ARC0146, American Radiolabeled Chemicals). La conversion des niveaux de gris en mesures de radioactivité (nCi/mg) a été réalisée avec la fonction de régression non-linéaire de Rodbard. Les résultats sont exprimés en valeurs normalisées obtenues à partir des mesures de radioactivité moyennes selon la formule: (BLA - bruit de fond Striatum)/(Cortex - bruit de fond Striatum) ± SEM. Test du t de student non apparié **p<0.01 (n=5 souris/condition). Les souris ont été sacrifiées 9 semaines après la chirurgie.

J'ai ensuite examiné si l'inhibition du transcript CCK modifie les réponses émotionnelles à l'aide d'une batterie de paradigmes comportementaux. Pour ce faire, des injections stéréotaxiques de virus AAV₂-shCCK ou AAV₂-shScramble ont été réalisées dans la BLA sur deux cohortes indépendantes de souris mâles de souche C57BL/6J, selon le Mouse Brain Atlas de Paxinos & Franklin (2001). La batterie de tests comportementaux a été conçue de façon à évaluer des comportements de type anxiété, des comportements de désespoir, le conditionnement de place aversif à la naloxone et le syndrome de sevrage à la morphine chronique. Les souris ayant reçu des injections de shCCK (souris shCCK) ont montré une

diminution significative de leur niveau d'anxiété dans le test du labyrinthe en croix surélevé, en passant plus de temps dans les bras ouverts que les souris contrôle ayant reçu des injections de shScramble (souris shScramble) (** $p < 0.001$) (Figure 4A). D'autres tests d'anxiété tels que le champ ouvert (open field) et la boîte lumière/obscurité (light/dark box) n'ont pas révélé de différence statistique significative entre les groupes, probablement due aux conditions d'éclairage anxiogène pendant les essais. Les souris shCCK ont également montré une réduction significative des comportements de désespoir dans le test de la nage forcée, montrant moins d'immobilité pendant les six minutes du test comparées aux souris shScramble (** $p < 0.001$) (Figure 4B). Le test de suspension par la queue a aussi été utilisé pour évaluer les comportements de désespoir, mais aucune différence significative n'a pu être observée entre les deux groupes, cependant, de trouver des différences de sensibilité lors de ces essais n'est pas surprenant. En ce qui concerne l'évaluation de l'état homéostatique hédonique, les souris shCCK présentaient un déficit dans le paradigme d'aversion de place conditionnée (CPA) induite par la naloxone (ns) comparé aux souris shScramble (** $p < 0.001$) (Figure 4C). Enfin, aucune différence n'a été observée entre les groupes dans l'évaluation des signes physiques de sevrage lorsque des souris dépendantes à la morphine ont été soumises à un sevrage précipité par la naloxone (Figure 4D). Au total, nos données identifient clairement la BLA comme site principal des effets anxiogènes et déprimeurs de la CCK cérébrale. Dans le contexte de l'abus de drogues, la CCK de la BLA peut contribuer à l'état dépressif qui caractérise l'abstinence.

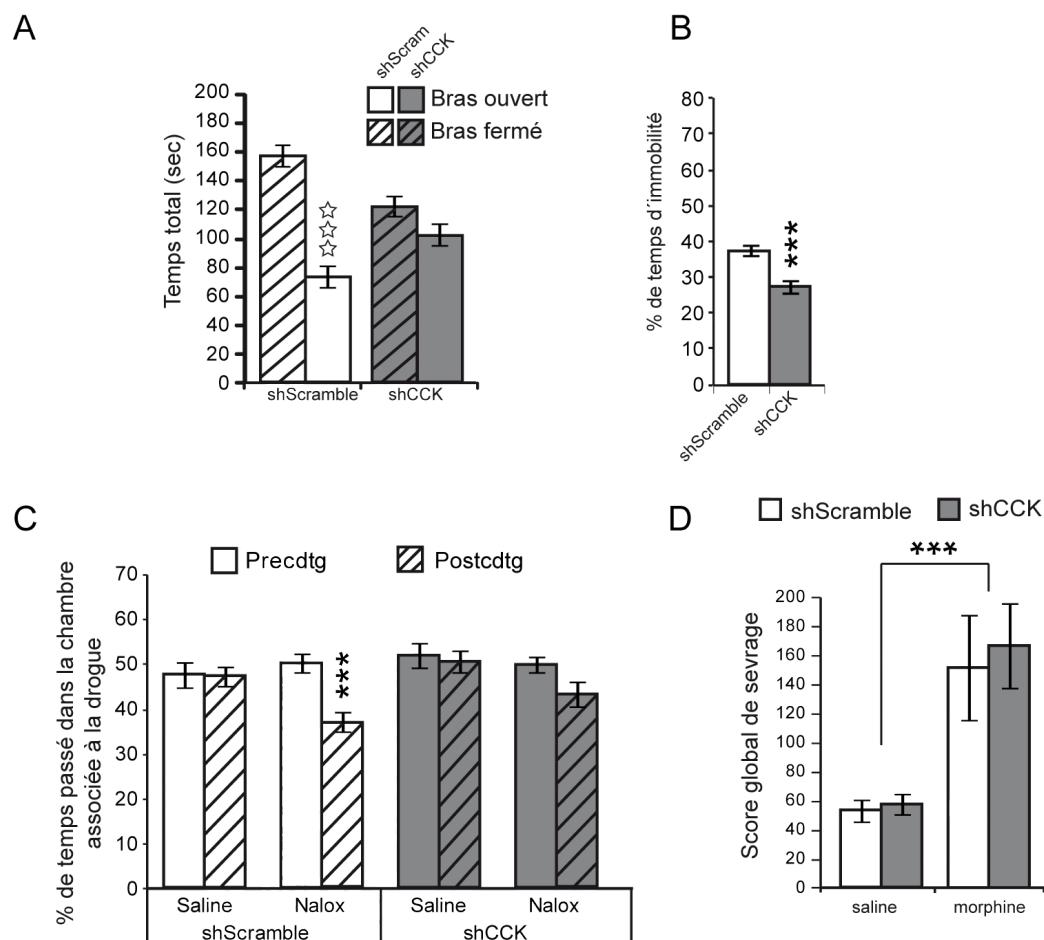


Figure 4 : Évaluation des réponses émotionnelles comportementales après inactivation fonctionnelle de la CCK dans la BLA de souris par injection de vecteurs viraux AAV2-shCCK. Les souris ayant reçu des injections de shCCK (souris shCCK) ont montré: (A) une diminution significative de leur niveau d'anxiété mesuré par le temps d'exploration dans le bras ouvert dans le test du labyrinthe en croix surélevé (ANOVA 2 voies, *** $p < 0.001$, $n = 21-23$ souris/groupe); (B) une diminution des comportements de type dépression mesuré par le pourcentage de temps d'immobilité au cours des 6 minutes du test de la nage forcée (ANOVA 2 voies, *** $p < 0.001$, $n = 9-11$ souris/groupe); (C) une réduction de l'aversion de place induite par la naloxone (test du t de Student, *** $p < 0.001$, $n = 11$ souris/groupe). (D) que l'injection de vecteur viral n'a pas eu d'effet sur le sevrage précipité par la naloxone après un traitement chronique à la morphine, mesuré par l'observation des signes somatiques de sevrage ($n = 4$ souris/groupe).

Conclusions et perspectives

Le but de ma thèse a été d'identifier les régions cérébrales à partir desquelles la CCK régule les comportements émotionnels et la dépendance aux drogues.

Nous avons d'abord quantifié les changements d'expression de l'ARNm de la CCK dans la BLA et le Ctx Cg suite à un traitement chronique à la morphine, et avons trouvé une tendance intéressante à des niveaux de l'ARNm de la CCK augmentés dans les deux régions après 4 semaines d'abstinence. Dans le cadre de ce projet, nous avons développé une méthodologie de cartographie autoradiographique quantitative qui permet des mesures anatomiques précises de l'expression des gènes et sera utile pour des projets ultérieurs de notre laboratoire. Une étude des modifications de l'expression de l'ARNm de la CCK dans nos deux régions d'intérêt après un traitement chronique à l'éthanol est déjà en cours. Enfin, nos résultats montrant la modification de l'expression de CCK dans la BLA suggèrent un rôle possible de ce gène dans l'émergence de l'état dépressif qui caractérise l'abstinence.

Nous avons également abordé le rôle de la CCK dans les réponses émotionnelles à l'aide d'une approche fonctionnelle de shRNA *in vivo*. Nous avons conçu un vecteur viral rAAV2-eGFP-shCCK afin de cibler l'ARNm de la CCK dans le cerveau de souris, et avons réussi à mettre en place les conditions expérimentales permettant de diminuer localement l'expression de l'ARNm CCK dans la BLA. Nous avons montré que l'inhibition locale de la CCK a des effets anxiolytiques et antidépresseurs, respectivement dans le test du labyrinthe en croix surélevé et celui de la nage forcée. De plus, les souris shCCK sont moins performantes dans le test de CPA induite par la naloxone. Une étude plus approfondie avec d'autres tests de préférence ou d'aversion de place, tels que la préférence de place conditionnée par la morphine, ou la CPA induite par le lithium serait intéressante afin de déterminer si notre observation reflète un rôle de la CCK dans l'apprentissage conditionné ou dans le tonus hédonique basal. Dans de futures expériences, nous envisageons de caractériser les effets de l'inhibition du gène de la CCK dans le cortex cingulaire, pour lequel les conditions expérimentales ont d'ores et déjà été mises en place. Cela permettra de déterminer si la CCK dans cette zone corticale contribue également à l'état émotionnel négatif présent dans l'abstinence prolongée.

« Chaque jour j'apprenais quelque chose sur la planète,
sur le départ, sur le voyage... »

LE PETIT PRINCE - Antoine de Saint-Exupéry

“Todos saben que las aves migratorias
siempre encuentran el camino de regreso...”

Zamba del Emigrante - Ismael Serrano

ABSTRACT

Cholecystokinin (CCK) is one of the major neuromodulatory peptides in the mammalian brain. Both peptides and receptors present a wide distribution in the CNS co-localizing with classic neurotransmitters (dopamine, glutamate, GABA and serotonin) in neurons of rewarding, motivational and emotional pathways. The CCKergic system modulates a broad variety of physiological functions, including feeding behavior, cardio-respiratory control, thermoregulation, nociception, anxiety, depression, memory processes and motivational responses. A previous study in our laboratory identified CCK as a mu-opioid dependent gene which mRNA showed remarkable modifications in the central extended amygdala, a neuroanatomical entity strongly implicated in drug seeking, craving and relapse, upon morphine treatment. CCK-expressing brain regions involved in all these effects remain unclear and their identification represents an important step towards understanding CCK function in the brain. Therefore, the aim of this thesis was to further investigate CCK transcriptional regulation in response to morphine throughout the mouse brain, and to examine the implication amygdalar CCK in emotional responses.

In the first part of my thesis, I developed a complete mapping of CCK mRNA distribution in the mouse brain to confirm reported locations of *mcck*, and I then focused on two brain structures implicated in the processing of emotional states and drug dependence, both showing high CCK transcript density: the Cingulate Cortex (Cg Ctx) and the Basolateral nucleus of the Amygdala (BLA). I evaluated the consequences of an escalating chronic morphine treatment and a period of 4 weeks of abstinence over CCK mRNA expression in these regions. To this aim I optimized a quantitative autoradiographic mapping methodology and our results show a trend for *mcck* up-regulation after 4 weeks abstinence in both Cg Ctx and BLA. Although these results need to be confirmed with an increased number of mice, the presented trends, detectable only in the abstinent mice, are consistent with an earlier study in our laboratory, which established the existence of depressive-like symptoms in morphine-abstinent mice.

In the second part of my thesis, I focused on the BLA, which is strongly involved in the generation of emotional states, and examined the role of amygdalar CCK in negative emotional responses in the mouse. To this aim we designed a double promoter-based rAAV-eGFP(CMV)-shRNA(mU6) viral vector to target the CCK mRNA *in vivo* and I optimized the experimental conditions to effectively and stable down-regulate the CCK transcript in Cg Ctx and BLA. Using this genetic approach, we demonstrated that CCK mRNA down-regulation in BLA has significant anxiolytic and antidepressant effects in the elevated plus-maze and forced swim test, respectively. Moreover, shCCK mice showed a reduction in naloxone-induced conditioned-place aversion, another paradigm involving negative emotional responses. This study is presented in the manuscript "Genetic silencing of cholecystokinin mRNA in basolateral amygdala has anxiolytic and antidepressant effects in mice". Del Boca C, Le Merrer J, Lutz PE, Koebel P, Kieffer BL.

Altogether, our data on this first local genetic approach of CCK role in emotional responses clearly identify BLA as a main site for anxiogenic and depressant effects of neural CCK, and strongly suggest that amygdalar CCK contributes to mood homeostasis and dysregulation of CCK expression in this region may be a causal factor in panic disorders and major depression. Besides, in the context of drug abuse, our results combined with preliminary data obtained in our laboratory, suggest that CCK in BLA may contribute to the depressive state that characterizes abstinence.

Finally, my contributions to two other studies of our laboratory are also presented in an ANNEX part in two manuscripts: "RSK2 signaling in brain habenula mediates place learning". Darcq E, Koebel P, Del Boca C, Pannetier S, Kirstetter AS, Garnier JM, Hanauer A, Befort K and Kieffer BL. 2011. Submitted; and "Deletion of the delta-opioid receptor gene impairs place conditioning but preserves morphine reinforcement". Le Merrer J, Plaza-Zabala A, Del Boca C, Matifas A, Maldonado R and Kieffer BL. Biol Psychiatry. 2011.